Universidade do Minho
Escola de Engenharia

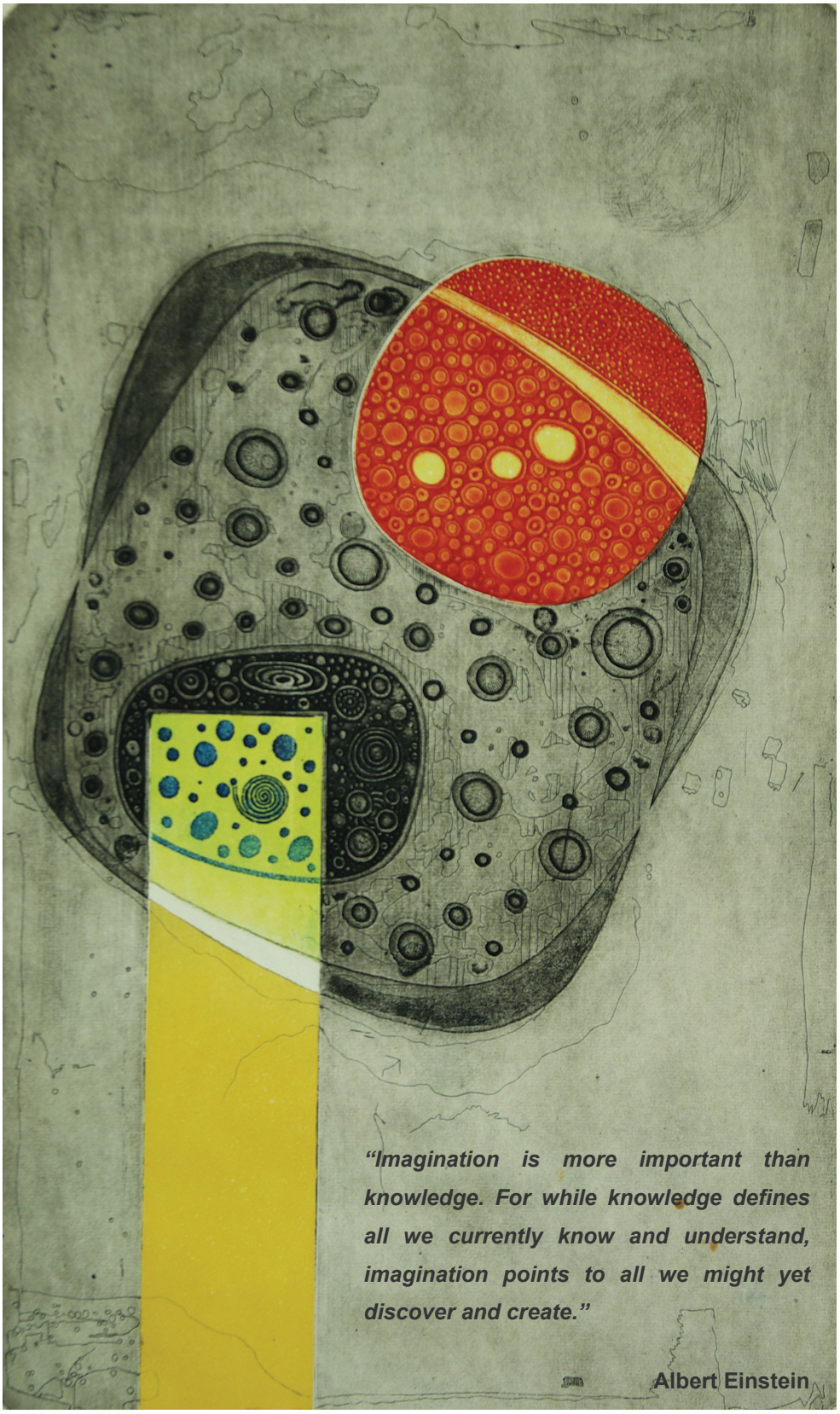
Ana Leite de Almeida Monteiro de Oliveira

New Biomimetic Approaches for Producing Bone-like Calcium-Phosphate Coatings on the Surface of Tissue Engineering 3D Architectures and Orthopaedic Implants

Tese de Doutoramento em Ciência e Engenharia de Polímeros
Área de conhecimento em Ciência de Materiais Poliméricos

Dezembro de 2007

“É AUTORIZADA A REPRODUÇÃO PARCIAL DESTA TESE APENAS PARA EFEITOS DE INVESTIGAÇÃO, MEDIANTE DECLARAÇÃO ESCRITA DO INTERESSADO, QUE A TAL SE COMPROMETE.”



“8-15Z”- António Leite

ACKNOWLEDGEMENTS

The preparation of this thesis would not be possible without the help of several persons and Institutions, to whom I am and will always be very grateful.

I start by expressing my gratitude to my main supervisor, Prof. Rui Reis, without whom I would never be able to go so far. He gave me the motivation and the freedom to follow my own ideas and in the more difficult moments has trusted in my judgments and supported my decisions. During these years, I have never stopped admiring his commitment to his dreams and his perseverance.
To Prof. Julio San Roman, my most sincere gratitude for all the support, encouragement and for the warm welcoming in his lab, where I felt like at home. Besides all his scientific achievements, I have always admired his sense of caring, joy and vitality. They are true life lessons.
To Dr. Panjian Li, in my opinion one of the most important researchers in the biomimetic coatings' field, whom I thank for giving me the opportunity to take research to the next level. I am also thankful for all his effort to make my staying at DePuy the best possible. All the guidance and constant interest in my work were very important, but they would not be useful without the knowledge he has willed to share. I truly admire his commitment to science and to life-time project.

I am very grateful to my colleagues and friends in my research group (without forgetting those that are not working with us anymore…). We share good and less good moments, and during these times I have found some really special people. I would like to thank Silvia Lopes, Silgia Costa, Miguel Oliveira, Simone Silva, Ana Martins, Catarina Alves, Vitor Correlo, João Oliveira, Ricardo Silva, Adriano Pedro, Marina Santos, Iva Paskuleva, Gabriela Silva and José Victor, not only colleagues, but also friends. My special "Thanks!" to our management team (Tânia Alves, Ariana Santos, Virginia Araújo e Berta Almeida) and our lab technician Liliana Gomes. I want also to acknowledge the technical support given by Elsa Ribeiro, conducting part of SEM analysis. I would like also to acknowledge to the technical staff of the Laboratório Central de Análises (Dr. Rosário Soares and Dr. Eugénio Soares, for all the support with the ICP and XRD analysis).

I had the wonderful opportunity to work in the group of Prof. Julio San Roman, at the CSIC, in Madrid were I acknowledge all, especially Gema Rodriguez and Carlos Elvira with whom I was lucky enough to work. Carlos, we met both in Madrid and Braga. I definitely learned a lot with you! You have been a good friend throughout the years.

During my period at the DePuy, in Warsaw, IN, I have worked in the group of Dr. Panjian Li, were I am thankful for all the support, especially the words of encouragement of Xiau Fang (Sofie), Hai Bo and Weidong Tong for the generosity in sharing their knowledge. Also to Todd Smith, for making this collaboration happen and receiving me so well.

I hereby acknowledge Fundação para a Ciência e Tecnologia, for financial support through a PhD grant (SFRH/BD/10956/2002). This work was partially supported by FCT through POCTI and/or FEDER programmes. I also acknowledge Fundação Calouste Gulbenkian for several travel awards to scientific meetings. This work was additionally supported by the EU Project HIPPOCRATES (NMP3-CT-2003-505758), developed in the scope of the EU EXPERTISSUES NoE (NMP-CT-2004-500283).

The support and cheering up of my closest friends was essential to keep me in the right mood during the preparation of this thesis. In all moments I was lucky enough to find people that (sometimes without knowing it) helped me going through these last working years. In no moment I felt alone. They have been very important and they still are today, as they all brighten my life. I want to address them a special “Thanks!”.

In Warsaw, I can not forget Caroline, Julie and Chip for making me part of their lives and for showing me the other side of “the orthopedic city of the world”, as well as João, such a good friend. I wonder if we will ever go Amish hunting again… In Madrid I must also thank Roby e Mario, for taking so good care of me, and for being true friends. I was literally spoiled with Italian pasta.

I want to express my deepest gratitude to my very best friends, Patricia, Pituca and Cristina. They are the friends for all moments and at the same time the friends with whom I share ideas and opinions. They have always been there for encouraging me. Besides being my very good friend, supporting me in the moments there I have most needed, Patricia has also participated as a co-author in some of the work presented herein. Thank you for always being around!

I would like to thank my family for always respecting my choices in life (not that they have always understood them) and for supporting me no matter what. I have to specially thank to the two most important women in my life, my mother and grandmother. Their generosity, strength and amazing ability to go through the difficulties in life have been true life lessons to me.

Finally, it is difficult to express gratefulness to someone so special to me, without whom it would have been much more difficult to go trough the course of this thesis. His love and care were essential for giving me the strength to keep going on. He was by my side in all moments and has always supported me no matter what. Thank you Rui for your unconditional love!

ABSTRACT

Bone is one of the most wonderful examples of nature's ability to engineer living materials. The processes by which the mineralized tissues are formed can be a source of information for the development of new materials for biomedical applications, capable of better mimicking living tissues, i.e. biomimetic materials. In the field of bone replacement and regeneration, this new concept can lead to innovative ideas towards the controlled fabrication of advanced materials.

When considering a particular material as being adequate for orthopaedics one should keep always in mind that it must be mechanical and biologically compatible with bone. Furthermore, it may be advantageous to exhibit a bone bonding behaviour, i.e. to express bioactivity by creating an environment compatible with osteogenisis (bone growth), having the mineralizing interface developing as a natural bonding junction between living and non-living materials. This interface can be generated by a calcium phosphate coating at the surface of the material. The techniques whereby Ca-P layers are produced have recently undergone a revolutionary change leading to profound consequences in their potential applications. Over the last years, calcium phosphate layers were deposited upon the surfaces of implants under non-physiological conditions, which limits their application in polymeric substrates. In the recent years, there has been an increasing interest in the so-called biomimetic preparation of calcium phosphate coatings, under physiological conditions of temperature, pH and pressure. This new generation of coating techniques as enlarged the spectrum of potential applications of such coatings from bone fixation improvement in traditional bone replacement applications, to coating of 3D scaffold architectures in Tissue Engineering applications. Due to their processing versatility, these coatings can be tailored in terms of chemical composition, crystallinity and resorbability or even be loaded with bioactive molecules and/or serve as scaffolds for the seeding of living cells, stimulating bone formation. To do this on a degradable polymer is not a very easy task, as the surface of the substrate (and pH around it) is continuously changing. These were the main challenges addressed in this thesis, having always in mind that to date scientists did not produce yet any material capable of mimicking the bone structure. In this way nature is, and will continue to be, the best material scientist, and the only one able to design complex structures and control intricate processing routes that lead to the final shape of living creatures.

Most of the experimental part of the work is focused on the development of tailored apatite layers on the surface of starch based biodegradable polymers, using a sodium silicate gel as an alternative nucleating agent. This methodology proved to be a very effective and simple mean of inducing the formation of a well-defined apatite-like layer at the surface of these polymers. One of the advantages when comparing with the traditional biomimetic coating methodology is that apatite is formed at a higher rate. Preliminary cell studies on these coatings have indicated a very good osteoblast adhesion and proliferation. When increasing the ionic product of the Simulated Body Fluid solution (SBF), it was possible to positively influence cell proliferation possibly due to an increase in the apatite crystallinity.

Sodium silicate biomimetic methodology was also employed to coat the surface of starch based scaffolds produced by a rapid prototyping technology (Bioplotter®), recently proposed for bone Tissue Engineering applications. This coating methodology is particularly suitable for complex-shaped materials since sodium silicate gel can reach the inner surfaces of the porous structures. In this work, several dynamic biomimetic coating routes are originally proposed with the aim of producing coatings homogeneously distributed throughout the thickness of the scaffolds, namely by using static, agitation and circulating flow perfusion conditions. A bioreactor was specially designed for the last operating condition. Bone-like poorly crystalline carbonated apatite layers were effectively produced at both the external and bulk surfaces of the developed scaffolds, by covering the surface of the fibres of the scaffold while maintaining its initial porous structure and interconnectivity. The composition, chemical structure and crystallinity of the obtained apatite layers grown under static, agitation and flow perfusion conditions were not significantly different. In case of the flow perfusion, the coating thickness was greatly enhanced. Besides the typical characterization techniques, Micro-Computed Tomography analysis (μ-CT) was here used for the first time to assess scaffold porosity and as a new tool for mapping apatite content. 2D histomorphometric analysis was performed and 3D virtual models were created using specific softwares for CT reconstruction. By this technique it was possible to observe, in a non-destructive way, that the interior of the scaffolds was effectively coated without compromising their overall morphology and interconnectivity. μ-CT analysis clearly demonstrated that flow perfusion was the most effective condition. Besides mimicking better the biological milieu, it allowed for the coating of complex architectures at higher rates of apatite formation, greatly reducing the time of the coating process step.

The possibility of tailoring an apatite layer by incorporating bioactive agents was also assessed in this work. A well known therapeutic agent from the family of bisphosphonates (BP) - sodium clodronate - was incorporated in an apatite coating, previously formed on the surface of a starch based polymer by a sodium silicate methodology, as a strategy to develop a site-specific drug delivery system for bone tissue regeneration. This drug, currently in use for the treatment of several bone- and calcium- related pathologies like hypercalcemia, Paget's disease or osteoporosis, was successfully incorporated, at different doses, in the structure of a biomimetic apatite layer. It is foreseen that these coatings can for instances be produced on the surface degradable polymers for regulating the equilibrium on osteoblastic/osteoclastic activity in the direction of a regenerative effect at the interface between biomaterial and bone.

The final study conducted in this work explores the possibility of incorporating Strontium into the structure of apatite coatings prepared by a solution-derived process according to an established biomimetic methodology for coating titanium based orthopaedic implants. It is believed that its localized presence at the interface between an implant and bone will enhance osteointegration and therefore, ensure the longevity of a joint prosthesis. By using this methodology it was possible to incorporate increasing amounts of Sr in the apatite layers. Sr was found to incorporate in the apatite lattice through a substitution mechanism by replacing Ca in the apatite lattice. The presence of Sr in solution induced an inhibitory effect on mineralization, leading to a decrease in the thickness of the mineral layers. The obtained Sr-substituted biomimetic coatings presented a bone-like structure similar to the one found in the human bone and are therefore expected to enhance bone formation and osteointegration.

The results herein presented demonstrate the potential and versatility of the proposed biomimetic strategies for improving the performance of biomaterials either in the context of regeneration or traditional substitution of bone.

Resumo

O processo através do qual os tecidos mineralizados são formados constitui uma fonte de inspiração para o desenvolvimento de novos materiais para aplicções biomédicas, capazes de mimetizar os tecidos vivos, i.e. materiais biomiméticos. Na área da substituição e regeneração óssea, este novo conceito é particularmente interessante, dando origem a ideias inovadoras para o fabrico de materiais avançados.

Considerar um material adequado para aplicação na área ortopédica pressupõe a sua respectiva compatibilidade ao nível mecânico e biológico. Para além destes requisitos poderá ser também vantajoso combinar a capacidade de promover a adesão ao tecido ósseo, isto é, induzir um comportamento bioactivo promovendo um ambiente compatível à osteogénese (crescimento ósseo) mediante o desenvolvimento de uma interface mineralizada, que assegure a ligação entre os materiais vivos e não vivos. Esta interface poderá ser criada por um revestimento de fosfato de cácio à superfície do material. As primeiras técnicas desenvolvidas para produzir este tipo de revestimentos utilizavam condições não fisiológicas, o que limitou o seu uso em substratos poliméricos. Nos últimos anos tem havido um crescente interesse na preparação biomimética de revestimentos de fosfato de cácio (Ca-P) em condições de temperatura, pH e pressão próximas das fisiológicas. Esta nova geração de técnicas de revestimento permitiu alargar o espectro de potenciais aplicações, não só no sentido de melhorar a interface com o osso em materiais para substituição óssea como também de estimular a regeneração óssea na superfície de estruturas de suporte tridimensionais (3D). Devido à sua versatilidade, estes revestimentos podem ser ajustados em termos da sua composição e estabilidade química, cristalinidade e resorbabilidade, ou mesmo carregados com moléculas bioactivas e/ou servirem como suporte para a cultura de células e posterior formação de novo osso. No entanto, aplicar este tipo de tratamento a um polímero biodegradável não é uma tarefa fácil, já que a superfície do substrato (e o pH envolvente) está continuamente em alteração. Estes são os desafios propostos nesta tese, tendo sempre presente que até à data, a ciência não foi capaz de produzir um material capaz de replicar a estrutura óssea. A natureza é, e continuará a ser, o melhor cientista de materiais, já que é capaz de desenhar estruturas complexas e controlar intricados processos que irão conduzir à forma final dos seres vivos.

Grande parte do trabalho experimental apresentado nesta tese é baseada no desenvolvimento de revestimentos de apatite na superfície de polímeros biodegradáveis à base de amido de milho, utilizando um gel de silicato de sódio como um agente alternativo de nucleação. Esta metodologia provou ser um meio simples e eficaz para induzir a formação de uma camada de apatite bem definida na superfície destes polímeros. Uma das vantagens quando comparado com o método biomimético tradicional, é o facto de a camada de apatite ser formada a uma velocidade superior. Estudos celulares preliminares utilizando células do tipo osteoblasto indicaram uma boa adesão a estes revestimentos. Quando o produto iónico da solução simuladora do plasma humano (*Simulated Body Fluid* – SBF) foi aumentado, foi possível influenciar positivamente a proliferação celular devido possivelmente a um aumento da cristalinidade do revestimento de apatite formado.

A metodologia de revestimentos biomiméticos por silicato de sódio foi também utilizada para revestir a superfície de estruturas de suporte à base de amido de milho produzidas por uma tecnologia de prototipagem

rápida (Bioplotter®), recentemente proposta para aplicações em Engenharia de Tecidos. Esta metodologia de revestimento é particularmente adequada a estruturas com formas complexas uma vez que o gel de silicato de sódio é capaz de penetrar nos poros e alcançar as suas superfícies interiores. Neste trabalho são originalmente propostas diversas condições de revestimento em regime estático e dinâmico (agitação, e fluxo por perfusão), com o objectivo de produzir revestimentos homogeneamente distribuídos em toda a estrutura de suporte. Para induzir a circulação de fluxo por perfusão foi especialmente desenhado um bioreactor. Através destas metodologias foi possível produzir camadas de apatite semelhantes ao osso (apatite carbonatada exibindo baixa cristalinidade) na superfície exterior e interior das estruturas de suporte, cobrindo toda superfície das fibras sem comprometer a sua porosidade inicial e respectiva interconectividade. A composição, estrutura química e cristalinidade das camadas de apatite formadas em condições estáticas, de agitação e de perfusão não foram significativamente diferentes. No entanto, no caso da perfusão, a espessura do revestimento aumentou consideravelmente. Para além das técnicas de caracterização usuais foi utilizada pela primeira vez a Micro Tomografia Computorizada (Micro-Computed Tomography, μ-CT) para quantificar a porosidade das estruturas de suporte e como nova forma de quantificar a quantidade de apatite formada na superfície das fibras. Através desta técnica foi possível observar, de uma forma não destrutiva, que o interior dos suportes foi efectivamente revestido sem comprometer a sua morfologia e interconectividade. A análise por μ-CT demonstrou de forma clara que a perfusão foi a condição mais eficaz. Para além de mimetizar melhor o ambiente biológico, permitiu revestir estruturas complexas com taxas de formação de revestimento superiores, reduzindo de forma significativa o tempo necessário para revestir estruturas porosas.

A possibilidade funcionalizar uma camada de apatite através da incorporação de agentes bioactivos foi também considerada neste trabalho. Foi possível incorporar nos revestimentos de apatite várias doses de um agente terapêutico da família dos bisfosfonatos (BP) – clodronato de sódio - utilizado no tratamento de diversas patologias relacionadas com o osso ou cálcio tais como a osteoporose, hipercalcémia ou a doença de Paget's. Admite-se que estes revestimentos possam, por exemplo, ser produzidos na superfície de polímeros degradáveis de forma a intervirem directamente na regulação da actividade osteoblática/osteoclástica, induzindo um efeito regenerativo na interface entre o osso e o biomaterial.

O estudo final apresentado nesta tese explora a possibilidade de incorporação de um outro agente terapêutico, o Estrôncio (Sr), na estrutura de revestimentos biomiméticos, preparados por um processo alternativo aplicado a implantes ortopédicos. Acredita-se que a presença localizada de Sr na interface entre um implante e o osso poderá também melhorar a osteointegração e consequentemente assegurar a longevidade de uma prótese ortopédica. Através desta metodologia foi possível incorporar quantidades crescentes de Sr nas camadas de apatite. A incorporação de Sr na estrutura da apatite deu-se através de um mecanismo de substituição. A sua presença teve um efeito inibidor na mineralização, dando origem a uma diminuição na espessura das camadas de Ca-P. Estes revestimentos, ainda que incorporando Sr, apresentaram uma estrutura semelhante ao osso e por isso é esperado que melhorem a formação óssea e a osteointegração.

Os resultados aqui apresentados demonstram o potencial e versatilidade das metodologias biomiméticas propostas como estratégias para melhorar a performance de biomateriais em contextos regenerativos e substitutivos.

TABLE OF CONTENTS

Acknowledgments……iii
Abstract……iv
Resumo……vi
Table of Contents……viii
List of Abbreviations……xiv
List of Figures……xvii
List of Tables……xxii
Short *Curriculum Vitae* ……xxiv
List of Publications……xxv
Introduction to the Thesis Format……xxix

SECTION 1

Chapter I

Part A. Nature-Inspired Calcium Phosphate Coatings: Present Status and Novel Advances in the Science of Mimicry 3
Abstract 3
I.1. Introduction 4
I.2. Biomineralized structures: lessons from Nature 4
I.3. Bone as a material 7
I.4. Ca-P coatings: present status 9
I.5. The biomimetic approach applied to produce Ca-P coatings 11
I.6. Biomimetic Ca-Ps coatings on biodegradable polymers and Tissue Engineering scaffolds 13
I.7. Conclusions 15
References 16

Part B. Bone-Like Apatite Coatings on Biodegradable Polymers as a Way to Induce Bone Mineralization: Current Developments and Future Trends 23
I.1. Introduction 23
I.2. Evolution of the coating methodologies 26
I.3. Bioinspired coatings 27
I.3.1. The biomimetic methodology 28
I.3.2. Other pre-mineralization routes 29
I.4. Coating starch based biodegradable polymers 33
I.4.1. Sodium silicate as a precursor for a Ca-P coating 34

I.4.1.1. Apatite formation 36
I.4.1.2. Cell adhesion 38
I.5. New opportunities for coated materials 38
I.6. Conclusions 39
References 40

SECTION 2

Chapter II

Materials and Methods 49
II.1. Materials 49
III.1.1. Starch based biodegradable polymers 49
II.1.1. Titanium alloy 51
II.1.4. Reagents 51
II.2. Processing routes of starch-based polymers 51
II.2.1. Compact samples 52
II.2.2. Porous 3D architectures 52
II.4. Biomimetic coating methodologies 54
II.4.1. Apatite coatings on biodegradable polymers 54
II.4.2. Apatite coatings on titanum alloy 59
II.5. Incorporation of a therapeutic molecule 61
II.6. Characterization methodologies 63
II.6.2. Surface wettabillity and hydration degree 63
II.6.2.1. Contact angle measurements 63
II.6.2.2. Water-uptake ability 64
II.6.3. Structural and elemental characterization 65
II.6.3.1. Fourier Transform Infrared Spectroscopy (FTIR) 65
II.6.3.2. Thin Film X-Ray Diffraction (TF-XRD) 65
II.6.3.3. Energy Dispersive Spectroscopy (EDS) 65

II.6.4. Morphological characterization 66
II.6.5. Apatite quantification 66
II.6.5. Solution analysis 67
II.6.3.1. Inductively Coupled Plasma Spectroscopy (ICP) 67
II.6.3.2. High Permeation Liquid Chromatography (HPLC) 69
II.6.3.3. Atomic Absorption Spectroscopy (AAS) 70
II.6.3.4. UV-light Spectrophotometry 70
II.6.5. Cell adhesion and proliferation 70
References 71

SECTION 3

Chapter III

Cell Adhesion and Proliferation on Biomimetic Calcium-Phosphate Coatings Produced by a Sodium Silicate Gel Methodology 77
Abstract 77
III. 1. Introduction 78
III.2. Materials and Methods 79
III.2.1. Materials 79
III.2.2. Sodium silicate methodology 80
III.2.3. Water-uptake ability 80
III.2.4. Contact angle measurements 81
III.2.5. Apatite formation 82
III.2.6. Scanning Electron Microscopy (SEM) and Energy Dispersive Spectroscopy (EDS) and X-ray Diffraction (TF-XRD) 83
III.2.7. Cell adhesion and proliferation 84
III.3. Results and Discussion 84
III.3.1. Water-uptake ability 84
III.3.2. Contact angle measurements 85
III.3.3. Apatite formation 86
III.3.4. Cell adhesion and proliferation 89
III.4. Conclusions 91
References 92

Chapter IV

Nucleation and Growth of Biomimetic Apatite Layers on 3D-Plotted Biodegradable Polymeric Scaffolds: Effect of Static and Dynamic Coating Conditions 95
Abstract 95
IV. 1. Introduction 96
IV.2. Materials and Methods 98
IV.2.1. Preparation of the scaffolds 98
IV.2.2. Apatite Coating Formation 99
IV.2.3. Scanning Electron Microscopy (SEM) and Energy Dispersive Spectroscopy (EDS) 101
IV.2.4. X-Ray Diffraction (TF-XRD) 101

IV.2.5. Fourier Transformed Infra-Red (FTIR) 101
IV.2.6. Inductively Coupled Plasma Spectroscopy (ICP) 101
IV.3. Results 102
IV.3.1. Nucleation of the apatite layer 102
IV.3.2. Growing of the apatite layer under static and dynamic conditions 109
IV.4. Discussion 115
IV.5. Conclusions 116
References 117

Chapter V

Micro-Computed Tomography (μ-CT) as a Potential Tool to Assess the Effect of Dynamic Coating Routes on the formation of Biomimetic Apatite Layers on 3D-Plotted Biodegradable Polymeric Scaffold 121

Abstract 121
V.1. Introduction 122
V.2. Materials and Methods 123
V.2.1. Preparation of the scaffolds 123
V.2.2. Apatite Coating Formation 124
V.2.3. Scanning Electron Microscopy (SEM) and Energy Dispersive Spectroscopy (EDS) 126
V.2.4. X-ray Diffraction (TF-XRD) 126
V.2.5. Fourier Transformed Infra-Red (FTIR) 126
V.2.6. Inductively Coupled Plasma Spectroscopy (ICP) 127
V.2.7. Micro-Computed Tomography (μ-CT) 127
V.3. Results and Discussion 127
V.3.1. Stabilization of the apatite layer 127
V.3.2. Growing of the apatite layer under static and dynamic conditions 129
V.3.3. μ-CT evaluation of the coated scaffolds 135
V.4. Conclusions 141
References 142

Chapter VI

Biomimetic Ca-P Coatings Incorporating Bisphosphonates Produced on Starch Based Degradable Biomaterials 145
Abstract 145
VI.1. Introduction 146

VI.2. Materials & Methods 149
VI.2.1. Preparation of the samples 149
VI.2.2. Sodium silicate methodology 149
VI.2.3. Apatite formation 149
VI.2.4. Incorporation of sodium clodronate 150
VI.2.5. Structural characterisation 151
VI.2.6. Mechanical behaviour 151
VI.2.7. Dissolution behaviour 152
VI.2.8. Sodium clodronate Release studies 153
VI.2.9. Cell adhesion and proliferation 154
VI.3. Results & Discussion 155
VI.3.1. Morphology, crystallinity and chemical structure of the apatite coatings 155
VI.3.2. Microhardness tests 159
VI.3.3. Dissolution of Ca and P 160
VI.3.4. Sodium clodronate release profiles 162
VI.3.5. Preliminary cell adhesion and proliferation results 163
VI.4. Discussion 165
VI.5. Conclusions 168
References 168

SECTION 4

Chapter VII

Strontium-Substituted Apatite Coating on Ti6Al4V Through Biomimetic Synthesis 175
Abstract 175
VII.1. Introduction 176
VII.2. Materials and Methods 178
VII.2.1. Materials 178
VII.2.2. Apatite coating formation 178
VII.2.3. Solution analysis 180
VII.2.4. Characterization of the apatite coatings 181
VII.3. Results 181
VII.3.1. Apatite formation: the solution side 181
VII.3.2. Apatite formation: the coating side 182
VII.4. Discussion 188
VII.5. Conclusions 190
References 190

SECTION 5

Chapter VIII

General Conclusions 195
VII.1. Biomimetic Calcium-Phosphate Coatings Produced by a Sodium Silicate Gel Methodology 196
VII.1.2 Influence of the ionic strength of the SBF solution 197
VII.1.3. Effect of Dynamic Conditions on coating the Surface and Bulk of Complex Architectures 197
VII.1.4. Incorporation of a therapeutic molecule: Sodium Clodronate 199
VII.2. Development of a Biomimetic Technology to produce a Strontium-Substituted Apatite Coating 199
V.II.3. Final Remarks and Future work 200
References 203

A

AA	Atomic Absorption Spectroscopy
ACP	Amorphous calcium phosphate
A.U.	Arbitrary Units

B

BMPs	Bone morphogenic proteins
BP	Bisphosphonate

C

Ca-P	Calcium phosphate
CDA	Calcium deficient apatite
CPTi	Commercially pure titanium

D

γ_l^d	Dispersive component
d	Mean diagonal length of the indentation
DCP	Dicalcium phosphate
DCPD	Dicalcium phosphate dihidrate (Brushite)
DMEM	Dulbecco's Modified Eagle's Medium
DR-FTIR	Diffuse Reflectance – Fourier Transformed Infrared

E

EDS	Energy Dispersive Spectroscopy
EDTA	Ethylene diamine tetraacetic acid
EVOH	Ethylene-vinyl alcohol copolymer

F

F	Forçe
FBS	Foetal Bovine Serum
FDM	Fused Deposition Modelling
FTIR - ATR	Fourier Transformed Infra-Red - Attenuated Total Reflectance

H

HA	Hydroxyapatite
HCA	Hydroxy carbonate apatite
HMWPE	High molecular weight polyethylene
HPLC	High Permeation Liquid Chromatography
$\mathbf{H_v}$	Vickers microhardness

I

ICP-OES	Inductively Coupled Plasma Optical Emission Spectroscopy
IP	Ionic activity product

J

JCPDS	Joint Committee for Powder Diffraction Studies

L

LB Langmuir Blodgett

M

M Mass
M Molar
Mg Milligrams
Ml Millilitres
mM Millimolar
µg Micrograms
µl Microliters
µm Micrometers
µ-CT Micro-Computed Tomography analysis
MCP Monocalcium phosphate
MCPM Monocalcium phosphate monohydrate
MPa Mega Pascal
MTS 3-(4,5-Dimethylthiazol-2-yl)-5(3-carboxyme-thonyphenol)-2-(4-sulfophenyl)-2H-tetrazolium

O

OCP Octacalcium phosphate
OD Optical density
OXA Oxyapatite

P

γ_l^p polar component
P Pressure
PA 6,6 Polyamide poly(vinyl alcohol)
PBS Phosphate Buffer Saline
PEO/PBT Polyethylene oxide/polybutylene terephthalate
PES Poly(ethersulfone)
PET Polyethylene terephthalate
pH Potential of Hydrogen
PHA Precipitated Hydroxyapatite
PIC A Tetrabutylammonium Hydrogen Sulphate solution
PLGA Poly(lactide-co-glicolide) copolymer sponge
PLLA poly(L-lactic acid)
PU Polyurethane

Q

Q Volume flow rate

R

RH Relative Humidity
RP Rapid prototyping
R-SBF Revised SBF

S

γ surface tension
SAM Self-Assembled Monolayer
SaOS-2 human osteoblast cell line
SBF Simulated Body Fluid
SCA Starch cellulose acetate
SEM Scanning Electron Microscopy
SEVA-C Starch poly(ethylene vinyl alcohol) blend

SPCL	starch polycaprolactone
Sr	Strontium
T	
3D	Three-dimensional
T	Temperature
TCP	Tricalcium phosphate
TEOS	Tetraethoxysilane
TetCP	Tetracalcium phosphate
TF-XRD	Thin-Film X-Ray Diffraction
Ti-6Al-4V	Titanium–Aluminum (6%wt)–Vanadium (4%wt) alloy
t_R	Residence Time
TRIS	Tris(hydroxymethyl)aminomethane
U	
UV	Ultraviolet irradiation
V	
VOI	Volume of Interest
W	
Wt	Weight

LIST OF FIGURES

SECTION 1

Chapter I

Part B. Bone-Like Apatite Coatings on Biodegradable Polymers as a Way to Induce Bone Mineralization: Current Developments and Future Trends

Figure 1. Schematic representation of the sodium silicate gel biomimetic methodology. Adapted from the procedure developed by Kokubo *et al.*[50,51] and adapted by Reis *et al.* [99,100].....**35**

Figure 2. Water-uptake (%) versus time for untreated and sodium silicate treated compact and porous SEVA-C samples.....**35**

Figure 3. SEM micrographs of: compact SEVA-C treated with a) sodium silicate and after b) 30 days of immersion in SBF and porous SEVA-C treated with c) sodium silicate and after d) 30 days of immersion in SBF.....**36**

Figure 4. Thin-film X-ray diffraction spectra of the films formed after treatment with sodium silicate. a) Compact and b) porous SEVA-C after 0, 15 and 30 days of immersion SBF.....**37**

Figure 5. SEM micrographs showing the morphology of the apatite coatings formed on the surface of SEVA-C and the typical aspect of the SaOs-2 cells adhered to it after 24 h of cell culturing. **38**

SECTION 2

Chapter II
Materials and Methods

Figure 1. Geometry of the produced compact SEVA-C samples: a) standard ASTM tensile test bar, b) disk sample. **52**

Figure 2. 3D Plotting Technology (Bioplotter®) used in the fabrication of SPCL scaffolds (collaboration established with the company EnvisionTec GmbH in the frame of the EU Project Hippocrates). **53**

Figure 3. Geometry of the scaffolds as produced by the 3D plotter technology. **54**

Figure 4. Schematic representation of the sodium silicate gel biomimetic methodology. Adapted from the procedure developed by Kokubo *et al.* [54, 56] and adapted by Reis *et al.* [3, 53]. **56**

Figure 5. Bioreactor designed for coating scaffolds with an apatite layer under flow perfusion. **58**

Figure 6. Possible sizes of the chambers made with disposable syringes. **59**

Figure 7. Schematic drawing of the coating experiments in double-jacked glass reactors.....**61**

Figure 8. Chemical structure of sodium clodronate [74]. **62**

Figure 9. Contact angle on a solid surface (a). interfacial tension at the 3-phase contact line (b).....**64**

Figure 10. HPLC release profiles of sodium clodronate in a) a solution buffered to pH 7.4, b) a solution buffered to pH 3 and c) de-ionized water. **69**

SECTION 3

Chapter III

Cell Adhesion and Proliferation on Biomimetic Calcium-Phosphate Coatings Produced by a Sodium Silicate Gel Methodology

Figure 1. Schematic representation of the sodium silicate gel biomimetic methodology. Adapted from the procedure developed by Kokubo *et al* [13,14] and adapted by Reis *et al* [17,18]. **82**

Figure 2. Water-uptake (%) versus time for untreated and sodium silicate treated SEVA-C samples. **85**

Figure 3. Ca/P and (Ca + Mg + Na + K)/P ratios of the apatites formed on compact SEVA-C substrates, after immersion in SBF 1X and after 7 days in SBF 1.5X or 2.0X. **87**

Figure 4. Thin-film X-ray diffraction patterns of the films formed on SEVA-C after treatment with sodium silicate and after 15 and 30 days of immersion in SBF. In a) the SBF solution was raised to 1.5X after 7 days, while in b) it was raised to 2.0X after the same period. **88**

Figure 5. SEM micrographs showing the morphology of the apatite coatings formed on the surface of SEVA-C and the typical aspect of the SaOS-2 cells adhered to it: a) 1.5X SBF or b) 2.0X SBF. **89**

Figure 6. Proliferation of osteoblast-like cells after culture over the different surfaces: 1.5X SBF for a) 1 day and b) 1 week; and 2.0X SBF for c) 1 day and d) 1 week. **90**

Chapter IV

Nucleation and Growth of Biomimetic Apatite Layers on 3D-Plotted Biodegradable Polymeric Scaffolds: Effect of Static and Dynamic Coating Conditions

Figure 1. Geometry of the scaffolds as produced by the 3D plotter technology. **98**

Figure 2. Schematic drawing of the bioreactor designed for coating an apatite layer under flow perfusion. **100**

Figure 3. SEM micrographs of the scaffolds produced by the Bioplotter® technology. **103**

Figure 4. SEM micrographs of the scaffolds a) treated with sodium silicate and after different periods in SBF: b) 6 and c) 24 hours, d) 2, e) 5 and f) 7 days, showing the evolution of the apatite layer in the nucleation stage. **104**

Figure 5. FTIR spectra of the scaffolds treated with sodium silicate and after different periods in SBF up to 7 days. ◘ -C-O-C-, ◈ C=O, ■ Si-O (stretch), O Si-O-Na (stretch), ✖ Si-O-Si (stretch), ❖ Si-O-Si (bend), ✱ H_2O, ⊙ CO_3^{2-}, ● O-P-O (ν_4, bend), ▲ P-O (bend)◆ P-O (ν_3, stretch). **105**

Figure 6. TF-XRD spectra of the scaffolds treated with sodium silicate and after different periods in SBF up to 7 days. ● main characteristic peaks assigned to hydroxyapatite. **106**

Figure 7. Evolution of the elemental concentration of SBF solution measured by ICP analysis for different periods up to 7 days showing a) the consumption of Ca, P and Mg ions and b) the release of Na and Si ions. **107**

Figure 8. Evolution of the elemental ratios of the obtained apatite layers for different periods up to 7 days. **108**

Figure 9. FTIR (a) and XRD (b) spectra obtained from the analysis of the SPCL scaffolds before and after immersion in SBF for 14 days from which the last 7 days were in static and dynamic conditions. **110**

Figure 10. SEM micrographs of the lateral sides of the scaffolds after immersion in SBF for 14 in a) static, b) agitation and c) flow perfusion. d) Bottom side of the sample c. **112**

Figure 11. Average thickness of the apatite coatings formed during the biomimetic process in static and dynamic conditions (n=6). **113**

Figure 12. Morphology of apatite coatings grown on the bottom side of the SPCL scaffolds after immersion in SBF for 14 days in a) static, b) agitation and c) flow perfusion conditions. d) Apatite coating grown on the upper side of sample in condition b....**114**

Figure 10. SEM micrographs of the lateral sides of the scaffolds after immersion in SBF for 14 in a) static, b) agitation and c) flow perfusion. d) Bottom side of the sample c. **110**

Figure 11. Average thickness of the apatite coatings formed during the biomimetic process in static and dynamic conditions (n=6). **111**

Figure 12. Morphology of apatite coatings grown on the bottom side of the SPCL scaffolds after immersion in SBF for 14 days in a) static, b) agitation and c) flow perfusion conditions. d) Apatite coating grown on the upper side of sample in condition b....**112**

Chapter V

Micro-Computed Tomography (µ-CT) as a Potential Tool to Assess the Effect of Dynamic Coating Routes on the formation of Biomimetic Apatite Layers on 3D-Plotted Biodegradable Polymeric Scaffold

Figure 1. Schematic drawing of the bioreactor designed for coating an apatite layer under flow perfusion. **125**

Figure 2. SEM micrographs of SPCL scaffolds a), b) as processed and c), d), e) f) after growing a biomimetic apatite layer for 7 days in SBF. **128**

Figure 3. FTIR spectra obtained from the analysis of apatite layers after immersion in SBF for 21 days from which 14 days under static and dynamic conditions. All the spectra were obtained from the same side of the scaffold. **129**

Figure 4. TF-XRD spectra obtained from the analysis of the SPCL scaffolds before and after immersion in SBF for a) 14 and 21 days in static and dynamic conditions. **130**

Figure 5. SEM micrographs of the coated lateral sides of the scaffolds after immersion in SBF in static (a,b), agitation (c,d) and flow perfusion (e,f) conditions for 14 (a, c, e) and 21 (b, d, f) days. **132**

Figure 6. SEM micrographs of the cross-sections of a fibre in the middle of the scaffolds after immersion in SBF in static (a,b), agitation (c,d) and flow perfusion (e,f) conditions for 14 (a, c, e) and 21 (b, d, f) days....**133**

Figure 7. Average thickness of the apatite coatings formed during the biomimetic process in static and dynamic conditions, measured by SEM analysis. **134**

Figure 8. *In vitro* apatite coating progress in the scaffolds measured by µ-CT as function of time and test conditions. **136**

Figure 9. SPCL porosity profile (---) and apatite content distribution (—) along the scaffolds after 21 days period as function of test condition. **137**

Figure 10. Selected volume of interest (VOI) of the central and inner area of the scaffolds. This selection was applied for all the scanned scaffolds....**138**

Figure 11. 2D X-Ray, 2D binary images and 3D models for the apatite coatings obtained for 21 days as function of static and dynamic conditions. **139**

Chapter VI

Biomimetic Ca-P Coatings Incorporating Bisphosphonates Produced on Starch Based Degradable Biomaterials

Figure 1. Chemical structure of sodium clodronate **150**

Figure 2. HPLC release profiles of sodium clodronate in a) a solution buffered to pH 7.4, b) a solution buffered to pH 3. ..... **153**

Figure 3. SEM micrographs performed on the apatite coatings grown on the surface of SEVA-C samples a), b) before and c), d) after the treatment with 8 mg/mL of sodium clodronate. **155**

Figure 4. EDS spectra showing the evolution of the elemental composition of the apatite layers with increasing doses of sodium clodronate. **156**

Figure 5. FTIR-ATR spectra of SEVA-C before and after forming an apatite layer and after the incorporation of 8 and 16 mg/mL of sodium clodronate. Sodium clodronate powder was used as reference. **157**

Figure 6. TF-XRD spectra of SEVA-C before and after forming an apatite layer and after the incorporation of 8 and 16 mg/mL of sodium clodronate. Sodium clodronate powder was used as reference. ✱ SEVA-C; ● Apatite; ▲ Sodium clodronate. **158**

Figure 7. Microhardness of the samples with different concentrations of sodium clodronate in the CaP coatings. The continuous line represents the average corresponding to the microhardness at the level of the bulk substrate (uncoated sample). **159**

Figure 8. Dissolution profile of Ca and P in a standard solutions buffered at a), b) at pH 7.4 and c),d) at pH 3. ..... **160**

Figure 9. Calibration curves of sodium clodronate and respective release profiles in a) a solution buffered at pH 7.4 and b) a solution buffered at pH 3. ..... **162**

Figure 10. SEM micrographs after 3 days in culture of Osteoblasts Cells (SaOs-2): a), b) SEM micrographs showing the osteoblasts adhesion onto surfaces of apatite coatings material without incorporation of Sodium Clodronate; c), d) SEM micrographs showing the osteoblasts adhesion onto surfaces of apatite coatings material with incorporation of Sodium Clodronate at 0,064 mg/mL and 0,32 mg/mL respectively. **163**

Figure 11. Quantification of the a) cell viability, b) protein quantification and c) ALP expression after different periods of culture on apatite coatings as function of sodium clodronate content. **164**

SECTION 4

Chapter VII

Strontium-Substituted Apatite Coating on Ti6Al4V Through Biomimetic Synthesis

Figure 1. Schematic drawing of the coating experiments in double-jacked glass reactors. **179**

Figure 2. Evolution of Ca, P and Sr composition of the different solutions during the coating process: a) solution in the absence of Sr and with b) 0.5 , c) 1.0 and d) 1.5 mg/mL of Sr. **181**

Figure 3. Morphologies of the apatite coatings formed after 7 days in the solutions containing: a) 0, b) 0.5, c) 1.0 and d) 1.5 mM of Sr, concerning a polished sample. **182**

Figure 4. Morphology and thickness of the apatite layers formed on polished (a,c,e,g) and grit-blasted (b,d,f,h) surfaces after 7 days in SBF containing increasing amounts of Sr in solution: 0 mM (a, b), 0.5 mM (c, d), 1.0 mM (e, f), 1.5 mM (g, h). **183**

Figure 5. Average thickness of the apatite layers formed in solutions containing increasing amounts of Sr.....**184**

Figure 6. Typical EDS spectra obtained for the formed Sr-apatite layers after 7 days of the coating process.....**185**

Figure 7. DR-FTIR of the apatite coatings formed in the solutions containing increasing concentrations of Sr.....**185**

Figure 8. TF-XRD of the apatite coatings formed in the solutions containing increasing concentrations of Sr.....**186**

Figure 9. Detail of the XRD peaks assigned to the (002) lattice plane indicating a shift to the left on coatings formed in solutions with increasing Sr.....**186**

SECTION 5

Chapter VIII

General Conclusions

Figure 1. New bioreactor including the cyclic inversion of the flow.....**199**

LIST OF TABLES

SECTION 1

Chapter I

Part B. Bone-Like Apatite Coatings on Biodegradable Polymers as a Way to Induce Bone Mineralization: Current Developments and Future Trends

Table 1. Main calcium phosphate compounds. Compiled from references [6-8]. **24**

SECTION 2

Chapter II
Materials and Methods

Table 1. Composition of Ti-6Al-4V used for the fabrication of bone-replacement implants [39]..... **51**

Table 2. Processing conditions to obtain the tensile bars and disks. **52**

Table 3. Ion concentrations and Ionic Activity Products (IP) of the human blood plasma and SBF solutions in the present study [55]..... **55**

Table 4. Static and dynamic conditions for coating apatite layers on the SPCL scaffolds. **57**

Table 5. Ionic concentration of the prepared solutions for coating Ti4AL6V. **60**

Table 6. Polar (γ_l^p) and disperse (γ_l^d) components of the water and the methylene iodide [76]. **64**

Table 7. Solutions used in the dissolution studies. **68**

SECTION 3

Chapter III
Cell Adhesion and Proliferation on Biomimetic Calcium-Phosphate Coatings Produced by a Sodium Silicate Gel Methodology

Table 1. Static and dynamic conditions for coating apatite layers on the SPCL scaffolds. **100**

Table 2. Variation of the elemental concentration of the solution from 7 to 14 days (mM/L) calculated from the ICP measured values. **110**

Table 3. Ca/P, (Ca+Na+Mg+K)/P, Mg/Ca and Na/Ca ratios calculated from the dissolved apatite layers after the biomimetic coating in static and dynamic conditions after 14 days of immersion in SBF..... **111**

Chapter IV

Nucleation and Growth of Biomimetic Apatite Layers on 3D-Plotted Biodegradable Polymeric Scaffolds: Effect of Static and Dynamic Coating Conditions

Table 1. Static and dynamic conditions for coating apatite layers on the SPCL scaffolds. **98**

Table 2. Variation of the elemental concentration of the solution from 7 to 14 days (mM/L) calculated from the ICP measured values. **108**

Table 3. Ca/P, (Ca+Na+Mg+K)/P, Mg/Ca and Na/Ca ratios calculated from the dissolved apatite layers after the biomimetic coating in static and dynamic conditions after 14 days of immersion in SBF.....**109**

Chapter V

Micro-Computed Tomography (μ-CT) as a Potential Tool to Assess the Effect of Dynamic Coating Routes on the formation of Biomimetic Apatite Layers on 3D-Plotted Biodegradable Polymeric Scaffold

Table 1. Static and dynamic conditions for coating apatite layers on the SPCL scaffolds. **125**

Chapter VI

Biomimetic Ca-P Coatings Incorporating Bisphosphonates Produced on Starch Based Degradable Biomaterials

Table 1. Solutions used in the dissolution studies. **152**

SHORT CURRICULUM VITAE

Ana L. Oliveira was born in 1974 in Porto, Portugal. She presently lives in Matosinhos and works, as a researcher, in the 3B's Research Group (Biomaterials, Biodegradables and Biomimetics), University of Minho, Portugal, under the supervision of Prof. Rui L. Reis.

Her background includes a five-year graduation in Metallurgical and Materials Science. During the final year of her graduation she developed two important works of initiation to scientific research on the general topic of "Biodegradable Polymers for Biomedical Applications", both oriented by Prof. Rui L. Reis at the University of Porto, Portugal.

In 1998 she was invited to help starting a new biomaterials group at the University of Minho known today as the 3B's Research Group, under the Direction of Prof. Rui Reis. She was accepted in the Master Degree on Materials Science Engineering at the University of Minho, in September 1999 and defended it in March 2002. Between October 2001 and January 2002 she was lecturing in the Polytechnic Institute of Engineering in Porto (ISEP), where she has taught the course of Materials Chemistry. In April 2002 she accepted an invitation to start her PhD in collaboration with the Bioceramic Group at Depuy Orthopaedics, a Johnson & Johnson company. She worked from April to December in a project in this company, co-supervised by Dr. Panjian Li. In January 2003 she was awarded with a grant from the Fundação para a Ciência e a Tecnologia (FCT) for continuing with her PhD at the facilities of 3B's Research Group and in the Consejo Superior de Investigaciones Cientificas (CSIC) – Institute for Science and Technology of Polymers, co-oriented by Prof. Julio S. Román.

As a researcher of the 3B's Research Group she has been involved in the supervision of senior research projects of undergraduate students, as well as in the organization of two NATO/ASI meetings, one in Tissue Engineering (2001) and another in Biomineralization (2003), and several Marie Curie Training Actions.

Ana L. Oliveira has also been involved in the preparation of several grant proposals, both at the National (Portuguese Foundation for Science and Technology) and European levels (frameworks V, VI and VII), including the only Tissue Engineering Network of Excellence of Europe, EXPERTISSUES, as well as other EU-funded projects, such as HIPPOCRATES and also ALEA JACTA EST, a Marie Curie Multi-Site Early Stage Training program.

As a result of her research work she attended several of the most important international meetings in her present field of research with more than 30 works of her authorship most being presented orally. In 2006 she was awarded with a Student Travel Achievement Recognition by The Society for Biomaterials to the work she presented at the 31st Annual Meeting of the Society from Biomaterials, Pittsburgh, "as an outstanding contribution to the Society For Biomaterials". Presently she is the author of 12 papers in international refereed journals (10 published, 2 submitted), 9 book chapters and 33 abstracts published in international conference proceedings.

LIST OF PUBLICATIONS

This thesis is based on the following publications:

International Journals with referee

A. L. Oliveira, J. F. Mano, R. L. Reis, “Nature-Inspired Calcium Phosphate Coatings: Present Status and Novel Advances In The Science Of Mimicry”, Current Opinion On Solid State & Materials Science, 7/4-5, 2003, 309-318.

A. L. Oliveira, C. M. Alves, R. L. Reis, “Cell adhesion and proliferation on biomimetic calcium-phosphate coatings produced by a sodium silicate gel methodology”, Journal of Materials Science: Materials in Medicine, 12, 2002, 1181-1188, invited paper.

A.L. Oliveira, S.A. Costa, R.A. Sousa, R.L. Reis, Nucleation and Growth of Biomimetic Apatite Layers on 3D-Plotted Biodegradable Polymeric Scaffolds: Effect of Static and Dynamic Coating Conditions, Biomaterials, 2007, submitted.

A.L. Oliveira, P. B. Malafaya, S.A. Costa, R.A. Sousa, R.L. Reis, “Micro-Computed Tomography (μ-CT) as a Potential Tool to Assess the Effect of Dynamic Coating Routes on the formation of Biomimetic Apatite Layers on 3D-Plotted Biodegradable Polymeric Scaffolds”, Journal of Materials Science: Materials in Medicine, 18(2), 2007, 211-223.

AL Oliveira, AJ Pedro, C Saiz Arroyo, JF Mano, G Rodriguez, J San Roman and RL Reis, “Biomimetic Ca-P Coatings Incorporating Bisphosphonates Produced on Starch Based Degradable Biomaterials”, Journal of Biomedical Materials Research Part A, 2007, submitted.

A.L. Oliveira, P. Li, R.L. Reis, Strontium-Substituted Apatite Coating Grown on TI6AL4V Substrate through Biomimetic Synthesis, Journal of Biomedical Materials Research. Part B: Applied Biomaterials, 1552-4973 (US Patent 6,569,489).

Book chapters

A. L. Oliveira, I. B. Leonor, C. Elvira, M. C. Azevedo, I. Pashkuleva, R. L. Reis, “Surface Treatments and Pre-calcification Routes to Enhance Cell Adhesion and Proliferation”, Ed. R. L. Reis and D. Cohn, in “Polymer Based Systems on Tissue Engineering, Replacement and Regeneration”, Eds. R. L. Reis and D. Cohn, NATO/ASI Series, Kluwer Press, Drodercht, (2002), 183-217, invited chapter.

A. L. Oliveira, I. B. Leonor, P. B. Malafaya, C. M. Alves, H. S. Azevedo, R. L. Reis, “Tailoring the bioactivity of natural origin based polymers systems: from bone-analogue composites to an all range of biomimetic calcium-phosphate coating methodologies”, in: Bioceramics 15, Sidney, Australia, Eds. B Ben-Nissan, D Sher, W Walsh, Trans Tech Pub, Zurich, (2002), 111-142, invited chapter.

I.B. Leonor, A.L. Oliveira, R.L. Reis, “Recubrimientos biomimeticos”, in Biomateriales, Ed. Sastre R., de Aza S. and San Román J., Faenza Editrice, Ibérica S.L., Italy, (2003), 307-322.

I. B. Leonor, H. S. Azevedo, I. Pashkuleva, A. L. Oliveira, C. M. Alves, R. L. Reis, “Learning From Nature How To Design Biomimetic Calcium-Phosphate Coatings”, in Learning from Nature How to Design New Implantable Biomaterials: From Biomineralization Fundamentals to Biomimetic Materials and Processing Routes, Eds. R. L. Reis and S. Weiner, NATO/ASI Series, Kluwer Press, Drodercht, (2004), 123-150.

A. L. Oliveira, R. L. Reis, “Bone-Like Apatite Coatings Nucleated on Biodegradable Polymers as a Way to Induce Bone Mineralization: Current Developments and Future Trends” in: Biodegradable Systems in Medical Functions: Design, Processing, Testing and Applications, Ed. Rui L. Reis, Julio San Roman, CRC Press, Boca Raton, USA, (2004), 205-221.

A. L. Oliveira, M. I. Santos, A. A. Pedro and R. L. Reis, “Bisphosphonates Incorporated on a Ca-P Biomimetic Coating Produced by a Sodium Silicate Based Methodology Stimulate Osteoblastic Activity”, in: Bioceramics 17, New Orleans, USA, Ed. Panjian Li, Trans. Tec. Publications, Zurich, (2004), 615-618.

A.L. Oliveira, R.L. Reis, P. Li, “Biomimetic Synthesis of a Strontium-Substituted Apatite Coating Grown on Ti6Al4V Substrate”, in: Bioceramics 19, Chengdu, China, Ed. Xingdong Zhang, Xudong Li, Hongsong Fan, Xuanyong Liu, Trans. Tec. Publications, Zurich, (2007), 558-588.

Communications in international meetings

A. L. Oliveira, P. B. Malafaya, M. E. Gomes, R. L. Reis, Biomimetic Strategies for Producing Calcium-Phosphate Coatings on Porous Biodegradable Polymeric Scaffolds, 28th Annual Meeting of the Society from Biomaterials, Tampa, Florida, (2002), 635, poster.

A. L. Oliveira, C. M. Alves, R. L. Reis, "Cell Adhesion and Proliferation on Biomimetic Calcium-Phosphate Coatings Produced by a Sodium Silicate Gel Methodology", 17th European Conference on Biomaterials, Barcelona, Spain, (2002), T82, oral presentation.

A. L. Oliveira, I. B. Leonor, P. B. Malafaya, C. M. Alves, H. S. Azevedo, R. L. Reis, "Tailoring the bioactivity of natural origin based polymers systems: from bone-analogue composites to an all range of biomimetic calcium-phosphate coating methodologies", Bioceramics 15, Sidney, Australia, December, (2002), 111-142, invited lecture.

A. L. Oliveira, R. L. Reis, "Strategies for Developing Natural Origin Materials for Biomedical Applications", Workshop on "Perspectives in Marine Bioadhesives Engineering: Mimicking Marine Bioadhesives towards Novel Applications", Brussels, Belgium, September (2003), oral presentation.

A. L. Oliveira, C. M. Alves, M. E. Gomes, P. B. Malafaya, R. L. Reis, "Silicate Gels as Precursors of Biomimetic Mineralization on Degradable Polymeric Scaffolds", NATO/ASI- Advanced Study Institute course on "Learning from Nature How to Design New Implantable Biomaterials: From Biomineralization Fundamentals to Biomimetic Materials and Processing Routes", Alvor, Portugal, October (2003), 31, oral presentation.

A. L. Oliveira, R. L. Reis, "Biomimetic Strategies for the Pre-Mineralization of Porous Biodegradable Polymeric Scaffolds with a Bone-Like Apatite Layer", 12th Annual POLYCHAR World Forum on Advanced Materials, Guimarães, Portugal, January (2004), poster.

A. L. Oliveira, C. M. Alves, R. L. Reis, "Biomimetic Routes for Inducing In Vitro Biomineralization on Starch-Based Polymeric Structures for Bone-Related Applications", XVIIth Aachen Colloquium on Biomaterials, Aachen, Germany, March (2004), p. 22, oral presentation.

A. L. Oliveira, M. I. Santos, O. P. Coutinho, R. L. Reis, Biomimetic Coatings Incorporating Bisphosphonates Aiming to Inhibit Bone Resorption, 7th World Biomaterial Congress, Sydney, Australia, May (2004), p. 325, oral presentation.

A. L. Oliveira, M. I. Santos, A. A. Pedro and R. L. Reis, "Bisphosphonates Incorporated on a Ca-P Biomimetic Coating Produced by a Sodium Silicate Based Methodology Stimulate Osteoblastic Activity", Bioceramics 17, New Orleans, USA, December (2004), oral presentation.

A. L. Oliveira, A. J. Pedro, C. Saiz Arroyo, J. F. Mano, G. Rodriguez, J. San Roman and RL Reis, "Biomimetic Ca-P Coatings Incorporating Bisphosphonates Produced on Starch Based Degradable Biomaterials", 19th European Conference on Biomaterials, Sorrento, Italy, (2005), poster presentation.

A. L. Oliveira, J. F. Mano, C. Saiz Arroyo, G. Rodriguez, J. San Roman and RL Reis, “Structure and Stability of Ca-P Biomimetic Coatings Incorporating a Bisphosphonate”, Frontiers in Biomedical Polymers, Granada, Spain, (2005), oral presentation.

A. L. Oliveira, S. A. Costa, R. A. Sousa, R. L. Reis, “Studies on the Formation of Biomimetic Apatite Layers on 3D-Printed Biodegradable Polymeric Scaffolds: Effect of Different Dynamic Coating Routes”, 2006 Annual Meeting of the Society from Biomaterials, Pittsburgh, US, (2006), oral presentation.

A. L. Oliveira, S. A. Costa, R. A. Sousa, R. L. Reis, “Static and Dynamic Coating Routes and its Influence on the Kinetics for Biomimetic Apatite Formation on 3D-Plotted Biodegradable Polymeric Scaffolds:”, 1st Marie Curie Cutting Edge Conference on New developments on polymers for tissue engineering: replacement and regeneration, Funchal, Madeira, Portugal, (2006), oral presentation

AL Oliveira, RA Sousa, PB Malafaya, SA Costa, RL Reis, “μ-CT a Valuable Tool to Study the Effect of Dynamic Coating Routes on the formation of Biomimetic Apatite Layers on 3D-Plotted Biodegradable Polymeric Scaffolds”, 20th European Conference on Biomaterials, Nantes, France, (2006), oral presentation.

A. L. Oliveira , S. A. Costa, R.A. Sousa and R. L. Reis. "Static and Dynamic Coating Routes and its Influence on the Kinetics for Biomimetic Apatite Formation on 3D-Plotted Biodegradable Polymeric Scaffolds", 1st Marie Curie Cutting Edge Conference on New developments on polymers for tissue engineering: replacement and regeneration, Funchal (Madeira), Portugal, (2006), oral presentation.

INTRODUCTION TO THE THESIS FORMAT

This thesis is divided in five sections containing nine different chapters, with six of them being experimental research. The contents of each are summarized bellow.

Section 1 (*Chapter I*) presents an extensive overview on the several aspects behind the concept of biomimetic mineralization and its application for the development of improved bone analogue materials. Chapter I starts by driving the attention to the importance of Nature as an inspirational source to develop calcium phosphate coatings similar to bone apatite. A review of the literature on the recently emerged coating methodologies is presented, revealing the importance of this strategy to enhance the interface bone-implant. At the same time the obstacles found in the different proposed coating methodologies are discussed and have constituted the basis for proposing more natural and simplified approaches for producing Ca-Ps coatings by novel biomimetic methodologies. The second part of the introduction presents once again the history and principles of biomimetic technology but extends its scope to the introduction of an innovative biomimetic approach based on sodium silicate, which has constituted the starting point of this dissertation. The emerging opportunities of this strategy, namely in the field of tissue engineering are also discussed, envisioning biomimetic coatings as carriers for the delivery of bioactive molecules towards bone regeneration. **Section 2** (*Chapter II*) presents in detail the materials and experimental procedures used for the development and characterization of the proposed biomimetic coating routes. In **Section 3** (*Chapters III, IV, V, VI*) are presented different studies that explore the proposed biomimetic methodology for producing tailored Ca-P layers on the surface of biodegradable starch-based biomaterials. In Chapter III, the effect of the solution concentration on the resulting apatite layers is evaluated, while in Chapters IV and V a different concept is proposed by means of originally introducing dynamic conditions to the biomimetic process aiming at specific applications in complex shaped 3D arquitectures for bone Tissue Engineering. In chapter VI, the possibility of including a therapeutic function to the produced apatite layers is also explored by incorporating a Bisphosphonate, a well known bone resorption inhibitor. The research work presented In **Section 4** (*Chapter VII*) although connected with the above-described studies by the concept of biomimetics, is a rather different study which have resulted from collaboration with the company DePuy Orthopaedics, Inc. In this study an alternative coating technology for producing biomimetic apatite layers is proposed, in which a therapeutic effect is envisioned by incorporating Strontium into its structure. The challenge was also to design a biomimetic process able to be scaled up for further industrialization and easy commercialization. Finally, **Section 5** (*Chapter VIII*) contains the general conclusions regarding the overall work carried out under the scope of this thesis, as well as some final remarks and future directions.

SECTION 1.

CHAPTER I

Chapter I

Calcium Phosphate Coatings: Form Man-made to Man-like

Part A. Nature-Inspired Calcium Phosphate Coatings: Present Status and Novel Advances in the Science of Mimicry*

Abstract

There has been a growing awareness in materials science that the adaptation of nature biological processes can lead to significant progresses in the controlled fabrication of advanced materials for an all range of applications. To learn from, understand and apply these natural processes for producing calcium phosphate coatings that are biologically similar to bone apatite, mimicking its properties, has driven the attention of many researchers in recent years.

This article reviews the most relevant advances in this emerging research field, pointing out several approaches being introduced and explored by distinct laboratories.

*This part of the chapter is based on the following publication:

A. L. Oliveira, J. F. Mano, R. L. Reis, "Nature-Inspired Calcium Phosphate Coatings: Present Status and Novel Advances in the Science of Mimicry", Current Opinion on Solid State & Materials Science, 7/4-5, 2003, 309-318.

I.1. Introduction

The present overview is intended to draw the attention of the readers to the processes by which mineralized tissues are formed. The main aim is to provide useful information that can be applied as a source of inspiration for the development of new materials to be used in the biomedical field, particularly in bone-related applications. That is the rational for searching materials capable of mimicking the living tissues, i.e. the so-called biomimetic materials. In the case of bone replacement innovative ideas can be generated by means of studying the mineralized tissues found in Nature. The main research question in this field is: if the basic strategies by which living organisms produce mineralized tissues are understood, how might these principles be exploited for the development of new biomaterials? If biomimetic is interpreted as the reproduction of the entire sequence of biomineralization steps, it is then clear that any developed process would be extremely complex and would lead to unbearable costs. Moreover, it must be understood that is not possible to compete with thousands of million years of Nature's "research work"! A less literal use of the term biomimetic should then be applied. If a materials scientist can be inspired by a biological prototype to apply its principles to his research area, then a biomimetic result can be achieved. At the moment lessons from Nature are already being taken, leading to the creation of new biomaterials and methodologies, particularly those that are able to stimulate the tissues for eliciting specific responses at the interface with bone, in order to create a continuous transition from tissue to implant material. Nevertheless, there is still much to be studied and understood and the potential of biomimetics is still not really being put to work for engineering better biomedical systems. This review will discuss some lessons that can be obtained from Nature in order to improve bone-related implants and tissue engineering scaffolds by means of developing adequate biomimetic coating routes.

I.2. Biomineralized structures: lessons from Nature

The traditional design of materials has been mainly motivated by basic concepts of Chemistry (choice of the type of material to be used – polymer, ceramic, metal, composite…; surface modifications; decoration with specific chemical groups), along with

some input from physics (e.g. for electronic, electrical or optical applications) and engineering (processing and macrostructure design, that should include internal size control from nano- to macro- dimensions). Nevertheless, there has been an increasing interest in the study of biological systems that could inspire the conception of new and better materials with tailored/engineered properties. The hypothesis is that materials in Nature should have been continuously improving their performance under evolutionary pressures in both design and function, since the appearance of life on Earth. As a trivial and straightforward example, Aramides, such as Kevlar®, are synthetic polyamides that are the gold standard in the production of high strength and modulus and low weight polymeric fibres for a variety of structural applications (ballistic and defence protection, high performance cables and ropes…). Their processing involves the use of sulphuric acid as the solvent and both high temperatures and pressures. It is interesting to compare such processing conditions with those of natural spider silk that is produced under aqueous solution (pH near 7) at both atmospheric temperature and pressure, and exhibits an even higher toughness than Kevlar® [1]. In the particular case of Biological hard tissues (such as bones, shells, teeth or spicules), there is the formation of hierarchical structures with complex architecture from the nanometre to the millimetre scales, combining minerals, structural biological polymers (proteins and polysaccharides) and lipids [2,3]; under the correct genetic control of the shape and pattern in time and space, the biocomposites are produced with minimum energy costs using an environmentally friendly biomineralization synthesis pathway. The resulting tissue tends to optimise its function, and often its multifunctions, preferentially minimizing the amount of materials required. Moreover, biological materials are also “smart” as they adapt internally to external events, which includes their “self-repairing” ability. Biomineralized structures exist in all five kingdoms of organisms and the functions are very diverse, including mainly structural and load-bearing purposes (e.g. bone, mollusc shells, teeth) but also sound reception, optical, magnetic and gravity sensing and temporary storage of ions or rejection of wastes [2,3]. In terms of length scale we can find structures that can go from single ~50 nm magnetite crystals, acting as magnetic domains in magnetotactic bacteria monitoring the Earth’s magnetic field [4], up to the huge molars of elephants made of ivory [5]. Such systems also cover a considerable range of organic component weight fraction that can go from 0.1% in cross lamellar shells and echinoderm calcite up to about 20% in bone [6]. One also finds a variety of morphological diversity and complexity in biological minerals (often exhibiting no resemblance to their inorganic counterparts), even for a common function [7]. And this is built using a limited number of mineral possibilities (including amorphous minerals and both inorganic and organic crystals [6,8]), where only a few minerals are the main component of endo- and exo-skeletons [9]. It should also be noted that none of such

minerals have, by themselves, particular outstanding characteristics – again, their success is the way they are assembled together with the organic phase. Among such biogenic minerals, calcium is present in some 50% of them [2]. This reflects both the natural abundance of this metal in the oceans and its importance as the cell's messenger (due to its efficient transport throughout the cell by membrane pumps) [2]. The two major calcium compounds that are found are calcium carbonate, appearing mainly in shells of marine creatures and eggshells, and calcium phosphate, e.g. in bone and dentin in vertebrates. In the former case, three main polymorphs are found (calcite, aragonite and vaterite), and among them, different shapes may be found [2,10]. An interesting study by Chateigner et al. [8] tried to systematise the great variety of crystallographic textures in shells from monoplacophoras, bivalves, cephalopods and gastropods. A good example occurs in shells of bivalves that exhibit two layers of differently shaped aragonite crystals, neither of them being similar to the crystals formed inorganically [2]. This is due to the precise calcium-binding sites that are dictated by the structure of the nucleating proteins (negatively charged, interacting electrostatically with the calcium ions), which are glycoproteins rich in aspartic acid, possibly with a β-sheet structure [2,10]. Such stereochemical self-assembled templates will control both the nucleation and the growth of the inorganic precipitation reactions, determining the final size, shape and orientation of the formed crystalline structure [11]. These "control macromolecules" [10] are usually the minor macromolecular component of a biological material, being intimately attached to the mineral phase; they are, in fact, difficult to extract or degrade without dissolving the mineral [10]. It is interesting to notice in this context that such acidic soluble proteins inhibit crystallization in solution, as rigidity and regularity is then lost. This is related with the way Nature controls the biomineralization process: minerals formed in organisms require a precise isolation in space [2], either delineated by macromolecular matrix frameworks (providing a 3D matrix for crystal formation and a substrate for the interaction between the control macromolecules and the mineral phase [10]), or else by confinement from cell membranes or vesicles [2,3]. These evidences suggest that analogous synthetic templates could be used in the production of tailor-made mineral structures. As described by Green et al. [12], surfactant micelles, lipid microstructures, and stacked bacterial filaments have been proposed to control precipitation and growth of inorganic minerals such as silica and iron oxides. In that particular work, an analysis is made where chemical and biological concepts of self-assembling and self-organization found in natural porous skeletons can be used in the development of bone-analogue structures for hard tissue engineering [12]. It should also be noticed in this context that apparently different biomineralized structures can exhibit physiological compatibility [13]. A good example is the bone-conductive properties of shells. For instance, implantation of nacre powder in

jawbone promotes osteoblasts activation and bone formation, with no inflammatory response [13]. However, no definitive explanation for this behaviour is really known, although the authors claim [13], for example, a matching between the nacre and bone organic matrices. These facts can be also in accordance with the ability of gastropod nacre to be converted hydrothermally into hydroxyapatite (the inorganic – calcium phosphate - component of bone) [14].

I.3. Bone as a material

As this review focuses on biomimetic mineralization, mainly aiming to find better ways for increasing the biocompatibility and the performance of biomaterials used in bone related applications (filling bone defects, fixation, bone tissue engineering scaffolding, etc.), one should look in more detail at relevant aspects of the structure and mineralization in bone. Properties of bone have been widely studied. It has been known for a long time that this material has multi-functional properties, which include structural support, protection and storage of healing cells, and mineral ion homeostasis [15]. The “material bone” should be understood herein as a family of materials built up of mineralised collagen fibrils. The structure of bone and its relation with the mechanical properties are very well discussed elsewhere [15,16]. Collagen is the “framework macromolecule” in bone, in contrast with the Gly- and Ala-rich proteins in mollusc shells [10]. Although many more protein exist in bone (e.g. phosphoproteins, that have an important role in the biomineralization process), collagen is the main component of the 3D matrix into which (or onto which) the hydroxylapatite ($Ca_{10}(PO_4)_6(OH)_2$) is deposited, in the form of thin plates with 50x25 nm of length and width and with 2-3 nm thickness [16,17]. In the lowest level of bone organization, type-I collagen is self-assembled into fibrils. First collagen peptides are assembled into the cells; however, further assembly into bundles occurs in the extracellular medium [18]. Collagen molecules in fibrils appear with 1.5 nm thick (thickness of one triple-helical molecule), 300 nm length and 40 nm gaps or holes between the ends [16]. The apatite crystals are nucleated at specific regions on or within the collagen fibrils [19]. They grow in the hole zones (channels) and in later stages they penetrate into the overlap zones that exists between neighbouring collagen molecules [16,20]. This compresses the triple-helical collagen framework, diminishing the average distance between collagen molecules from 1.5 to 1.2 nm with crystal growth [2]. Such highly anisotropic fibrils are then arranged in higher order organizations. In lamellar bone, there are parallel arrays of fibrils, with crystals aligned (sub-layers). The consecutive sub-

layers rotate though the lamellar plane by an average of 30º, forming a so-called plywood-like structure [12]. As each lamella is composed of 5 sub-layers, the total rotation is 150 º, thus forming an asymmetric structure. Moreover, the collagen fibril bundles rotate around their axis within the five sub-layers. These two events reduce strongly the macroscopic anisotropy of bone. This tendency, that is found in lamellar bone, seems to be general in Nature. Weiner et al. [6] presented several examples in which organisms use different strategies to reduce anisotropy in biomineralized structures. Lessons such as these may be useful to design better materials that will substitute or be in contact with living tissues. For instance, biomimetic coatings have been developed in order to be functionally efficient, being produced using an environmental benign process [21]. This leads to new technological materials that can be used in bone repair. Up to now, as it will be seen in this review, we are still in the stage of engineering the substrate surfaces using more or less complex Chemical and Physical methods. For example, important contributions have been resulting from the works of Mann *et al.* [22,23], that achieved the orientation of the crystallisation of calcium carbonate from homocharge cation layers in supersaturated $CaCO_3$ solutions. Also, calcite nucleation could be obtained in polystyrene substrates decorated with sulfonate and carboxylate moieties [24], which corresponds to a nice model of the mineralization occurring in molluscs [11]. A nucleating matrix isolated from Abalone shells also induced the formation of aragonite, when proteins also extracted from Abalone shell were added to it [25]. Despite such nice results, the nucleation mechanism involved in-vitro (and of course in-vivo) is far from being understood.

It will then be always very difficult to mimic exactly the calcification process that occurs in bone. This is further complicated as all mineralization processes are ultimately controlled through the cells directly associated to the tissue formation [26]. Nevertheless, the great understanding that currently exists of bone biology may provide key concepts that may be adapted within a synthetic context. As done with the calcium carbonate mineralization studies, a step further would be to control the precipitation of the minerals using templates of biomineralization proteins for the control of crystal organization and properties. This would allow enhancement of the biological activity with the bone/cartilage mineral structure for bone cell adhesion, alignment, spreading and differentiation. This is of course not an easy task, as the extraction of such macromolecules directly from the natural composites involves complex procedures such as protein isolation and purification, amino acid analysis and sequencing [27]; the use of similar existing proteins is also inefficient as the binding to the inorganic surfaces is non-specific. As discussed by Sarikaya [27], a better solution would be the molecular design of recombinant proteins via genetic engineering techniques. As in other biomimetic strategies, the conventional engineering and chemical approach must gradually be substituted by endeavours in areas such as

genetics, proteonics and nano-technologies, i.e., to learn how to use the same tools of the living organisms. This would include the mastering of molecular and supra-molecular organization (self-assembling). This area has having an increasing interest in many fields [28-30], and includes, for example, the production of electronic devices [29] or micro-patterning of single crystals [30] using biomimetic approaches.

Besides the surface composition (that will dictate the chemical environment) the osteogenic process of bone cells will also depend on the roughness and topography of the surface. An important issue for the case of 3D porous structures (e.g. in scaffolds for tissue engineering) is also their meso/macro-organization. As referred by Green et al. [12] pore diameters between 15 and 50 μm stimulate fibrovascular growth, between 50 and 150 μm stimulate osteoid formation and in the range of 150-500 μm lead directly to mineralised bone. Other authors [31-33] indicate different figures for these porosities. Despite such insights, the ideal porous structure which would maximise bone growth, in terms of pore dimension distribution and interconnectivity is still unknown. In such complex structures it is often not straightforward to engineer uniform coatings for bone compatibility enhancement. In this review some biomimetic coating procedures that have potential to surpass this shortcoming will be presented and discussed in detail.

I.4. Ca-P coatings: present status

When considering an ideal material to replace and mimic bone, synthetic calcium phosphates (currently designated as Ca-Ps or “apatites”) can be an obvious answer, since they can replicate the structure and composition of bone mineral –hydroxylapatite (HA)- in a reproducible way. Unsurprisingly, Ca-Ps have a biocompatible behaviour with most of the cell types such as osteoblasts, osteoclasts, fibroblasts, and periodontal ligament cells, being found in the calcified tissues [34-37]. Furthermore, Ca-Ps disclose osteoconductive properties allowing for the formation of bone on its surface by attachment, migration, proliferation, and differentiation of bone-forming cells [38,39]. However, despite having a similar composition and chemistry to that of human bone, the mechanical properties of Ca-Ps are far from being close to those of human bone, which limits their use for load-bearing applications. In fact Ca-Ps are too stiff and often very brittle.

Today’s solutions of materials for bone replacement are still far from being ideal. In fact, metallic implants are still the first choice for load-bearing applications, despite all the

problems associated with stress-shielding [40] and long term application [41]. Although progress is being made at this very moment, the right balance between surface and bulk properties of an orthopaedic material is still to be achieved. At the present, one of the most interesting solutions to this problem is to use Ca-Ps as a coating on the surface of load-bearing implants [38,42-45]. Therefore, and in spite of their low mechanical properties, these types of coatings have great potential for bone fixation applications, or to be used on scaffolds for tissue engineering. In fact, these coatings can be tailored in terms of chemical composition, crystallinity and resorbability [46,47] and also can be loaded with osteogenic biological molecules [48-50] or serve as beds for the seeding of living cells that will stimulate bone formation [45,51].

At the moment the commercially available methods to produce such Ca-P coatings are in fact just a few and still the same as proposed a decade ago, having several disadvantages like difficulties in controlling the calcium-phosphate (Ca-P) layer composition, resorbability, weak adhesion to the substrates, the use of high temperatures or the costs involved in the process. Moreover, these methodologies are not effective in coating complex shapes. On the other hand new challenges are now being raised: to coat the interior of a porous material would be highly interesting when thinking about the immerging concepts linked to Tissue Engineering. These coatings would facilitate the cell attachment and proliferation in the interior of a scaffold, which will eventually and ideally be followed by the process of vascularization. For the last 30 years there has been a great amount of research aiming at the development of effective coating methodologies. But, if so, shouldn't we be more ahead? Why has this particular area progressed so little? In our opinion, there is more than one straight answer…

The plasma-spraying technique is, to date, the major commercially available method, used for coating Ca-P on metallic implants [52-55]. The first coated implant was commercialized in 1980 by Valen for dental applications. It is amazing to imagine that the same technique is still being used, if we think how much we have progressed from then (how would our lives be if we were still using computers from that time?!). But the fact is that the reproducibility and economic efficiency of the process are clear advantages that can not be disregarded, hence its popularity from 20 years ago to the present day [53,54]. However, this method presents some crucial drawbacks affecting the long-term performance and lifetime of the implant. The most significant are the poor coating-substrate adhesion [54] and lack of uniformity of the coating in terms of morphology and crystallinity [55,56]. Since plasma-spraying is a high-temperature and line-of-sight process, there are also some aspects that were not solved yet, such as the deteriorating

effect of intense heat on substrates, non-uniformity in coating density, wide range of band strength and the unavoidable limitations when trying to coat implant devices with complex shapes [53-56]. Other studied approaches have been sputter coating techniques that have been shown to be able to increase the bond strength between the coating and the substrates [57-59]. However, the inherent drawbacks are that the deposition and the process itself are very slow, the coatings quite thin, or their cohesion not adequate. A collection of other methodologies have been proposed such as: dip coating sintering [60], chemical vapour deposition [61,62], sol-gel deposition [63-65], ion implanting [66] laser deposition [67-69], laser cladding [70] and electrochemical processes like electrophoretic deposition [71], electrocrystallization [72,73], anode oxidation [74], or electroless coatings [75] to name just a few examples. Despite all of the investigations carried out, the produced coatings can suffer from at least one of the following problems [42]: lack of coating adherence to the substrate, thickness non-uniformity, poor structure integrity, non-stoichiometric composition of the coatings and limitations on choosing the type of substrate due to high temperatures of the process. In fact, each of the above mentioned techniques has its own technical limitations, and so far, an optimal technique for producing physiologically stable and interfacially adherent apatite coatings is yet to be developed. Thus, there is a demand to develop innovative methods able to face new challenges such as a technique when engineering bone implants or designing tissue engineering scaffolds to form an apatite layer (with properties similar to those of bone calcium-phosphates on the surface of new emerging materials) on various complex shaped materials, so that both biocompatibility as well as bioactivity are enhanced. Within this context a very attractive idea is to develop processes in which biologically active molecules, such as growth factors, could be incorporated in the coating.

I.5. The biomimetic approach applied to produce Ca-P coatings

As described above, Ca-P minerals found in natural hard tissues are produced spontaneously in a physiological environment at low temperatures from moderately supersaturated mineralizing solutions [76]. To learn, understand and apply these natural processes for producing Ca-P coatings biologically identical to bone apatite has been the focus of the attention of many researchers in recent years [77-81]. The so-called biomimetic preparation of calcium phosphate coatings on implant materials has then emerged as a new concept, and several methodologies have been proposed. This type of

approach is particularly suitable to coat polymeric materials [77,81-87], as it can be carried out at low temperature reaction conditions.

A calcium phosphate coating was first grown on a substrate by a biomimetic process by Kokubo et al in 1990 [81]. For this purpose, a bioactive $CaO\text{-}SiO_2$-based glass was used in the form of particles that were set in contact with the substrates to induce apatite nucleation on their surface in a simulated body fluid (SBF) with ion concentrations nearly equal to those of the human blood plasma and at body temperature. This solution was developed also in 1990 by the same author [21]. The mechanism of apatite formation is well known: the silanol groups (Si-OH) contained in the silicate ions are released from the bioactive glass and adsorbed on the substrate surface to induce the formation of a Ca-P layer [81,88,89]. Another very important aspect of this methodology is that it is highly dependent on the conditions of SFB immersion. In fact, parameters like time, temperature, agitation, renovation or ion concentration of the SBF solution are extremely important in tailoring the apatite formed. For example, Kim et al [90] have reported that different apatite layers can be produced on polyethylene terephthalate (PET) substrates in solutions where the ion concentrations were changed from 0.75 to 2.00 times those of SBF. Increasing the ionic activity product then resulted in lower Ca/P ratios of the apatites. The same author [91] has also reported that by increasing the carbonate ion content, apatites with composition and structure nearly identical to those of bone carbonated apatite could be produced. In fact, SBF solution is known to be deficient in relation to the HCO^{3-} content, when comparing to the human blood plasma [21,91]. Therefore, this group has now proposed a new revised SBF (R-SBF) with an ion composition closer to the human blood plasma (higher amounts of HCO^{3-}), to replace conventional SBF [92]. Although this new solution has already been proposed 3 years ago, the original SBF is still the one being widely used by different groups all over the world [84,93-100].

There is a quite considerable amount of published work using other different biomimetic routes for the formation of apatite layers on the surface of different materials [82,85,95,98,99,101-103]. Some of them are based on surface modifications, by chemical or physical means that are claimed [85,95,98], to induce direct bioactivity in the surface of the materials. Other methodologies use nucleating agents to induce the formation of the bioactive layer [77,82]. In both cases the basic principle is the formation at the surface (either by chemical bond or adsorption) of certain functional groups that seem to be favourable for inducing apatite formation. The works developed by Kobubo and his group [96,104] provide researchers with information that helps to understand better what would be the ideal surface chemistry for promoting apatite formation. They found that not only Si-

OH but other negatively charged groups at physiological conditions are favourable for apatite formation, for example Ti-OH, Zr-OH, Ta-OH, and Nb-OH groups [96]. In contrast, positively charged Al-OH groups are not effective. However, besides the charge, the spatial arrangement of the groups also play a very important role since, for example, not all titania gel structures lead to the formation of Ti-OH groups with an ability to form apatite [105].

In another very interesting study carried out by by Tanashi et al [46] the ability of various surface functional groups to nucleate a Ca-P layer after immersion in SBF was evaluated on a self-assembled monolayer (SAM) of alkanethiols over a gold substrate. They were able to establish a hierarchy of functional groups. The most potent nucleating group was -PO_4H_2 followed by –COOH. The groups –$CONH_2$, -OH and -NH_2 were considered as groups with a weaker nucleating ability. Finally –CH_3 was found to have no ability to promote apatite formation in the presence of the ions from SBF. Only the first two groups were charged negatively which explains their ability to form a Ca-P layer. These different studies demonstrate that there is more than one approach for inducing the formation of a Ca-P on a surface. In fact, each coating methodology should be designed while considering the desired substrate in terms of its chemistry, structure and surface morphology. The authors of this review really believe that different biomimetic routes should be applied to different materials/substrates.

I.6. Biomimetic Ca-Ps coatings on biodegradable polymers and Tissue Engineering scaffolds

Over the last few years the 3B's Research Group at the University of Minho has been giving special attention to the biomimetic preparation of Ca-P coatings, particularly to be applied on the surface of biodegradable polymers. Starch-based biodegradable polymers are particularly interesting for bone replacement [106-114]. Besides being biodegradable, inexpensive (when compared to other biodegradable polymers) and available in large quantities [115-117], these polymers can be converted into complex geometries that exhibit interesting mechanical properties, by using standard processing routes for synthetic polymers [106,110,118-120] or by means of using distinct innovative methodologies [109,112,121,122]. Furthermore, in addition to their processing versatility, they exhibit a biocompatible behaviour, already demonstrated on different *in vitro* [111,123,124] and *in vivo* [125] studies. To induce a bioactive behaviour on the surface of

these biodegradable polymers, via different surface modifications and biomimetic routes, has been one of the major goals of the works of Reis and co-workers, even with all the difficulties arising from the pH changes and continuous degradation of the polymeric surfaces.

The first biomimetic studies have used an adaptation of the standard biomimetic methodology [108] in which the samples were rolled in a bed of wet bioactive glass particles before immersion in an SBF solution. The methodology was effective in coating different types of polymers and shapes, such as a high molecular polyethylene, a biodegradable starch poly (ethylene vinyl alcohol) blend (SEVA-C) and a polyurethane foam. Nevertheless, problems associated with a lack of coating adhesion were observed. Therefore, different surface modifications were then experimented with, some of which have already led to some interesting results. Surface treatments like potassium hydroxide (KOH), UV radiation and overexposure to ethylene oxide sterilization, on SEVA-C substrates, applied before the biomimetic process have proved to be very effective in increasing the adhesion to the substrate and reducing the incubation periods for apatite formation [78]. In later studies, there was a need to develop alternative biomimetic methodologies in order to better control the nucleation and growing of bioactive Ca-P layers on the surface of our materials. Since starch base polymers have a high swelling ability, they are able to uptake ions from the surrounding medium, when immersed in SBF. Based on this idea new biomimetic methodologies were developed based on different approaches like: “impregnation” with a sodium silicate gel [51,84], pre-coating with a calcium silicate layer [126] or incubation in several supersaturated salt solutions ($CaCl_2$, KCl and $MgCl_2$) [127]. These surface treatments were performed prior to immersion in a simulated body fluid (SBF), in order to generate nucleating sites for the formation of the apatite layers. The developed methodologies aimed at: (i) the reduction of the incubation periods for apatite formation; (ii) the improvement of the adhesion strength between the coating and substrate; (iii) the production of Ca-P layers with different (tailored) Ca-P ratios. (iv) the coating of the inside of pores in porous 3D architectures to be used on tissue replacement and as tissue engineering scaffolds. Silicate-based methodologies in particular have been demonstrated to be extremely effective in coating porous scaffolds with different morphologies. Since gels were used, it was possible to cover inside the cell walls of different porous structures [84,126]. Therefore, one of the most promising aspects of the developed biomimetic methodologies is that they can be suitable to produce apatite coatings onto complex-shaped materials. In case of the sodium silicate gel methodology, the influence of the ion concentration of the SBF solution was also studied, and it was possible to observe that when increasing the ionic product of the solution, there was a

slight increase on the apatite crystallinity which had a positive effect on cell adhesion and proliferation kinetics [51,84].

At the present Reis and co-workers are starting to use these methodologies for designing systems for the release of bioactive molecules at the coating level. As a result, there are new opportunities for applying this type of coatings in the field of tissue engineering, as a way to enhance the cell adhesion and proliferation and the extra-cellular matrix production. Some possibilities are presently being considered, based on the incorporation of osteogenic biological molecules in some biomimetic coatings [50]. Due to the physiological coating conditions used, it is expected that, when applying these methodologies, the bioactive factors can preserve their biological activities. Therefore, considering the slow, but definite degradation of Ca-Ps as well as their high hydrophilicity [128], they may be very suitable to serve as carriers for these molecules. The options for creating a delivery system in these coatings are numerous. For example, certain molecules like protein growth factors can regulate various cell functions such as growth, differentiation, secretion, and apoptosis [129]. The authors do believe that producing these hybrid coatings on 3D biodegradable porous scaffolds, with adequate resorbability, can represent a very promising opportunity for introducing coated biodegradable scaffolds in the field of tissue engineering. Although in this review we have been mainly discussing biomimetic coating methodologies applied to biodegradable starch based polymers, other authors have also been able to coat by biomimetic routes several other polymers. Some examples are coatings produced on cotton [95], silk [103], chitosan [130] and collagen [131]. Du *et al*. [132] presented a 1-day one-step incubation method to obtain either amorphous or bone-like apatitic calcium phosphate coating on dense plates or three-dimensional porous blocks of PEO/PBT (Polyactive®) 1000/70/30. However this was only possible by means of bubbling CO_2 gas in a derived concentrated simulated body fluid. Bone-like apatite coating on poly(L-lactic acid) (PLLA) fibres was also obtained by Yuan *et al.* [133] by immersing the fibres in a modified simulated body fluid (SBF) at 37 ºC and pH 7.3 after hydrolysis of the fibres in water.

I.7. Conclusions

Novel biomimetic coating routes have been developed in order to produce Ca-P layers on orthopaedic implants and tissue engineering scaffolds. There is already available in the

literature a range of possible biomimetic coating routes that researchers and industry can choose from. However, these methodologies are still to be introduced in industrial plants and then in clinical practice. It is, nevertheless, the belief of the authors that by means of continuing to learn from Nature, and by incorporating bioactive agents into the coatings, it will be possible to use this coated systems in the clinical practice. Many research groups and already some major companies are pursuing that demanding goal. Nature will continue to lead us all!

References

1. Guinea GV, Elices M, Perez-Rigueiro J, Plaza G. Self-tightening of spider silk fibers induced by moisture. Polymer 2003;44(19):5785-5788.
2. Addadi L, Weiner S. Control and Design Principles in Biological Mineralization. Angewandte Chemie-International Edition in English 1992;31(2):153-169.
3. Mann S. Biomineralization, Principles and Concepts in Bioinorganic Materials Chemistry. Oxford: Oxford University Press; 2001.
4. Webb J, Macey DJ, Chua-anusorn W, St Pierre TG, Brooker LR, Rahman I, Noller B. Iron biominerals in medicine and the environment. Coordination Chemistry Reviews 1999;192:1199-1215.
5. Su XW, Cui FZ. Hierarchical structure of ivory: from nanometer to centimeter. Materials Science & Engineering C-Biomimetic and Supramolecular Systems 1999;7(1):19-29.
6. Weiner S, Addadi L, Wagner HD. Materials design in biology. Materials Science & Engineering C-Biomimetic and Supramolecular Systems 2000;11(1):1-8.
7. Mann S. The chemistry of form. Angewandte Chemie-International Edition 2000;39(19):3393-3406.
8. Chateigner D, Hedegaard C, Wenke HR. Mollusc shell microstructures and crystallographic textures. Journal of Structural Geology 2000;22(11-12):1723-1735.
9. Lowenstam HA, Weiner S. On Biomineralization. New York: Oxford University Press; 1989.
10. Weiner S, Addadi L. Design strategies in mineralized biological materials. Journal of Materials Chemistry 1997;7(5):689-702.
11. Addadi L, Weiner S. Interactions between acidic proteins and crystals: stereochemical requirements in biomineralization. Proc Natl Acad Sci U S A 1985;82(12):4110-4.
12. Green D, Walsh D, Mann S, Oreffo ROC. The potential of biomimesis in bone tissue engineering: Lessons from the design and synthesis of invertebrate skeletons. Bone 2002;30(6):810-815.
13. Atlan G, Balmain N, Berland S, Vidal B, Lopez E. Reconstruction of human maxillary defects with nacre powder: histological evidence for bone regeneration. Comptes Rendus De L Academie Des Sciences Serie Iii-Sciences De La Vie-Life Sciences 1997;320(3):253-258.
14. Zaremba CM, Morse DE, Mann S, Hansma PK, Stucky GD. Aragonite-hydroxyapatite conversion in gastropod (abalone) nacre. Chemistry of Materials 1998;10(12):3813-3824.
15. Rho JY, Kuhn-Spearing L, Zioupos P. Mechanical properties and the hierarchical structure of bone. Medical Engineering & Physics 1998;20(2):92-102.
16. Weiner S, Wagner HD. The material bone: Structure mechanical function relations. Annual Review of Materials Science 1998;28:271-298.
17. Robinson RA. An electron-microscopic study of the crystalline inorganic component of bone and its relationship to the organic matrix. J Bone Joint Surg A 1952;34:389.
18. Birk DE, Zycband EI, Winkelmann DA, Trelstad RL. Collagen Fibrillogenesis Insitu - Discontinuous Segmental Assembly in Extracellular Compartments. Annals of the New York Academy of Sciences 1990;580:176-194.
19. Jackson SF. The Fine Structure of Developing Bone in the Embryonic Fowl. Proceedings of the Royal Society of London Series B-Biological Sciences 1957;146(923):270-279.

20. Arsenault AL. Crystal-Collagen Relationships in Calcified Turkey Leg Tendons Visualized by Selected-Area Dark Field Electron-Microscopy. Calcified Tissue International 1988;43(4):202-212.
21. Kokubo T, Kushitani H, Sakka S, Kitsugi T, Yamamuro T. Solutions able to reproduce in vivo surface-structure changes in bioactive glass-ceramic A-W. J Biomed Mater Res 1990;24(6):721-34.
22. Mann S, Heywood BR, Rajam S, Birchall JD. Controlled Crystallization of Caco3 under Stearic-Acid Monolayers. Nature 1988;334(6184):692-695.
23. Heywood BR, Mann S. Molecular Construction of Oriented Inorganic Materials - Controlled Nucleation of Calcite and Aragonite under Compressed Langmuir Monolayers. Chemistry of Materials 1994;6(3):311-318.
24. Addadi L, Moradian J, Shay E, Maroudas NG, Weiner S. A Chemical-Model for the Cooperation of Sulfates and Carboxylates in Calcite Crystal Nucleation - Relevance to Biomineralization. Proceedings of the National Academy of Sciences of the United States of America 1987;84(9):2732-2736.
25. Belcher AM, Wu XH, Christensen RJ, Hansma PK, Stucky GD, Morse DE. Control of crystal phase switching and orientation by soluble mollusc-shell proteins. Nature 1996;381(6577):56-58.
26. Simkiss K, Wilbur, KM. Biomineralization. Cell Biology and Mineral Deposition. San Diego: Academic Press; 1989.
27. Sarikaya M. Biomimetics: Materials fabrication through biology. Proceedings of the National Academy of Sciences of the United States of America 1999;96(25):14183-14185.
28. Whitesides GM, Grzybowski B. Self-assembly at all scales. Science 2002;295(5564):2418-2421.
29. Boncheva M, Gracias DH, Jacobs HO, Whitesides GM. Biomimetic self-assembly of a functional asymmetrical electronic device. Proceedings of the National Academy of Sciences of the United States of America 2002;99(8):4937-4940.
30. Aizenberg J, Muller DA, Grazul JL, Hamann DR. Direct fabrication of large micropatterned single crystals. Science 2003;299(5610):1205-1208.
31. Yeni YN, Norman TL. Calculation of porosity and osteonal cement line effects on the effective fracture toughness of cortical bone in longitudinal crack growth. Journal of Biomedical Materials Research 2000;51(3):504-509.
32. Ayers RA, Simske SJ, Bateman TA, Petkus A, Sachdeva RLC, Gyunter VE. Effect of nitinol implant porosity on cranial bone ingrowth and apposition after 6 weeks. Journal of Biomedical Materials Research 1999;45(1):42-47.
33. Kujala S, Ryhanen J, Danilov A, Tuukkanen J. Effect of porosity on the osteointegration and bone ingrowth of a weight-bearing nickel-titanium bone graft substitute. Biomaterials 2003;24(25):4691-4697.
34. Midy V, Dard M, Hollande E. Evaluation of the effect of three calcium phosphate powders on osteoblast cells. Journal of Materials Science-Materials in Medicine 2001;12(3):259-265.
35. Heymann D, Guicheux J, Rousselle AV. Ultrastructural evidence in vitro of osteoclast-induced degradation of calcium phosphate ceramic by simultaneous resorption and phagocytosis mechanisms. Histology and Histopathology 2001;16(1):37-44.
36. Suzuki T, Ohashi R, Yokogawa Y, Nishizawa K, Nagata F, Kawamoto Y, Kameyama T, Toriyama M. Initial anchoring and proliferation of fibroblast L-929 cells on unstable surface of calcium phosphate ceramics. Journal of Bioscience and Bioengineering 1999;87(3):320-327.
37. Shirakata Y, Oda S, Kinoshita A, Kikuchi S, Tsuchioka H, Ishikawa I. Histocompatible healing of periodontal defects after application of an injectable calcium phosphate bone cement. A preliminary study in dogs. Journal of Periodontology 2002;73(9):1043-1053.
38. Ducheyne P, Qiu Q. Bioactive ceramics: the effect of surface reactivity on bone formation and bone cell function. Biomaterials 1999;20(23-24):2287-2303.
39. Kanazawa T. General Background on Phosphate Materials. Amsterdam: Elsevier; 1989. 1 p.
40. Mcnamara BP, Toni A, Tayor D. Effects of Implant Material Properties and Implant-Bone Bonding on Stress Shielding in Cementless Total Hip-Arthroplasty. Advances in Engineering Materials 1995;99-1:309-314.
41. Gomez J, Rodriguez MA, Banos V, Martinez L, Claver MA, Ruiz J, Simarro E, Canovas JA, Medina M, Clavel M. Orthopedic implant infection: Prognostic factors and influence of long-

term antibiotic treatment on evolution. Prospective study, 1992-1999. Enfermedades Infecciosas Y Microbiologia Clinica 2003;21(5):232-236.
42. Thomas KA. Hydroxyapatite Coatings. Orthopedics 1994;17(3):267-278.
43. Greenspan DC. Bioactive ceramic implant materials. Current Opinion in Solid State & Materials Science 1999;4(4):389-393.
44. Hench LL, Wilson J. Surface-Active Biomaterials. Science 1984;226(4675):630-636.
45. de Bruijn JD, van den Brink, I., Mendes, S., Dekker, R., Bovell, Y.P., van Blitterswijk, C.A. Bone Induction by Implants Coated with Cultures Osteogenic Bone Marrow Cells. Advents in Dental Research 1999;13:74.
46. Tanahashi M, Matsuda T. Surface functional group dependence on apatite formation on self-assembled monolayers in a simulated body fluid. J Biomed Mater Res 1997;34(3):305-15.
47. ter Brugge PJ, Wolke JGC, Jansen JA. Effect of calcium phosphate coating crystallinity and implant surface roughness on differentiation of rat bone marrow cells. Journal of Biomedical Materials Research 2002;60(1):70-78.
48. Liu Y, Hunziker EB, Randall NX, de Groot K, Layrolle P. Proteins incorporated into biomimetically prepared calcium phosphate coatings modulate their mechanical strength and dissolution rate. Biomaterials 2003;24(1):65-70.
49. Wen HB, Moradian-Oldak J. Modification of calcium-phosphate coatings on titanium by recombinant amelogenin. Journal of Biomedical Materials Research Part A 2003;64A(3):483-490.
50. Leonor IB, Azevedo HS, Alves CM, Reis RL. Effects of the incorporation of proteins and active enzymes on biomimetic calcium-phosphate coatings. Bioceramics 15 2003;240-2:97-100.
51. Oliveira AL, Alves CM, Reis RL. Cell adhesion and proliferation on biomimetic calcium-phosphate coatings produced by a sodium silicate gel methodology. Journal of Materials Science-Materials in Medicine 2002;13(12):1181-1188.
52. Kohn DH. Metals in medical applications. Current Opinion in Solid State & Materials Science 1998;3(3):309-316.
53. Weng J, Liu Q, Wolke JGC, Zhang XD, deGroot K. Formation and characteristics of the apatite layer on plasma-sprayed hydroxyapatite coatings in simulated body fluid. Biomaterials 1997;18(15):1027-1035.
54. Zheng XB, Huang MH, Ding CX. Bond strength of plasma-sprayed hydroxyapatite/Ti composite coatings. Biomaterials 2000;21(8):841-849.
55. Gledhill HC, Turner IG, Doyle C. In vitro dissolution behaviour of two morphologically different thermally sprayed hydroxyapatite coatings. Biomaterials 2001;22(7):695-700.
56. Fazan F, Marquis PM. Dissolution behavior of plasma-sprayed hydroxyapatite coatings. Journal of Materials Science-Materials in Medicine 2000;11(12):787-792.
57. Yamashita K, Arashi T, Kitagaki K, Yamada S, Umegaki T, Ogawa K. Preparation of Apatite Thin-Films through Rf-Sputtering from Calcium-Phosphate Glasses. Journal of the American Ceramic Society 1994;77(9):2401-2407.
58. Burke EM, Haman JD, Weimer JJ, Cheney AB, Rigsbee JM, Lucas LC. Influence of coating strain on calcium phosphate thin-film dissolution. Journal of Biomedical Materials Research 2001;57(1):41-47.
59. Wang CX, Chen ZQ, Wang M, Liu ZY, Wang PL, Zheng SX. Functionally graded calcium phosphate coatings produced by ion beam sputtering/mixing deposition. Biomaterials 2001;22(12):1619-1626.
60. Kim CS, Ducheyne P. Compositional Variations in the Surface and Interface of Calcium-Phosphate Ceramic Coatings on Ti and Ti-6al-4v Due to Sintering and Immersion. Biomaterials 1991;12(5):461-469.
61. Hamdi M, Hakamata S, Ektessabi AM. Coating of hydroxyapatite thin film by simultaneous vapor deposition. Thin Solid Films 2000;377:484-489.
62. Hamdi M, Ide-Ektessabi A. Preparation of hydroxyapatite layer by ion beam assisted simultaneous vapor deposition. Surface & Coatings Technology 2003;163:362-367.
63. Li P, Ohtsuki C, Kokubo T, Nakanishi K, Soga N, de Groot K. The role of hydrated silica, titania, and alumina in inducing apatite on implants. J Biomed Mater Res 1994;28(1):7-15.
64. Li P, Ohtsuki C, Kokubo T, Nakanishi K, Soga N, Nakamura T, Yamamuro T. Effects of ions in aqueous media on hydroxyapatite induction by silica gel and its relevance to bioactivity of bioactive glasses and glass-ceramics. J Appl Biomater 1993;4(3):221-9.

65. Peltola T, Patsi M, Rahiala H, Kangasniemi I, Yli-Urpo A. Calcium phosphate induction by sol-gel-derived titania coatings on titanium substrates in vitro. Journal of Biomedical Materials Research 1998;41(3):504-510.
66. Hanawa T, Ukai H, Murakami K, Asaoka K. Structure of Surface-Modified Layers of Calcium-Ion-Implanted Ti-6al-4v and Ti-56ni. Materials Transactions Jim 1995;36(3):438-444.
67. Mayor B, Arias J, Chiussi S, Garcia F, Pou J, Fong BL, Perez-Amor M. Calcium phosphate coatings grown at different substrate temperatures by pulsed ArF-laser deposition. Thin Solid Films 1998;317(1-2):363-366.
68. Fernandez-Pradas JM, Cleries L, Martinez E, Sardin G, Esteve J, Morenza JL. Calcium phosphate coatings deposited by laser ablation at 355 nm under different substrate temperatures and water vapour pressures. Applied Physics a-Materials Science & Processing 2000;71(1):37-42.
69. Fernandez-Pradas JM, Sardin G, Cleries L, Serra P, Ferrater C, Morenza JL. Deposition of hydroxyapatite thin films by excimer laser ablation. Thin Solid Films 1998;317(1-2):393-396.
70. Lusquinos F, Pou J, Arias JL, Larosi M, de Carlos A, Leon B, Amor MP, Best S, Bonfield W, Driessens FCM. Laser surface cladding: A new promising technique to produce calcium phosphate coatings. Bioceramics 14 2002;218-2:187-190.
71. Zhitomirsky I. Electrophoretic hydroxyapatite coatings and fibers. Materials Letters 2000;42(4):262-271.
72. Chen JS, Juang HY, Hon MH. Calcium phosphate coating on titanium substrate by a modified electrocrystallization process. Journal of Materials Science-Materials in Medicine 1998;9(5):297-300.
73. Shirkhanzadeh M. Calcium-Phosphate Coatings Prepared by Electrocrystallization from Aqueous-Electrolytes. Journal of Materials Science-Materials in Medicine 1995;6(2):90-93.
74. Ishizawa H, Ogino M. Hydrothermal precipitation of hydroxyapatite on anodic titanium oxide films containing Ca and P. Journal of Materials Science 1999;34(23):5893-5898.
75. Leonor IB, Reis RL. An innovative auto-catalytic deposition route to produce calcium-phosphate coatings on polymeric biomaterials. Journal of Materials Science-Materials in Medicine 2003;14(5):435-441.
76. Rey C. Calcium Phosphate Biomaterials and Bone Mineral. Differences in Composition, Structures and Properties. Biomaterials 1990;11:13.
77. Tanahashi M, Yao T, Kokubo T, Minoda M, Miyamoto T, Nakamura T, Yamamuro T. Apatite Coating on Organic Polymers by a Biomimetic Process. Journal of the American Ceramic Society 1994;77(11):2805-2808.
78. Oliveira AL, Elvira, C., Vásquez, B., San Roman, J., Reis, R. L. Surface Modifications Tailors the Characteristics of Biomimetic Coatings Nucleated on Starch Based Polymers. Journal of Materials Science: Materials in Medicine 1999;10:827.
79. Habibovic P, Barrere F, van Blitterswijk CA, de Groot K, Layrolle P. Biomimetic hydroxyapatite coating on metal implants. Journal of the American Ceramic Society 2002;85(3):517-522.
80. Li F, Feng QL, Cui FZ, Li HD, Schubert H. A simple biomimetic method for calcium phosphate coating. Surface & Coatings Technology 2002;154(1):88-93.
81. Abe Y, Kokubo T, Yamamuro T. Apatite Coating on Ceramics, Metals and Polymers Utilizing a Biological Process. Journal of Materials Science-Materials in Medicine 1990;1(4):233-238.
82. Miyaji F, Kim HM, Handa S, Kokubo T, Nakamura T. Bonelike apatite coating on organic polymers: novel nucleation process using sodium silicate solution. Biomaterials 1999;20(10):913-919.
83. Taguchi T, Muraoka Y, Matsuyama H, Kishida A, Akashi M. Apatite coating on hydrophilic polymer-grafted poly(ethylene) films using an alternate soaking process. Biomaterials 2001;22(1):53-58.
84. Oliveira AL, Malafaya PB, Reis RL. Sodium silicate gel as a precursor for the in vitro nucleation and growth of a bone-like apatite coating in compact and porous polymeric structures. Biomaterials 2003;24(15):2575-2584.
85. Kim HM, Uenoyama M, Kokubo T, Minoda M, Miyamoto T, Nakamura T. Biomimetic apatite formation on polyethylene photografted with vinyltrimethoxysilane and hydrolyzed. Biomaterials 2001;22(18):2489-2494.

86. Oyane A, Kawashita M, Kokubo T, Minoda M, Miyamoto T, Nakamura T. Bonelike apatite formation on ethylene-vinyl alcohol copolymer modified with a silane coupling agent and titania solution. Journal of the Ceramic Society of Japan 2002;110(4):248-254.
87. Oyane A, Kawashita M, Nakanishi K, Kokubo T, Minoda M, Miyamoto T, Nakamura T. Bonelike apatite formation on ethylene-vinyl alcohol copolymer modified with silane coupling agent and calcium silicate solutions. Biomaterials 2003;24(10):1729-35.
88. Takadama H, Kim HM, Kokubo T, Nakamura T. TEM-EDX study of mechanism of bonelike apatite formation on bioactive titanium metal in simulated body fluid. J Biomed Mater Res 2001;57(3):441-8.
89. Hata K, Kokubo T, Nakamura T, Yamamuro T. Growth of a Bonelike Apatite Layer on a Substrate by a Biomimetic Process. Journal of the American Ceramic Society 1995;78(4):1049-1053.
90. Kim HM, Kishimoto K, Miyaji F, Kokubo T, Yao T, Suetsugu Y, Tanaka J, Nakamura T. Composition and structure of the apatite formed on PET substrates in SBF modified with various ionic activity products. Journal of Biomedical Materials Research 1999;46(2):228-235.
91. Kim HM, Kishimoto K, Miyaji F, Kokubo T, Yao T, Suetsugu Y, Tanaka J, Nakamura T. Composition and structure of apatite formed on organic polymer in simulated body fluid with a high content of carbonate ion. Journal of Materials Science-Materials in Medicine 2000;11(7):421-426.
92. Oyane A, Kim HM, Furuya T, Kokubo T, Miyazaki T, Nakamura T. Preparation and assessment of revised simulated body fluids. J Biomed Mater Res 2003;65A(2):188-95.
93. Lin FH, Hsu YS, Lin SH, Sun JS. The effect of Ca/P concentration and temperature of simulated body fluid on the growth of hydroxyapatite coating on alkali-treated 316L stainless steel. Biomaterials 2002;23(19):4029-4038.
94. Barrere F, van Blitterswijk CA, de Groot K, Layrolle P. Nucleation of biomimetic Ca-P coatings on Ti6Al4V from a SBF x 5 solution: influence of magnesium. Biomaterials 2002;23(10):2211-2220.
95. Mucalo MR, Yokogawa Y, Toriyama M, Suzuki T, Kawamoto Y, Nagata F, Nishizawa K. Growth of Calcium-Phosphate on Surface-Modified Cotton. Journal of Materials Science-Materials in Medicine 1995;6(10):597-605.
96. Kokubo T, Kim HM, Kawashita M, Nakamura T. Process of calcification on artificial materials. Z Kardiol 2001;90 Suppl 3:86-91.
97. Huang J, DiSilvio L, Wang M, Tanner KE, Bonfield W. In vitro mechanical and biological assessment of hydroxyapatite-reinforced polyethylene composite. Journal of Materials Science-Materials in Medicine 1997;8(12):775-779.
98. Tretinnikov ON, Kato K, Ikada Y. In-Vitro Hydroxyapatite Deposition onto a Film Surface-Grafted with Organophosphate Polymer. Journal of Biomedical Materials Research 1994;28(11):1365-1373.
99. Liu X, Ding C, Wang Z. Apatite formed on the surface of plasma-sprayed wollastonite coating immersed in simulated body fluid. Biomaterials 2001;22(14):2007-12.
100. Du C, Meijer GJ, van de Valk C, Haan RE, Bezemer JM, Hesseling SC, Cui FZ, de Groot K, Layrolle P. Bone growth in biomimetic apatite coated porous Polyactive((R)) 1000PEGT70PBT30 implants. Biomaterials 2002;23(23):4649-4656.
101. Yokogawa Y, Reyes JP, Mucalo MR, Toriyama M, Kawamoto Y, Suzuki T, Nishizawa K, Nagata F, Kamayama T. Growth of calcium phosphate on phosphorylated chitin fibres. Journal of Materials Science-Materials in Medicine 1997;8(7):407-412.
102. Rhee SH, Tanaka J. Hydroxyapatite formation on cellulose cloth induced by citric acid. Journal of Materials Science-Materials in Medicine 2000;11(7):449-452.
103. Takeuchi A, Ohtsuki C, Miyazaki T, Tanaka H, Yamazaki M, Tanihara M. Deposition of bone-like apatite on silk fiber in a solution that mimics extracellular fluid. Journal of Biomedical Materials Research Part A 2003;65A(2):283-289.
104. Kokubo T, Kim HM, Kawashita M. Novel bioactive materials with different mechanical properties. Biomaterials 2003;24(13):2161-75.
105. Uchida M, Kim HM, Kokubo T, Fujibayashi S, Nakamura T. Structural dependence of apatite formation on titania gels in a simulated body fluid. J Biomed Mater Res 2003;64A(1):164-70.
106. Reis R. L. CAM, Allan P. S., Bevis M. J. Mechanical behaviour of injection-moulded starch based polymers. Polymer Advanced Technology 1996;7:784-790.

107. Reis RL, Cunha A. M. Characterization of two biodegradable polymers of potential application within the biomaterials field. Journal of Materials Science: Materials in Medicine 1995;6:786-792.
108. Reis RL, Cunha, A. M., Fernandes, M. H., Correia, R. N. Treatments to Induce the Nucleation and Growth of Apatite Like Layers onto Polymeric Surfaces and Foams. Journal of Materials Science: Materials in Medicine 1997;8:897.
109. Malafaya PB, Elvira C, Gallardo A, San Roman J, Reis RL. Porous starch-based drug delivery systems processed by a microwave route. J Biomater Sci Polym Ed 2001;12(11):1227-41.
110. Gomes ME, Ribeiro AS, Malafaya PB, Reis RL, Cunha AM. A new approach based on injection moulding to produce biodegradable starch-based polymeric scaffolds: morphology, mechanical and degradation behaviour. Biomaterials 2001;22(9):883-9.
111. Gomes ME, Reis RL, Cunha AM, Blitterswijk CA, de Bruijn JD. Cytocompatibility and response of osteoblastic-like cells to starch-based polymers: effect of several additives and processing conditions. Biomaterials 2001;22(13):1911-7.
112. Gomes M. E. SAJ, Reis R. L. Bone Tissue Engineering Using Starch Based Scaffolds Obtained by Different Methodologies. Ed., R.L.Reis and D.Cohn, NATO/ASI Series, Kluwer Press, Drodercht, 2002:221-249.
113. Gomes M. E. SVI, Behravesh E., Reis R.L., Mikos Antonios G. Effect of Flow Perfusion on the Osteogenic Differentiation of Bone Marrow Stromal Cells Cultured on Starch Based Three-Dimensional Scaffolds. Journal of Biomedical Materials Research 2003;67A:87-95.
114. Oliveira AL, Leonor IB, Malafaya PB, Alves CM, Azevedo HS, Reis RL. Tailoring the bioactivity of natural origin inorganic-polymeric based systems. Bioceramics 15 2003;240-2:111-142.
115. Galliard T. Starch: properties and potential. New-York: John Wiley & Sons; 1987.
116. Poutanen K, Forssell P. Modification of starch properties with plasticizers. Trends in Polymer Science 1996;4(4):128-132.
117. Andreopoulos AG, Theophanides T. Degradable Plastics - a Smart Approach to Various Applications. Journal of Elastomers and Plastics 1994;26(4):308-326.
118. Sousa RA, Reis RL, Cunha AM, Bevis MJ. Processing and properties of bone-analogue biodegradable and bioinert polymeric composites. Composites Science and Technology 2003;63(3-4):389-402.
119. Sousa RA, Reis RL, Cunha AM, Bevis MJ. Structure and properties of hydroxylapatite reinforced starch bone-analogue composites. Bioceramics 2000;192-1:669-672.
120. Sousa RA, Kalay G, Reis RL, Cunha AM, Bevis MJ. Injection molding of a starch/EVOH blend aimed as an alternative biomaterial for temporary applications. Journal of Applied Polymer Science 2000;77(6):1303-1315.
121. Malafaya PB, Gomes ME, Salgado AJ, Reis RL. Polymer based scaffolds and carriers for bioactive agents from different natural origin materials. Tissue Engineering, Stem Cells and Gene Therapies 2003;534:201-233.
122. Sousa RA, Oliveira AL, Reis RL, Cunha AM, Bevis MJ. Bi-composite sandwich moldings: Processing, mechanical performance and bioactive behavior. Journal of Materials Science-Materials in Medicine 2003;14(5):385-397.
123. Marques AP, Reis RL, Hunt JA. The biocompatibility of novel starch-based polymers and composites: in vitro studies. Biomaterials 2002;23(6):1471-1478.
124. Mendes SC, Bezemer J, Claase MB, Grijpma DW, Bellia G, Degli-Innocenti F, Reis RL, De Groot K, Van Blitterswijk CA, De Bruijn JD. Evaluation of two biodegradable polymeric systems as substrates for bone tissue engineering. Tissue Engineering 2003;9:S91-S101.
125. Mendes SC, Reis RL, Bovell YP, Cunha AM, van Blitterswijk CA, de Bruijn JD. Biocompatibility testing of novel starch-based materials with potential application in orthopaedic surgery: a preliminary study. Biomaterials 2001;22(14):2057-64.
126. Oliveira AL, Gomes ME, Malafaya PB, Reis RL. Biomimetic coating of starch based polymeric foams produced by a calcium silicate based methodology. Bioceramics 15 2003;240-2:101-104.
127. Oliveira AL, Leonor, IB, Elvira, C, Azevedo, MC, Pashkuleva, I, Reis, RL. Surface Treatments and Pre-calcification Routes to Enhance Cell Adhesion and Proliferation. In: Cohn RLRaD, editor. Polymer Based Systems on Tissue Engineering, Replacement and Regeneration. Drodercht: Kluwer Press; 2002. p 183-217.

128. Nagano M, Nakamura T, Kokubo T, Tanahashi M, Ogawa M. Differences of bone bonding ability and degradation behaviour in vivo between amorphous calcium phosphate and highly crystalline hydroxyapatite coating. Biomaterials 1996;17(18):1771-1777.
129. Ito Y. Tissue engineering by immobilized growth factors. Materials Science & Engineering C-Biomimetic and Supramolecular Systems 1998;6(4):267-274.
130. Varma HK, Yokogawa Y, Espinosa FF, Kawamoto Y, Nishizawa K, Nagata F, Kameyama T. Porous calcium phosphate coating over phosphorylated chitosan film by a biomimetic method. Biomaterials 1999;20(9):879-884.
131. Girija EK, Yokogawa Y, Nagata F. Bone-like apatite formation on collagen fibrils by biomimetic method. Chemistry Letters 2002(7):702-703.
132. Du C, Klasens P, Haan RE, Bezemer J, Cui FZ, de Groot K, Layrolle P. Biomimetic calcium phosphate coatings on Polyactive (R) 1000/70/30. Journal of Biomedical Materials Research 2002;59(3):535-546.
133. Yuan XY, Mak AFT, Li JL. Formation of bone-like apatite on poly(L-lactic acid) fibers by a biomimetic process. Journal of Biomedical Materials Research 2001;57(1):140-150.

Part B. Bone-Like Apatite Coatings on Biodegradable Polymers as a Way to Induce Bone Mineralization: Current Developments and Future Trends*

I.1. Introduction

Bone is one of the most wonderful examples of nature's ability to engineer living materials by combining different organic/inorganic materials into complex shapes with a controlled specific function. This highly organized mineralized tissue consists of a hierarchy of collagen-based microstructures in association with cartilage and connective tissue. Therefore, when considering an ideal material to replace and mimic bone, synthetic calcium phosphates (currently designated as Ca-Ps or "apatites") can be an obvious answer, since they can replicate the structure and composition of bone mineral – hydroxylapatite (HA)- in a reproducible way.

In the 1970's Ca-Ps (mostly HA) were synthesized, characterized, and applied in the biomedical field [1-4]. Since then, the interest in these materials has increased, mostly in dental and bone related applications, but have simultaneously rendered the field more complex to the everyday user, since only subtle differences in composition and structure of Ca-P compounds may have a profound effect on their *in vivo* behaviour [5].

*This part of the chapter is based on the following publication:

A. L. Oliveira, J. F. Mano, R. L. Reis, "Nature-Inspired Calcium Phosphate Coatings: Present Status and Novel Advances in the Science of Mimicry", Current Opinion on Solid State & Materials Science, 7/4-5, 2003, 309-318.

Most calcium phosphates previously used *in vivo* have been calcium orthophosphates, i.e. they contain the orthophosphate group PO_4^{3-}. Two different categories of Ca-Ps should be distinguished [6]: (i) Ca-P obtained by precipitation from an aqueous solution at or around room temperature (low-temperature Ca-P), and (ii) Ca-P obtained by a thermal reaction (high temperature Ca-P). All calcium phosphate cements belong to the first category whereas most other Ca-P products belong to the second category. Table 1 summarizes the main calcium phosphate compounds according with each category. The first sixth compounds precipitate at room temperature in aqueous systems and last sixth are obtained by thermal decomposition or thermal synthesis.

Table 1. Main calcium phosphate compounds. Compiled from references [6-8].

	CHEMICAL FORMULA	(Ca/P) MOLAR RATIO	ABREVIATION
PRECIPITATED CaP			
Dicalcium phosphate	$CaHPO_4$	1.00	DCP
Monocalcium phosphate monohydrate	$Ca(HPO_4)_2 \cdot H_2O$	0.50	MCPM
Dicalcium phosphate dihidrate (Brushite)	$Ca(HPO_4)_2 \cdot 2H_2O$	1.00	DCPD
Octacalcium phosphate	$Ca_8H_2(PO_4)_6 \cdot 5\ H_2O$	1.33	OCP
Precipitated hydroxiapatite ("Tricalcium phosphate")	$Ca_{10-x}(HPO_4)_x(PO_4)_{6-x}(OH)_{2-x}$ $0 \le x \le 2$	1.50-1.67	PHA
Amorphous calcium phosphate	$Ca_3(PO_4)_2 \cdot n\ H_2O$ n=3-4.5; 15-20% H_2O	1.50	ACP
HIGH TEMPERATURE CaP			
Monocalcium phosphate	$Ca(HPO_4)_2$	0.50	MCP
α-Tricalcium phosphate	α-$Ca_3(HPO_4)_2$	1.50	α-TCP
β-Tricalcium phosphate	β-$Ca_3(PO_4)_2$	1.50	β-TCP
Sintered hydroxylapatite	$Ca_5(PO_4)_3OH$	1.67	HA
Oxyapatite	$Ca_{10}(PO_4)_6O$	1.67	OXA
Tetracalcium phosphate	$Ca_4(PO_4)_2O$	2.00	TetCP

The most important property of Ca-Ps is probably the solubility in water since it allows predicting the *in vivo* behaviour of Ca-Ps to large extent. If the solubility of a Ca-P is less than the mineral part of bone, it degrades extremely slowly if at all. If the solubility of a Ca-P is greater than that of the mineral part of bone, it is degraded. The solubility of Ca-Ps is inversely proportional to the Ca/P ratio [9]. At body temperature only two calcium phosphates are stable in contact with aqueous media, such as body fluids [6,10-12]: at pH < 4.2 the stable phase is dicalcium phosphate or brushite ($CaHPO_4 \cdot 2H_2O$), whereas at

pH ≥ 4.2 the stable phase is $Ca_{10}(PO_4)_6(OH)_2$ (HA). All the high-temperature calcium phosphate phases interact with water or body fluids at 37 ºC to form HA [10].

It is clear that the material that forms the mineral component of bone should represent the ideal ceramic for bone replacement. In fact, HA presents an excellent biocompatibility and bioactive behaviour being the mechanical properties dependent on the method of preparation [13,14]. In fact, HA materials have been used in many forms, for non load-bearing applications [12,13]. It is important to distinguish between precipitated hydroxylapatite (PHA) and high temperature hydroxylapatite (HA) (See Table 1). The first is obtained by precipitation in an aqueous solution and is normally poorly crystalline [6]. The molar Ca/P ratio can vary between 1.50 and 1.67 and resembles the mineral of bone. PHA with a Ca/P molar ratio of 1.50 is often called calcium-deficient hydroxylapatite (CDHA) or tricalcium phosphate (TCP). The latter name has led to confusion with β-TCP, which has almost the same chemical composition, but a different crystalline structure [6]. The term “HA” is more applied to the hydroxylapatite obtained by thermal treatment, typically above 800 ºC. Due to the thermal treatment, HA is crystalline, stoichiometric and less soluble than the mineral part of bone [13,14].

Despite of having a similar composition and chemistry, the mechanical properties of Ca-Ps are far from being close to those of human bone, which limits their use for load bearing applications. In fact Ca-Ps are too stiff and very brittle [15]. The fact is that today’s solutions of materials for bone replacement are still far from being ideal, being the metallic implants still the first choice for load-bearing applications, despite all the problems associated with stress-shielding and long term application. Although progress is currently being made, the right balance between surface and bulk properties of a material is still to be achieved. For the nearest future, one of the most interesting solutions is to use Ca-Ps with ideal bone tissue growth effects as coatings on the surface of load-bearing materials [8,13,16-20]. Ca-Ps disclose osteoconductive properties allowing for the formation of bone on its surface by attachment, migration, proliferation, and differentiation of bone-forming cells [19,21]. Therefore, despite their low mechanical properties, these types of coatings have great potential for bone fixation applications, or on scaffolds for tissue engineering. In fact, these coatings can be tailored in terms of chemical composition, crystallinity and resorbability [22,23] and also can be loaded with osteogenic biological molecules [24-26] or serve as beds for the seeding of living cells that will stimulate bone formation.

At the present the commercially available methods to produce such Ca-P of coatings are just a few and typically still the same proposed a decade ago, having several

disadvantages like difficulties on controlling the calcium-phosphate (Ca-P) layer composition, resorbability, weak adhesion to the substrates, the use of high temperatures or the costs of the process. Moreover, these methodologies are not effective on coating complex shapes. On the other hand new challenges are now being raised: to coat the interior of a porous material would be highly interesting when thinking about the fashionable concept of Tissue Engineering. These coatings would facilitate the cell attachment and proliferation in the interior of the scaffold, followed by the process of vascularization. For the last 30 years there has been a great amount of research in this particular area, to face the need of developing effective coating methodologies.

I.2. Evolution of the coating methodologies

In the history of bone replacement, various orthopaedic implant materials have been introduced, particularly metallic materials like stainless steel or titanium alloys [27]. Because a stable fixation of these implants to the bone was found to be critical to the long term stability in applications like joint replacement, an input was made for the development of different Ca-P coating methodologies to induce bone bonding ability and therefore, to create more stable interfaces [15,28].

The plasma-spraying technique is, to date, the major commercially available method, used for coating Ca-P on metallic implants [29-32]. The first coated implant was commercialized in 1980 by Valen [33]for dental applications. It is outstanding to imagine that the same technique is still being used, if we think on how much we have progressed from then (How would our life be if we were still using computers from that time?!). But the fact is that reproducibility and economic efficiency of the process are advantages, that made it famous from 20 years ago to nowadays [30,31]. However, this method presents some crucial drawbacks affecting the long-term performance and lifetime of the implant. The most significant are the poor coating-substrate adherence [31] and lack of uniformity of the coating in terms of morphology and crystallinity [32,34]. Since plasma-spraying is a high-temperature and line-of-sight process, there are also some aspects that were not solved yet, such as the deteriorating effect of intense heat on substrates, non-uniformity in coating density, wide range of band strength and limitation in coating implant devices with complex shapes [31,32,34].

Other studied approaches have been sputtering coating techniques that are able to increase the bond strength between the coating and the substrates [35-37]. However, the

drawback inherent to this technique is that the deposition and the process itself are very slow. By using a magnetically enhanced variant of radiofrequent sputtering, this problem can be solved but the endurance and the Ca/P ratio of the coating require further in vitro and in vivo studies before it can be applied routinely to produce crystalline pure Ca/P ceramic coatings on implant surfaces [10]. A collection of other methodologies have been proposed such as: dip coating sintering [38], chemical vapour deposition [39], sol-gel deposition [11,40], ion implanting [41] laser deposition [42-44], laser cladding [45] and electrochemical processes like electrophoretic deposition [46], electrocrystallization [47] and anode oxidation [48]. Despite of all the investigations carried out, the produced coatings can suffer from at least one of the following problems (that differ from method to method) [17]: lack of coating adherence to the substrate, thickness non-uniformity, poor structure integrity, and non-stoichiometric composition of the coatings. In fact, each of the above mentioned techniques has its own technical limitations, and so far, an optimal technique for producing physiologically stable and interfacially adherent apatite coatings has yet to be developed. Thus, there is a demand to develop new methods able to face new challenges like: to form an apatite layer with properties similar to those of bone calcium-phosphates on the surface of new emerging materials, on various complex shaped materials, that is capable to enhance biocompatibility as well as bioactivity, when engineering bone implants or designing tissue engineering scaffolds. On the other hand the ability to incorporate bioactive agents in these coatings can be a very promising therapeutic strategy for a site-specific delivery system for stimulating bone tissue regeneration.

I.3. Bioinspired coatings

The Ca-P minerals found in natural hard tissues are produced spontaneously in a physiological environment at low temperatures from moderately supersaturated mineralizing solutions [9]. In the recent years, there has been an increasing interest in the natural formation of Ca-Ps as a way to learn, understand and apply natural processes for producing Ca-P coatings biologically identical to bone apatite. The so-called biomimetic preparation of calcium phosphate coatings on implant materials as then emerged as a new concept. Rapid progress has been made in the development of these coatings and several methodologies have been proposed. This type of approach is particularly suitable to coat polymeric materials [16,49], as it can be carried out at low temperature reaction conditions.

I.3.1. The biomimetic methodology

A calcium phosphate coating was first grown on a substrate by a biomimetic process by Kokubo *et al.* [50] in 1990 using bioactive $CaO\text{-}SiO_2$-based glass particles that were set in contact with the substrates to induce apatite nucleation on their surface in a simulated body fluid (SBF) with ion concentrations nearly equal to those of the human blood plasma and at body temperature. This solution was developed also in 1990 by the same author [51]. Silicate ions containing silanol groups (Si-OH) are supposed to be released from the bioactive glass and adsorbed on the substrate surface to induce apatite formation. After one week (the time established for apatite nuclei to form a layer), the apatite grew subsequently by immersing the substrates in 1.5 SBF with ion concentrations 1.5 times higher of those of SBF. By this method, apatite layer has been coated on ceramics [50,52], metals [50,52] and polymers [50,52], such as alumina glass, zirconia, titanium, polyethylene, polymethylmethacrylate, ethylene-vinyl alcohol copolymer, polyethylene terephthalate (PET), poly(ethersulfone) (PES), polyamide (PA 6,6), poly(vinyl alcohol) and silicone. It was also shown that this apatite layer could be formed not only on flat surfaces but also on curved surfaces of small particles, long fibers and woven cloths of various materials [49,52].

The adhesion strength of the apatite layer to the polymeric (or other) surfaces by this process was, however, not sufficient for clinical applications [49]. Surface modifications, were then applied, prior to the biomimetic treatment, to improve the adhesion strength by increasing the amount of polar groups on the substrate surface [53-56]. These groups were found to act as favourable nucleating sites for apatite formation in the surface of the polymers. Various methods for surface modification of different polymers were reported by Kokubo and co-workers [53-56]. Chemical treatments with sodium hydroxide (NaOH) [53] or (hydrocloric acid) HCl [54] solutions before biomimetic coating have shown to improve the adhesion strength and to reduce the induction periods for apatite formation, being strictly dependent of the type of polymer. Surface modifications induced by a glow-discharge treatment [55] and ultraviolet irradiation (UV) [56] were also tested for the same polymers and similar effects were described.

An adaptation of the biomimetic methodology was also used by Reis *et al.* [57] in which the samples were rolled on a bed of wet bioactive glass particles before immersion in an SBF solution. The methodology was effective on coating different types of polymers and

shapes like a high molecular polyethylene [57], a biodegradable starch poly (ethylene vinyl alcohol) blend (SEVA-C) and a polyurethane foam [57]. Nevertheless, the same problem associated with a lack of coating adhesion was also observed. Therefore, different surface modifications are presently being experimented, some of which have already lead to some results. Surface treatments like potassium hydroxide (KOH), UV radiation and overexposure to ethylene oxide sterilization, on SEVA-C substrates, before to the biomimetic process have proved to be very effective in increasing the adhesion to the substrate and reducing the incubation periods for apatite formation [58].

Another way of tailoring the properties of apatite layer formed by the herein described biomimetic methodology is by the side of the solution, i.e. changing the composition of the SBF [59,60]. Kim *et al* [60] have reported that different apatite layers can be produced on polyethylene terephthalate (PET) substrates in solutions were the ion concentrations were changed from 0.75 to 2.00 times those of SBF. Increasing the ionic activity product has then resulted in lower Ca/P ratios of the apatites. The same author [59] have also reported that by increasing the carbonate ion content, apatites with composition and structure nearly identical to those of bone apatite could be produced. In fact, this solution is known to be deficient in relation to the HCO_3^- content, when comparing to the human blood plasma [59,61]. Therefore, this group is now proposing a new revised SBF (R-SBF) with an ion composition closer to the human blood plasma (higher amounts of HCO_3^-), to replace conventional SBF [61].

I.3.2. Other pre-mineralization routes

There is an enormous amount of published work [56,62-66] using other different biomimetic routes for the formation of apatite layers on the surface of different materials. Some of them are based in surface modifications, by chemical and physical means that are claimed to induce direct bioactivity in the surface of the materials [64-66]. Other methodologies use nucleating agents to induce the formation of the bioactive layer [56,63].

Bonelike apatite was successfully formed on organic polymers by a biomimetic process using sodium silicate solution as a nucleating agent, instead of bioactive glass particles, as reported by Miyaji *et al.* [63]. A dense apatite layer was formed not only on limited surfaces but also on whole surfaces of fine PET fibers constituting a fabric. Therefore, this method enabled to produce apatite coatings on various materials with complex shapes.

The “traditional” biomimetic process is not so effective on coating materials with complex shapes, since the apatite nuclei are formed only on the material surface which is facing the glass grains [63]. On the other hand it was also possible to reduce the incubating periods for apatite formation to only 6 hours [63].

The grafting technique has also become very popular as a way to immobilize functional groups at the surface of polymers that can encourage apatite formation. For instances, Oyane *et al.* [67] developed a different methodology in which ethylene-vinyl alcohol copolymer (EVOH) substrates were modified by grafting silane coupling agents at its surface, in order to produce silanol groups, like tetraethoxysilane (TEOS). Their apatite forming ability was examined in SBF and 1.5 SBF. Only in the later case it was possible to observe the formation of an apatite layer after 21 days [67]. Nevertheless, the Ca/P molar ratio of the apatite formed in 1.5 SBF was much lower than that of the apatite in the natural bone. Therefore, the same authors [68] tried also to incorporate calcium ions in the silicate phase, by using a calcium silicate solution prepared with the coupling agent. The release of these ions accelerated the apatite nucleation by increasing ionic activity product of the apatite locally near the surface [68]. Recently, Kim *et al.* [64] proposed a different methodology to incorporate silanol groups at a polyethylene substrate via photografting of vinyltrimethoxysilane and hydrolysis. The substrate modified in this way formed a dense and homogeneous bone-mineral-like apatite layer in a 1.5X SBF solution, after 7 days.

Tretinnikov *et al.* [62] developed a bioactive polymer by using also surface modification by grafting to immobilize organic compounds. An organophosphate polymer was chemically bound on to a polymer film by surface graft polymerization of a phosphate-containing monomer [62]. As the phosphate group is one of the building blocks of HA and has a high affinity toward calcium ions, polymeric materials modified by surface grafted water soluble organophosphate polymer induce bone deposition of Ca and PO_4 ions in the form of a hydroxy carbonate apatite (HCA) layer [62]. It is then expected that covalent immobilization of organophosphates will open the way for developing bioactive bone-bonding polymers.

More recently, Elvira, Reis *et al.* [69] have used plasma and chemical induced graft polymerization of different acrylic hydrophilic monomers on starch-based blends, in order to improve the cell adhesion and proliferation. After this treatment the materials were incubated in a solution of calcium chloride ($CaCl_2$). Subsequent immersion in a SBF solution, lead to the formation of an apatite layer after 15 days, for all surface

modifications. Furthermore, these treatments were also effective on improving the cell adhesion and proliferation with respect to the original starch based blends.

Another approach was used by Mucalo *et al.* [65] to coat apatite in cotton substrates, by grafting phosphate groups at the surface of the substrates using a phosphorylation methodology and subsequent SBF immersion. Yokogawa *et al.* [66] found that soaking in $Ca(OH)_2$ treated phosphorylated chitin fibers, also lead to the deposition of an apatite layer, after SBF immersion.

The Langmuir Blodgett (LB) technique, another very interesting approach, is a type of supramolecular assembly which can be used to produce an organic template with a specific head group for the nucleation of calcium phosphate crystals [64]. The LB process produces a thin organic film with a very organized structure, fulfilling the requirements of an organic template for a controlled mineralization process. Costa *et al.* [70], investigated apatite formation in SBF using a ω-tricosenoic acid monolayer film that was prepared by the LB method, using calcium carboxylate as a functional group. They reported that the nucleation of apatite was induced by carboxyl groups that reduced the interface energy between the nucleus and substrate. The morphology of the apatite crystals grown was strongly affected by the structure of the monolayer. It was further indicated the crystal orientation between the apatite and organic material took place *in vitro*, possibly due to the similar mechanisms observed in the biogenic materials [70].

Besides the use of SBF as a mineralizing environment, other biomimetic solutions have been developed for the formation of an apatite layer. For example, Taguchi *et al.* [71] developed an apatite formation process using hydrogels – an alternate soaking process – to form large amounts of apatite in SBF for a considerable short period of time (42 hours). The soakings have alternated every hour between $CaCl_2$ and di-hydrogen phosphate (H_2PO_4) solutions. The same methodology was also effectively applied by Furuzono *et al.* [72] to coat a silk fabric proposed as a biomaterial for bone replacement. Nevertheless, this methodology does not seem very practical since it requires a constant change of solutions every hour. Kim *et al.* [73] have used a simple method of coating thin films of low crystalline apatite crystals by using a filtrated solution containing calcium and phosphate ions to coat a poly(lactide-co-glicolide) copolymer sponge (PLGA). The material was coated by this process within 24 hours. The work of X. Yuan *et al.* [74], indicates that an apatite layer was formed in the surface of poly(L-lactic acid) (PLLA) after two weeks without the aid of a nucleating agent, by immersing the substrates in a solution inspired in SBF but with 1.5 times its ion concentration. S.-H. Rhee *et al.* [75,76], have shown that an

apatite layer could be formed in the surface of a collagen membrane after one week with the same 1.5X SBF solution, but to which citric acid was also added. This same solution is able to induce the formation of an apatite layer, after the same period, in the surface of a cellulose cloth [77]. The results therefore suggest that citric acid has a nucleating ability and can accelerate the nucleation of apatite on the non-bioactive studied substrates.

Recently, a new alternative methodology was proposed by Leonor, Reis *et al.* [78], through a novel auto-catalytic deposition process. The developed coating methodology uses a deposition route that is totally “electroless”, i.e., does not require the use of electric current application for its application, being based on redox reactions. It was possible to produce a Ca-P coating on the surface of three types of polymers (HMWPE, SCA, SEVA-C). Two types of solutions: “alkaline” and “acid” baths were studied to produce the novel proposed auto-catalytic Ca-P coatings. With these solutions well adherent apatite coatings could be formed on the surface of both biodegradable and bionert polymers [78]. The developed route seems to be a very promising and simple methodology for being used as a pre-implantation treatment to coat several types of materials previously to their clinical application.

Herein are just described some examples that can well illustrate the variety of possibilities that can be explored when using/developing a biomimetic approach. All these surface modifications and pre-mineralization routes described before can play an important role in enhancing the biocompatibility and bioactivity of a biomaterial, particularly polymers. In fact cells are sensitive to several surface properties such as roughness, energy, chemistry and even to more subtle characteristics such as relative crystallinity.

It is possible to find several advantages of the biomimetic approach over the methodologies previously described. In fact, a biomimetic coating is expected to show higher bone-bonding ability due to its similarity to the mineral of bone. On the other hand, the adhesion to the substrate can be enhanced by means of several methodologies or by different surface pre-treatments. Tailored apatite coatings with different Ca/P ratios and crystallinities are also possible to be obtained. Another very important advantage is that no adverse effect of heat on substrate occurs, since these methodologies work at operating temperatures, which allow them to be applied to a range of different materials such as biodegradable polymers. It is also the simplest and more cost effective of the approaches available to create a biological-like apatite layer. Taking advantage of all this, different biomimetic approaches are being developed by our group to be able to effectively

coat a range of bioinert and biodegradable polymers processed into a large variety of shapes for bone related applications.

I.4. Coating starch based biodegradable polymers

Bone-like calcium phosphate coatings have a great potential when applied to biodegradable polymers since they can stimulate the tissue regeneration at the interface bone/implant, while the material is being resorbed (ideally at the same rate that bone is being formed). To achieve this ideal synchronized behaviour, being the stress slowly transferred from implant to bone, has been the main goal for scientists in this area.

Starch-based polymers are particularly interesting for bone related applications (replacement, tissue engineering scaffolding, etc). Besides being biodegradable, inexpensive (when compared to other biodegradable polymers such as polylactic acid) and available in large quantities [79-81], starch-based polymers can be converted into complex geometries that exhibit interesting mechanical properties, by using standard equipment developed for the processing of synthetic polymers or by means of using distinct innovative methodologies. Furthermore, in addition to their processing versatility, they exhibit a biocompatible behaviour, already demonstrated by *in vitro* [82-84] and in vivo studies [85]. Therefore, they are under consideration for a wide range of biomedical applications like bone replacement/fixation [86,87], novel hydrogels and partially degradable bone cements [88,89], drug delivery carriers [89,90] or temporary scaffolds for tissue engineering applications [90,91].

In case of bone related applications like tissue replacement/fixation, or tissue engineering scaffolds to be applied in load-bearing sites, these systems must exhibit mechanical properties that match those of human bone, associated to degradation kinetics adequate to the healing of the tissues to be replaced or fixed [92]. It was reported by our group that the physical and mechanical properties of these materials could be optimized by controlling the morphologic developments within the moulds, using non-conventional processing routes [93,94]. On the other hand, the incorporation of bone-like inorganic fillers, such as hydroxylapatite (HA) [95,96] or bioactive glasses [97] is another interesting approach, allowing for the development of degradable composites that can combine an attractive range of mechanical properties with the so-desirable bone-bonding behaviour. Since the essential condition for materials to bond to living bone is the formation of a

biologically active bone-like apatite layer on their surfaces different coating methodologies are also being developed through biomimetic processes for producing such type of layers on the proposed materials [57,58]. Finally, a novel emerging application is also currently being proposed, on which starch based polymers would serve as temporary scaffolds for the transplanted cells to attach, grow and maintain differentiated functions in a range of tissue engineering applications [90,91]. In fact it was already possible to develop distinct porous architectures based on these starch based biodegradable blends [90,98] by means of using different and innovative processing routes either based on melt-processing technologies [98] or on microwave baking [90] and subsequently to produce biomimetic coatings on these materials that are not only aimed at enhancing cell adhesion and proliferation but also tissue ingrowth.

I.4.1. Sodium silicate as a precursor for a Ca-P coating

As mentioned before, when considering materials with complex shapes, such as porous 3D architectures, the traditional biomimetic methodology is not so effective. This can be explained by the considerable difficulty on forming an apatite coating, since the apatite nuclei will preferentially grow in the surfaces which are facing the bioactive glass particles. In order to overcome this obstacle a new biomimetic methodology to produce bioactive coatings on the surface of starch based or other polymeric biomaterials is being proposed by Oliveira *et al.* [99], using a sodium silicate gel as alternative nucleating agent. Sodium silicate gel can reach inside the pores of porous 3D architectures to be used on tissue replacement and in tissue engineering scaffolding. This new methodology is aimed at [99]: (i) reducing the incubation periods; (ii) improving of the adhesion strength between the coating and substrate; (iii) being able to coat the inside of pores in porous 3D architectures to be used on tissue replacement and as tissue engineering scaffolds; (iv) producing Ca-P layers with different (tailored) Ca-P ratios.

The studied materials included typically different starch based blends processed into different shapes. To produce the bioactive coatings the materials were “impregnated” with a commercially available sodium silicate gel, that acted as an alternative Ca-P nucleating agent. After the sodium silicate treatment the samples were soaked in a simulated body fluid (SBF) at 37 ºC. After 7 days the ion concentration of SBF solution was raised to 1.5X in order to make the apatite nuclei to grow. The procedure is schematized in figure 1.

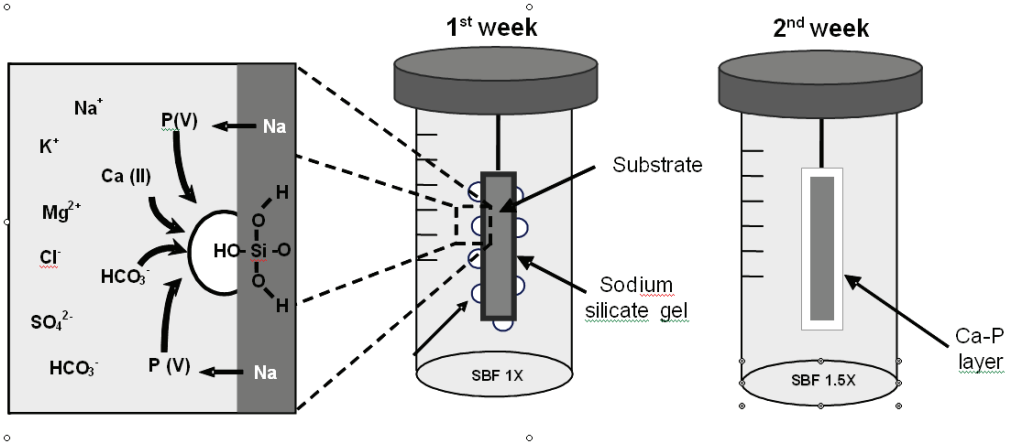


Figure 1. Schematic representation of the sodium silicate gel biomimetic methodology. Adapted from the procedure developed by Kokubo *et al.* [50,51] and adapted by Reis *et al.* [99,100].

Figure 2 shows the water-uptake versus time for SEVA-C compact and porous structures, untreated and treated with sodium silicate.

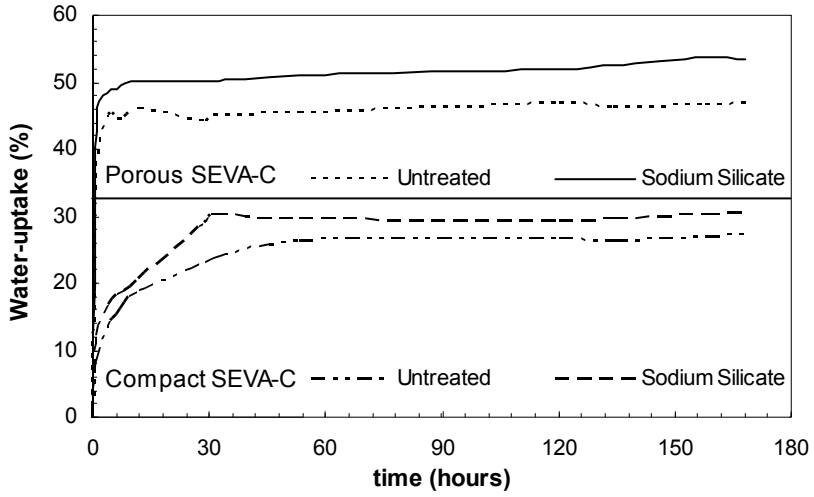


Figure 2. Water-uptake (%) versus time for untreated and sodium silicate treated compact and porous SEVA-C samples.

For compact structures, the equilibrium hydration degree of untreated samples is about 25%, after 50 hours. This hydrophilic behaviour is mainly a result of the presence of starch and vinyl alcohol hydroxyl groups, as it has been previously described [58,101]. Untreated porous structures achieve the equilibrium hydration degree, around 45%, after the first 10 hours of water uptaking. This higher hydrophilicity may result from the existence of high amounts of polar groups available in the structure after reaction of hydrogen peroxide with starch. On the other hand, porous structures have a higher specific surface then compact ones, which allows for a higher water-uptake. With sodium silicate treatment the amount of water uptaked increases around 5% in both types of structures, being this observation more significant in the case of the compact material. The materials used as controls

(compact HMWPE and porous PU) did not uptake water after sodium silicate treatment (Data not shown).

I.4.1.1. Apatite formation

After immersion in SBF for several periods, the formation of an apatite layer was studied. Figure 3. shows the SEM photographs of the evolution of the typical films formed on the surface of the treated materials.

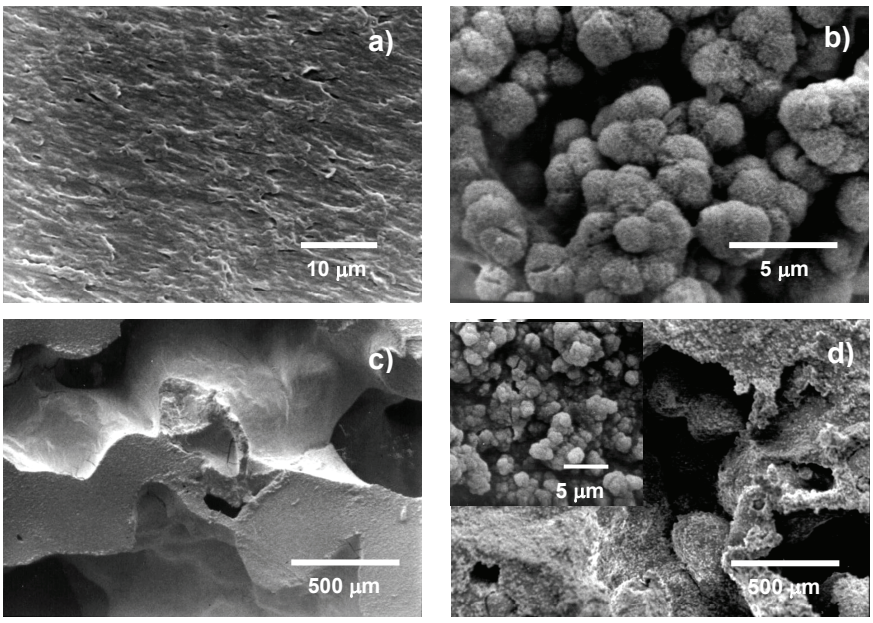


Figure 3. SEM micrographs of: compact SEVA-C treated with a) sodium silicate and after b) 30 days of immersion in SBF and porous SEVA-C treated with c) sodium silicate and after d) 30 days of immersion in SBF.

In sodium silicate treated materials only after 6 hours of immersion in SBF it was possible to observe the formation of very cohesive apatite-like layers that became fragmented due to the swelling of the polymers (Data not shown) [99]. For the porous materials, the apatite layer could be also observed inside the pores, clearing covering the cell walls. When comparing with the traditional biomimetic treatment, the later was not so effective on reaching the bulk of porous structures. This result is very promising for the developing of cancellous bone replacement materials and for pre-calcifying bone tissue engineering scaffolds. For the SEVA-C compact material the corresponding Ca/P ratios for the apatite formed in this earlier stage of nucleation is around 1.5, which is typical of tri-calcium

phosphate (TCP). After 30 days the morphology of the layers tended to develop to the so-called cauliflower morphology [57], which is clearly showed in both compact and porous structures. On the other hand, the respective Ca/P ratios are very close to the value attributed to hydroxyapatite (1.67). The biomimetic methodology proposed in this case lead to an increasing on the water-uptake ability of the polymers (Figure 1), allowing the materials to absorb higher quantities of Ca^{2+} ions from the SBF solution. As a consequence, the Ca^{2+} ion concentration in the surface will be increased, leading to the formation of additional nucleating sites for the Ca-P coating formation. On the other hand, the increase of the surface hydrophilicity (data not shown) [99] raising the amount of polar groups in the surface could be a contribute to the formation of silanol groups that are well known apatite inductors. This theory has been previously described by Kokubo *et al.* [16,49,51]. Figure 4 presents the TF-XRD patterns of the surface of compact (Figure 4.a) and porous (Figure 4.b) SEVA-C, before and after immersion in SBF.

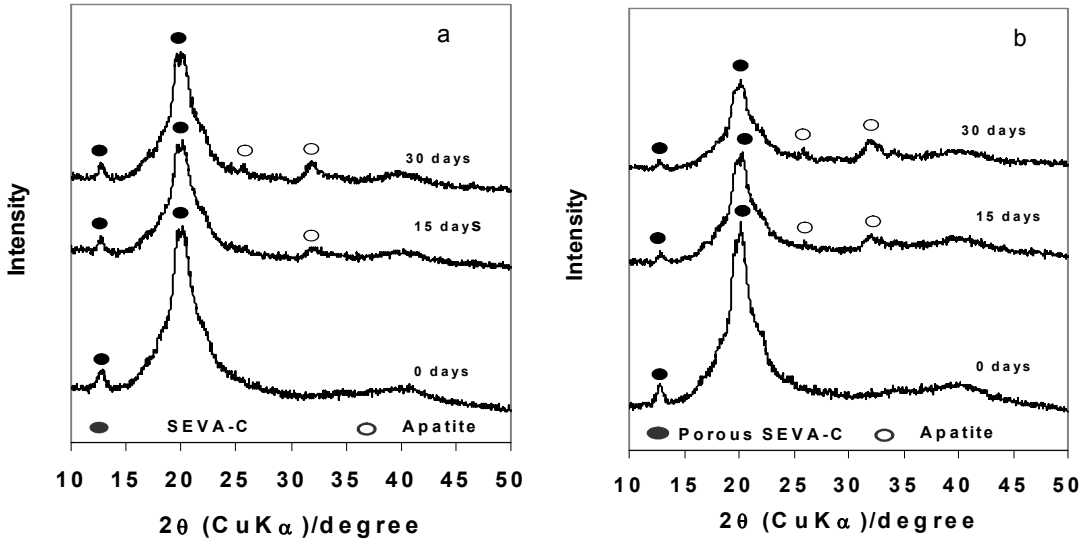


Figure 4. Thin-film X-ray diffraction spectra of the films formed after treatment with sodium silicate. a) Compact and b) porous SEVA-C after 0, 15 and 30 days of immersion SBF.

TF-XRD spectra exhibited the formation of a partially amorphous Ca-P film with the crystalline peaks mainly corresponding to hydroxylapatite, for the longer SBF immersion periods. On materials used as controls (compact HMWPE and porous PU) it was not possible to observe apatite formation (data not shown) [99], which have indicated that this methodology is only highly adequate for materials that have a strong swelling ability. In this case, even with the correspondent difficulties associated to biodegradable polymers raising from continuous pH and surface changes as function of time, the methodology was successful on generating Ca-P coatings.

I.4.1.2. Cell adhesion

Figures 5 shows the SEM micrographs of the morphology of SEVA-C surface after immersion in SBF for 15 days and subsequent SaOs-2 cell culturing for the first 24 hours.

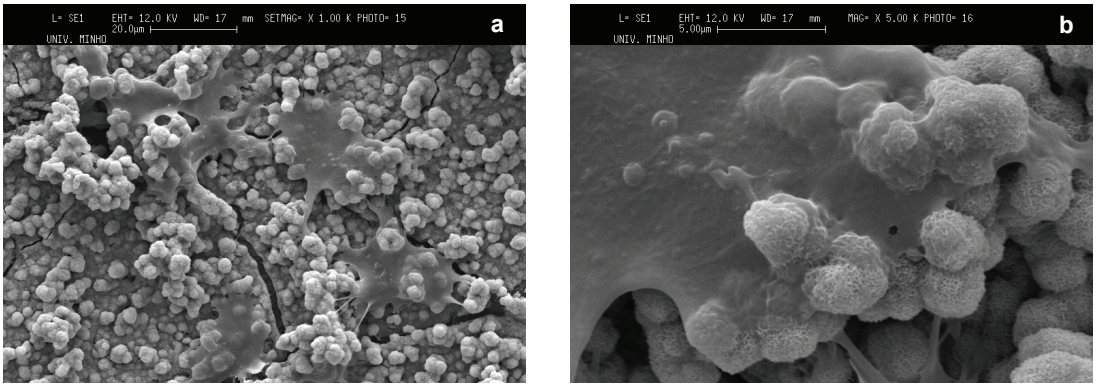


Figure 5. SEM micrographs showing the morphology of the apatite coatings formed on the surface of SEVA-C and the typical aspect of the SaOs-2 cells adhered to it after 24 h of cell culturing.

In the presented figures is possible to observe that the apatite layer is formed by aggregates of nucleus that have grown into the previously described *cauliflower* morphology [57,58] , after 15 days of immersion in SBF (please remember that SBF concentration was raised to 1.5x after 7 days).

On what concerns to the study of cell adhesion it is possible to observe, on the same SEM micrographs (Figure 5.a and 5.b), that these preliminary results indicate good cell attachment to both types of coated surfaces. In fact, the crystallinity of a biomaterial surface is known to determine specific cell responses like the organisation of cytoskeleton filaments and cell proliferation mechanisms [102,103]. Furthermore, it can be said that SBF treatment or more specifically, the obtained characteristics of the coatings, influence positively cell proliferation kinetics (data not shown) [104]. In this study cell behaviour seems to depend on coatings crystallinity being slower for more amorphous surfaces.

I.5. New opportunities for coated materials

One of the most promising characteristics of several biomimetic methodologies is that they can be suitable to produce apatite coatings onto complex-shaped materials [16,100,105]. As a result, there are new opportunities for these types of coatings in the field of tissue engineering, as a way to enhance the formation of bone tissue. Some possibilities are

presently being considered, based on the incorporation of osteogenic biological molecules in the biomimetic coatings [24,26,106,107]. Due to the physiological coating conditions presented by some methodologies it is expected that these bioactive factors can preserve their biological activities. Therefore, considering the slow, but definite degradation of such coatings [9,108-110], they may be very suitable to serve as carriers for these molecules. The options for creating a delivery system in these coatings are numerous.
Certain molecules like protein growth factors can regulate various cell functions such as growth, differentiation, secretion, and apoptosis [111]. Bone morphogenic proteins (BMPs) are an important class of bone growth factors that might revolutionize how clinicians treat such diverse orthopaedic applications as the healing of broken bones or increasing bone density lost through aging [111-113]. Murphy et al [107] developed a system for sustained release of a bioactive vascular endothelial growth factor from poly(lactide-co-glycolide) scaffolds. These scaffolds were previously mineralized in a SBF solution [114]. For example, De Bruijn *et al*. [115] reported that by a co-precipitation process it was possible to incorporate a bone morphogenic protein, rhBMP2, in an apatite coating on a Ti alloy substrate.

A more biologically driven approach involves the addition to the apatite layer of living osteogenic cells to create an autologous bone-graft substitute. Due to the similarity of the formed layers with bone mineral, they represent friendly surfaces for cell attachment and proliferation which subsequently, will stimulate the formation of bone tissue either ex vivo or after implantation. Studies developed by de Bruijn *et al.* [115] show that rat-, goat- and human-derived bone marrow cells can be expanded in vitro and maintain their osteogenic potential in vitro and in vivo when grown under specific osteogenic culture conditions. These results indicate that new developments such as bone tissue engineering are promising to obtain a whole new generation of osteoinductive implant coatings derived from patients own tissues.

I.6. Conclusions

A number of biomimetic coating routes are presently being developed in order to produce Ca-P layers on orthopaedic implants and tissue engineering scaffolds.

The Ca-P minerals in natural hard tissues are formed in a physiological environment at low temperatures from moderately supersaturated mineralizing solutions. Therefore, in the recent years, there has been an increasing interest in the so-called biomimetic preparation

of calcium phosphate coatings on implant materials, in contrast to the major commercially available method in use nowadays, which is still the plasma spraying technique. Rapid progress has been made in the development of these bioinspired coatings and several methodologies have emerged. This approach is particularly suitable to coat polymeric materials (as it can be carried out at low temperature reaction conditions) and complex-shaped scaffolds for tissue engineering. Furthermore, other possibilities are presently being considered based on the incorporation of bioactive factors in the biomimetic coatings, like osteogenic biological molecules. The herein presented biomimetic methodology, using a sodium silicate gel as nucleating agent, was successfully developed and allowed to produce a well-defined calcium-phosphate layer on the surface of a starch based biodegradable polymer. With this treatment it was possible not only to reduce the induction period for the formation of a well defined apatite-like layer. Furthermore, when applied to porous materials, this methodology was highly effective, since a clear apatite-like layer was observed inside the pores, clearly covering the pore walls. It also can be said that the obtained characteristics of the coatings, influence positively cell adhesion and proliferation kinetics. This proposed route is quite simple and very promising for developing cancellous bone replacement materials and for pre-calcifying bone tissue engineering scaffolds.

References

1. Getter L., Bhaskar S. CD, Perez B., Brady J., Driskell T., O´Hara M. Three Biodegradable Calcium Phosphate Slurry Implants in Bone. Journal of Oral and Maxillofacial Surgery 1972;30:263-268.
2. Peelen J., Rejda B. VJ, de Groot K. Sintered Tricalcium Phosphate as Bioceramic. Science of Ceramics 1977;9:226-236.
3. Jarcho M., Kay J. GK, Doremus R., Drobeck H. Tissue, cellular and subcellular events at a bone-ceramic hydroxyapatite interface. Journal of Bioengineering 1977;1:79-92.
4. Roy D., S. L. Hydroxyapatite formed from coral skeletal carbonate by hydrothermal change. Nature 1974;247:220-222.
5. Delecrin J, Daculsi G, Passuti N, Duquet B. Specific Resorbable Calcium-Phosphate Coating to Enhance Osteoconduction. Cells and Materials 1994;4(1):51-62.
6. Bohner M. Calcium orthophosphates in medicine: from ceramics to calcium phosphate cements. Injury-International Journal of the Care of the Injured 2000;31:S37-S47.
7. Driessens FC. Physiology of Hard Tissues in Comparison With the Solubility of Synthetic Calcium Phosphates. In: P. Ducheyne JEL, editor. Bioceramics: Materials Characterizations versus In Vivo Behaviour. New York: Academy of Sciences; 1988. p 131.
8. J. C. Heughebaert GB. Composition, Structures and Properties of Calcium Phosphates of Biological Interest. In: P. Christel AM, A. J. C. Lee, editor. Biological and Biomechanical Performance of Biomaterials. Amsterdam: Elsevier Science Publishers; 1986.
9. Rey C. Calcium Phosphate Biomaterials and Bone Mineral. Differences in Composition, Structures and Properties. Biomaterials 1990;11:13.
10. Cao WP, Hench LL. Bioactive materials. Ceramics International 1996;22(6):493-507.
11. Ducheyne P, Hench LL. The Processing and Static Mechanical-Properties of Metal Fiber Reinforced Bioglass. Journal of Materials Science 1982;17(2):595-606.
12. Hench LL. Bioceramics. Journal of the American Ceramic Society 1998;81(7):1705-1728.

13. Hench LL, Wilson J. Surface-Active Biomaterials. Science 1984;226(4675):630-636.
14. Barralet JE, Best SM, Bonfield W. Effect of sintering parameters on the density and microstructure of carbonate hydroxyapatite. Journal of Materials Science-Materials in Medicine 2000;11(11):719-724.
15. Hench LL. Bioceramics - from Concept to Clinic. Journal of the American Ceramic Society 1991;74(7):1487-1510.
16. Kokubo T, Kim HM, Kawashita M, Nakamura T. Process of calcification on artificial materials. Z Kardiol 2001;90 Suppl 3:86-91.
17. Thomas KA. Hydroxyapatite Coatings. Orthopedics 1994;17(3):267-278.
18. Greenspan DC. Bioactive ceramic implant materials. Current Opinion in Solid State & Materials Science 1999;4(4):389-393.
19. Ducheyne P, Qiu Q. Bioactive ceramics: the effect of surface reactivity on bone formation and bone cell function. Biomaterials 1999;20(23-24):2287-2303.
20. Ratner BD, Hoffman, A.S. Thin films, Grafts and Coatings. In: Ratner BD, Hoffman, A. S., Schoen, F. J., Lemnons, J. E., editor. Biomaterial Science. San Diego: Academic Press; 1996. p 105-118.
21. Kanazawa T. General Background on Phosphate Materials. Amsterdam: Elsevier; 1989. 1 p.
22. Tanahashi M, Matsuda T. Surface functional group dependence on apatite formation on self-assembled monolayers in a simulated body fluid. J Biomed Mater Res 1997;34(3):305-15.
23. ter Brugge PJ, Wolke JGC, Jansen JA. Effect of calcium phosphate coating crystallinity and implant surface roughness on differentiation of rat bone marrow cells. Journal of Biomedical Materials Research 2002;60(1):70-78.
24. Liu Y, Hunziker EB, Randall NX, de Groot K, Layrolle P. Proteins incorporated into biomimetically prepared calcium phosphate coatings modulate their mechanical strength and dissolution rate. Biomaterials 2003;24(1):65-70.
25. Wen HB, Moradian-Oldak J. Modification of calcium-phosphate coatings on titanium by recombinant amelogenin. Journal of Biomedical Materials Research Part A 2003;64A(3):483-490.
26. Leonor IB, Azevedo HS, Alves CM, Reis RL. Effects of the incorporation of proteins and active enzymes on biomimetic calcium-phosphate coatings. Bioceramics 15 2003;240-2:97-100.
27. Silver FH. Scope and Markets for Medical Implants. In: Silver FH, editor. Biomaterials, Medical Devices and Tissue Engineering: An Integrated Approach. London: Chapman & Hall; 1994. p 2.
28. Puleo DA, Nanci A. Understanding and controlling the bone-implant interface. Biomaterials 1999;20(23-24):2311-2321.
29. Kohn DH. Metals in medical applications. Current Opinion in Solid State & Materials Science 1998;3(3):309-316.
30. Weng J, Liu Q, Wolke JGC, Zhang XD, deGroot K. Formation and characteristics of the apatite layer on plasma-sprayed hydroxyapatite coatings in simulated body fluid. Biomaterials 1997;18(15):1027-1035.
31. Zheng XB, Huang MH, Ding CX. Bond strength of plasma-sprayed hydroxyapatite/Ti composite coatings. Biomaterials 2000;21(8):841-849.
32. Gledhill HC, Turner IG, Doyle C. In vitro dissolution behaviour of two morphologically different thermally sprayed hydroxyapatite coatings. Biomaterials 2001;22(7):695-700.
33. Valen M. The relationship between endosteal implant design and function: maximum stress distribution with computer-formed, three dimensional Flexi-Cup blades. J Oral Implantol 1983;11(1):49-71.
34. Fazan F, Marquis PM. Dissolution behavior of plasma-sprayed hydroxyapatite coatings. Journal of Materials Science-Materials in Medicine 2000;11(12):787-792.
35. Yamashita K, Yagi T, Umegaki T. Bonelike coatings onto ceramics by reactive magnetron sputtering. Journal of the American Ceramic Society 1996;79(12):3313-3316.
36. Wang CX, Chen ZQ, Wang M, Liu ZY, Wang PL, Zheng SX. Functionally graded calcium phosphate coatings produced by ion beam sputtering/mixing deposition. Biomaterials 2001;22(12):1619-1626.
37. Burke EM, Haman JD, Weimer JJ, Cheney AB, Rigsbee JM, Lucas LC. Influence of coating strain on calcium phosphate thin-film dissolution. Journal of Biomedical Materials Research 2001;57(1):41-47.

38. Kim CS, Ducheyne P. Compositional Variations in the Surface and Interface of Calcium-Phosphate Ceramic Coatings on Ti and Ti-6al-4v Due to Sintering and Immersion. Biomaterials 1991;12(5):461-469.
39. Hamdi M, Ide-Ektessabi A. Preparation of hydroxyapatite layer by ion beam assisted simultaneous vapor deposition. Surface & Coatings Technology 2003;163:362-367.
40. Peltola T, Patsi M, Rahiala H, Kangasniemi I, Yli-Urpo A. Calcium phosphate induction by sol-gel-derived titania coatings on titanium substrates in vitro. Journal of Biomedical Materials Research 1998;41(3):504-510.
41. Hanawa T, Ukai H, Murakami K, Asaoka K. Structure of Surface-Modified Layers of Calcium-Ion-Implanted Ti-6al-4v and Ti-56ni. Materials Transactions Jim 1995;36(3):438-444.
42. Mayor B, Arias J, Chiussi S, Garcia F, Pou J, Fong BL, Perez-Amor M. Calcium phosphate coatings grown at different substrate temperatures by pulsed ArF-laser deposition. Thin Solid Films 1998;317(1-2):363-366.
43. Fernandez-Pradas JM, Cleries L, Sardin G, Morenza JL. Characterization of calcium phosphate coatings deposited by Nd : YAG laser ablation at 355 nm: influence of thickness. Biomaterials 2002;23(9):1989-1994.
44. Fernandez-Pradas JM, Sardin G, Cleries L, Serra P, Ferrater C, Morenza JL. Deposition of hydroxyapatite thin films by excimer laser ablation. Thin Solid Films 1998;317(1-2):393-396.
45. Lusquinos F, Pou J, Arias JL, Larosi M, de Carlos A, Leon B, Amor MP, Best S, Bonfield W, Driessens FCM. Laser surface cladding: A new promising technique to produce calcium phosphate coatings. Bioceramics 14 2002;218-2:187-190.
46. Zhitomirsky I. Electrophoretic hydroxyapatite coatings and fibers. Materials Letters 2000;42(4):262-271.
47. Shirkhanzadeh M. Calcium-Phosphate Coatings Prepared by Electrocrystallization from Aqueous-Electrolytes. Journal of Materials Science-Materials in Medicine 1995;6(2):90-93.
48. Ishizawa H, Ogino M. Hydrothermal precipitation of hydroxyapatite on anodic titanium oxide films containing Ca and P. Journal of Materials Science 1999;34(23):5893-5898.
49. Tanahashi M, Yao T, Kokubo T, Minoda M, Miyamoto T, Nakamura T, Yamamuro T. Apatite Coating on Organic Polymers by a Biomimetic Process. Journal of the American Ceramic Society 1994;77(11):2805-2808.
50. Abe Y, Kokubo T, Yamamuro T. Apatite Coating on Ceramics, Metals and Polymers Utilizing a Biological Process. Journal of Materials Science-Materials in Medicine 1990;1(4):233-238.
51. Kokubo T, Kushitani H, Sakka S, Kitsugi T, Yamamuro T. Solutions able to reproduce in vivo surface-structure changes in bioactive glass-ceramic A-W. J Biomed Mater Res 1990;24(6):721-34.
52. Hata K, Kokubo T, Nakamura T, Yamamuro T. Growth of a Bonelike Apatite Layer on a Substrate by a Biomimetic Process. Journal of the American Ceramic Society 1995;78(4):1049-1053.
53. Tanahashi M, Yao T, Kokubo T, Minoda M, Miyamoto T, Nakamura T, Yamamuro T. Apatite coated on organic polymers by biomimetic process: improvement in its adhesion to substrate by NaOH treatment. J Appl Biomater 1994;5(4):339-47.
54. Tanahashi M, Yao T, Kokubo T, Minoda M, Miyamoto T, Nakamura T, Yamamuro T. Apatite Coated on Organic Polymers by Biomimetic Process - Improvement in Adhesion to Substrate by Hcl Treatment. Journal of Materials Science-Materials in Medicine 1995;6(6):319-326.
55. Tanahashi M, Yao T, Kokubo T, Minoda M, Miyamoto T, Nakamura T, Yamamuro T. Apatite coated on organic polymers by biomimetic process: improvement in its adhesion to substrate by glow-discharge treatment. J Biomed Mater Res 1995;29(3):349-57.
56. Liu GJ, Miyaji F, Kokubo T, Takadama H, Nakamura T, Murakami A. Apatite organic polymer composites prepared by a biomimetic process: improvement in adhesion of the apatite layer to the substrate by ultraviolet irradiation. Journal of Materials Science-Materials in Medicine 1998;9(5):285-290.
57. Reis RL, Cunha AM, Fernandes MH, Correia RN. Treatments to induce the nucleation and growth of apatite-like layers on polymeric surfaces and foams. Journal of Materials Science-Materials in Medicine 1997;8(12):897-905.

58. Oliveira AL, Elvira, C., Vásquez, B., San Roman, J., Reis, R. L. Surface Modifications Tailors the Characteristics of Biomimetic Coatings Nucleated on Starch Based Polymers. Journal of Materials Science: Materials in Medicine 1999;10:827.
59. Kim HM, Kishimoto K, Miyaji F, Kokubo T, Yao T, Suetsugu Y, Tanaka J, Nakamura T. Composition and structure of the apatite formed on PET substrates in SBF modified with various ionic activity products. J Biomed Mater Res 1999;46(2):228-35.
60. Kim HM, Kishimoto K, Miyaji F, Kokubo T, Yao T, Suetsugu Y, Tanaka J, Nakamura T. Composition and structure of apatite formed on organic polymer in simulated body fluid with a high content of carbonate ion. Journal of Materials Science-Materials in Medicine 2000;11(7):421-426.
61. Oyane A, Kim HM, Furuya T, Kokubo T, Miyazaki T, Nakamura T. Preparation and assessment of revised simulated body fluids. J Biomed Mater Res 2003;65A(2):188-95.
62. Tretinnikov ON, Kato K, Ikada Y. In-Vitro Hydroxyapatite Deposition onto a Film Surface-Grafted with Organophosphate Polymer. Journal of Biomedical Materials Research 1994;28(11):1365-1373.
63. Miyaji F, Kim HM, Handa S, Kokubo T, Nakamura T. Bonelike apatite coating on organic polymers: novel nucleation process using sodium silicate solution. Biomaterials 1999;20(10):913-919.
64. Kim HM, Uenoyama M, Kokubo T, Minoda M, Miyamoto T, Nakamura T. Biomimetic apatite formation on polyethylene photografted with vinyltrimethoxysilane and hydrolyzed. Biomaterials 2001;22(18):2489-2494.
65. Mucalo MR, Yokogawa Y, Toriyama M, Suzuki T, Kawamoto Y, Nagata F, Nishizawa K. Growth of Calcium-Phosphate on Surface-Modified Cotton. Journal of Materials Science-Materials in Medicine 1995;6(10):597-605.
66. Yokogawa Y, Reyes JP, Mucalo MR, Toriyama M, Kawamoto Y, Suzuki T, Nishizawa K, Nagata F, Kamayama T. Growth of calcium phosphate on phosphorylated chitin fibres. Journal of Materials Science-Materials in Medicine 1997;8(7):407-412.
67. Oyane A, Minoda M, Miyamoto T, Takahashi R, Nakanishi K, Kim HM, Kokubo T, Nakamura T. Apatite formation on ethylene-vinyl alcohol copolymer modified with silanol groups. J Biomed Mater Res 1999;47(3):367-73.
68. Oyane A, Kawashita M, Nakanishi K, Kokubo T, Minoda M, Miyamoto T, Nakamura T. Bonelike apatite formation on ethylene-vinyl alcohol copolymer modified with silane coupling agent and calcium silicate solutions. Biomaterials 2003;24(10):1729-35.
69. Oliveira AL, Leonor IB, Elvira C, Azevedo MC, Pashkuleva I, Reis RL. Surface Treatments and Pre-calcification Routes to Enhance Cell Adhesion and Proliferation. In: Reis RL, Cohn D, editors. Polymer Based Systems on Tissue Engineering, Replacement and Regeneration. Drodercht: Kluwer Press; 2002. p 183-217.
70. Costa N, Maquis PM. Biomimetic processing of calcium phosphate coating. Medical Engineering & Physics 1998;20(8):602-606.
71. Taguchi T, Muraoka Y, Matsuyama H, Kishida A, Akashi M. Apatite coating on hydrophilic polymer-grafted poly(ethylene) films using an alternate soaking process. Biomaterials 2001;22(1):53-58.
72. Furuzono T, Taguchi T, Kishida A, Akashi M, Tamada Y. Preparation and characterization of apatite deposited on silk fabric using an alternate soaking process. Journal of Biomedical Materials Research 2000;50(3):344-352.
73. Kim HM, Kim Y, Park SJ, Rey C, Lee HM, Glimcher MJ, Ko JS. Thin film of low-crystalline calcium phosphate apatite formed at low temperature. Biomaterials 2000;21(11):1129-1134.
74. Yuan XY, Mak AFT, Li JL. Formation of bone-like apatite on poly(L-lactic acid) fibers by a biomimetic process. Journal of Biomedical Materials Research 2001;57(1):140-150.
75. Rhee SH, Tanaka J. Hydroxyapatite coating on a collagen membrane by a biomimetic method. Journal of the American Ceramic Society 1998;81(11):3029-3031.
76. Rhee SH, Tanaka J. Effect of citric acid on the nucleation of hydroxyapatite in a simulated body fluid. Biomaterials 1999;20(22):2155-2160.
77. Rhee SH, Tanaka J. Hydroxyapatite formation on cellulose cloth induced by citric acid. Journal of Materials Science-Materials in Medicine 2000;11(7):449-452.
78. Leonor IB, Reis RL. An innovative auto-catalytic deposition route to produce calcium-phosphate coatings on polymeric biomaterials. Journal of Materials Science-Materials in Medicine 2003;14(5):435-441.
79. Galliard T. Starch: properties and potential. New-York: John Wiley & Sons; 1987.

80. Andreopoulos AG, Theophanides T. Degradable Plastics - a Smart Approach to Various Applications. Journal of Elastomers and Plastics 1994;26(4):308-326.
81. Poutanen K, Forssell P. Modification of starch properties with plasticizers. Trends in Polymer Science 1996;4(4):128-132.
82. Gomes ME, Reis RL, Cunha AM, Blitterswijk CA, de Bruijn JD. Cytocompatibility and response of osteoblastic-like cells to starch-based polymers: effect of several additives and processing conditions. Biomaterials 2001;22(13):1911-7.
83. Marques AP, Reis RL, Hunt JA. The biocompatibility of novel starch-based polymers and composites: in vitro studies. Biomaterials 2002;23(6):1471-8.
84. Mendes SC, Bezemer J, Claase MB, Grijpma DW, Bellia G, Degli-Innocenti F, Reis RL, De Groot K, Van Blitterswijk CA, De Bruijn JD. Evaluation of two biodegradable polymeric systems as substrates for bone tissue engineering. Tissue Engineering 2003;9:S91-S101.
85. Mendes SC, Reis RL, Bovell YP, Cunha AM, van Blitterswijk CA, de Bruijn JD. Biocompatibility testing of novel starch-based materials with potential application in orthopaedic surgery: a preliminary study. Biomaterials 2001;22(14):2057-64.
86. Reis RL, Cunha A. M. Characterization of two biodegradable polymers of potential application within the biomaterials field. Journal of Materials Science: Materials in Medicine 1995;6:786-792.
87. Reis R. L. CAM, Allan P. S., Bevis M. J. Mechanical behaviour of injection-moulded starch based polymers. Polymer Advanced Technology 1996;7:784-790.
88. Elvira C, Mano JF, San Roman J, Reis RL. Starch-based biodegradable hydrogels with potential biomedical applications as drug delivery systems. Biomaterials 2002;23(9):1955-66.
89. Pereira C. S. CAM, Reis R. L., Vázquez B., San Roman J. New starch-based thermoplastic hydrogels for use as bone cements or drug-delivery carriers. Journal of Materials Science: Materials in Medicine 1998;9:825-33.
90. Malafaya PB, Elvira C, Gallardo A, San Roman J, Reis RL. Porous starch-based drug delivery systems processed by a microwave route. J Biomater Sci Polym Ed 2001;12(11):1227-41.
91. Gomes ME, Ribeiro AS, Malafaya PB, Reis RL, Cunha AM. A new approach based on injection moulding to produce biodegradable starch-based polymeric scaffolds: morphology, mechanical and degradation behaviour. Biomaterials 2001;22(9):883-9.
92. Demirgoz D, Elvira C, Mano JF, Cunha AM, Piskin E, Reis RL. Chemical modification of starch based biodegradable polymeric blends: effects on water uptake, degradation behaviour and mechanical properties. Polymer Degradation and Stability 2000;70(2):161-170.
93. Sousa RA, Reis RL, Cunha AM, Bevis MJ. Processing and properties of bone-analogue biodegradable and bioinert polymeric composites. Composites Science and Technology 2003;63(3-4):389-402.
94. Reis RL, Cunha AM, Bevis MJ. Oriented composites meet tough orthopedic demands. Modern Plastics 1999;76(5):73-75.
95. Reis RL, Cunha AM, Allan PS, Bevis MJ. Structure development and control of injection-molded hydroxylapatite-reinforced starch/EVOH composites. Advances in Polymer Technology 1997;16(4):263-277.
96. Sousa RA, Mano JF, Reis RL, Cunha AM, Bevis MJ. Mechanical performance of starch based bioactive composite biomaterials molded with preferred orientation. Polymer Engineering and Science 2002;42(5):1032-1045.
97. Leonor IB, Sousa RA, Cunha AM, Reis RL, Zhong ZP, Greenspan D. Novel starch thermoplastic/Bioglass((R)) composites: Mechanical properties, degradation behavior and in-vitro bioactivity. Journal of Materials Science-Materials in Medicine 2002;13(10):939-945.
98. Gomes ME, Ribeiro AS, Malafaya PB, Reis RL, Cunha AM. A new approach based on injection moulding to produce biodegradable starch-based polymeric scaffolds: morphology, mechanical and degradation behaviour. Biomaterials 2001;22(9):883-889.
99. Oliveira AL, Malafaya PB, Reis RL. Sodium silicate gel as a precursor for the in vitro nucleation and growth of a bone-like apatite coating in compact and porous polymeric structures. Biomaterials 2003;24(15):2575-2584.
100. Reis RL, Cunha, A. M., Fernandes, M. H., Correia, R. N. Treatments to Induce the Nucleation and Growth of Apatite Like Layers onto Polymeric Surfaces and Foams. Journal of Materials Science: Materials in Medicine 1997;8:897.

101. Reis RL, Mendes SC, Cunha AM, Bevis MJ. Processing and in vitro degradation of starch/EVOH thermoplastic blends. Polymer International 1997;43(4):347-352.
102. Ball MD, Downes S, Scotchford CA, Antonov EN, Bagratashvili VN, Popov VK, Lo WJ, Grant DM, Howdle SM. Osteoblast growth on titanium foils coated with hydroxyapatite by pulsed laser ablation. Biomaterials 2001;22(4):337-347.
103. Chou L, Marek B, Wagner WR. Effects of hydroxylapatite coating crystallinity on biosolubility, cell attachment efficiency and proliferation in vitro. Biomaterials 1999;20(10):977-985.
104. Oliveira AL, Alves CM, Reis RL. Cell adhesion and proliferation on biomimetic calcium-phosphate coatings produced by a sodium silicate gel methodology. Journal of Materials Science-Materials in Medicine 2002;13(12):1181-1188.
105. Oliveira AL, Gomes ME, Malafaya PB, Reis RL. Biomimetic coating of starch based polymeric foams produced by a calcium silicate based methodology. Bioceramics 15 2003;240-2:101-104.
106. Wen HB, de Wijn JR, van Blitterswijk CA, de Groot K. Incorporation of bovine serum albumin in calcium phosphate coating on titanium. Journal of Biomedical Materials Research 1999;46(2):245-252.
107. Murphy WL, Peters MC, Kohn DH, Mooney DJ. Sustained release of vascular endothelial growth factor from mineralized poly(lactide-co-glycolide) scaffolds for tissue engineering. Biomaterials 2000;21(24):2521-2527.
108. Nagano M, Nakamura T, Kokubo T, Tanahashi M, Ogawa M. Differences of bone bonding ability and degradation behaviour in vivo between amorphous calcium phosphate and highly crystalline hydroxyapatite coating. Biomaterials 1996;17(18):1771-1777.
109. Barrere F, Stigter M, Layrolle P, van Blitterswijk CA, de Groot K. In vitro dissolution of various calcium-phosphate coatings on Ti6Al4V. Bioceramics 2000;192-1:67-70.
110. Barrere F, van der Valk CM, Dalmeijer RAJ, van Blitterswijk CA, de Groot K, Layrolle P. In vitro and in vivo degradation of biomimetic octacalcium phosphate and carbonate apatite coatings on titanium implants. Journal of Biomedical Materials Research Part A 2003;64A(2):378-387.
111. Ito Y. Tissue engineering by immobilized growth factors. Materials Science & Engineering C-Biomimetic and Supramolecular Systems 1998;6(4):267-274.
112. Li RH, Wozney JM. Delivering on the promise of bone morphogenetic proteins. Trends in Biotechnology 2001;19(7):255-265.
113. Kirker-Head CA. Potential applications and delivery strategies for bone morphogenetic proteins. Advanced Drug Delivery Reviews 2000;43(1):65-92.
114. Murphy WL, Kohn DH, Mooney DJ. Growth of continuous bonelike mineral within porous poly(lactide-co-glycolide) scaffolds in vitro. Journal of Biomedical Materials Research 2000;50(1):50-58.
115. J. D. de Bruijn IB, S. Mendes, R. Dekker, Y. P. Bovell, C. A. van Blitterswijk. Bone Induction by Implants Coated with Cultures Osteogenic Bone Marrow Cells. Advents in Dental Research 1999;13:74.

SECTION 2

CHAPTER II

Chapter II

Materials and Methods

This chapter intends to give an overview on the experimental work behind the studies presented in this dissertation. All the ground work that support the achieved results (presented in Sections 3 and 4) will be herein described in detail. Additionally, in order to orient the reading, some considerations will be made on the selection of materials and characterization techniques and on the underlying principles that sustain the proposed methodologies. This is expected to leave the reader with a more clear vision of the purpose of each studied subject and of the way they can be correlated.

II.1. Materials

The increased demands placed on biomaterials for both currently approved and novel emerging applications continues to stimulate the interest in improving the performance of existing medical-grade metallic implants and inspires the development of new alternative solutions based on polymeric systems. In this thesis both of the approaches are present, reflecting the large spectrum of applicability of biomimetic coatings which can be applied either to bon-replacement materials or to more complex tissue engineering scaffolds.

In this section a short introduction on the emerging applications of starch based biodegradable polymers in the biomedical field intends to give a comprehensive perspective on the rational for choosing these materials as the basis for the studies herein presented in Chapters III to VII. The last chapter presents a study that is, as said before, quite different from the previous which has resulted from a collaboration established with the company DePuy Orthopaedics, Inc. One of the company goals is to overcome problems associated with the lack of stability between the implant surface and the underlying bone which in most of the cases results in implant failure.

III.1.1. Starch based biodegradable polymers

Over the last years 13 years Reis and co-workers [1] at the 3B's Research Group, University of Minho have been giving a special attention to starch-based biodegradable

polymers. These polymers present an enormous potential to be widely used in bone-related biomedical applications [1-15]. Besides being biodegradable, inexpensive (when compared to other biodegradable polymers) and available in large quantities [16-18], these polymers can be converted into complex geometries with interesting mechanical properties, by using standard processing routes for synthetic polymers [2, 5, 19-21] or by means of using novel processing methodologies [4, 7, 14, 22, 23]. In this way, this class of materials has recently been proposed for a wide range of novel emerging biomedical applications besides the traditional bone replacement/fixation [2, 21], such as hydrogels [24, 25] and microparticles [10, 12, 26] for drug delivery applications [10, 24, 27], bone cements [15, 28-30] and primarily temporary scaffolds for Tissue Engineering applications [5, 13, 14, 31, 32]. Furthermore, in addition to their processing versatility, they exhibit a biocompatible behaviour, already demonstrated on different *in vitro* [6, 11, 32, 33] and *in vivo* [34, 35] studies.

The herein studied materials are based on blends of corn starch obtained from native maize. The starch typical composition was 70% amylopectin and 30% amylase (wt%) [36]. This type of starch based blends displays a semi-crystalline behaviour, as it has been previously shown for several systems, by X-ray Diffraction [1]. The amount of water, the type of plasticizer, the amyopectin/amylose ratio, and the blending conditions are the parameters that determine the crystallinity of these types of blends [36].

The following grades were selected for the different studies presented in this thesis:

i. an interpenetrated network (IPN) of starch and poly(ethylene vinyl alcohol) (SEVA-C). The blend contains around 50% (wt%) starch by weight, while the copolymer discloses a composition of 60/40 mol/mol.
ii. a blend of starch with poly(epsilon-caprolactone) (SPCL). The blend contains around 30% (wt%) in starch.

These materials present distinct mechanical properties and degradation behaviours [37]. Different compact samples and porous 3D architectures were produced from these materials as described in section II.2.

II.1.1. Titanium alloy

DePuy Orthopaedics, Inc. (www.depuy.com) has a strong background on producing metallic implants for bone replacement applications like hip, shoulder, elbow, etc. Titanium and its alloys are particularly attractive for medical applications because of their excellent biocompatibility and imaging qualities [38]. Titanium–Aluminum–Vanadium alloys have better mechanical properties than commercially pure titanium (CPTi) and are used more widely in total joint implants [39-42]. The substrate used in the study presented in Chapter VII was a commercially available Titanium alloy (Ti-6Al-4V) with a composition as presented in Table II.1, to be applied specifically in hip replacement.

Table 1. Composition of Ti-6Al-4V used for the fabrication of bone-replacement implants [39].

Component	Al	Fe	O	Ti	V
Wt. %	6	Max 0.25	Max 0.2	90	4

Disks with a 16 mm in diameter and 2 mm in thickness were used as substracts for the coating of biomimetic apatite layers. To study the effect of the surface roughness on the formation of these coatings one set of samples was polished to have a reflective mirror-like finish, and another was grit blasted using 20-μm alumina particles.

II.1.4. Reagents

All the reagents described on the experimental results, in Sections III and IV, were supplied by MERCK and SIGMA-ALDRICH. They presented analytical purity and were not submitted to further purification.

II.2. Processing routes of starch-based polymers

In this thesis different processing routes were used to produce compact and porous structures that served as substrates for exploring the different aspects of the nucleation and growth of biomimetic coatings. Chapters III and VI from Section III have included studies on compact starch-based biodegradable polymers produced by injection moulding. In Chapters IV and V the aim was to expand the study to more complex shapes like porous 3D architectures. In this case the studies were conducted using constructs produced by a 3D plotting technique. These architectures are currently being proposed for bone Tissue Engineering applications. In Chapter VII compact sample disks of a

commercially available Titanium alloy were used as substrates for coating the biomimetic layers.

II.2.1. Compact samples

SEVA-C granules were injection moulded on a Klockner Desma FM-20, using a nozzle temperature of 170 ºC, in order to produce standard ASTM tensile test bars with a cross-section of 2x4 mm^2 and disks with 10 mm in diameter and 1,5 mm in thickness (Figure II.1). The processing parameters of these materials are presented in Table II.2.



Figure 1. Geometry of the produced compact SEVA-C samples: a) standard ASTM tensile test bar, b) disk sample.

Table 2. Processing conditions to obtain the tensile bars and disks.

	T_1 (ºC)	Flow rate (cm^3/s)	T_{mol} (ºC)	P_i (MPa)	P_h (MPa)	$T_{cool.}$ (s)
SEVA-C Tensile bars	140-150-175-185	172	40	12	5	15
SEVA-C disks	135-145-170-180	100	40	12	8	20

T_1 – Termic profile of the cylinder;
$T_{mol.}$ – Temperature of the mould;
P_i – Injection pressure;
P_h – Holding pressure;
T_{cool} – Cooling time

II.2.2. Porous 3D architectures

Methods for manufacturing porous materials in a reproducible manner are crucial to their success, and must allow for the necessary scale-up of the developed tissue engineering technology. The technique used to manufacture scaffolds for tissue engineering is dependent on the properties of the polymer and its intended application [43-47]. It must

allow the preparation of scaffolds with complex 3D geometries with controlled porosity and pore size, since these factors are associated with supplying of nutrients to transplanted factors in tissue regeneration [43, 48].

Rapid prototyping (RP) technologies are considered as potential routes for the production of complex scaffolds for Bone TE applications, as they present superior control over design, manufacturing and reproducibility of TE scaffolds [49-52]. Moreover, when coupled with adequate image acquisition software, RP allows for the production of anatomically adapted 3D scaffolds based on the patient's own defect. SPCL scaffolds were produced using a 3D plotting technology (Bioplotter®, EnvisionTec GmbH, Germany) as presented in Figure II.2. In this case, consecutive alternated layers were plotted with a 0º/90º/…/0º/90º orientation pattern to produce cubic samples with a lateral side of L= 5 mm. Each layer was plotted using a distance of 2 mm between layer strands and an in-plane absolute offset distance of 1 mm between consecutive equivalent layers. 3D plotting RP enables high control over scaffold morphology, namely controlled porosity and interconnectivity.

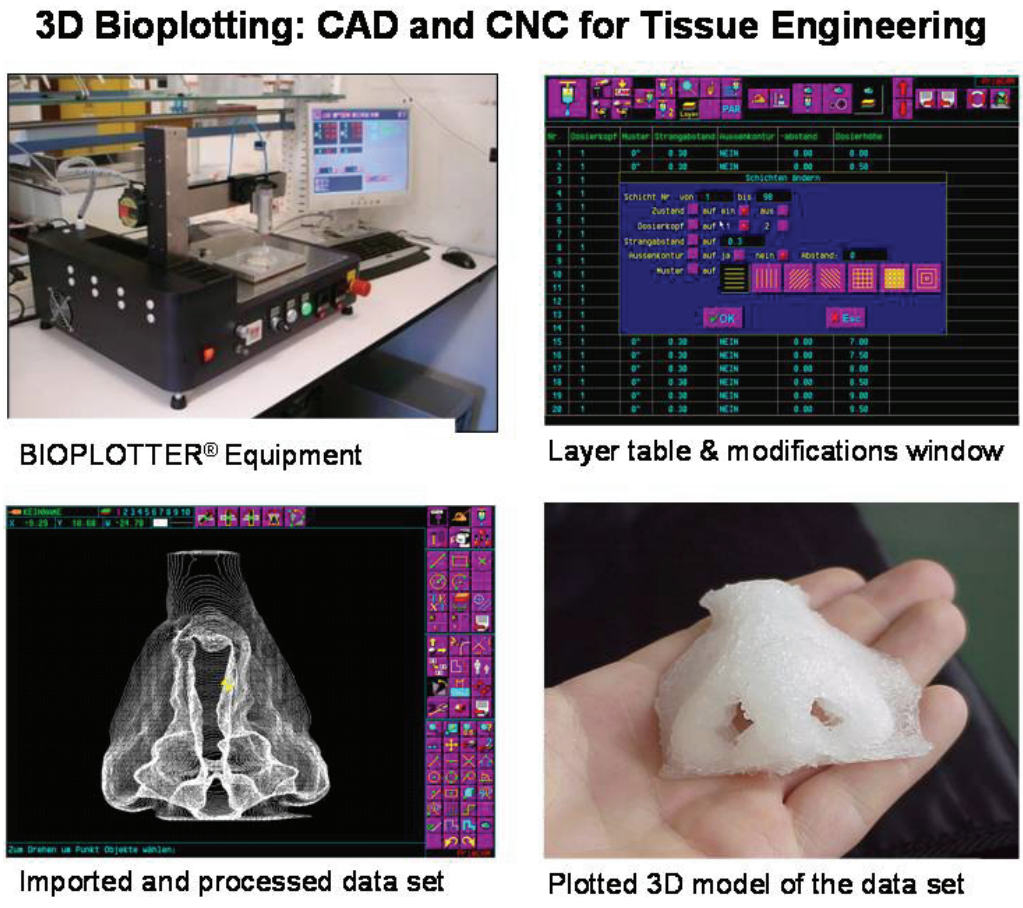


Figure 2. 3D Plotting Technology (Bioplotter®) used in the fabrication of SPCL scaffolds (collaboration established with the company EnvisionTec GmbH in the frame of the EU Project Hippocrates).

Figure II.3. illustrates the geometry of the obtained scaffolds.

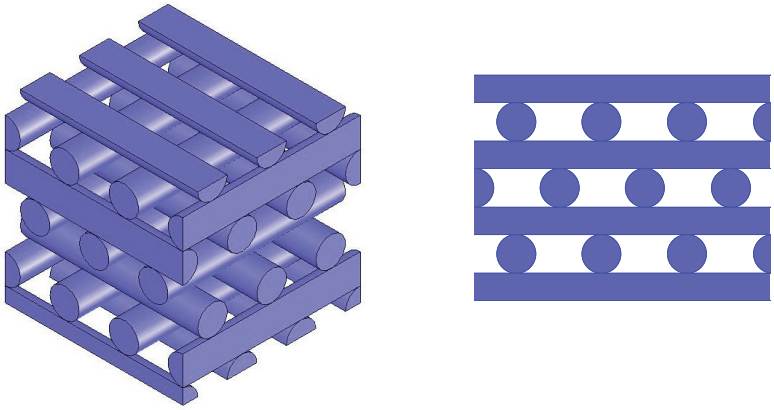


Figure 3. Geometry of the scaffolds as produced by the 3D plotter technology.

II.4. Biomimetic coating methodologies

As it as been stressed along this thesis, when coated with a bone-like apatite layer, a biomaterial has a great potential to be used for bone-repairing applications, since it can exhibit not only mechanical properties analogous to the natural bone but also a bioactive character.

Presently available methods to produce such type of coatings are usually difficult to control on what concerns the calcium-phosphate (Ca-P) layer composition, its resorbability, and ability to generate strong bonds with substrates. All these aspects dictate the success of a certain coating methodology and are dependent on the nature of the substrate to be coated, its geometry and intended application. To design a biomimetic methodology according with these specific requirements constitutes a main challenge addressed in this work. In that perspective, several biomimetic approaches for coating different biomaterials were proposed so that tailor made apatite layers could be produced.

II.4.1. Apatite coatings on biodegradable polymers

To produce an apatite coating on the surface of the different studied starch biodegradable polymers several biomimetic approaches were developed, being based on a previously proposed sodium silicate methodology [53]. This methodology is especially effective in coating the proposed starch based polymers due to their high hydration degree, which allows for an impregnation with the sodium silicate gel. Moreover, this gel can penetrate

the interior of 3D porous architectures, allowing for coating of the inner pores of the constructs and maintaining its original morphology.

For the several proposed biomimetic routes sodium silicate gel was used with concentration and SiO_2/Na_2O molar ratio as received ($Na_2SiO_3 \cdot H_2O$, containing ~14% NaOH and ~27% SiO_2, pH ≈13). The samples were "impregnated" with the gel under mild agitation. The relatively high viscosity of the gel (6 x 10-2 Pa.s-1) allows for the impregnation of the materials other than uptaking, which would seriously affect their mechanical and degradation behaviour. After this treatment the solution with the samples was diluted with 50% vol. of distilled water and stirred. This procedure was aimed at diminishing the viscosity of the gel in order to produce a homogeneous and thin layer of vitrified sodium silicate in the surface of the materials. The time for the impregnation and dilution steps was adjusted according with the nature of the type of sample and its geometry. The scaffolds were then removed from the solution and then dried in vacuum for 3 hours and in a controlled atmosphere (23 ± 1 ºC; 55% RH) for 24 hours.

An aqueous solution comprising all major inorganic ions present in the body in concentrations nearly equal to those of human blood plasma was first proposed by Kokubo *et al.* [54] as an *in vitro* model to study apatite formation on the surface of different kinds of materials. This SBF solution was used to nucleate and grow biomimetic apatite layers on the surface of starch base materials, after the sodium silicate treatment. This solution was prepared with different ion concentrations, as presented in Table II.3, by dissolving the different reagents into bi-distilled water and adjusting the pH to 7.4 with tris(hydroxymethyl)aminomethane ($(CH_2OH)_3CNH_2$) and hydrochloric acid (HCl) at 37 ºC. The ionic activity products (IP) of SBF at the different concentrations are also presented in the following table.

Table 3. Ion concentrations and Ionic Activity Products (IP) of the human blood plasma and SBF solutions in the present study [55].

Solution	Concentration (mM)								Log IP
	Na^+	K^+	Ca^{2+}	Mg^{2+}	Cl^-	HCO_3^-	HPO_4^{2-}	SO_4^{2-}	
Human plasma	142.0	5.0	2.5	1.5	103.0	27.0	1.0	0.5	-96.6
SBF 1.0X	142.0	5.0	2.5	1.5	147.8	4.2	1.0	0.5	-96.6
SBF 1.5X	213.0	7.5	3.8	2.6	223.0	6.3	1.5	0.8	-93.8
SBF 2.0X	284.0	10.0	5.0	3.0	297.6	8.4	2.0	1.0	-91.9

In Chapter III and VI of Section III, SEVA-C compact samples were submitted, after the sodium silicate treatment, to the following coating procedure (Figure II.4):

i. immersion in SBF up to 7 days, in order to nucleate an apatite layer – Nucleation stage;
ii. immersion in another solution with ion concentrations of 1.5X SBF up to 15 days, for making apatite layer to grow – Growth stage.

In the study presented in Chapter III the concentration of SBF was also raised to 2X during growth stage in order to evaluate the effect of an increase in the ionic strength of the SBF solution on the resulting apatite layers. During these coating procedures the solutions were renewed every 2 days.

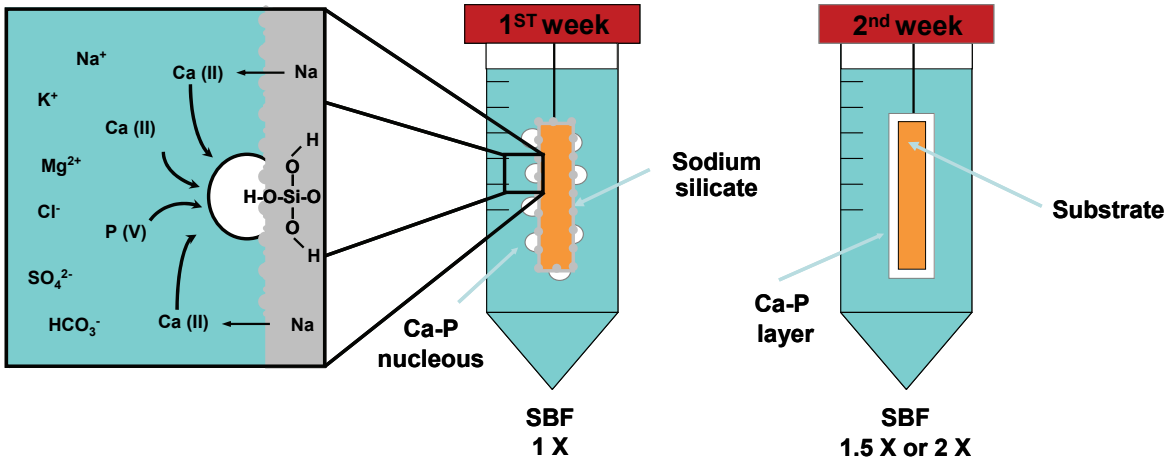


Figure 4. Schematic representation of the sodium silicate gel biomimetic methodology. Adapted from the procedure developed by Kokubo *et al.* [54, 56] and adapted by Reis *et al.* [3, 53].

In Chapters IV and V a different biomimetic concept was introduced. The influence of dynamic conditions on the growth of bone-like apatite layers at the surface of the 3D plotted SPCL scaffolds was evaluated. After the sodium silicate treatment SPCL scaffolds were immersed in the SBF solution for several periods up to 7 days and an apatite layer was allowed to nucleate and grow on the surface of the samples. During this time the solution was renewed every 2 days. Following this period, the samples were divided into 3 different groups and placed in contact with a renewed SBF solution under different conditions: static, agitation by shaking in a thermostatic bath (Selecta, Unitronic, Spain, 80 strokes/min.) and circulating flow perfusion in a bioreactor (volume flow rate (Q) of 4mL/min; Residence Time (t_R) of 15 s) for periods up to 14 days. In all the conditions the total volume of SBF available per sample was 50 mL and the solution was renewed every

2 days (solid-to-liquid ratio of 1g/400mL/week). The different conditions herein studied were selected based on preliminary experimental results. After each period the samples were removed from solution, washed in distilled water and dried in a controlled atmosphere (23 ± 1 ºC; 55% RH). Table II.4 summarizes the different coating conditions.

Table 4. Static and dynamic conditions for coating apatite layers on the SPCL scaffolds.

Periods (Days)	**SBF**	**Conditions**		
7	1 X	Static		
14	1 X	Static	Agitation	Flow perfusion
Volume of SBF available per sample		50 mL	50 mL	50 mL
Solid-to-liquid ratio		1g/400mL/week	1g/400mL/week	1g/400mL/week
Fluid Flow		None	Turbulent flow (80 Strokes/min)	Laminar flow (Q=4 mL/min; t_R=15s)

For the last condition a special bioreactor was designed according Figure II.5.

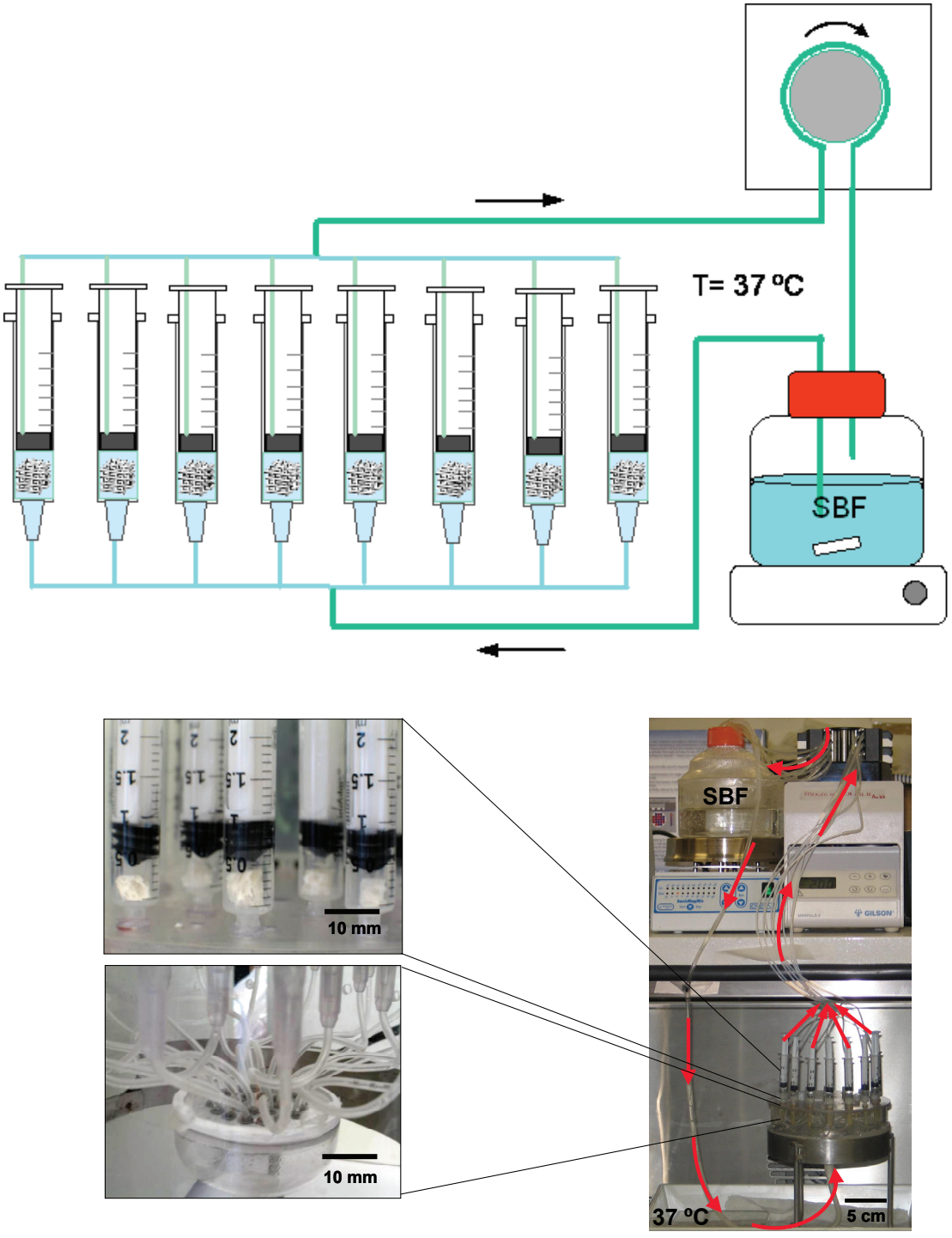


Figure 5. Bioreactor designed for coating scaffolds with an apatite layer under flow perfusion.

This bioreactor was built with the aim of being as simple as possible and easy to assemble and clean. On the other hand, since the chambers are made of disposable syringes it increases its versatility since it is possible to used any kind of syringe size, as presented if Figure II.6.

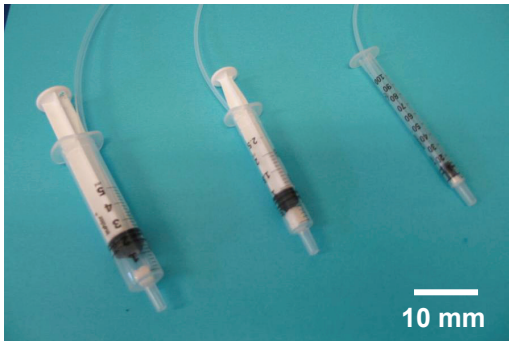


Figure 6. Possible sizes of the chambers made with disposable syringes.

On the other hand it is also possible to play with other parameters like: temperature, flow rate, residence time of the fluid, pressure with the piston to the material, etc. In this way, the study possibilities with this bioreactor are numerous. Besides the here presented mineralization studies, it is also possible to perform for instances degradation/dissolution tests, release studies and cell studies.

II.4.2. Apatite coatings on titanium alloy

As a way to enhance biological performance and consequently implant long-term viability a biomimetic coating process has been developed to be applied to the surface of a commercially available titanium alloy currently used in load-bearing cementless metallic implants [39].

A biomimetic nano-crystalline apatite coating was grown on the titanium specimens according to a procedure which was adapted from a previously developed process described by Li *et al.* [57, 58]. An aqueous solution was prepared comprising all major inorganic ions present in the body, adapted from the simulated body fluid solution (SBF) initially proposed by Kokubo *et al.* [54]. The reagents were dissolved in de-ionized H_2O and the pH adjusted to neutral using tris(hydroxymethyl)aminomethane-hydrochloric acid. The solution was buffered at time 0. The concentrations of NaCl, KCl, $NaHCO_3$, $MgCl_2$ and $NaSO_4$ were designed to correspond to the nominal levels of human blood plasma, whereas the concentrations of Ca^{2+} and HPO_4^{2-} were 5.0 and 2.4 mM, respectively. Three other solutions were prepared based on the same procedure with the supplement of 0.5, 1.0 and 1.5 mM $SrCl_2$ that results in the atomic ratio of Ca to Sr in solution of 10:1, 5:1 and 10:3, respectively [59]. Table II.5 summarizes the composition of each of the prepared solutions.

Table 5. Ionic concentration of the prepared solutions for coating Ti4AL6V.

Solution	Concentration (mM)					
	[Ca]	[Sr]	[P]	[Mg]	[HCO_3]	Tris
S1	5.0	-	2.4	2.5	8.0	17.5
S2	5.0	0.5	2.4	2.5	8.0	17.5
S3	5.0	1.0	2.4	2.5	8.0	17.5
S4	5.0	1.5	2.4	2.5	8.0	17.5

The lowest concentration of Sr is in the therapeutic range, when compared to the values found in human blood plasma in a study carried out in patients receiving a daily strontium supplement [60]. Concerning the ideal concentration of Sr in bone a consensus has not been reached. In the literature several studies report different amounts of strontium found in bone [60-66] which, however, cannot be directly compared, since they are referred to either different animal models or human subjects and different Sr therapies. Nevertheless based on studies by Boivin et al. [67] 10:1 was indicated as the theoretical maximum of the Ca to Sr ratio in bone.

The as-prepared solutions were loaded in a 2L double-jacketed glass reactor and the temperature was kept constant at 45 ºC using a water circulating controller. The samples were fixed in tailor-made Teflon holders and placed in the reactors standing vertically in order for the surfaces to be coated. Such arrangement ensures that the coating formed on the surface of Ti disks will not result from sedimentation of precipitates in the solution. Figure II.7. illustrates schematically the process. The disks were removed from solution after 7 days and cleaned with de-ionized water.

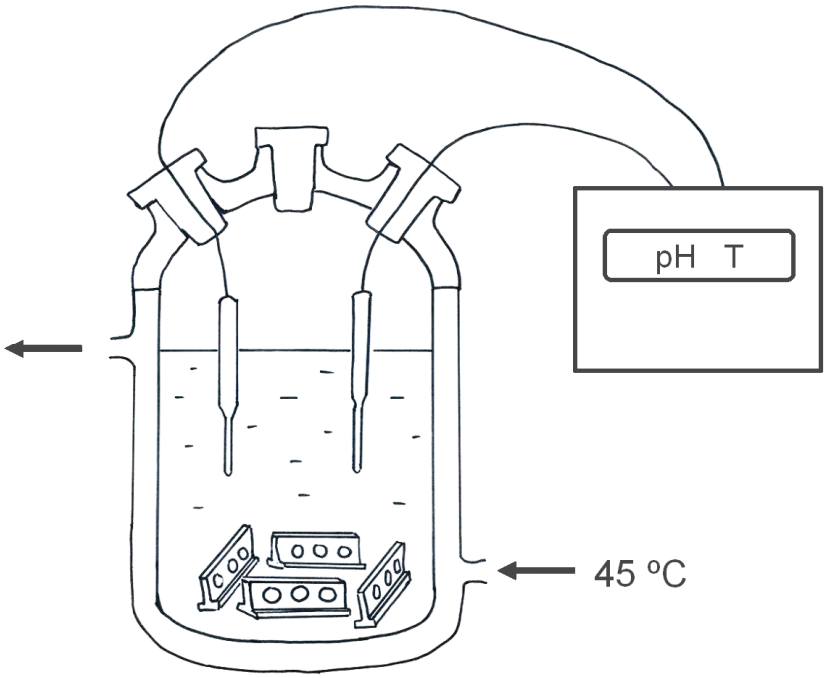


Figure 7. Schematic drawing of the coating experiments in double-jacked glass reactors.

II.5. Incorporation of a therapeutic molecule

Biomimetic apatite coatings offer an opportunity to incorporate different bioactive molecules without compromising its functionality/activity, as they are generated under physiological conditions. However, this process is highly dependent on specific properties of the therapeutic agent to be incorporated. Bisphosphonates (BPs) are an important family of drugs in various bone- and calcium- related pathologies like hypercalcemia, Paget's disease or osteoporosis [68-71]. The affinity of BPs to bone mineral hydroxylapatite is the basis for their use as inhibitors of bone resorption. They are pyrophosphate (P-O-P) analogues in which the oxygen in the P-O-P has been replaced by a carbon to yield a P-C-P backbone. Substitutions on the carbon give raise to a large family of compounds with different properties and potencies which are determined by the nature of the side chains [70]. The physicochemical effects of BPs include binding strongly to the calcium phosphate crystals and inhibiting their growth, aggregation and dissolution [70, 71]. Their biological effects in calcium-related disorders are due to the direct interaction with osteoclasts (bone forming cells) and/or osteoblasts (bone resorbing cells) though a variety of biochemical pathways. It is now generally accepted that BPs inhibit osteoclast activity [68-70]. However, the major drawback of the clinically utilized BPs is their pharmacokinetics and poor oral absorption [70, 71].

It has been also discovered that BPs can be beneficial when administrated after bone replacement, decreasing the primary failure mode of total hip arthroplasty: aseptic loosening [72, 73]. Nevertheless, this effect could be improved if the time for the administered bisphosphonate to reach the interface bone-implant could be reduced. In this case localized delivery of the drug could have a favourable effect in order to produce a more stable and integrated interface between the implant and bone at the early stage of implantation.

The bisphosphonate used in this study was a sodium clodronate (dichloromethylene-bisphosphonate) in which the side chains R_1 and R_2 are replaced by chloride. The structure of this drug is presented in Figure II.8.

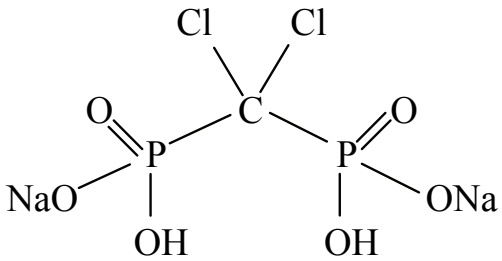


Figure 8. Chemical structure of sodium clodronate [74].

Sodium Clodronate is one of the best documented bisphosphonates that is used effectively in medical applications [74]. In the literature the ideal concentration of this BP for inducing a positive effect in bone cells varies from study to study. Therefore, we have chosen two lower concentrations that are considered to be in the therapeutic range [74] and two higher concentrations in order to scale up the effects of this BP in the structure of the apatite coating in order to be detectable by Infra-red and X-ray Spectroscopies. Solutions of 0.064, 0.32, 8 and 16 mg/mL of sodium clodronate (SIGMA-ALDRICH) were prepared with the pH adjusted to 7.4 with NaOH (1M). Aliquots of 50 μl of each solution were added to the coated disks left for 3 hours followed by drying at 60ºC. The effective concentration of the BP in the coated samples is approximately as follows: 0.004, 0.02, 0.5 and 1 mg/cm2.

II.6. Characterization methodologies

For the characterization of the bulk and surface properties of the studied materials as well as of the formed apatite coatings, different techniques were used in this thesis.

II.6.2. Surface wettability and hydration degree

Understanding the surface behaviour of a biomaterial in contact with hydrated media is of great importance to predict interactions of a certain material with the surrounding tissues, when applied in a particular biomedical application. These parameters are determined, in general, by means of wetting experiments, using the sessile drop technique [75]. Water-uptake studies are also of great importance [37] for a biodegradable material, because when implanted, it will be inevitably in the presence of the body fluids that will diffuse into the bulk of the polymer. The hydration degree of the materials was investigated, since the biomimetic strategy applied in this case relies on the capacity of these polymers to uptake ions from the surrounding fluids. These studies were performed to the starch based materials before and after treatment with sodium silicate, in Chapter III.

II.6.2.1. Contact angle measurements

Contact angle measurements were obtained by the sessile drop method using a standard contact angle apparatus (Krüss, Hamburg, Germany). The measurements were performed automatically with the aid of an image analysis system (G2/G40) installed in the apparatus. Duplicate measurements were recorded for each drop deposition. The average values were recorded after 5 seconds of the drop deposition (settling time). Ten average values were recorded for each condition and a final average value was calculated. All the measurements were made at room temperature and the probe liquids were water and methylene iodide (CH_2I_2).

The obtained results from both liquids were used to calculate the surface tension (γ) according to a method proposed by Owens and Went [76], which is particularly indicated for the determination the surface energy of low energy surfaces (polymers). According to this method the surface tension of each phase can be resolved into a polar (γ_l^p) and disperse (γ_l^d) parts that are known and are present in Table II.6.

Table 6. Polar (γ^p) and disperse (γ^d) components of the water and the methylene iodide [76].

	γ_l	γ_l^d	γ_l^p
Water	72.8	21.8	51.0
Methylene iodide	50.8	50.8	0.0

Figure II.9. shows the interfacial tension at the 3-phase contact line.

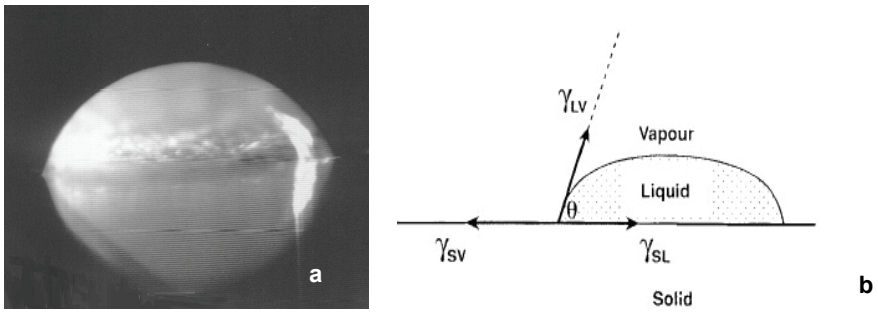


Figure 9. Contact angle on a solid surface (a). interfacial tension at the 3-phase contact line (b).

The contribution of the disperse and polar interactions to the surface energy was calculated by considering that the intermolecular attraction which causes surface energy, γ, results from a variety of intermolecular forces according to an additive rule.

II.6.2.2. Water-uptake ability

For water-uptake measurements all the samples were weighted before being immersed on distilled water (at room temperature) and then each 2 hours, during the first 12 hours of immersion. After that period, the weights started to be registered each 24 hours, until the end of the experiment time (15 days). The samples were carefully removed from the water containing flasks and immediately weighted for the determination of the wet weight as function of the immersion time. Water-uptake is given by:

$$W_{absorbed} = \frac{(m_f - m_i)}{m_i} \times 100\%$$

(Equation 1)

Were m_i is the initial weight of the sample, and m_f is the sample wet weight after a given time of immersion.

II.6.3. Structural and elemental characterization

II.6.3.1. Fourier Transform Infrared Spectroscopy (FTIR)

The chemical structure of the substrates and apatite coatings, were analysed by Fourier Transform Infrared Spectroscopy (FTIR) in a Perkin-Elmer System 1600 Series, USA. In Chapters IV and V the surface of the fibres was scratched and the resulting particles were milled with KBr powder and shaped by compression into pellets for further analysis. In Chapter VI an Attenuated Total Reflectance (ATR) device, from SPECAC was used to perform the data acquisition. The formed apatite coatings in Chapter VII, were analyzed using Diffuse Reflectance Fourier Transform Infra-Red spectroscopy (DR-FTIR, Magna-IR 550, Nicolet, Madison, WI). All spectra were recorded using 64 scans and 2 cm^{-1} resolution.

II.6.3.2. Thin Film X-Ray Diffraction (TF-XRD)

In order to identify the crystalline phases present in the several Ca-P layers formed in the surface of the compact and porous structures during the coating processes Thin-Film X-Ray Diffraction (TF-XRD, 1º incidence angle) spectroscopy was used. In Chapter III a Rigaku equipment at 60 kV at 30 mA was used while in remaining Chapters the analysis were performed in a Philips X'Pert (The Netherlands). The data collection was performed by 2θ scan method with 1º as incident beam angle using CuKα X-ray line and a scan speed of 0.05 º/min in 2θ.

II.6.3.3. Energy Dispersive Spectroscopy (EDS)

A half-quantitative characterization, using well established calibration sub-routines, of the atomic concentrations of the Ca-P coatings was performed by Energy Dispersive Spectroscopy (EDS), in a Noran Instruments spectrometer or in a Rontec spectometer. Ca, P, Mg, K and Na amounts were quantified. From these results Ca/P ratios were calculated. Considering the possibility of Mg^{2+}, Na^{+} and K^{+}, present in the SBF, substituting the Ca^{2+} in the cristalline network of the apatite, the following relation was also calculated: (Ca+Na+Mg+K)/P. The presence of Cl was investigated in Chapter VI when sodium clodronate was incorporated in the apatite layers.

II.6.4. Morphological characterization

The porous and compact structures of the studied materials were characterized by Scanning Electron Microscopy (SEM), in a Leica Cambridge S360 in case of Chapters III to VI or in a Hitachi S-3500N, Japan in Chapter VII. All the samples were previously gold coated in a Sputter Jeol JFC 1100 equipment. The electron beam energy was between 10 and 15 KeV. The SEM analysis allowed for evaluating the morphology of the compact and porous materials before and after the formation of the biomimetic coatings.

In Chapters IV and V the scaffolds were observed in 3 different orientations: from the top, lateral side and bottom, for the different tested periods and conditions in SBF. The corresponding cross-sections were also analysed and the thickness of the apatite layers was calculated by performing measurements in six fibres per scaffold (3 measurements per fibre). Since these coatings are constituted by fused spherical apatite nuclei they present an irregular surface. Therefore, in order to ensure that the measure would be done in the same way for all the conditions the basis of these nuclei was established as the limit for the coating. In this was the measured average values are the minimum thickness values for all the samples.

In Chapter VII the cross-sections of the coatings were also observed and its thickness calculated from the average of measurements performed in 5 equidistant points (5 μm) along the coating.

II.6.5. Apatite quantification

In Chapter V Micro-Computerized Tomography (μ-CT) is proposed for the first time, as a tool for mapping apatite coating content and distribution on the surface of polymer complex 3D architectures. In fact, to assess the apatite content in the inner parts of a scaffold is a relevant issue that needs to be taken into consideration. Tomography using x-rays is a well established technique that is gaining popularity since the interior of the specimen can be studied in great detail, without resorting to physical sectioning nor using toxic chemicals. On the other hand, it provides precise quantitative and qualitative information on the 3D morphology of the specimen [77]. After scanning, the intact samples can be subjected to other tests, therefore resolving the problem of sample scarcity. One of the main advantages of μ-CT is that it is able to evaluate the material (polymeric or ceramic) volume based on 3D spatial distribution.

Micro-Computed Tomography (μ-CT) of the uncoated and coated scaffolds was carried out using μ-CT 20 equipment (SCANCO Medicals, Switzerland). The X-ray scans were performed in high resolution mode of 11 μm x/y/z and an integration time of 250ms x 2 (500 ms). The rotation step used was 500/180º. The energy of the scanner used was 50 keV with 180 μA current. Around 400 slices of the materials were obtained in order to scan the entire scaffolds. Mimics from Materialise (Belgium), CT Analyser and CT Vol Realistic 3D Visualization both from SkyScan (Belgium) were used as image processing softwares, for CT reconstruction, to create and visualize the 3D representation. The 2-D histomorphometric analysis of the scaffolds was performed using a threshold of 51 to determine the porosity and a threshold of 133 to identify the apatite content along the scaffold (from 0-4500 μm) (grey values).

II.6.5. Solution analysis

II.6.3.1. Inductively Coupled Plasma Spectroscopy (ICP)

In Chapters IV and V the composition of the Ca-P coatings was assessed by analysing the solution resulting from dissolving the coated scaffolds in 0.1 M HCl, under agitation for 24 hours (the scaffolds were examined by SEM afterwards to confirm the total dissolution of the coating at the surface). The elemental concentration was measured by Inductively Coupled Plasma Optical Emission Spectroscopy (ICP-OES, JY 70 plus, Jobin Yvon, France). Duplicate samples were analysed for each condition and immersion time. From these results Ca/P ratios were calculated. Considering the possibility of Mg2+, Na+ and K+, present in the SBF, substituting the Ca2+ in the crystalline network of the apatite, the following relations were also considered: (Ca+Na+Mg+K)/P; (Ca+Mg+K)/P; Na/Ca; Mg/Ca; K/Ca.

The evolution of the elemental composition of the solution during the coating formation was also monitored by ICP. The concentration of Ca, P, Na, Mg, K and Si elements was measured after 3, 6 and 24 hours, 2, 5, 7 and 15 days. From the obtained concentration of ions consumed or released to the solution at each time point the cumulative concentration was calculated according to the following equation:

$$C = \Sigma ([C_n] - [C_{n+1}]) \qquad \text{(Equation 2)}$$

C_n- Concentration in solution;
C_{n+1}-Subsequent measured concentration.

To predict the behaviour of the apatite coating when facing the biological milieu is of extreme importance. However, to design a method capable of fully replicate it, is extremely difficult, considering the complexity of the biological fluids, going from minerals to proteins, enzymes and cells. In vitro dissolution tests, although far from the ideal method, can give some insights on the stability of the materials prior to implantation. In fact, since these studies are carried out in solution they always simulate the worst case low-end service environment. In Chapter VI dissolution tests were carried out on the coated samples before and after loading with increasing doses of sodium clodronate. Two different media were used in this study, according to the International Standard ISO/DIS 10993-14 procedure [78] and are presented in Table II.7.

Table 7. Solutions used in the dissolution studies.

Solution #	Description	pH (at 37ºC)
1	Simulated Tris/HCl solution	7,4
2	Acidic Buffered solution (simulating osteoclastic activity)	3

Solution 1 simulates, in a very simplistic way, the in vitro physiological environment. In this case a solution in the absence of Ca or P ions was used in order to avoid the precipitation of these ions in the apatite coating, which would be interfering with the coating dissolution profile. Nevertheless, once the coatings are immersed in the solution the dissolution and reprecipitation phenomena will still occur. Solution 2 is aimed at reproducing the worse predictable scenario in which bone is resorbed due to osteoclastic activity. The coated disks, incorporating different amounts of sodium clodronate, were immersed in a volume of 5 mL of each solution. Two replicates of each condition were studied. The experiment was carried out at 37ºC for periods up to 15 days. Aliquots of 2 mL were removed at different periods and replaced by the same volume of fresh solution. The obtained samples were analysed by Induced Coupled Plasma emission (ICP) spectroscopy for the quantification of Ca and P. The final cumulative concentration values were calculated according to the following equation:

$$\Sigma [V_n-(V_{n-1} \times 2/5)]_n \qquad \text{(Equation 3)}$$

V_n- Volume aliquoted;

V_{n-1}- Subsequent volume aliquoted;

II.6.3.2. High Permeation Liquid Chromatography (HPLC)

The release of sodium clodronate from the Ca-P in the previously described solutions was studied in Chapter VI. The analysed solutions and periods of time were the same in which Ca and P were quantified. The release of the drug was monitorized by means of High Permeation Liquid Chromatography (HPLC). The analysis was performed by using a mixture (60:40) of methanol/aqueous solution of PIC A (a solution of Tetrabutylammonium Hydrogen Sulphate in water, supplied by Waters) as the mobile phase and a flow rate of 1 mL/min. The system consisted in a Perkin Elmer LC-250 pump, an UV/VIS detector Perkin Elmer LC-95 and a Waters μBoundapak C-18 column of 3.9 × 300 mm. Measurements were made at 204 nm. The obtained profiles for each solution are presented in Figure II.10.

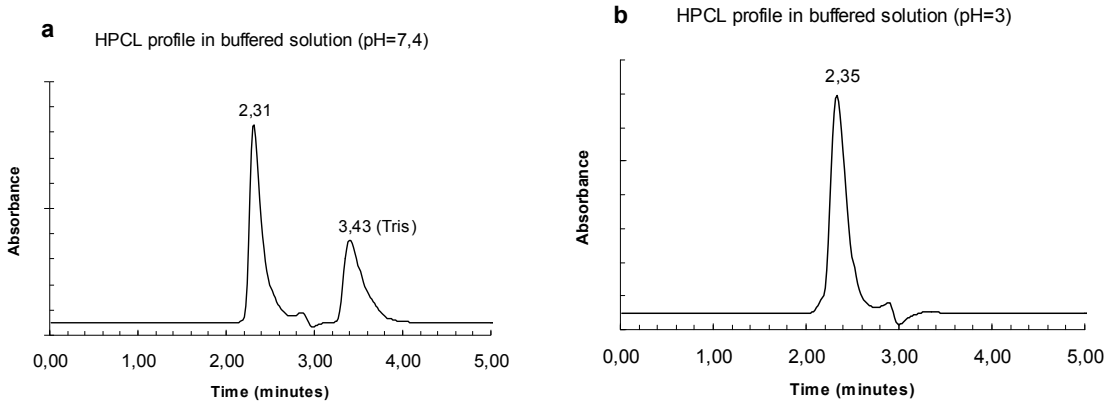


Figure 10. HPLC release profiles of sodium clodronate in a) a solution buffered to pH 7.4, b) a solution buffered to pH 3 and c) de-ionized water.

The concentration of sodium clodronate studied was 8 mg/mL which is in the highest concentration range studied. The studied concentrations of 0,32 and 0,064 were out of the detection limit of the HPCL equipment. The effective concentration loaded in the was 0,4 mg per coated disk, which is the result of a 50 μL aliquot of a solution with concentration 8 mg/mL. The results were plotted according with Equation 3.

II.6.3.3. Atomic Absorption Spectroscopy (AAS)

In Chapter VII the evolution of Ca and Sr concentrations in the coating solutions was followed by means of removing aliquots of 5 mL of solution every 10 to 12 hours during the coating process. Atomic Absorption Spectroscopy (AA800, Perkin-Elmer, Norwalk, CT) was used to quantify the amount of the Ca and Sr present. To eliminate the interference of phosphate in the measurement of calcium and strontium, 0.1 mL of the sample solution was diluted in 5 mL of 0,625 %wt of $LaCl_3$ that acts as a release agent. For each time point 3 repetitions *per* 5 replicates were analyzed, and the average values calculated.

II.6.3.4. UV-light Spectrophotometry

The P concentration was analyzed in Chapter VII by the "molybdenum blue" method [79] using a UV-light spectrophotometer (Genesys 2, Spectronic Instruments). The same 5 mL aliquots of solution that were analysed by AAS were also used to perform this assay. Again for each time point 3 repetitions *per* 5 replicates were analysed, and the average values calculated.

II.6.5. Cell adhesion and proliferation

In order to study the morphology, attachment and proliferation of osteoblast-like cells over pre-calcified loaded SEVA-C surfaces, a human osteoblast-like cell line (SaOS-2) obtained from the European Collection of Cell Cultures was selected. Dulbecco's Modified Eagle's Medium (DMEM, Sigma, USA), supplemented with 10% Foetal Bovine Serum (FBS, Biochrome, Germany) and 1% antibiotic/antimicotic solution (Sigma, USA) was used as cell incubation medium and growth to confluency in controlled atmosphere conditions (37ºC, 5% CO2, 100% humidity). Detachment of confluent low passage cells was performed using 0,25% Trypsin/EDTA solution (Sigma, USA). Subsequently, osteoblast-like cells were cultured over samples in a concentration of 3.3×10^4 cell/mL and incubated in controlled atmosphere conditions for 24 hours and 7 days in case of Chapter III and 3, 5 and 7 days in case of Chapter VI. Tissue culture grade polystyrene was used as control and replicates were prepared. After each incubation period, samples were washed with Phosphate Buffer Saline (PBS, Sigma, USA) solution and fixed in Gluteraldehyde 2.5% (V/V) for observation by means of Scanning Electronic Microscopy.

After fixation, samples were dehydrated in crescent ethanol concentrations (50%, 70%, 90% and 100%), air-dried and sputter coated with gold.

Cell proliferation of SaOs-2 was assessed using the Micro BCA Protein Assay Kit from PIERCE to quantify the total protein quantity. At each time period each sample was washed with PBS (phosphate-buffered saline), the cells were lysed through cycles of freeze and thawing and the protein present on each lysed suspension was measured. This total protein quantification is directly related with cell proliferation, once it is directly proportional to the cell number.

Cell viability was measured through the MTS test, using the CellTiter 96® AQueous One Solution from PROMEGA, that is based on bioreduction of a substrate (MTS), into a brown product by dehydrogenase enzymes in metabolically active cells and is commonly used for cell viability evaluation. Cells were then incubated for 3 h at 37°C in a humidified atmosphere containing 5% CO2. At this time optical density (OD) was measured with a plate reader at 490 nm. The mean OD value obtained for the positive control (cell seeded on culture plate without any coating) was considered as 100% metabolic activity.
Alkaline phosphatase activity was assessed by the p-nitrophenol phosphate method witch consists on the use of the lysed cells (that contains the Enzyme ALP) to cleave the p-nitrophenol phosphate that is added to that solution as a substrate. The resultant products are phosphate and p-nitrophenol. The last is turns resultant solution into yellow, which can be measured by optical density (OD) at 405nm. The obtained OD is directly related with the enzyme activity.

References

1. Reis, R.L., Cunha A. M., *Characterization of two biodegradable polymers of potential application within the biomaterials field.* Journal of Materials Science: Materials in Medicine, 1995. **6**: p. 786-792.
2. Reis R. L., C.A.M., Allan P. S., Bevis M. J., *Mechanical behaviour of injection-moulded starch based polymers.* Polymer Advanced Technology, 1996. **7**: p. 784-790.
3. Reis, R.L., Cunha, A. M., Fernandes, M. H., Correia, R. N., *Treatments to Induce the Nucleation and Growth of Apatite Like Layers onto Polymeric Surfaces and Foams.* Journal of Materials Science: Materials in Medicine, 1997. **8**: p. 897.
4. Malafaya, P.B., et al., *Porous starch-based drug delivery systems processed by a microwave route.* J Biomater Sci Polym Ed, 2001. **12**(11): p. 1227-41.
5. Gomes, M.E., et al., *A new approach based on injection moulding to produce biodegradable starch-based polymeric scaffolds: morphology, mechanical and degradation behaviour.* Biomaterials, 2001. **22**(9): p. 883-9.
6. Gomes, M.E., et al., *Cytocompatibility and response of osteoblastic-like cells to starch-based polymers: effect of several additives and processing conditions.* Biomaterials, 2001. **22**(13): p. 1911-7.

7. Gomes M. E., S.A.J., Reis R. L., *Bone Tissue Engineering Using Starch Based Scaffolds Obtained by Different Methodologies.* Ed., R.L.Reis and D.Cohn, NATO/ASI Series, Kluwer Press, Drodercht,, 2002: p. 221-249.
8. Gomes M. E., S.V.I., Behravesh E., Reis R.L., Mikos Antonios G., *Effect of Flow Perfusion on the Osteogenic Differentiation of Bone Marrow Stromal Cells Cultured on Starch Based Three-Dimensional Scaffolds.* Journal of Biomedical Materials Research, 2003. **67A**: p. 87-95.
9. Oliveira, A.L., et al., *Tailoring the bioactivity of natural origin inorganic-polymeric based systems.* Bioceramics 15, 2003. **240-2**: p. 111-142.
10. Silva, G.A., et al., *Starch-based microparticles as vehicles for the delivery of active platelet-derived growth factor.* Tissue Eng, 2007. **13**(6): p. 1259-68.
11. Santos, M.I., et al., *Response of micro- and macrovascular endothelial cells to starch-based fiber meshes for bone tissue engineering.* Biomaterials, 2007. **28**(2): p. 240-8.
12. Malafaya, P.B., F. Stappers, and R.L. Reis, *Starch-based microspheres produced by emulsion crosslinking with a potential media dependent responsive behavior to be used as drug delivery carriers.* Journal of Materials Science-Materials in Medicine, 2006. **17**(4): p. 371-377.
13. Gomes, M.E., et al., *Influence of the porosity of starch-based fiber mesh scaffolds on the proliferation and osteogenic differentiation of bone marrow stromal cells cultured in a flow perfusion bioreactor.* Tissue Engineering, 2006. **12**(4): p. 801-809.
14. Tuzlakoglu, K., et al., *Nano- and micro-fiber combined scaffolds: a new architecture for bone tissue engineering.* J Mater Sci Mater Med, 2005. **16**(12): p. 1099-104.
15. Boesel, L.F., et al., *The in vitro bioactivity of two novel hydrophilic, partially degradable bone cements.* Acta Biomater, 2007. **3**(2): p. 175-82.
16. Galliard, T., *Starch: properties and potential*. Critical Report on Applied Chemistry. 1987, New-York: John Wiley & Sons.
17. Poutanen, K. and P. Forssell, *Modification of starch properties with plasticizers.* Trends in Polymer Science, 1996. **4**(4): p. 128-132.
18. Andreopoulos, A.G. and T. Theophanides, *Degradable Plastics - a Smart Approach to Various Applications.* Journal of Elastomers and Plastics, 1994. **26**(4): p. 308-326.
19. Sousa, R.A., et al., *Processing and properties of bone-analogue biodegradable and bioinert polymeric composites.* Composites Science and Technology, 2003. **63**(3-4): p. 389-402.
20. Sousa, R.A., et al., *Structure and properties of hydroxylapatite reinforced starch bone-analogue composites.* Bioceramics, 2000. **192-1**: p. 669-672.
21. Sousa, R.A., et al., *Injection molding of a starch/EVOH blend aimed as an alternative biomaterial for temporary applications.* Journal of Applied Polymer Science, 2000. **77**(6): p. 1303-1315.
22. Malafaya, P.B., et al., *Polymer based scaffolds and carriers for bioactive agents from different natural origin materials.* Tissue Engineering, Stem Cells and Gene Therapies, 2003. **534**: p. 201-233.
23. Sousa, R.A., et al., *Bi-composite sandwich moldings: Processing, mechanical performance and bioactive behavior.* Journal of Materials Science-Materials in Medicine, 2003. **14**(5): p. 385-397.
24. Elvira, C., et al., *Starch-based biodegradable hydrogels with potential biomedical applications as drug delivery systems.* Biomaterials, 2002. **23**(9): p. 1955-66.
25. Baran, E.T., J.F. Mano, and R.L. Reis, *Starch-chitosan hydrogels prepared by reductive alkylation cross-linking.* J Mater Sci Mater Med, 2004. **15**(7): p. 759-65.
26. Silva, G.A., et al., *Microparticulate release systems based on natural origin materials.* Adv Exp Med Biol, 2004. **553**: p. 283-300.
27. Malafaya, P.B., G.A. Silva, and R.L. Reis, *Natural-origin polymers as carriers and scaffolds for biomolecules and cell delivery in tissue engineering applications.* Adv Drug Deliv Rev, 2007. **59**(4-5): p. 207-33.
28. Espigares, I., et al., *New partially degradable and bioactive acrylic bone cements based on starch blends and ceramic fillers.* Biomaterials, 2002. **23**(8): p. 1883-1895.
29. Pereira, C.S., et al., *New starch-based thermoplastic hydrogels for use as bone cements or drug-delivery carriers.* Journal of Materials Science-Materials in Medicine, 1998. **9**(12): p. 825-833.

30. Boesel, L.F., M.H. Fernandes, and R.L. Reis, *The behavior of novel hydrophilic composite bone cements in simulated body fluids.* J Biomed Mater Res B Appl Biomater, 2004. **70**(2): p. 368-77.
31. Salgado, A.J., O.P. Coutinho, and R.L. Reis, *Novel starch-based scaffolds for bone tissue engineering: cytotoxicity, cell culture, and protein expression.* Tissue Eng, 2004. **10**(3-4): p. 465-74.
32. Mendes, S.C., et al., *Evaluation of two biodegradable polymeric systems as substrates for bone tissue engineering.* Tissue Engineering, 2003. **9**: p. S91-S101.
33. Marques, A.P., R.L. Reis, and J.A. Hunt, *The biocompatibility of novel starch-based polymers and composites: in vitro studies.* Biomaterials, 2002. **23**(6): p. 1471-1478.
34. Mendes, S.C., et al., *Biocompatibility testing of novel starch-based materials with potential application in orthopaedic surgery: a preliminary study.* Biomaterials, 2001. **22**(14): p. 2057-64.
35. Salgado, A.J., et al., *In vivo response to starch-based scaffolds designed for bone tissue engineering applications.* J Biomed Mater Res A, 2007. **80**(4): p. 983-9.
36. Yuryev, V.P., P. Tomasik, and E. Bertoft, *Starch: Structure, Properties And New Technologies*. Tomasik, P., Bertoft, E. ed. 2006: Nova Science Pub Inc.
37. Demirgoz, D., et al., *Chemical modification of starch based biodegradable polymeric blends: effects on water uptake, degradation behaviour and mechanical properties.* Polymer Degradation and Stability, 2000. **70**(2): p. 161-170.
38. Taksali, S., J.N. Grauer, and A.R. Vaccaro, *Material considerations for intervertebral disc replacement implants.* The Spine Journal, 2004. **4**(6, Supplement 1): p. S231.
39. R. Boyer, G. Welsh, and E.W. Collings, *Materials Properties Handbook: Titanium Alloys*, ed. R. Boyer, G. Welsh, and E.W. Collings. 1994, Materials Park, OH: ASM International.
40. Johansson, C.B., et al., *A quantitative comparison of machined commercially pure titanium and titanium-aluminum-vanadium implants in rabbit bone.* Int J Oral Maxillofac Implants, 1998. **13**(3): p. 315-21.
41. Linder, L., *Osseointegration of metallic implants. I. Light microscopy in the rabbit.* Acta Orthop Scand, 1989. **60**(2): p. 129-34.
42. Katsikeris, N., R.D. Listrom, and J.M. Symington, *Interface between titanium 6,4 alloy implants and bone.* Int J Oral Maxillofac Surg, 1987. **16**(4): p. 473-6.
43. Thomson, R., M. Yaszemski, and A. Mikos, *Polymer Scaffold Processing*. Principles of Tissue Engineering, ed. R. Lanza, R. Langer, and W. Chick. 1997, New York: Academic Press. 263.
44. Yang, Y. and A.J. El Haj, *Biodegradable scaffolds - delivery systems for cell therapies.* Expert Opinion on Biological Therapy, 2006. **6**(5): p. 485-498.
45. Karageorgiou, V. and D. Kaplan, *Porosity of 3D biornaterial scaffolds and osteogenesis.* Biomaterials, 2005. **26**(27): p. 5474-5491.
46. Hutmacher, D.W. and A.J. Garcia, *Scaffold-based bone engineering by using genetically modified cells.* Gene, 2005. **347**(1): p. 1-10.
47. Salgado, A.J., O.P. Coutinho, and R.L. Reis, *Bone tissue engineering: State of the art and future trends.* Macromolecular Bioscience, 2004. **4**(8): p. 743-765.
48. Langer, R. and J.P. Vacanti, *Tissue Engineering.* Science, 1993. **260**(5110): p. 920-926.
49. Hutmacher, D.W., M. Sittinger, and M.V. Risbud, *Scaffold-based tissue engineering: rationale for computer-aided design and solid free-form fabrication systems.* Trends in Biotechnology, 2004. **22**(7): p. 354-362.
50. Sun, W. and P. Lal, *Recent development on computer aided tissue engineering - a review.* Computer Methods and Programs in Biomedicine, 2002. **67**(2): p. 85-103.
51. Sodian, R., et al., *Tissue engineering of vascular conduits: Fabrication of custom-made scaffolds using rapid prototyping techniques.* Thoracic and Cardiovascular Surgeon, 2005. **53**(3): p. 144-149.
52. Chen, V.J., L.A. Smith, and P.X. Ma, *Bone regeneration on computer-designed nano-fibrous scaffolds.* Biomaterials, 2006. **27**(21): p. 3973-3979.
53. Oliveira, A.L., P.B. Malafaya, and R.L. Reis, *Sodium silicate gel as a precursor for the in vitro nucleation and growth of a bone-like apatite coating in compact and porous polymeric structures.* Biomaterials, 2003. **24**(15): p. 2575-2584.
54. Kokubo, T., et al., *Solutions able to reproduce in vivo surface-structure changes in bioactive glass-ceramic A-W.* J Biomed Mater Res, 1990. **24**(6): p. 721-34.

55. Kim, H.M., et al., *Composition and structure of the apatite formed on PET substrates in SBF modified with various ionic activity products.* J Biomed Mater Res, 1999. **46**(2): p. 228-35.
56. Abe, Y., T. Kokubo, and T. Yamamuro, *Apatite Coating on Ceramics, Metals and Polymers Utilizing a Biological Process.* Journal of Materials Science-Materials in Medicine, 1990. **1**(4): p. 233-238.
57. Li, P.J., *Biomimetic nano-apatite coating capable of promoting bone ingrowth.* Journal of Biomedical Materials Research Part A, 2003. **66A**(1): p. 79-85.
58. Li, P., *Bioactive ceramic coating and method*, U.P.o. trademark, Editor. 2000, DePuy Orthopaedics, Inc.: USA. p. 19.
59. Li, P., *Strontium-substituted apatite coating*, U.P.o. trademark, Editor. 2005, DePuy Products, Inc.: USA.
60. Skoryna, S.C., *Effects of Oral Supplementation with Stable Strontium.* Canadian Medical Association Journal, 1981. **125**(7): p. 703-712.
61. Morohashi, T., T. Sano, and S. Yamada, *Effects of Strontium on Calcium-Metabolism in Rats .1. A Distinction between the Pharmacological and Toxic Doses.* Japanese Journal of Pharmacology, 1994. **64**(3): p. 155-162.
62. Marie, P.J., et al., *An Uncoupling Agent Containing Strontium Prevents Bone Loss by Depressing Bone-Resorption and Maintaining Bone-Formation in Estrogen-Deficient Rats.* Journal of Bone and Mineral Research, 1993. **8**(5): p. 607-615.
63. Marie, P.J. and M. Hott, *Short-Term Effects of Fluoride and Strontium on Bone Forming and Bone Resorbing Cells in the Mouse.* Calcified Tissue International, 1986. **38**(Ns): p. S17-S17.
64. Marie, P.J., et al., *Effect of Low-Doses of Stable Strontium on Bone Metabolism in Rats.* Mineral and Electrolyte Metabolism, 1985. **11**(1): p. 5-13.
65. Grynpas, M.D., et al., *Strontium increases vertebral bone volume in rats at a low dose that does not induce detectable mineralization defect.* Bone, 1996. **18**(3): p. 253-259.
66. Grynpas, M.D. and P.J. Marie, *Effects of Low-Doses of Strontium on Bone Quality and Quantity in Rats.* Bone, 1990. **11**(5): p. 313-319.
67. Boivin, G., et al., *Strontium distribution and interactions with bone mineral in monkey iliac bone after strontium salt (S 12911) administration.* Journal of Bone and Mineral Research, 1996. **11**(9): p. 1302-1311.
68. Rodan, G.A. and T.J. Martin, *Therapeutic approaches to bone diseases.* Science, 2000. **289**(5484): p. 1508-1514.
69. Rodan, G.A. and H.A. Fleisch, *Bisphosphonates: Mechanisms of action.* Journal of Clinical Investigation, 1996. **97**(12): p. 2692-2696.
70. Fleisch, H., *Bisphosphonates: mechanisms of action.* Expert Opinion on Therapeutic Patents, 2001. **11**(9): p. 1371-1381.
71. Ezra, A. and G. Golomb, *Administration routes and delivery systems of bisphosphonates for the treatment of bone resorption.* Adv Drug Deliv Rev, 2000. **42**(3): p. 175-95.
72. Venesmaa, P.K., et al., *Alendronate reduces periprosthetic bone loss after uncemented primary total hip arthroplasty: A prospective randomized study.* Journal of Bone and Mineral Research, 2001. **16**(11): p. 2126-2131.
73. Yamaguchi, K., et al., *Cyclic therapy with etidronate has a therapeutic effect against local osteoporosis after cementless total hip arthroplasty.* Bone, 2003. **33**(1): p. 144-149.
74. Plosker, G.L. and K.L. Goa, *Clodronate - a Review of Its Pharmacological Properties and Therapeutic Efficacy in Resorptive Bone-Disease.* Drugs, 1994. **47**(6): p. 945-982.
75. Bikerman, J.J., *Physical Surfaces*, ed. B.J. J. 1970, New York: Academic Press.
76. Owens, D.K. and R.C. Wendt, *Estimation of Surface Free Energy of Polymers.* Journal of Applied Polymer Science, 1969. **13**(8): p. 1741-&.
77. Mulder, L., J.H. Koolstra, and T.M.G.J. Van Euden, *Accuracy of MicroCT in the quantitative determination of the degree and distribution of mineralization in developing bone.* Acta Radiologica, 2004. **45**(7): p. 769-777.
78. *Biological evaluation of medical devices – Part 14: Identification and quantification of degradation products from ceramics, ISO/DIS 10993-14. Geneva: International Organization of Standardization.* 1997.
79. Dick, W.A. and M.A. Tabatabai, *Determination of Orthophosphate in Aqueous-Solutions Containing Labile Organic and Inorganic Phosphorus-Compounds.* Journal of Environmental Quality, 1977. **6**(1): p. 82-85.

SECTION 3.

CHAPTER III

Chapter III

Cell Adhesion and Proliferation on Biomimetic Calcium-Phosphate Coatings Produced by a Sodium Silicate Gel Methodology

Abstract

The present study describes a methodology to produce bioactive coatings on the surface of starch based biodegradable polymers or other polymeric biomaterials. As an alternative to the more typical bioactive glass percursors, a sodium silicate gel is being employed as a nucleating agent, for inducing the formation of a calcium-phosphate (Ca-P) layer. The method has the advantage of being able to coat efficiently both compact materials and porous 3D architectures aimed at being used on tissue replacement applications and as bone tissue engineering scaffolds. This treatment is also very effective in reducing the incubation periods, being possible to observe the formation of an apatite-like layer, only after 6 hours of immersion in a simulated body fluid (SBF). The influence of the SBF concentration on the formation of the apatite coating was also studied. The apatite coatings formed under different conditions were analysed and compared in terms of morphology, chemical composition and structure. After the first days of SBF immersion, the apatite-like films exhibit the typical cauliflower like morphology. With increasing immersion times, these films exhibited a partially amorphous nature and the Ca/P ratios became very closer to the value attributed to hydroxyapatite (1.67).

---

*This part of the chapter is based on the following publication:

A. L. Oliveira, C. M. Alves, R. L. Reis, “Cell adhesion and proliferation on biomimetic calcium-phosphate coatings produced by a sodium silicate gel methodology”, Journal of Materials Science: Materials in Medicine, 12, 2002, 1181-1188, invited paper.

The obtained results are very promising for pre-calcifying bone tissue engineering scaffolds. Therefore, in order to study cell behaviour and response to these apatite coatings, adhesion, morphology and proliferation of a human osteoblast cell line (SaOS-2) was also analysed after being cultured in the coatings formed after 15 days of immersion in SBF. Results indicate a good correlation between crystallinity of the apatite like coatings formed in these conditions and respective cell spreading and morphology. In general, higher cell proliferation was observed for higher crystalline Ca-P coatings.

III. 1. Introduction

Biodegradable materials are a promising alternative for a range of bone related applications. Starch-based biodegradable polymers are particularly interesting for bone replacement. Besides being biodegradable, inexpensive (when compared to other biodegradable polymers) and available in large quantities [1,2], starch-based polymers can be converted into complex geometries that exhibit interesting mechanical properties, by using standard equipment developed for the processing of synthetic polymers [3] or by means of using distinct innovative methodologies [4,5]. Furthermore, in addition to their processing versatility, they exhibit a biocompatible behaviour, already demonstrated by in vitro [6-8] and in vivo studies [9]. Therefore, they are under consideration for a wide range of biomedical applications like bone replacement/fixation [10,11], novel hydrogels and partially degradable bone cements [12], drug delivery carriers [4] or temporary scaffolds for tissue engineering applications [4,5].

In case of bone related applications like tissue replacement/fixation, or tissue engineering scaffolds to be applied in load-bearing sites, these systems must exhibit mechanical properties that match those of human bone, associated to degradation kinetics adequate to the healing of the tissues to be replaced or fixed [10,11]. Additionally, when coated with a bone-like apatite layer, they can also exhibit a bone-bonding behaviour. In the recent years, there has been an increasing interest in the so-called biomimetic preparation of calcium phosphate coatings on implant materials. A biomimetic process for coating an apatite layer on organic polymers or other type of materials was first developed by Kokubo and co-workers [13,14]. In this methodology, the materials were immersed in a simulated body fluid (SBF) with a composition similar to the human blood plasma, in order to promote the nucleation and growth of a calcium phosphate (Ca-P) bone-like layer on its surface. This was achieved using bioactive silica based glass particles as nucleating agents.

The Ca-P minerals found in natural hard tissues are fabricated in a physiological environment at low temperatures from moderately supersaturated mineralising solutions [15]. Therefore, a biomimetic approach is particularly suitable to coat polymeric materials [14,16], as it can be carried out at low temperature reaction conditions. Due to that fact it is expectable that these types of coatings would be very friendly surfaces for cell adhesion and proliferation, which is a key issue for bone regeneration These type of coatings have been previously produced on the surface of biodegradable materials by using different biomimetic routes, in spite of all the difficulties arising from the pH changes and continuous degradation of substrates surface [17,18].

The herein described biomimetic methodology reports on the use of a sodium silicate gel as an alternative nucleating agent applied before the subsequent immersion in a simulated body fluid (SBF) to promote apatite nucleation and growth. With this method, it was possible to reduce the incubation period for the formation of an apatite coating, when compared to the traditional biomimetic methodology, which uses bioactive glass particles as nucleating agents [17]. On the other had it can either be applied to coat compact or porous 3D architectures to be used on tissue replacement and in tissue engineering scaffolding [21]. The present study describes the influence of the SBF concentration on the formation of the apatite coatings for this recently developed biomimetic methodology. The apatite coatings formed under different conditions were analysed and compared in terms of morphology, chemistry and structure. In order to study cell behaviour and response to these apatite coatings, adhesion, morphology and proliferation of human osteoblast-like cells (SaOS-2) culture on coating surfaces were also analysed.

III.2. Materials and Methods

III.2.1. Materials

Natural origin starch based polymers, exhibit a great potential to be used in several al applications. In this particular work, the studied material is based on a blend of starch/ethylene vinyl alcohol (SEVA-C) supplied by Novamont, Italy. The blend contains around 50% starch by weight, while the copolymer discloses a composition of 60/40 mol/mol. Compact samples were produced by injection moulding on a Klockner Desma FM-20, using a nozzle temperature of 170 ºC. All samples were standard ASTM tensile

test bars, with a cross-section of 2x4 mm2, being produced on previously optimised processing conditions.

III.2.2. Sodium silicate methodology

To produce the bioactive coatings a commercially available sodium silicate gel from SIGMA-ALDRICH ($Na_2SiO_3 \bullet H_2O$, containing ~14% NaOH and ~27% SiO_2, pH ≈13) was used. The viscosity of the gel is 6 x 10^{-2} Pa.s^{-1}. Other authors have used before solutions based on sodium silicate gels [19,20]. However, to design this methodology as simple as possible (and that means to look at it as a possible future easy to apply industrial technology), the sodium silicate gel was herein used with a concentration and SiO_2/Na_2O molar ratio as received. On the other hand the relatively high viscosity of the gel allows for the impregnation of the materials instead of gel uptaking, which would seriously affect the bulk mechanical and degradation behaviour of the material. The materials were "impregnated" for 24 hours with the gel, in a controlled atmosphere (23 ± 1 ºC; 55% RH). After this treatment the solution, containing the samples, was diluted with 50% vol. of distilled water and stirred for 5 minutes. This procedure was aimed at diminishing the viscosity of the gel in order to produce a homogeneous and thin layer of vitrified sodium silicate in the surface of the materials. The samples were then removed from the solution and then dried in controlled atmosphere (23 ± 1 ºC; 55% RH).

III.2.3. Water-uptake ability

Water-uptake studies are of a great importance for a biodegradable material, because when implanted, it will be inevitably in the presence of the body fluids that will diffuse into the bulk of the polymer as degradation is taking place. For water-uptake measurements all the samples were weighted before being immersed on distilled water (at room temperature) and then each 2 hours, during the first 12 hours of immersion. After that period, the weights started to be registered each 24 hours, until the end of the experiment time (7 days). The samples were carefully removed from the water containing flasks and immediately weighted for the determination of the wet weight as function of the immersion time. Water-uptake is given by:

$$\text{Water absorbed} = [(m_f - m_i)/m_i] * 100 \qquad (1)$$

Were m_i is the initial weight of the sample, and m_f is the sample weight after a given time of immersion.

III.2.4. Contact angle measurements

In previous works SEVA-C has demonstrated to be a quite hydrophilic substrate [18,22]. It is also known that the presence of OH^- groups on the surface seems to facilitate the connection with an apatite layer, when it is nucleated by a biomimetic treatment [18,22]. Alkali attack, namely with KOH has already proved to be very effective in increasing the number of OH^- groups at the surface [18]. Since the used sodium silicate gel contains ~14% of NaOH, it is expected an increase in the hydrophilicity of the surface which will have an important role during apatite formation. Contact angle measurements were performed, for compact SEVA-C samples that were submitted to the sodium silicate gel treatment for 24 hours, in order to detect any eventual modification in the surface of the material. After treatment, the samples were washed in distilled water and dried in a controlled atmosphere (23 ± 1 ºC; 55% RH). Contact angle measurements were obtained by the sessile drop method using a standard contact angle apparatus (Krüss, Hamburg, Germany). The measurements were performed with the aid of an image analysis system (G2/G40) installed in the apparatus. Duplicate measurements were recorded for each drop deposition. The average values were recorded after 5 seconds of the drop deposition (settling time). Ten average values were recorded for each condition and a final average value was calculated. All the measurements were made at room temperature and the probe liquids were water and methylene iodide. The obtained results from both liquids were used to calculate the surface tension (γ) according to a method proposed by Owens and Wendt [23]. According to this method the surface tension of each phase can be resolved into a polar (γ_l^p) and dispersive (γ_l^d) parts, as presented in Table 1.

Table 1. Surface tension (γ_l) of water and methylene iodide and its polar (γ_l^p) and disperse (γ_l^d) components.

	γ_l	γ_l^d	γ_l^p
Water	72.8	21.8	51.0
Methylene iodide	50.8	50.8	0.0

Using these two test liquids the resulting values of the surface tension were calculated by this method, which is particularly useful for determination of the surface energy of low energy surfaces (such as polymers).

III.2.5. Apatite formation

To produce control biomimetic apatite coatings the substrates were submitted to a procedure inspired in the so-called biomimetic treatment, previously described by Kokubo and co-workers [13,14] and adapted by Reis et al. [17,18]. The procedure is schematised in Figure 1.

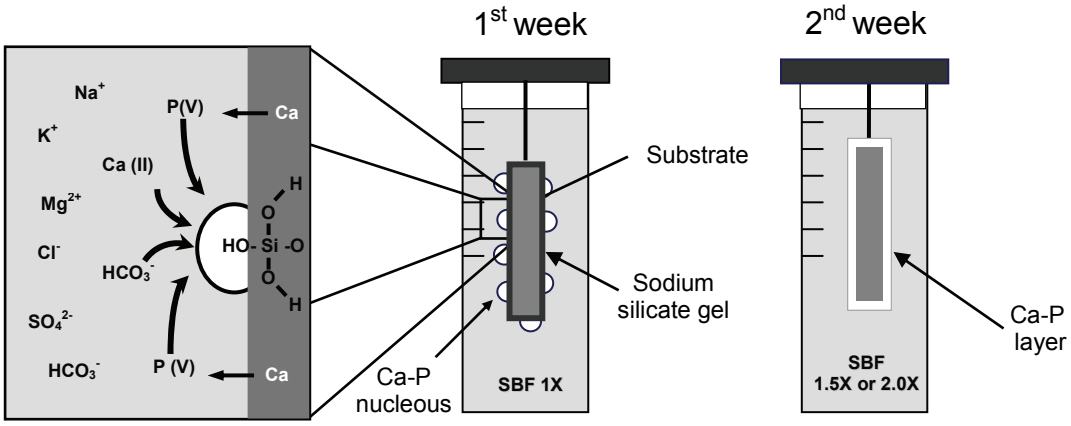


Figure 1. Schematic representation of the sodium silicate gel biomimetic methodology. Adapted from the procedure developed by Kokubo *et al* [13,14] and adapted by Reis *et al* [17,18].

This standard biomimetic methodology was used as a control – reference for comparative purposes. In this way it was possible to evaluate the efficacy of the hereby newly proposed methodology. For the standard biomimetic coatings production, the treated samples were:

i. first soaked in a 1.0x simulated body fluid (SBF) with an ion concentration nearly equal to human's blood plasma (Table 2) in order to form apatite nuclei;
ii. and then, after 7 days, soaked in another solution, with ion concentrations 1.5x SBF for making apatite nuclei to grow. Another group of samples was submitted to step (i) but, after 7 days they were soaked in a solution with ion concentrations of 2.0x SBF.

Table 2. Ion concentrations and Ionic Activity Products (IP) of the human blood plasma and SBF solutions in the present study [24].

Solution	Concentration (mM)								Log IP
	Na^+	K^+	Ca^{2+}	Mg^{2+}	Cl^-	HCO_3^-	HPO_4^{2-}	SO_4^{2-}	
Human plasma	142.0	5.0	2.5	1.5	103.0	27.0	1.0	0.5	-96.6
SBF 1.0X	142.0	5.0	2.5	1.5	147.8	4.2	1.0	0.5	-96.6
SBF 1.5X	213.0	7.5	3.8	2.6	223.0	6.3	1.5	0.8	-93.8
SBF 2.0X	284.0	10.0	5.0	3.0	297.6	8.4	2.0	1.0	-91.9

In fact, it is believed that the concentration of SBF solution influences the nature of the apatite formed during the growth stage [24]. Increasing the SBF concentration in 1.5 or 2x, after the first week of apatite formation will raise the ionic activity product from $10^{-96.6}$ to $10^{-1.9}$ respectively. In this way it is expectable that it might be possible to produce different (tailored) apatite coatings with different Ca-P ratios and relative crystallinities. In both cases, studied times were an incubation period up to 7 days (to understand the nucleation process) and a growing period up to 15 days.

III.2.6. Scanning Electron Microscopy (SEM) and Energy Dispersive Spectroscopy (EDS) and X-ray Diffraction (TF-XRD)

The morphological characterisation was carried out by Scanning Electron Microscopy (SEM) analysis, in a JEOL JSM 7301 F. All the samples were coated with a thin film of carbon, by ion sputtering, prior to any observation. The electron beam energy was changed between 10 KeV and 12 KeV.

A half-quantitative characterisation, using well established calibration sub-routines for analysing the atomic concentrations of Ca and P within the coatings was performed by means of Energy Dispersive Spectroscopy (EDS), in a Rontec spectrometer. Ca, P, Mg, K and Na amounts were quantified. From these results Ca/P ratios were calculated. Considering the possibility of Mg^{2+}, Na^+ and K^+, present in the SBF, substituting the Ca^{2+} in the crystalline network of the apatite, the following relation was also calculated: (Ca+Na+Mg+K)/P.

Thin-film X-ray Diffraction (TF-XRD, 1º incidence angle) spectra were acquired in a Rigaku equipment at 60 kV at 30 mA in order to identify the crystalline phases present in the several Ca-P layers, and their relative crystallinity.

III.2.7. Cell adhesion and proliferation

In order to study the morphology, attachment and proliferation of osteoblast-like cells over pre-calcified SEVA-C surfaces, a human osteoblasts SaOS-2 cell line obtained from the European Collection of Cell Cultures was selected. Dulbecco's Modified Eagle's Medium (DMEM, Sigma, USA), supplemented with 10% Foetal Bovine Serum (FBS, Biochrome, Germany) and 1% antibiotic/antimicotic solution (Sigma, USA) was used as cell incubation medium and growth to confluency in controlled atmosphere conditions (37ºC, 5% CO_2, 100% humidity). Detachment of confluent low passage cells was performed using 0,25% Trypsin/EDTA solution (Sigma, USA). Subsequently, osteoblast-like cells were cultured over samples in a concentration of 3.3 x 10^4 cell/mL and incubated for 24 hours and 7 days in controlled atmosphere conditions. Tissue culture grade polystyrene was used as control and replicates were prepared. After each incubation period, samples were washed with Phosphate Buffer Saline (PBS, Sigma, USA) solution and fixed in Gluteraldehyde 2.5% (V/V) for observation by means of Scanning Electronic Microscope. After fixation, samples were dehydrated in crescent ethanol concentrations (50%, 70%, 90% and 100%), air-dried and sputter coated with gold.

III.3. Results and Discussion

III.3.1. Water-uptake ability

Figure 2 shows the water-uptake versus time for the SEVA-C material, untreated and treated with sodium silicate.

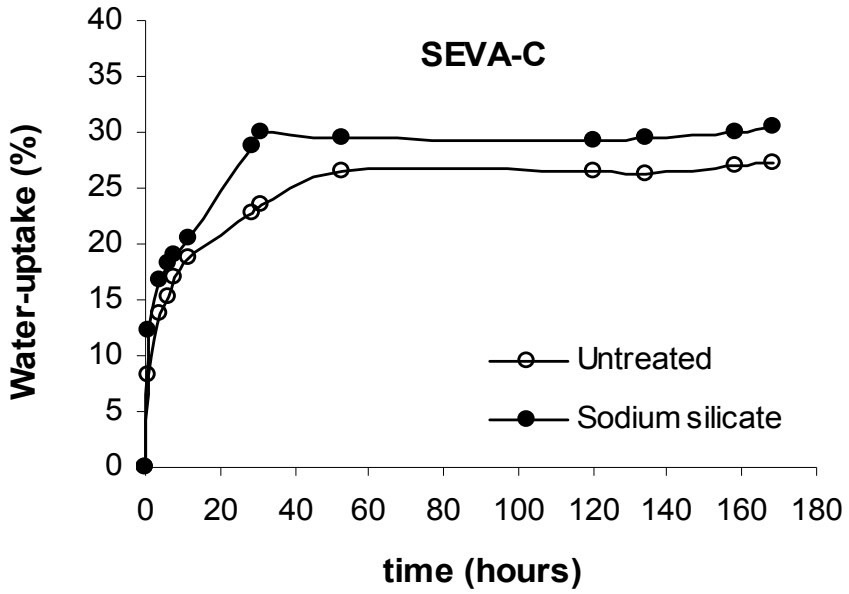


Figure 2. Water-uptake (%) versus time for untreated and sodium silicate treated SEVA-C samples.

After 50 hours, the equilibrium hydration degree of untreated samples is about 25%. This hydrophilic behaviour is mainly a result of the presence of starch and vinyl alcohol hydroxyl groups, as it has been previously described [25]. With sodium silicate treatment the amount of water uptake increases around 5%. This result can be justified by the fact that the commercially available sodium silicate that was used contains 14% of NaOH in its composition and discloses a pH around 13. This type of alkali attack can be compared to the previously studied KOH surface pre-treatment performed on SEVA-C [26]. The increase of hydrophilicity after this treatment can be justified by the molecular hydroxy-NaOH hydrogen bonding complexes, which are easily solvated by water molecules.

III.3.2. Contact angle measurements

Understanding the surface behaviour of a biomaterial in contact with hydrated media is of great importance to predict interactions of a certain material with the surrounding tissues, when it is applied in a particular biomedical application. In this work, contact angle measurements were performed on compact SEVA-C samples. Table 3 presents the results concerning the average water/methylene iodide contact angle (θ_w/θ_m) and the average surface tension (γ_s) of the sodium silicate treated surfaces. This treatment, performed on the SEVA-C samples did modify the surface parameters.

Table 3. Water (θ_w) and methylene iodide (θ_m) contact angle and surface energy measurements of SEVA-C untreated and after sodium silicate treatment for 24 hours.

	θ_w (º)	θ_m (º)	γ_s (mN/m)	γ_s^d (mN/m)	γ_s^p (mN/m)
Untreated SEVA-C	63.4 ± 1.85	53.2 ± 0.67	45.9 ± 1.09	32.5 ± 0.38	13.4 ± 1.08
Treated SEVA-C	29.7 ± 3.79	43.8 ± 2.02	68.0 ± 2.02	37.6 ± 1.07	30.3 ± 1.83

The average water contact angle decreased from 63.4 to 29.7º. An increment in the total surface energy, as a consequence of the increase of the polar contribution, was observed. Values changed from 45.9 to 68.0º after treatment. These significant changes can mainly be attributed to an increase in the polar contribution γ_s^p (from 13.4 to 30.32º) that resulted from an alkali attack by the sodium silicate gel, which can be compared to the previously studied KOH surface pre-treatment performed on SEVA-C substrates [18].

III.3.3. Apatite formation

Previous studies [21] have demonstrated that a very cohesive apatite-like layer can be formed when using the sodium silicate gel methodology only after 6 hours or immersion in SBF. This indicates that the number of the nucleating sites on the surface of the substrates during the first hours of immersion is rather high, allowing for the formation of a dense and uniform apatite layer [21]. SEVA-C is a polar and quite hydrophilic substrate, where the presence of OH^- groups in the surface tends to facilitate the connection with the apatite layer. It seems that a fairly strong bond could be formed between the polar groups and calcium ions of the apatite layer.

It has been shown by Li *et al*. [27], and Cho *et al*. [28] that heterogeneous nucleation of apatite can be induced from metaestable solutions, including physiologic solutions on those specific superficial sites, where there are OH^- containing groups. The proposed biomimetic methodology leads to an increase of the hydrophilicity (Table 3) and water-uptake ability (Figure 2) of the polymers, resulting in the increase of polar groups in the surface. In this way, the polymers tend to absorb higher quantities of Ca^{2+} ions from the SBF solution. As a consequence, the Ca^{2+} ion concentration at the surface will be increased, leading to the formation of additional nucleating sites for the Ca-P coating formation. This phenomenon has already been reported before for PEO/PBT copolymers [29], being related to a chelation effect. On the other hand, the formation at the surface of

silanol groups (Si-OH), will act as favourable sites for the apatite nucleation. As a result, a large number of apatite nuclei are rapidly formed on the surface. Subsequently, they grow spontaneously by consuming the calcium and phosphate ions from the surrounding fluids (the body fluid is already saturated with respect to the apatite).

Degradation of the starch-based polymers induces a greater degree of complexity to the reactions since it is continuously changing the composition of the solution adjacent to the interface, namely the pH and the polymer surface itself. This phenomenon has been previously described by Reis *et al* [17]. Nevertheless, the apatite-like layer could be formed in the proposed polymeric material by means of adapted biomimetic coating routes

Figure 3 presents the evolution of the Ca/P and (Ca+Mg+Na+K)/P ratios of the apatites formed on SEVA-C after immersion in SBF (1.5x or 2.0x after 7 days) for different periods up to 30 days.

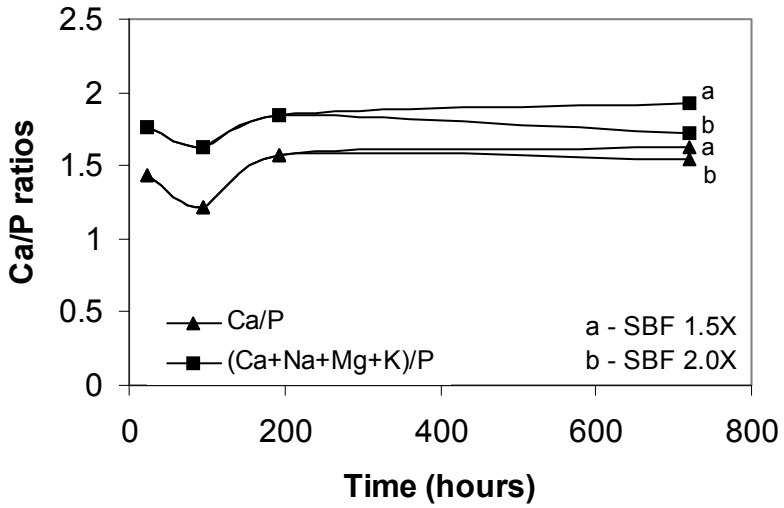


Figure 3. Ca/P and (Ca + Mg + Na + K)/P ratios of the apatites formed on compact SEVA-C substrates, after immersion in SBF 1X and after 7 days in SBF 1.5X or 2.0X.

Apatites formed in a solution often replace the Ca^{2+} ion site with small amounts of Na^{+}, Mg^{2+}, or K^{+} ions. The presence of these ions in the crystalline network of the apatite was evaluated. In fact, for the first stages of immersion in SBF there is a considerable difference between Ca/P and (Ca+Mg+Na+K)/P, being Na^{+} and Mg^{+} the main contributors for the presented values (data not shown). The presence of considerable amounts of Na^{+} in the apatites formed in the first hours can be justified by the existence of these ions at the surface, resulting from adsorption during impregnation with sodium silicate gel. Considerable amounts of Mg^{2+} were also detected for the first hours. This phenomenon is presently under study. The Ca/P ratios, tend to increase with immersion time in SBF, to values in the range between tricalcium phosphate (TCP, 1.5) and HA (1.67). When an

apatite layer is formed from an aqueous solution, some sites for the PO_4^{3-} are partially substituted by HPO_4^{2-} and CO_3^{2-} ion substituting for the PO_4^{3-} when comparing to the currently found for bone apatite (5.80 wt%) [24]. This result can be justified by a lower concentration of HCO_3^- in the produced SBFs when compared to human blood plasma (Table 1). After 30 days it is possible to observe a decrease in the Ca/P values of the apatites formed in the materials immersed in SBF 2.0x after 7 days, when comparing with values resulting from a second immersion in SBF 1.5X (from a to b). This decrease with increasing of the ionic activity product (IP) of the SBF solution was already reported by Kim *el al* [24] that calculated $H_2PO_4^-$, HPO_4^{2-} and PO_4^{3-} concentration of SBF with different IPs. Since $H_2PO_4^-$ ion concentration increases appreciably with increasing IP, comparing with the other phosphate ions, it is possible to assume that the degree of substitution of these ions for the PO_4^{3-} ions also increases appreciably with increasing IP, comparing with the other phosphate ions, it is possible to assume that the degree of substitution of these ions for the PO_4^{3-} ions also increases, leading to an increase in the Ca^{2+} deficiency [24]. This deficiency results from vacancies produced in the sites for the Ca^{2+} ions to maintain electrical neutrality.

Figure 4 presents the TF-XRD patterns of the surface of SEVA-C, before and after immersion in SBF, which was raised to a) 1.5x or b) 2.0x after the first week.

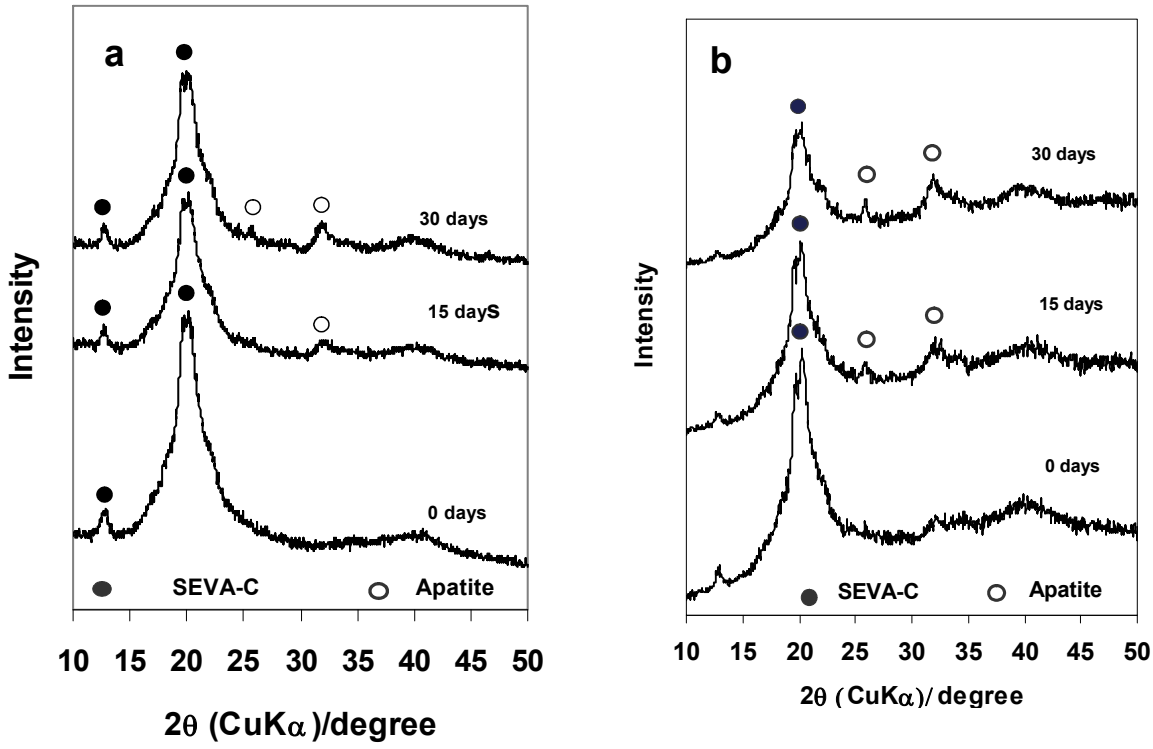


Figure 4. Thin-film X-ray diffraction patterns of the films formed on SEVA-C after treatment with sodium silicate and after 15 and 30 days of immersion in SBF. In a) the SBF solution was raised to 1.5X after 7 days, while in b) it was raised to 2.0X after the same period.

These patterns evidence poorly crystalline peaks mainly corresponding to hydroxylapatite on a mainly amorphous calcium-phosphate coating, for the longer SBF immersion periods. Nevertheless, when increasing the IP to 2X SBF, the crystallinity of the formed layers seems to be higher. It is well known that bone apatite also presents a highly amorphous content. The layers formed are consequently approaching bone apatite structure and are expected resorbed faster than highly crystalline coatings. The obtained results seem to indicate that it will be possible to tailor the coating relative crystallinity (and consequently its resorbability) by means of playing with the gel composition and the SBF concentration.

III.3.4. Cell adhesion and proliferation

Figures 5 and 6 show the SEM micrographs of the morphology of SEVA-C surface after immersion in SBF for 15 days and subsequent SaOS-2 cell culturing for 1 and 7 days.

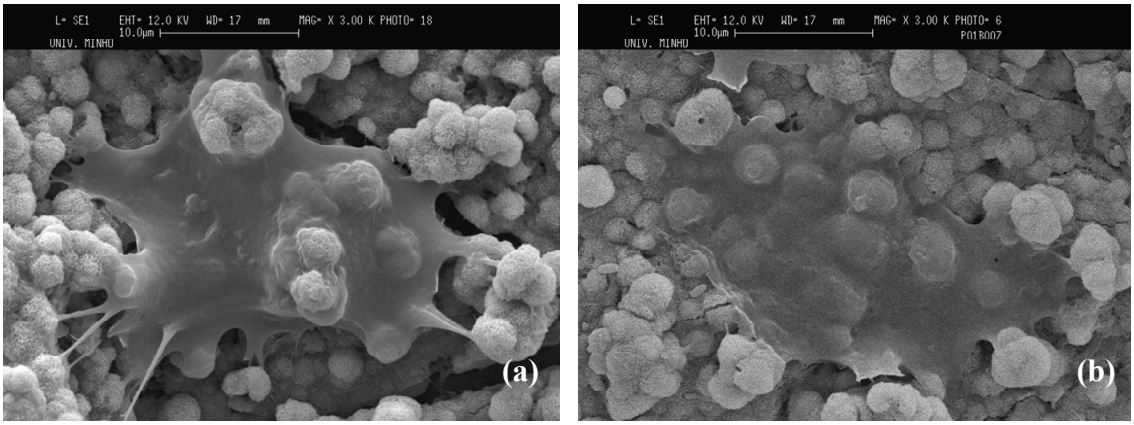


Figure 5. SEM micrographs showing the morphology of the apatite coatings formed on the surface of SEVA-C and the typical aspect of the SaOS-2 cells adhered to it: a) 1.5X SBF or b) 2.0X SBF.

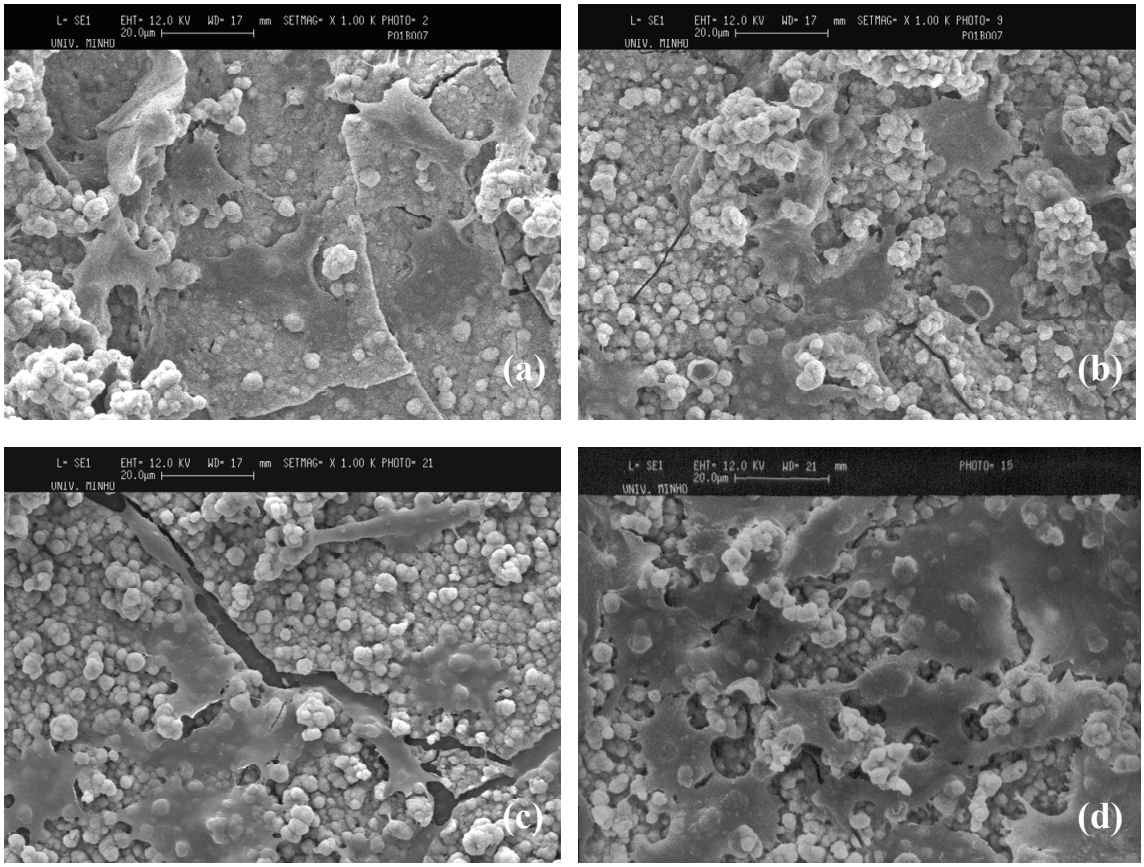


Figure 6. Proliferation of osteoblast-like cells after culture over the different surfaces: 1.5X SBF for a) 1 day and b) 1 week; and 2.0X SBF for c) 1 day and d) 1 week.

In the presented figures is possible to observe that the apatite layer is formed by aggregates of nucleus that have grown into the so-called *cauliflower* morphology, after 15 days of immersion in SBF (please remember that SBF concentration was raised to 1.5x after 7 days). This type of morphology was already reported for biomimetic coatings on the surface of similar polymers nucleated using bioactive silica glasses, produced in this type of materials [17,18]. For higher magnifications it is possible to observe a needle-like structure, which is typical of this type of coatings. This morphology is particularly evident after immersing in SBF 2.0x.

On what concerns to the study of cell adhesion and proliferation it is possible to observe, on the same SEM micrographs (Figure 5 and 6), that these preliminary results indicate good cell attachment to both types of coated surfaces. In addition, cell morphology was shown to be influenced by the type of coating produced, as the formation of characteristic lamellipodium structures was mainly detected for samples immersed in 1.5X SBF (please compare Figure 5a and 5b that are typical reproducible examples of cells behaviour on these surfaces). Even though 24 h of incubation was not enough to detect differences in cell number and distribution over both surfaces, after 7 days higher proliferation was

observed for 2.0X SBF samples (Figure 6). In fact, the crystallinity of a biomaterial surface is known to determine specific cell responses like the organisation of cytoskeleton filaments and cell proliferation mechanisms [30,31]. More specifically, results reported indicate that osteoblast spreading/proliferation is slower for more amorphous surfaces [30,31] mainly due to the development of less organised cytoskeleton [30]. Without minimising the influence of other factors, these results although still non-conclusive present a good reproducibility and a good correlation between crystallinity of apatite like coatings (see Figure 4) and cell spreading (see Figure 5) and morphology (see Figure 6).

III.4. Conclusions

Sodium silicate gel methodology proved to be a very effective and simple methodology to reduce the induction period for the formation of a well-defined apatite-like layer on the surface of starch based biodegradable polymers. Furthermore, when raising the concentration of the SBF solution during the growing period, it was possible to produce an apatite like layer more similar to bone apatite. Nevertheless in both cases a very good osteoblast adhesion and an undisrupted morphology were obtained, corresponding to a preliminary indicator of the biocompatibility of the apatite coatings. Furthermore, it can be said that SBF treatment or more specifically, the obtained characteristics of the coatings, influence positively cell proliferation kinetics. Cell behaviour seems to depend on coatings crystallinity being its activity slower for more amorphous surfaces.

References

1. T. Galliard, in: Starch: Properties and Potential, Critical Report on Applied Chemistry (John Wiley & Sons, New-York, 1987).
2. P. Forssell, K. Poutanen, Modification of Starch Properties with Plasticizers, *Biotechnology and Food Research* 4 (1996) 128.
3. M.E. Gomes, A.S. Ribeiro, P.B. Malafaya, R.L. Reis, A.M. Cunha, A New Approach Based on Injection Moulding to Produce Biodegradable starch-Based Polymeric Scaffolds: Morphology, Mechanical and Degradation Behaviour, *Biomaterials*, 22 (2001) 883.
4. P.B. Malafaya, C. Elvira, A. Gallardo, J. San Román, R.L. Reis, Porous Starch-Based Drug Delivery Systems Processed by a Microwave Route, *Journal of Biomedical Science - Polymer Edition*, 12 (2001) 1227.
5. M. E. Gomes, J. S. Godinho, D. Tchalamov, A. M. Cunha, R. L. Reis, Alternative Tissue Engineering Scaffolds Based On Starch: Processing Methodologies, Morphology, Degradation, Mechanical Properties And Biological Response, *Materials Science & Engineering C* 20 (2002) 19.
6. M.E. Gomes, R.L. Reis, A.M. Cunha, C.A. Blitterswijk, J. De Bruijn, Cytocompatibility and Response of Osteoblastic-like Cells to Starch-Based Polymers: Effect of Several Additives and Processing Conditions, *Biomaterials* 22 (2001) 1911.
7. A.P. Marques, R.L. Reis, J.A. Hunt, The Biocompatibility of Novel Starch-Based Polymers and Composites: *In Vitro* Studies, *Biomaterials* 23 (2002) 1471.
8. S.C. Mendes, J. Bezemer, M.B. Claase, D.W. Grijpma, V. Bellia, F. Degli-Innocenti, R.L. Reis, K .de Groot, C. Van Blitterswijk, J. De Bruijn, Evaluation of Two Biodegradable Polymeric Systems as Substrates for Bone Tissue Engineering, *Tissue Engineering* (2002), *in press*.
9. S.C. Mendes, R.L. Reis, Y.P. Bovell, A.M. Cunha, C. Van Blitterswijk, J. De Bruijn, Biocompatibility Testing of Novel Starch Based Materials with Potential Application in Orthopaedic Surgery: a Preliminary Study, *Biomaterials* 22 (2001) 2057.
10. R.L. Reis, A.M. Cunha, Characterization of Two Biodegradable Polymers of Potential Application within the Biomaterials Field, *Journal of Materials Science: Materials in Medicine* 6 (1995) 786.
11. R.L. Reis, A.M. Cunha, P.S. Allan, M.J. Bevis, Mechanical Behaviour of Injection-Moulded Starch Based Polymers, *Polymers Advanced Technologies* 7 (1996) 1.
12. C.S. Pereira, A.M. Cunha , R.L. Reis , B. Vázquez, J. San Roman, New Starch-Based Thermoplástic Hydrogels for Use as Bone Cements or Drug-delivery Carriers, *Journal of Materials. Science: Materials in Medicine* 9 (1998) 825.
13. Y. Abe, T. Kokubo, T. Yamamuro, Apatite coating on ceramics, metals and polymers utilizing a biological process, *Journal of Materials. Science: Materials in Medicine* 1 (1990) 233.
14. M. Tanashi, T. Yao, T. Kokubo, M. Minoda, T. Miyamoto, T. Nakamura, T. Yamamuro Apatite coating on organic polymers by biomimetic process. *Journal of American Ceramic Society* 7 (1994) 2805.
15. C. Rey, Calcium Phosphate Biomaterials and Bone Mineral. Differences in Composition, Structures and Properties, *Biomaterials*, 11 (1990) 13.
16. M. Tanashi, K. Hata, T. Kokubo, M. Minoda, T. Miyamoto, T. Nakamura, T. Yamamuro, Effect of Substrate on Apatite Formation by a Biomimetic Process, in Bioceramics 5, edited by: T. Yamamuro, T. Kokubo, T. Nakamura (Kobunshi-Kankokai, Kyoto, 1992), p.57.
17. R.L. Reis, A.M. Cunha, M.H. Fernandes, R.N. Correia, Treatments to induce the nucleation and growth of apatite-like layers on polymeric surfaces and foams, *Journal of Materials. Science: Materials in Medicine* 8 (1997) 897.
18. A.L. Oliveira, C. Elvira, B. Vázquez, J. San Roman, R. L. Reis, Surface Modifications Tailors the Characteristics of Biomimetic Coatings Nucleated on Starch Based Polymers, *Journal of Materials Science: Materials in Medicine* 10 (1999) 827.
19. F. Miyaji, S. Handa, T. Kokubo, T. Nakamura, Apatite formation on polymers by biomimetic process using sodium silicate solution, in: Bioceramics 10, edited by: L. Sedel, C. Rey (Elsevier Science, Amsterdam, 1997) p.7.

20. F. Miyaji, H. Kim, S. Handa, T. Kokubo, T. Nakamura, Bonelike apatite coating on organic polymers: novel nucleation process using sodium silicate solution, *Biomaterials* 20 (1999) 913.
21. A.L. Oliveira, P.B. Malafaya, R.L. Reis, Sodium silicate gel induced self-mineralization of different compact and porous polymeric structures, in Bioceramics 13, edited by: S. Giannini, A. Moroni (Trans Tech. Publications, Zurich, 2000) p.75.
22. D. Demirgöz, C. Elvira, J. F. Mano, A.M. Cunha, E. Piskin, R.L. Reis Chemical Modification of Starch Based Biodegradable Polymeric Blends: Effects on Water, Degradation Behaviour and Mechanical Properties, *Polymer Degradation and Stability* 70 (2000) 161.
23. D.K. Owens, R.C. Wendt, Estimation of Surface Free Energy of Polymers, *Journal of Applied Polymer Science* 13 (1969) 1741.
24. H.-M. Kim, K. Kishimto, F. Miyaji, T. Kokubo, T. Yao, Y. Suetsugu, J. Tanaka, T. Nakamura, Composition and structure of the apatite formed on PET substrates in SBF modified with various ionic activity products. *Journal of Biomedical Materials Research* 46 (1999) 228.
25. R.L. Reis, S.C. Mendes, A.M. Cunha, M.J. Bevis, Processing and in-vitro degradation of starch/EVOH thermoplastic blends, *Polymer International* 43 (1997) 3473.
26. I. Espigares, C. Elvira, J.F. Mano, B. Vasquez, J. San Roman, R.L. Reis, New biodegradable and bioactive acrylic bone cements based on starch blends and ceramic fillers, *Biomaterials* 23 (2002) 883.
27. P. Li, C. Ohtsuki, T. Kokubo et al, Apatite coating on organic polymers by a biomimetic process. *Journal of American Ceramics Society* 75 (1992) 2094.
28. S Cho, F Miyaji, T Kokubo, K Nakanishi, N Soga, T Nakamura, Apatite-forming ability of silicate ion dissolved from silica gels, *Journal of Biomedical Materials Research* 32 (1996) 375.
29. D. Bakker, J.J. Grote, C.M.F. Vrouenraets, S.C. Heseling, J.R. De Wijn, C.A. Van Blitterswijk, in: Clinical Implant Materials, edited by: G. Heimke, U. Soltesz, A.J.C. Lee (Elsevier, Amsterdam,1990) p.99.
30. M. D. Ball, S. Downes, C. A. Scatchford, E. N. Antonov, V. N. Bagratashvili, V. K. Popov, W. J. Grant, S. M. Howdle, Osteoblast growth on titanium foils coated with hydroxylapatite by pulsed laser ablation, *Biomaterials* 22 (2001) 337.
31. L. Chou, B. Marek, W. R. Wagner, Effects of hydroxylapatite coating crystallinity on biosolubility, cell attachment efficiency and proliferation in vitro, *Biomaterials* 20 (1999) 977.

CHAPTER IV

Chapter IV

Nucleation and Growth of Biomimetic Apatite Layers on 3D-Plotted Biodegradable Polymeric Scaffolds: Effect of Static and Dynamic Coating Conditions

Abstract

This work originally proposes biomimetic coating routes for the production of an apatite layer on the surface of newly developed starch/polycaprolactone (SPCL) based scaffolds by a 3D-plotting technology. To produce the biomimetic coatings a sodium silicate gel was used as nucleating agent, followed by immersion in a simulated body fluid solution (SBF). After stabilizing the apatite layer for 7 days, different conditions were studied: static, agitation (80 U/min.) and circulating flow perfusion (Q=4mL/min; t_R=15s) up to 14 days. The scaffolds and apatite coatings were characterized by Scanning Electron Microscopy (SEM)/Electron Dispersive Spectroscopy (EDS), Fourier Transformed Infra-Red (FTIR) and Thin-Film X-Ray Diffraction (TF-XRD). Cross-sections were obtained and the coatings' thickness was measured. The elemental composition of solution and coatings was followed by Induced Coupled Plasma Spectroscopy (ICP). After only 6 hours of immersion in SBF it was possible to observe the formation of small nuclei of an amorphous calcium phosphate (ACP) layer. After subsequent SBF immersion from 7 to 14 days in static, agitation and circulating flow perfusion conditions this layers have grown into bone-like nanocrystalline carbonated apatites. The layers produced under the different conditions have clearly covered each scaffold fibre without compromising its initial morphology. No differences in the composition and chemical structure of the apatites were detectable between the coating conditions. However, in case of flow perfusion the coating thickness was significantly higher. This condition, besides mimicking better the biological milieu, allowed for the coating of complex architectures at higher rates for the production of apatite layers, which can greatly reduce the coating step.

---

*This part of the chapter is based on the following publication:

A.L. Oliveira, S.A. Costa, R.A. Sousa, R.L. Reis, Nucleation and Growth of Biomimetic Apatite Layers on 3D-Plotted Biodegradable Polymeric Scaffolds: Effect of Static and Dynamic Coating Conditions, Biomaterials, (2007), *submitted*.

IV. 1. Introduction

The field of tissue engineering continues to advance with the discovery of new biomaterials, growth factors and scaffold fabrication techniques. In addition to demineralised bone matrix, numerous synthetic [1-3] and naturally [4-6] derived biodegradable porous scaffolds are being proposed to be used as bone graft substitutes and as delivery vehicles for bioactive factors and osteogenic cells. Among these, starch-based polymeric systems are particularly interesting due to their well-established biocompatibility [7,8] and processing versatility [9-13]. Concurrently, a variety of techniques for the processing of porous scaffolds have been reported [1-3,14-16]. However, most of the conventional fabrication techniques, available, do not yet meet the desired properties, as many of the processing routes still depend heavily on manual intervention. This will result in inconsistent and inflexible processing procedures. Rapid prototyping (RP) technologies are considered as potential routes for the production of complex scaffolds for TE applications, as they present superior control over design, manufacturing and reproducibility of TE scaffolds [16,17]. Moreover, when coupled with adequate image acquisition software, RP allows for the production of anatomically adapted 3D scaffolds based on the patient's own defect. In addition, the scaffold architecture can be tailored to present different symmetries. A clear example of the potential of these technologies is the work carried out by Hutmacher and co-workers [1] in exploring Fused Deposition Modeling (FDM) technique for the development of polycaprolactone (PCL) scaffolds.

From a TE point of view, the advantageous characteristics of fibre-based scaffolds include large surface area for enhancing cell attachment and rapid diffusion of nutrients which favours cell survival and proliferation [18]. Moreover, to provide the appropriate surface chemistry for cell attachment and proliferation is another key issue that needs to be addressed. In this sense a challenging, but yet attractive approach to better induce bone formation is to promote the mineralization of a bone-like calcium phosphate (generically designated as Ca-P or "apatite") layer on the outermost surface of the scaffold. Ca-P minerals found in natural hard tissues are produced spontaneously in a physiological environment at low temperatures from moderately supersaturated mineralizing solutions [19]. To learn, understand and apply these natural processes for producing Ca-P coatings

biologically identical to bone apatite has been the focus of the attention of many researchers in the recent years, as reviewed elsewhere [20].

The so-called biomimetic preparation of calcium phosphate coatings on implant materials as then emerged as a new concept, and has been initially proposed by Kokubo and co-workers [21] by using solutions able to mimic the inorganic composition of the human blood plasma, i.e. simulated body fluid solutions (SBFs). Besides its osteoconductive properties, a biomimetic apatite layer discloses a carrier potential due to the physiological operating conditions of temperature and pH. In fact, these coatings can serve as vehicles for the release of biologically relevant molecules such as protein growth factors, enzymes or pharmaceutical drugs used in bone related diseases. So far, this potential has not been fully exploited.

To effectively coat an apatite layer on the surface of a biodegradable polymeric scaffold, while ensuring a homogeneous coating distribution throughout the entire surface of the pores without compromising its initial shape represents an enormous challenge, due to complex features such as the coating composition, thickness distribution or the adhesion to the substrate. Moreover, pH changes due to possible degradation of substrates surface during the coating process have also to be taken into consideration. Nevertheless, in our research group these biomimetic coatings could be effectively produced on the surface of starch based biodegradable polymers [22,23], namely by developing a biomimetic methodology using a sodium silicate gel as nucleating agent.

In the latest years, the majority of the biomimetic routes proposed for coating of calcium phosphate (Ca-P) layers on surface of biomaterials have been limited to static conditions [22,24-30]. However *in vivo*, the mineralization of bone tissue occurs in the presence of body fluids that continuously circulate in the body [31]. Therefore, an *in vitro* biomimetic approach including dynamic studies is of great significance as it comes closer to the *in vivo* scenario, were the flow of human body fluids may have an effect on the formation of bone apatite [32]. Few authors [33-37] have studied the mineralization of apatite layers under dynamic conditions, being these studies only intended to better assess the bioactive behaviour of silica-based bioceramics. These materials are highly reactive causing a local decrease of Ca^{2+} and PO_4^{3-} in the surrounding solution, during apatite formation in static conditions, which will compromise the progress of the mineralization process. When considering 3D porous architectures that are not bioactive *per se*, dynamic mineralization environments can also be suitable to promote a homogeneous formation of the Ca-P layer on its interior. This work studies the nucleation of apatite layers on the surface of starch

poly-caprolactone (SPCL) scaffolds produced by a 3D-plotting technology, and its subsequent growth by under different static and dynamic mineralizing conditions.

IV.2. Materials and Methods

IV.2.1. Preparation of the scaffolds

As a natural origin polymer, starch based biomaterials exhibit a great potential to be used in bone related applications [38-41]. In this work, the studied material is based on a blend of starch/polycaprolactone (SPCL). The blend contains around 30% starch by weight. The selected biomaterial presents a good biological behaviour and has been proposed for bone Tissue Engineering applications by using other fibre-based processing routes such as fibre bonding [12,42-44] and by combining this technique with electrospinning to generate nano- and micro-fibre 3D architectures [12].

SPCL scaffolds were produced, for the first time, using a 3D plotting technology (Bioplotter, EnvisionTec GmbH, Germany). In this case alternated layers with a 0º/90º/0º/90º orientation period were plotted. The resulting pattern has generated an off-set which will increase the asymmetry level. Figure 1 illustrates the geometry of the obtained scaffolds. Cubic samples with a lateral side of L= 5 mm were produced.

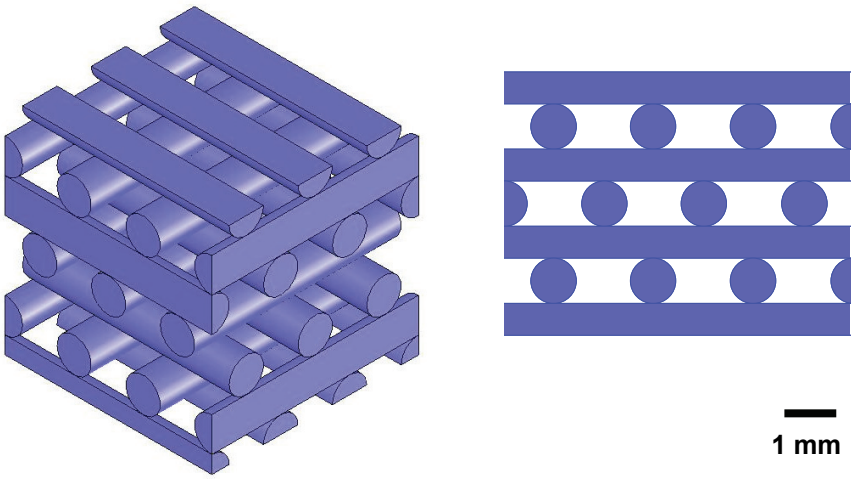


Figure 1. Geometry of the scaffolds as produced by the 3D plotter technology.

IV.2.2. Apatite Coating Formation

To produce an apatite coating on the surfaces of the obtained SPCL scaffolds a biomimetic methodology was used based in a previously developed sodium silicate methodology [22]. The samples were "impregnated" for 1 hour with a sodium silicate gel from SIGMA-ALDRICH ($Na_2SiO_3 \bullet H_2O$, containing ~14% NaOH and ~27% SiO_2, pH ≈13), under mild agitation. Sodium silicate gel was herein used with concentration and SiO_2/Na_2O molar ratio as received. After this treatment the solution with the samples was diluted with 50% vol. of distilled water and stirred for 5 minutes. This procedure was aimed at diminishing the viscosity of the gel in order to produce a homogeneous and thin layer of vitrified sodium silicate in the surface of the materials. The scaffolds were then removed from the solution and then dried in vacuum for 3 hours and in a controlled atmosphere (23 ± 1 ºC; 55% RH) for 24 hours. A more detailed description on the coating methodology can be found elsewhere [22].

An aqueous solution was prepared comprising all major inorganic ions present in the human's blood plasma and presenting its approximate ion concentration, in order to promote *in vitro* apatite formation. The different salts were dissolved in de-ionized H_2O and the pH adjusted to neutral using tris(hydroxymethyl)aminomethane and hydrochloric acid. This simulated body fluid solution (SBF) was developed by Kokubo and co-workers [45].

The as-treated scaffolds were immersed in the SBF solution for 7 days. During this period the solution was renewed every 2 days and an apatite layer was allowed to nucleate and grow on the surface of the samples. Following this period, the samples were divided into 3 different groups and placed in contact with a renewed SBF solution under different conditions: static, agitation by shaking in a thermostatic bath (Selecta, Unitronic, Spain, 80 strokes/min.) and circulating flow perfusion in a bioreactor (volume flow rate (Q) of 4mL/min; Residence Time (t_R) of 15 s) for periods up to 14 days. In all the conditions the total volume of SBF available per sample was 50 mL and the solution was renewed every 2 days (solid-to-liquid ratio of 1g/400mL/week). Table 1 summarizes the different coating conditions.

Table 1. Static and dynamic conditions for coating apatite layers on the SPCL scaffolds.

Periods (Days)	**SBF**	**Conditions**		
7	1 X	Static		
14	1 X	Static	Agitation	Flow perfusion
Volume of SBF available per sample		50 mL	50 mL	50 mL
Solid-to-liquid ratio		1g/400mL/week	1g/400mL/week	1g/400mL/week
Fluid Flow		None	Turbulent flow (80 Strokes/min)	Laminar flow (Q=4 mL/min; t_R=15s)

For the last condition a special bioreactor [46] was designed according with the schematic drawing of Figure 2.

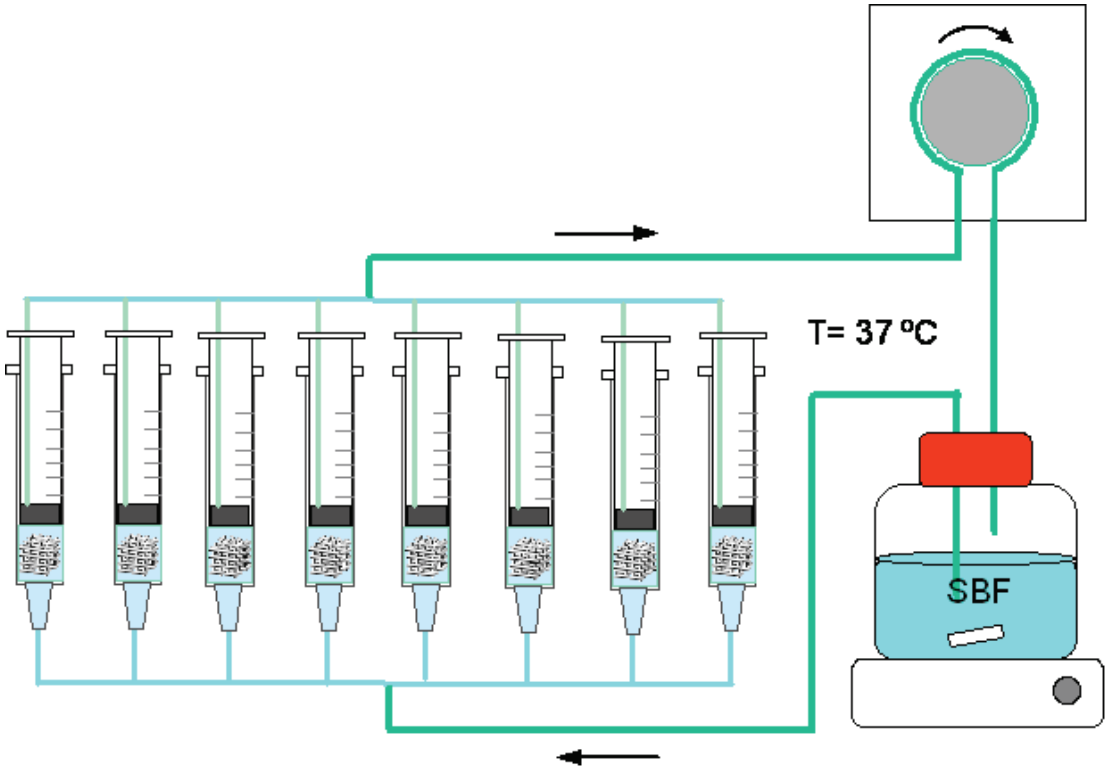


Figure 2. Schematic drawing of the bioreactor designed for coating an apatite layer under flow perfusion.

After 7 and 14 days the samples were removed from solution, washed in distilled water and dried in a controlled atmosphere (23 ± 1 ºC; 55% RH).

IV.2.3. Scanning Electron Microscopy (SEM) and Energy Dispersive Spectroscopy (EDS)

The morphological characterisation of the scaffolds was carried out by Scanning Electron Microscopy (SEM), in a LEICA Cambridge S360, United Kingdom. All the samples were coated with a thin film of carbon, by ion sputtering, prior to any observation. The electron beam energy was 10 and 12 KeV. The scaffolds were observed in 3 different orientations: from the top, lateral side and bottom, for the different tested periods and conditions in SBF. The corresponding cross-sections were also analysed and the thickness of the apatite layers was calculated by performing measurements in six fibres *per* scaffold (3 measurements *per* fibre). Since these coatings are constituted by fused spherical apatite nuclei they present an irregular surface. Therefore, in order to ensure that the measure would be done in the same way for all the conditions the basis of these nuclei was established as the limit for the coating. In this was the measured average values are the minimum thickness values for all the samples.

IV.2.4. X-Ray Diffraction (TF-XRD)

Thin-Film X-Ray Diffraction (TF-XRD, Philips X'Pert MPD, The Netherlands) was used to identify any crystalline phases present in the apatite layers formed during the immersion in SBF. The data collection was performed by 2θ scan method with 1º as incident beam angle using Cu$K\alpha$ X-ray line and a scan speed of 0.05 º/min in 2θ.

IV.2.5. Fourier Transformed Infra-Red (FTIR)

The chemical structure of the apatite coatings formed on the surface of the SPCL scaffold fibres after the different periods and conditions in SBF was analysed by Fourier Transform Infrared Spectroscopy (FTIR). The surface of the fibres was scratched and the resulting particles were milled with KBr powder and shaped by compression into pellets for further analysis. All spectra were recorded using 64 scans and 2 cm^{-1} resolution in an FTIR spectrophotometer (Perkin-Elmer 1600 Series, USA).

IV.2.6. Inductively Coupled Plasma Spectroscopy (ICP)

The composition of the Ca-P coatings was assessed by analysing the solution resulting from dissolving the coated scaffolds in 0.1 M HCl, under agitation for 24 hours (the

scaffolds were examined by SEM afterwards to confirm the total dissolution of the coating at the surface). The elemental concentration was measured by Inductively Coupled Plasma Optical Emission Spectroscopy (ICP-OES, JY 70 plus, Jobin Yvon, France). Duplicate samples were analysed for each condition and immersion time. From these results Ca/P ratios were calculated. Considering the possibility of Mg^{2+}, Na^{+} and K^{+}, present in the SBF, substituting the Ca^{2+} in the crystalline network of the apatite, the following relations were also considered: (Ca+Na+Mg+K)/P; (Ca+Mg+K)/P; Na/Ca; Mg/Ca; K/Ca.

The evolution of the elemental composition of the solution during the coating formation was also monitored by ICP. The concentration of Ca, P, Na, Mg, K and Si elements was measured after 3, 6 and 24 hours, 2, 5, 7 and 15 days. From the obtained concentration of ions consumed or released to the solution at each time point the cumulative concentration was calculated according to the following equation:

$$C = \Sigma ([C_n] - [C_{n+1}]) \qquad \text{(Equation 1)}$$

IV.3. Results

IV.3.1. Nucleation of the apatite layer

Figure 3 presents SEM micrographs of the obtained SPCL scaffolds' morphology after plotting using the Rapid Prototyping Technology.

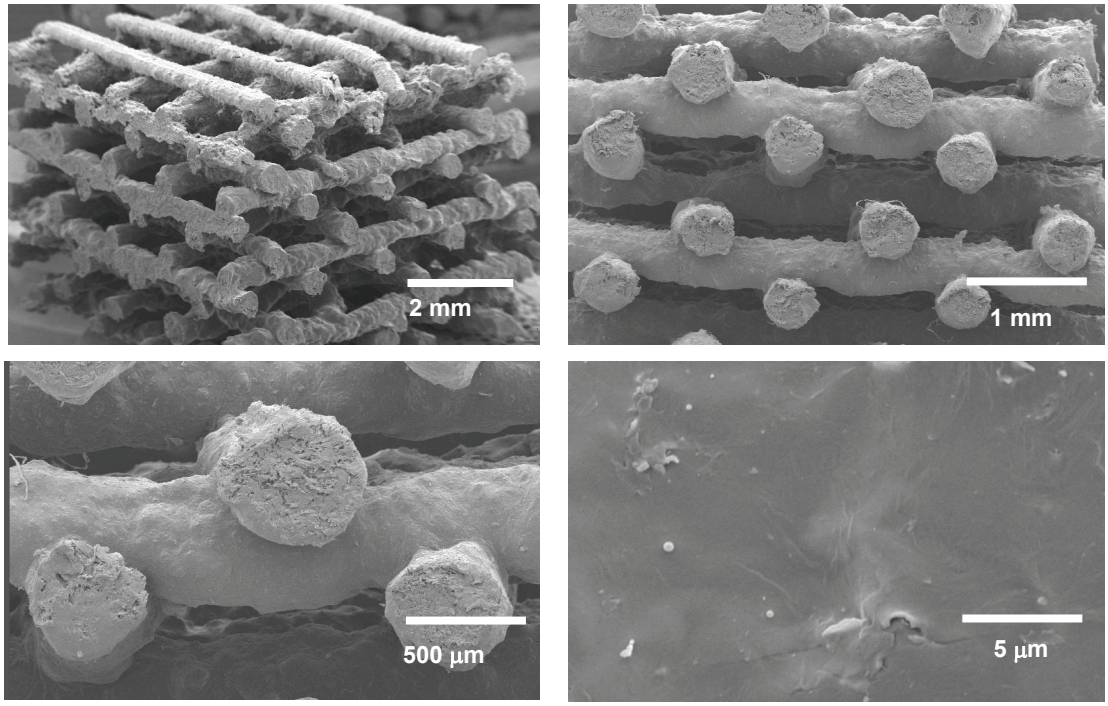


Figure 3. SEM micrographs of the scaffolds produced by the Bioplotter® technology.

This technology has enabled a superior control over scaffold morphology, resulting in the fabrication of scaffolds with controlled porosity and interconnectivity. Moreover, the applied plotting technique allowed for the processing of fibre-based 3D constructs with a controlled morphology and porosity (around 70 %) in a reproducible manner. The average diameter of the produced fibres was around 500 μm.

Figure 4 presents the scaffolds treated with sodium silicate and after different periods in SBF up to 7 days.

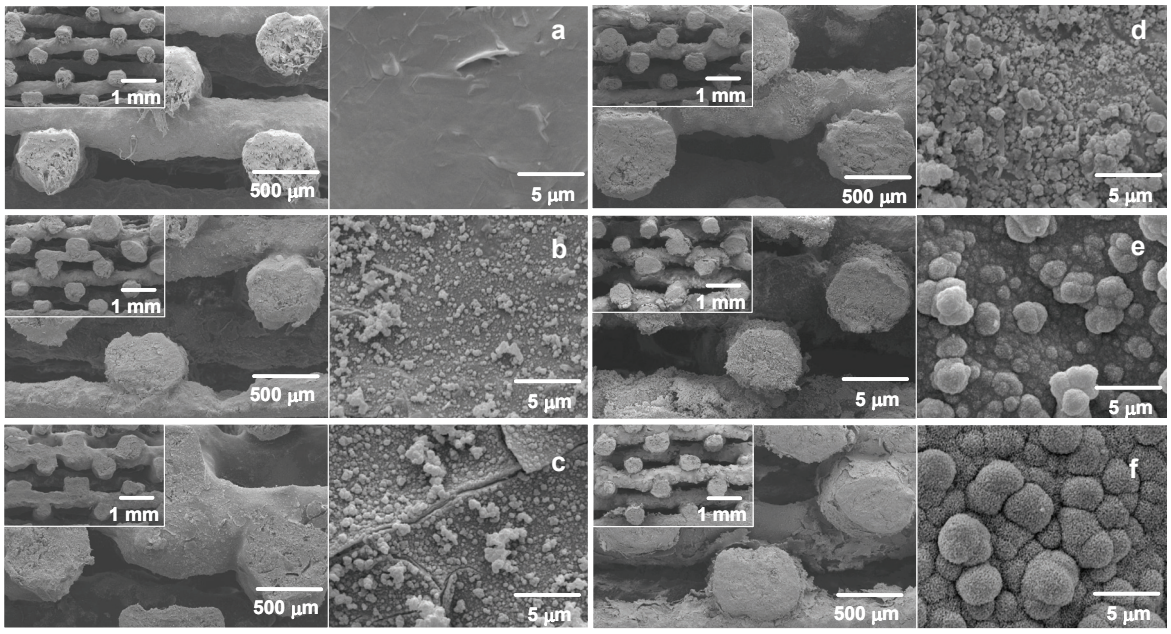


Figure 4. SEM micrographs of the scaffolds a) treated with sodium silicate and after different periods in SBF: b) 6 and c) 24 hours, d) 2, e) 5 and f) 7 days, showing the evolution of the apatite layer in the nucleation stage.

Sodium silicate treatment followed by immersion in the SBF solution for 7 days has resulted in the nucleation of a well-defined apatite layer covering the entire surface of the fibres while maintaining their initial porous structure and interconnectivity (Figures. 4.a to f). This biomimetic methodology was for the first time applied to coat 3D-plotted starch biodegradable scaffolds. After only 6 hours of immersion in SBF (Figure 4.b) it was possible to observe the formation of small nuclei at the surface of the scaffolds with an approximate size of few tens of nanometres, aggregated into a layer. With increasing time of immersion the initially formed nuclei have grown to form a continuous layer composed of a globular structure clearly observed after 5 days of immersion and later on (Figures 4.e and f). At higher magnifications, it is possible to detect a needle-like nano-structure that is characteristic of Ca-P coatings formed under the present biomimetic conditions.

In Figure 5 are presented the FTIR spectra performed on the scaffolds untreated, after the treatment with sodium silicate and after subsequent immersion in SBF up to 7 days. The IR bands were assigned according with previous studies [47-49].

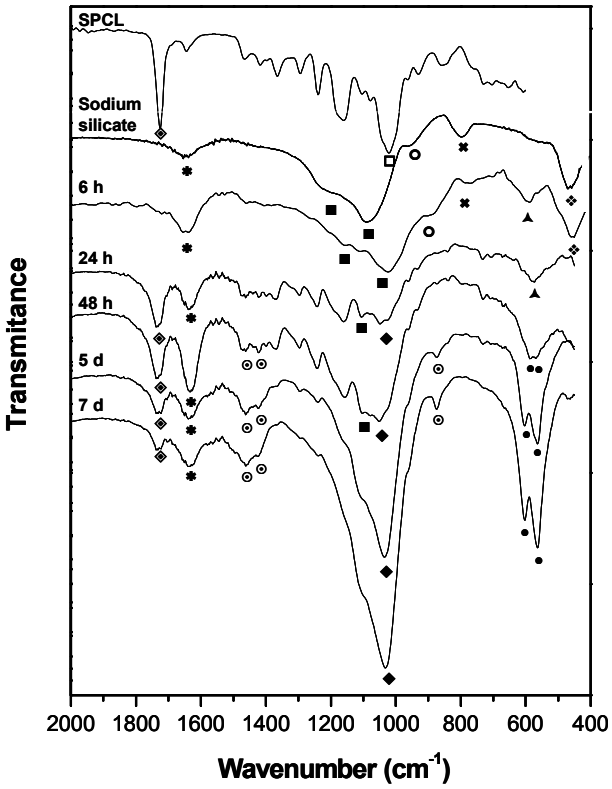


Figure 5. FTIR spectra of the scaffolds treated with sodium silicate and after different periods in SBF up to 7 days. ◘ -C-O-C-, ◈ C=O,■ Si-O (stretch), O Si-O-Na (stretch), ✖ Si-O-Si (stretch), ❖ Si-O-Si (bend), ✱ H_2O, ⊙ CO_3^{2-}, ● O-P-O (ν_4, bend), ▲ P-O (bend)◆ P-O (ν_3, stretch).

The IR spectrum of the SPCL blend revealed the presence of the main characteristic bands of corn starch and polycaprolactone (PCL). The band at 1150-1040 cm^{-1} is related to the -C-O-C- in glycosidic bonds of starch [47]. The characteristic band of PCL is located at 1726 cm^{-1}, corresponding to the C=O stretch ester carbonyl group [48]. The peaks at 1600-1580 and 1200-1000 cm^{-1} are related to asymmetric stretch of -COO- and the stretch of the -C-O bond at the main polymer chain [48].

Analyzing the spectrum correspondent to sodium silicate removed form the surface of the scaffolds before immersion in the SBF solution it is possible to detect 5 different bands, as reported before by Takadama *et al.* [49]. At 470 cm^{-1} a band corresponding to the bending of the Si-O-Si bond is identified; another band appears at 800 cm^{-1}, corresponding to the stretching mode of the same bond; the band identified at 950 cm^{-1} corresponds to the Si-O-Na stretching bond; the bands at 1090 e 1200 cm-1, are related to the stretch of the Si-

O bond. The bands detected at 1638 cm^{-1} are assigned to water molecules present in the sodium silicate structure.

The IR analysis performed to the coatings removed form the surface of the scaffolds during the first periods of immersion in SBF (up to 48 hours), revealed the presence of Si-O stretching bonds which are ascribed to the sodium silicate, abundant in Si-OH groups [50]. After 6 hours a band ascribed to P-O bending bonds is revealed at 590 cm^{-1} attributed to the formation of amorphous calcium phosphate (ACP) [51]. This band started to dissociate into two new bands after 48 hours being assigned to the ν_4 bending mode of the O-P-O bonds which are characteristic of more crystalline apatites. After 5 and 7 days these two bands have increased in intensity and could be detected at 602 and 564 cm^{-1}. The band at 1032 cm^{-1} indicates the ν_3 stretching mode of P-O bonds [51], and has also increased in intensity with time. The bands at 876, 1424 and 1462 cm^{-1} result from the presence of carbonate (CO_3^{2-}) incorporated in the apatite lattice [51,52]. The presence of these bands clearly indicates that a carbonated apatite was formed, similar to the one found in bone apatite.

In Figure 6 is presented the TF-XRD spectra performed on the scaffolds untreated, after the treatment with sodium silicate and after subsequent immersion in SBF up to 7 days. The XRD peaks were assigned according with previous studies [22,23].

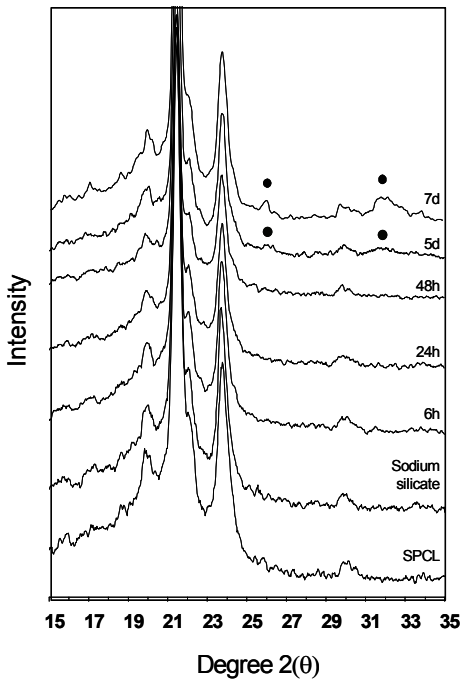


Figure 6. TF-XRD spectra of the scaffolds treated with sodium silicate and after different periods in SBF up to 7 days. ● main characteristic peaks assigned to hydroxyapatite.

The peaks detected at 2θ=20º, 21º and 24º are assigned to SPCL crystalline phases [23]. After the treatment with sodium silicate and subsequent immersion in SBF no changes in the XRD profiles were detected in the first 48 hours, indicating that the initially formed Ca-P layer exhibited and amorphous character. After 5 days the main two characteristic peaks attributed to HA started to be detected, and have increased in intensity after 7 days, due to an increase of the crystallinity and in the thickness of the apatite layer. The broad peak at 2θ = 26º is assigned to (002) plane in the lattice of the apatite crystals. Another important diffraction peak is detected around 2θ = 32º and is related to the overlapping of planes (211), (112) and (300). Together with FTIR data it was possible to confirm that a poorly crystalline carbonated apatite similar to bone was formed.

The variation of Ca, P, Si, Mg, Na, K and Si concentrations in the SBF solution as function of immersion time during the first week of the biomimetic treatment are shown in Figure 7.

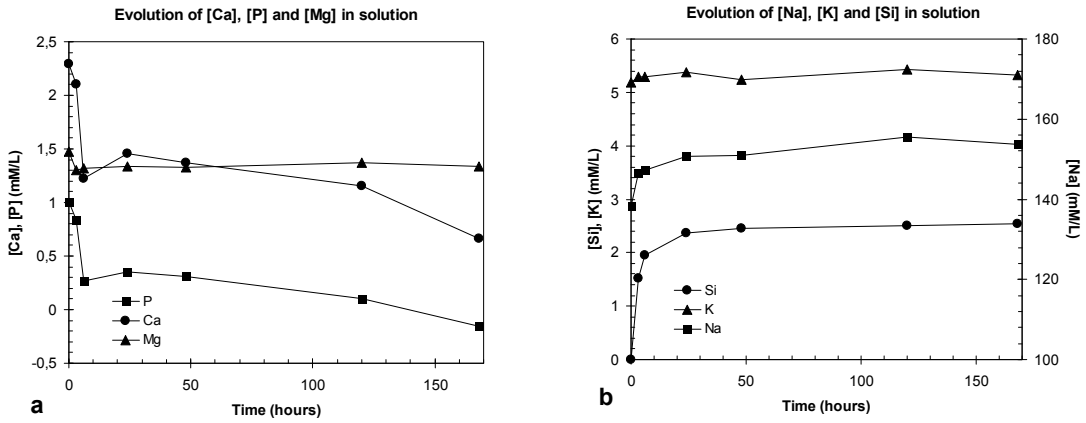


Figure 7. Evolution of the elemental concentration of SBF solution measured by ICP analysis for different periods up to 7 days showing a) the consumption of Ca, P and Mg ions and b) the release of Na and Si ions.

When considering the ionic composition of the SBF solution, it was observed that during the coating process a simultaneous drop of the concentration levels of Ca and P ions is observed, indicating that a Ca-P is being formed by consuming these ions from solution (Figure 7a). During this process, Ca and P are being consumed at a higher rate in the first hours and from then on more gradually. Initially, the presence of the sodium silicate at the surface of the scaffolds have induced the formation of a large number of Ca-P nuclei during the first 6 hours of immersion in SBF, as shown in Figure 4. Once stabilized, these nuclei have grown to form a continuous apatite layer, consuming Ca and P at a lower rate. On the other hand, when analysing the evolution of Na and Si in solution, an accentuated increase of their concentrations was observed initially, which is attributed to the dissolution

of the sodium silicate from the surface, thus creating at the near surface the adequate environment for the apatite to nucleate and grow (Figure 6a). A small decrease in the Mg concentration was observed in the first hours of immersion, indicating that this element could be incorporating the structure of the first formed apatite nuclei. The variation of the K concentration was considered irrelevant during the studied period of apatite formation, indicating that this element is not participating in the nucleation process.

Figure 8 presents the elemental ratios calculated from values measured by ICP, after dissolution of apatite layers formed during different periods in SBF up to 7 days.

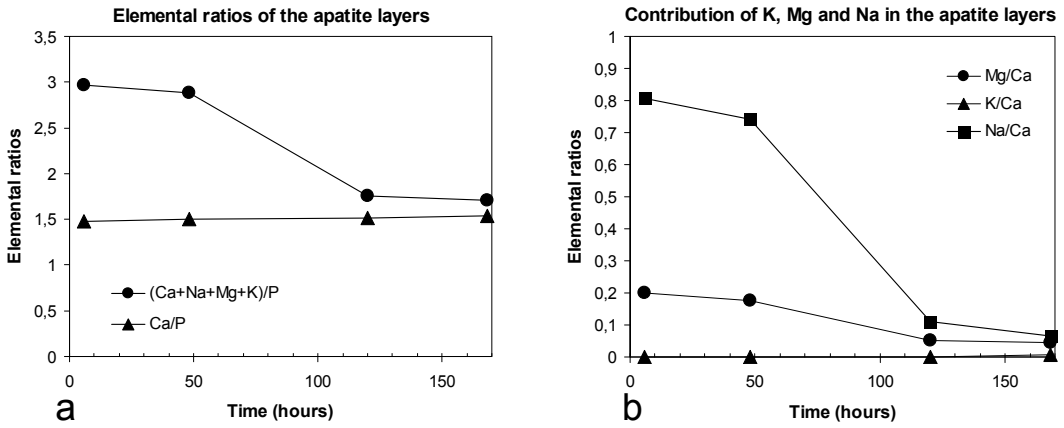


Figure 8. Evolution of the elemental ratios of the obtained apatite layers for different periods up to 7 days.

The Ca/P ratio of the apatite nuclei formed after the first 6 hours of immersion in SBF (Figure 8.a) was around 1.48, which is close to the value attributed to tricalcium phosphate (TCP, Ca/P=1.50). The results obtained from FTIR and XRD analysis (Figures 5 and 6) indicate that the first calcium phosphate nuclei to be formed presented an amorphous nature. In this way an amorphous phase (ACP) corresponding to a TCP-like composition was formed. A slow increase of the Ca/P ratio up to 1.54 was observed over time of immersion in SBF up to 7 days. The Ca/P ratio of stoichiometric hydroxyapatite ($Ca_{10}(PO_4)_6(OH)_2$*$10H_2O$) is 1.67. In this way, the obtained apatite is Ca defective. When considering the presence of Na, Mg or K in the apatite structure, the obtained values for the elemental ratios increased mostly in the first days of immersion in the SBF (Figure 7.a). By analyzing the individual contribution of each element (Figure 7.b) it is possible to observe that this increase has been attributed to Na and Mg. The detection of considerable amounts of Na in the apatites formed in the first hours can be justified by the presence of sodium silicate during the nucleation stage. This ion will be mostly physically adsorbed in the apatite structure. On the other hand, it is known that Mg can be easily accommodated in the structure of ACP by substituting Ca, causing local deformation with

eventual shrinking of the columns of calcium and distortion of PO_4 polyhedra, as magnesium has a lower ionic radius than calcium (0.66 versus 0.99 Á) and a shorter bond length with oxygen (Mg-O is about 2.1 Á, whereas Ca-O in HA is in the range 2.443-2.555 Á) [53]. The presence of this ion will stabilize the initially formed amorphous Ca-P nuclei and, and it is believed to ensure their chemical bonding to the substrate [28]. Due to mechanical strains induced by Mg ions, nucleation of HA is hindered and will only start to form when Mg ions will leave the structure. In fact, after 48 hours of immersion in SBF the presence Mg decreases together with Na, indicating that these ions will leave the Ca-P structure. This compositional evolution occurred together with an increase in the crystallinity of the apatite structure. The mechanism for the nucleation and growth of an apatite layer on a sodium silicate gel has been previously studied by Takadama *et al.* [49,50] and Miyagi *et al.* [54]. In brief, a calcium phosphate layer is grown as a consequence of electrostatic interactions of negatively charged Si-O units, formed by dissociation of the Si-OH groups, with the positively charged calcium ions in the fluid. A positively charged calcium silicate layer is then formed which will interact with the negatively charged phosphate ions in the fluid to form an ACP, which then stabilizes into a nano-crystalline apatite layer. The resulting Ca-P coating presents a needle-like structure (Figs. 2d) corresponding to the typical morphology obtained by this biomimetic route in previous work by the authors [22]. This coating was present both in the outside and in the interior of the scaffold. Apatite nucleation was clearly controlled by the surface, which has served as a template for the mineralization process to take place.

IV.3.2. Growing of the apatite layer under static and dynamic conditions

After 7 days of immersion in static SBF, the samples were divided into 3 groups and immersed in another SBF solution under 3 different hydrodynamic conditions: static, agitation and flow perfusion for periods up to 14 days. As said before, this new biomimetic approach intends to produce, for the first time, apatite coatings on the surface of the newly developed SPCL scaffolds without compromising its initial porosity or interconnectivity. Figure 9 presents the typical FTIR and TF-XRD spectra of the apatite coatings produced in the different SBF conditions, for the period of 14 days.

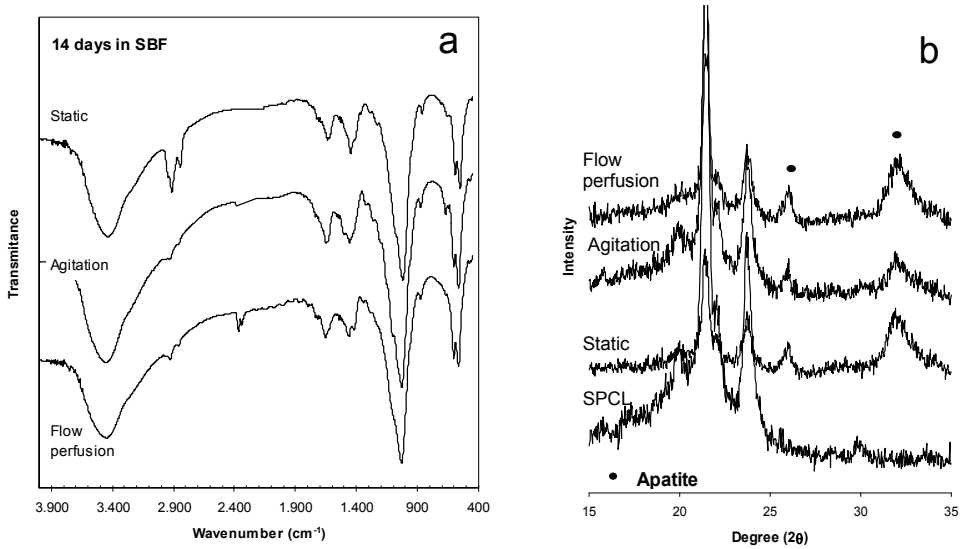


Figure 9. FTIR (a) and XRD (b) spectra obtained from the analysis of the SPCL scaffolds before and after immersion in SBF for 14 days from which the last 7 days were in static and dynamic conditions.

FTIR and TF-XRD (Figures 9a. and 9b., respectively) allowed to confirm that a poorly crystalline carbonated apatite similar to bone was formed after 14 days of immersion in SBF. By the present techniques it was not possible to assess any clear modification of the chemical structure or crystallinity of the apatite layers when dynamic flows were present. In the same way, the analysis performed to the top and bottom sides of each scaffold did not reveal any significant modification of the obtained spectra, being the presented results representative of the obtained profiles for the overall coated scaffolds.

The variation of Ca, P, Mg, Na and Si concentrations in the SBF solution from 7 to 14 days under the different studied conditions is presented in Table 2.

Table 2. Variation of the elemental concentration of the solution from 7 to 14 days (mM/L) calculated from the ICP measured values.

Condition	Consumed (mM/L)			Released (mM/L)		Ca/P from solution
	Δ [Ca]	Δ [P]	Δ [Mg]	Δ [Si]	Δ [Na]	
Static	0.86	0.58	0.01	0.01	0.26	1.51
Agitation	0.94	0.60	0.01	0.00	0.83	1.57
Flow Perfusion	1.05	0.70	0.06	0.02	1.10	1.49

From 7 to 14 days of immersion in SBF under the different studied conditions a decrease in Ca and P ions was observed resulting from the growth of the apatite layer. Particularly in case of flow perfusion the amount of Ca and P consumed from solution was clearly higher, indicating that the apatite has grown at a faster rate. The decrease of Mg ions in solution was very low in all the conditions, indicating that this ion is substituting for Ca at a very low amount. On the other hand dynamic conditions have allowed for the release of more Na ions from the coating during the growing of the apatite layer. This can be explained considering that the SBF will flow through the coating, reaching the first layers near the surface and leaching out any adsorbed ions in the in its structure, particularly Na from the sodium silicate treatment. The Ca/P ratio obtained from the Ca and P consumed in solution indicates that a Ca-deficient apatite is being formed and when dynamic conditions were present this deficiency has increased.

Table 3 presents the elemental ratios calculated from obtained after dissolution of apatite layers formed under the different condition in SBF after 14 days.

Table 3. Ca/P, (Ca+Na+Mg+K)/P, Mg/Ca and Na/Ca ratios calculated from the dissolved apatite layers after the biomimetic coating in static and dynamic conditions after 14 days of immersion in SBF.

Time (days)	Ca/P	Na/Ca	Mg/Ca	K/Ca	(Ca+Na+Mg+K)/P
Static	1.53	0.05	0.042	-	1.67
Agitation	1.57	0.04	0.039	-	1.69
Flow Perfusion	1.51	0.04	0.042	-	1.64

ICP analysis to the solutions obtained from dissolving the apatite coatings allowed for comparing the chemical composition of the coatings prepared under the different biomimetic conditions in SBF after 14 days. The Ca/P ratios obtained for the apatite layers formed under static, agitation and flow perfusion conditions are consistent with obtained values calculated from solution (Figure 7.a). A higher amount of Na was detected in the case of static condition, which is also in agreement with the obtained values from solution. In case of Mg no significant differences were detected in the obtained apatites. Besides the chemical structure and crystallinity, the chemical composition of the apatite layers was also not significantly altered by the presence of the dynamic flow conditions.

The morphology of the resulting apatite layers formed under these conditions was compared by means of SEM examination to the top, bottom and lateral sides of the cubic scaffolds.

Figure 10 presents the lateral sides of the scaffolds after being coated for 14 days in the different studied conditions, and the bottom side of the scaffold after coating by flow perfusion.

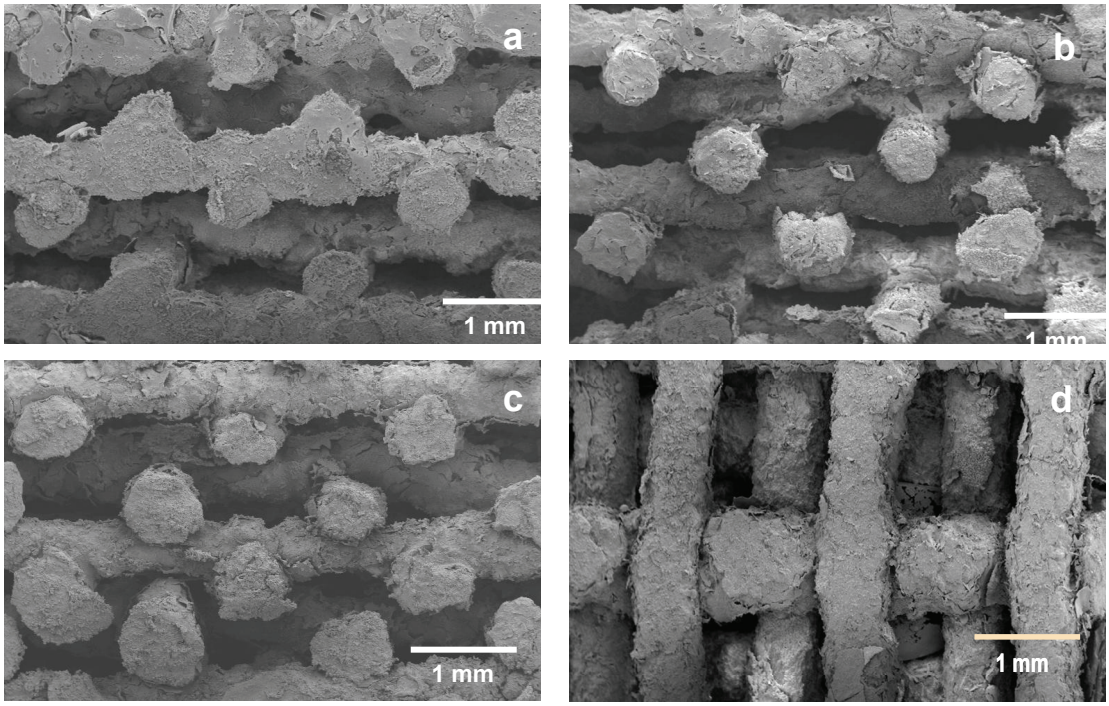


Figure 10. SEM micrographs of the lateral sides of the scaffolds after immersion in SBF for 14 in a) static, b) agitation and c) flow perfusion. d) Bottom side of the sample c.

For all the studied conditions the integrity of the apatite layer nucleated in static SBF (Figure 4) was maintained during the growth stage, even when dynamic conditions were present. The apatite layers have grown clearly covering the fibres without compromising the overall morphology and porosity of the scaffold. This indicates that the mineralization process was clearly controlled by the surface, which acted as a template for the nucleation and growing of the apatite layer. Nevertheless, in case of the static condition (Figure 10.a) apatite tended to accumulate in some of the intersections of the fibres, particularly those in its outer region. A possible explanation for this effect can be a local increase of the concentration of Ca^{2+} and PO_4^{3-} ions of SBF which will induce a higher formation of apatite

in those restricted areas. In case of agitation (Figure 10.b) and flow perfusion (Figure 10.c and d) conditions apatite coating has shown to better follow the fibres contour.

The average thickness of the produced apatite layers was measured by SEM observation of the obtained cross-sections in the centre of the scaffolds. In figure 11 is plotted the calculated average thickness of the apatite layers measured *per* condition (n=6). The SEM micrograph illustrates the procedure used to perform the measurements, starting from the basis of the apatite nuclei to the interface.

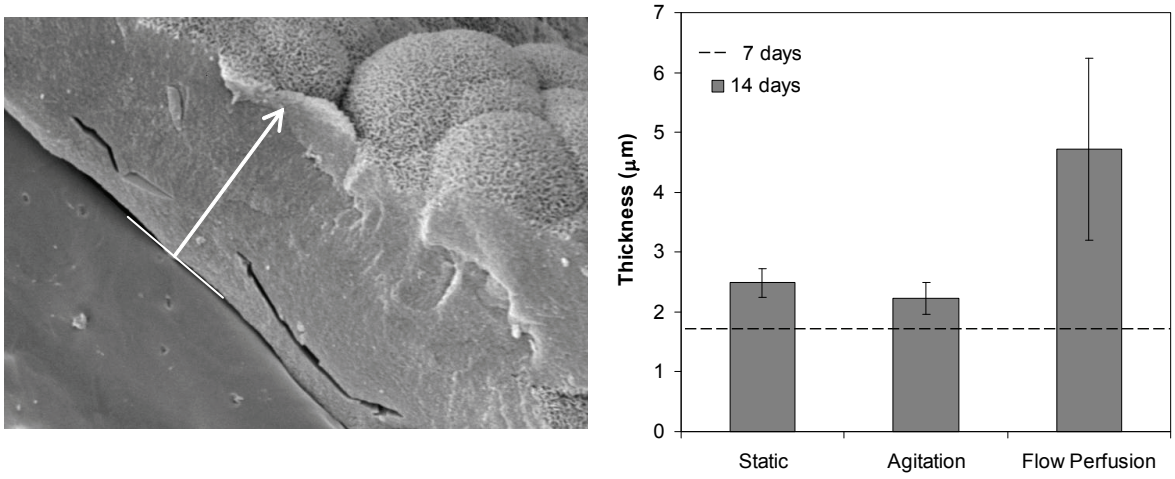


Figure 11. Average thickness of the apatite coatings formed during the biomimetic process in static and dynamic conditions (n=6).

When considering the cross-sections of the centre of the scaffolds it was possible to confirm the presence of an apatite layer in all the studied conditions, which did not detached even after being subjected to high vacuum environments during sputtering and SEM analysis, and also to shear stresses during cross-section preparation.

After the 7 days of immersion in SBF the measured apatite thickness was 1.77 $\pm$ 0.31 μm. Subsequent immersion in SBF allowed for the apatite layer to grow, particularly in case of the flow perfusion condition were the rate for apatite formation was significantly higher. After 14 days, the calculated average thickness for the coatings grown in static conditions was 2.49 $\pm$ 0.23 μm; similar values (2.22 $\pm$ 0.26 μm) were obtained when agitation of the SBF was present, while for the flow perfusion condition the coating thickness was greatly enhanced to values of 4.70 $\pm$ 1.51 μm. In this case, the calculated thickness presented a higher standard deviation, due to a thickness gradient observed from the bottom to the top of the apatite scaffolds. In fact the fibres from the bottom surface which were facing the flow presented a higher thickness, corresponding to the values in the upper limit of the

error bar. This result can be explained from a hydrodynamic perspective. During apatite growth Ca^{2+} and PO_4^{3-} ions will be depleted from the surrounding SBF leading to local concentration gradients. The rate for apatite formation will be dependent on the rate of diffusion of these ions at the boundary layer present at the interface between the growing apatite crystals and the fluid [55]. In a flowing system these concentration gradients will be eliminated. However, the side facing the flow will have more access to ions in SBF, since the SBF flow rate is higher in the entrance of the camber than in its centre.

Figure 12 presents high magnifications of the typical morphologies of the apatite coatings grown on the surfaces of the SPCL scaffolds under the different static and dynamic conditions. Figures 12.a, 12.b and 12.c correspond to the same side of the scaffold, the side facing down during the biomimetic process. Figure 12.d corresponds to the same condition as Figure 12.c (flow perfusion) and to the upper side of the scaffold.

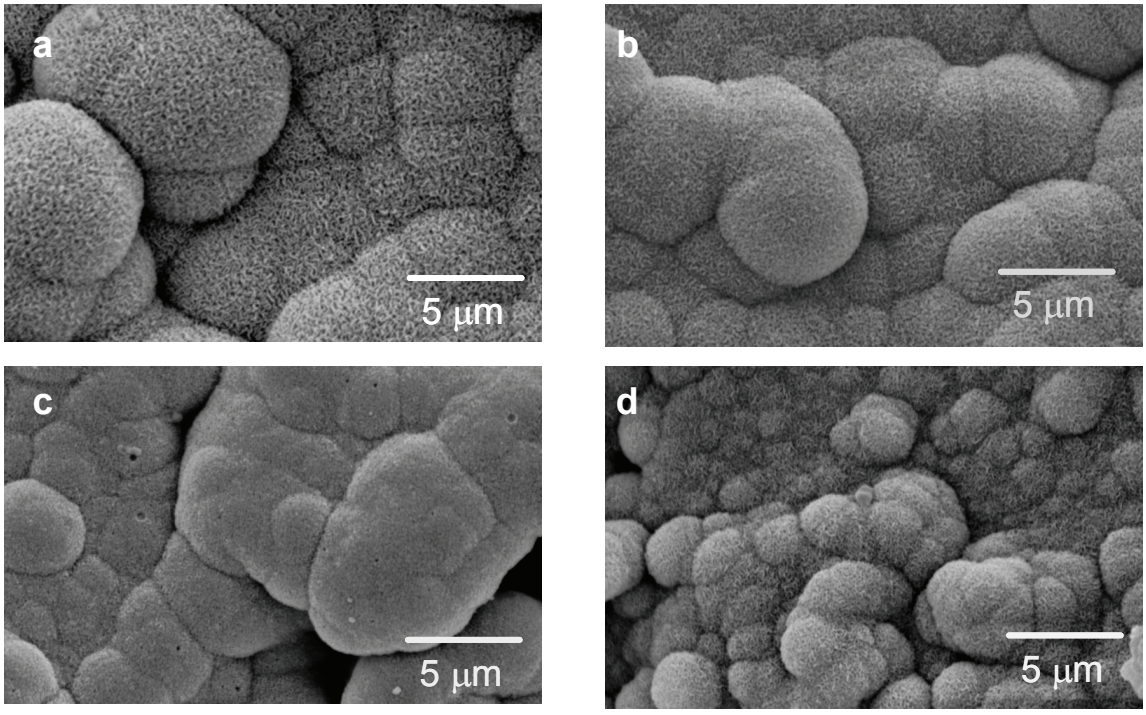


Figure 12. Morphology of apatite coatings grown on the bottom side of the SPCL scaffolds after immersion in SBF for 14 days in a) static, b) agitation and c) flow perfusion conditions. d) Apatite coating grown on the upper side of sample in condition b.

The produced apatite layers present the typical needle-like morphology. This nano-apatite structure was well-defined in case of static conditions (Figure 12.a). When agitation was present (Figure 12.b) the needle's size tended to decrease. In case of flow perfusion this decrease was more accentuated leading to a densification of the apatite structure in the

side of the scaffold facing the flow (Figure 12.c). However, on the opposite side a different morphology was observed (Figure 12.d). In this case the needle-like structure was again more defined and smaller globular structures were formed in the coating. In this sense, the surface morphology of the apatite layers was influenced by the different studied conditions.

IV.4. Discussion

When the concept of biomimetic coatings emerged in the early 90s there was an immediate concern on improving coating efficiency by (among others) reducing the required time for apatite formation [56]. This was immediately reflected in a study by Hata and Kokubo [27] in which the apatite formation rate was greatly enhanced by increasing the concentration of the SBF, its temperature, or even by including agitation in the system. The first option has been quite explored in the last few years [57,58]. For example, Barrere *et al.* [57] accelerated the classical biomimetic process from 7 to 14 days to 1 day by immersing substrates into supersaturated SBF (5x SBF), and illustrated systematically the interdependence of ionic strength, pH, carbonate concentration, and their collective influence on the formation of the resultant apatite. However, extremely high concentrated SBF solutions can frequently lead to spontaneous precipitation caused by homogeneous nucleation phenomena, making the coating process unstable and difficult to control, which can lead apatite layers with lower adhesion to the substrates. Moreover, the obtained Ca-Ps can vary from those formed at more physiological concentrations. Other approaches include the use of highly reactive nucleating agents at the surface [22], to perform several surface modifications [40,59], varying the SBF composition [60] or even increasing the temperature of the process [29,55].

As demonstrated in the present study, dynamic conditions can also accelerate the process for apatite formation in a pre-established apatite layer while maintaining the composition, crystallinity and chemical structure of the apatites. Nevertheless, only a few authors [33-37] have studied the induction and growth of an apatite layer on the surface of bioactive materials on dynamic SBF. In fact, to the authors knowledge, this kind of approach has been only proposed for accessing the SBF *in vitro* mineralization of materials in with intrinsic bioactivity like silica-based ceramics [33,35-37] or their composites [34]. Besides better mimicking bone mineralization, the rational for these studies was also intended to avoid the local build up of released silicic acid and ions from the silica-containing materials to the SBF solutions, which will influence the formation of the apatite layers. In a study to

test the bioactivity of $CaSiO_3$ ceramics Siriphannon *et al.* [36] obtained thinner apatite layers by using dynamic conditions. Salinas *et al.* [37] have also studied the apatite formation ability of similar systems and reported a delay on apatite formation. Although no straight comparison can be establish due to the different conditions used (e.g. solid/liquid ratio, flow rate) the high dissolution ability of the substrate is certainly playing a role during apatite formation. These results support the authors chosen strategy of promoting the nucleation of a stable apatite layer in static conditions prior to the studies in dynamic conditions.

Flow perfusion was the most effective apatite coating procedure, leading to a higher rate for apatite formation. In this case the time necessary for the coating process can be greatly reduced. Other advantages of this system when comparing with simple agitation and static conditions can be found like to avoid the accumulation of precipitates, allowing for a higher control of coating process by controlling the flow rate. On the other hand the scaffolds can better preserve their integrity since they are static in the chamber, which does not occur for agitation condition. A disadvantage of flow perfusion was the thickness gradient found in the apatite layer from the bottom to the top of the scaffold. Nevertheless, this effect can be clearly overcome by periodically alternating the flow direction inside the chamber, allowing for a more homogeneous distribution of the layers' thickness.

IV.5. Conclusions

Bone-like apatite layers could be effectively produced, for the first time, on the surface and in the interior of newly developed SPCL scaffolds produced by a Rapid Prototyping Technology. Sodium silicate treatment followed by immersion in SBF has resulted, after only 6 hours, in the nucleation of an amorphous Ca-P layer that have grown into a bone-like poorly crystalline carbonated apatite layer covering the entire surface of the fibres while maintaining their initial porous structure and interconnectivity. This indicates that the mineralization process was clearly controlled by the surface, which acted as a template for the nucleation and growing of the apatite layer. During the growing stage apatite layers were formed under static, agitation and flow perfusion conditions. This last condition was able to accelerate the process for apatite formation while maintaining its composition, crystallinity and chemical structure. Moreover, besides mimicking better the biological environment, this dynamic process allowed for the coating of more stable and well-defined apatite layers on the surface of complex 3D architectures.

References

1. Hutmacher DW, Schantz T, Zein I, Ng KW, Teoh SH, Tan KC. Mechanical properties and cell cultural response of polycaprolactone scaffolds designed and fabricated via fused deposition modeling. Journal of Biomedical Materials Research 2001;55(2):203-216.
2. He S, Timmer MD, Yaszemski MJ, Yasko AW, Engel PS, Mikos AG. Synthesis of biodegradable poly(propylene fumarate) networks with poly(propylene fumarate)-diacrylate macromers as crosslinking agents and characterization of their degradation products. Polymer 2001;42(3):1251-1260.
3. Mooney DT, Mazzoni CL, Breuer C, McNamara K, Hern D, Vacanti JP, Langer R. Stabilized polyglycolic acid fibre based tubes for tissue engineering. Biomaterials 1996;17(2):115-124.
4. Sachlos E, Reis N, Ainsley C, Derby B, Czernuszka JT. Novel collagen scaffolds with predefined internal morphology made by solid freeform fabrication. Biomaterials 2003;24(8):1487-1497.
5. Solchaga LA, Dennis JE, Goldberg VM, Caplan AI. Hyaluronic acid-based polymers as cell carriers for tissue-engineered repair of bone and cartilage. Journal of Orthopaedic Research 1999;17(2):205-213.
6. Tuzlakoglu K, Alves CM, Mano JF, Reis RL. Production and characterization of chitosan fibers and 3-D fiber mesh scaffolds for tissue engineering applications. Macromol Biosci 2004;4(8):811-9.
7. Marques AP, Cruz HR, Coutinho OP, Reis RL. Effect of starch-based biomaterials on the in vitro proliferation and viability of osteoblast-like cells. J Mater Sci Mater Med 2005;16(9):833-42.
8. Gomes ME, Reis RL, Cunha AM, Blitterswijk CA, de Bruijn JD. Cytocompatibility and response of osteoblastic-like cells to starch-based polymers: effect of several additives and processing conditions. Biomaterials 2001;22(13):1911-7.
9. Malafaya PB, Gomes ME, Salgado AJ, Reis RL. Polymer based scaffolds and carriers for bioactive agents from different natural origin materials. Tissue Engineering, Stem Cells and Gene Therapies 2003;534:201-233.
10. Gomes ME, Ribeiro AS, Malafaya PB, Reis RL, Cunha AM. A new approach based on injection moulding to produce biodegradable starch-based polymeric scaffolds: morphology, mechanical and degradation behaviour. Biomaterials 2001;22(9):883-9.
11. Gomes ME, Sikavitsas VI, Behravesh E, Reis RL, Mikos AG. Effect of flow perfusion on the osteogenic differentiation of bone marrow stromal cells cultured on starch-based three-dimensional scaffolds. J Biomed Mater Res A 2003;67(1):87-95.
12. Tuzlakoglu K, Bolgen N, Salgado AJ, Gomes ME, Piskin E, Reis RL. Nano- and micro-fiber combined scaffolds: a new architecture for bone tissue engineering. J Mater Sci Mater Med 2005;16(12):1099-104.
13. Silva GA, Coutinho OP, Ducheyne P, Shapiro IM, Reis RL. Starch-based microparticles as vehicles for the delivery of active platelet-derived growth factor. Tissue Eng 2007;13(6):1259-68.
14. Yang SF, Leong KF, Du ZH, Chua CK. The design of scaffolds for use in tissue engineering. Part 1. Traditional factors. Tissue Engineering 2001;7(6):679-689.
15. Salgado AJ, Coutinho OP, Reis RL, Davies JE. In vivo response to starch-based scaffolds designed for bone tissue engineering applications. J Biomed Mater Res A 2007;80(4):983-9.
16. Chim H, Hutmacher DW, Chou AM, Oliveira AL, Reis RL, Lim TC, Schantz JT. A comparative analysis of scaffold material modifications for load-bearing applications in bone tissue engineering. Int J Oral Maxillofac Surg 2006;35(10):928-34.
17. Hutmacher DW, Sittinger M, Risbud MV. Scaffold-based tissue engineering: rationale for computer-aided design and solid free-form fabrication systems. Trends in Biotechnology 2004;22(7):354-362.
18. Gomes M. E. SAJ, Reis R. L. Bone Tissue Engineering Using Starch Based Scaffolds Obtained by Different Methodologies. Ed., R.L.Reis and D.Cohn, NATO/ASI Series, Kluwer Press, Drodercht, 2002:221-249.
19. Rey C. Calcium Phosphate Biomaterials and Bone Mineral. Differences in Composition, Structures and Properties. Biomaterials 1990;11:13.

20. Oliveira AL, Mano JF, Reis RL. Nature-inspired calcium phosphate coatings: present status and novel advances in the science of mimicry. Current Opinion in Solid State & Materials Science 2003;7(4-5):309-318.
21. Abe Y, Kokubo T, Yamamuro T. Apatite Coating on Ceramics, Metals and Polymers Utilizing a Biological Process. Journal of Materials Science-Materials in Medicine 1990;1(4):233-238.
22. Oliveira AL, Malafaya PB, Reis RL. Sodium silicate gel as a precursor for the in vitro nucleation and growth of a bone-like apatite coating in compact and porous polymeric structures. Biomaterials 2003;24(15):2575-2584.
23. Oliveira AL, Reis RL. Pre-mineralisation of starch/polycrapolactone bone tissue engineering scaffolds by a calcium-silicate-based process. Journal of Materials Science: Materials in Medicine 2004;15(4):533-540.
24. Leonor IB, Kim HM, Balas F, Kawashita M, Reis RL, Kokubo T, Nakamura T. Functionalization of different polymers with sulfonic groups as a way to coat them with a biomimetic apatite layer. J Mater Sci Mater Med 2007;18(10):1923-30.
25. Oliveira AL, Mano JF, Reis RL. Nature-inspired calcium phosphate coatings: present status and novel advances in the science of mimicry. Current Opinion in Solid State and Materials Science 2003;7(4-5):309-318.
26. Tuzlakoglu K, Reis RL. Formation of bone-like apatite layer on chitosan fiber mesh scaffolds by a biomimetic spraying process. J Mater Sci Mater Med 2007;18(7):1279-86.
27. Hata K, Kokubo T, Nakamura T, Yamamuro T. Growth of a Bonelike Apatite Layer on a Substrate by a Biomimetic Process. Journal of the American Ceramic Society 1995;78(4):1049-1053.
28. Barrere F, van Blitterswijk CA, de Groot K, Layrolle P. Nucleation of biomimetic Ca-P coatings on Ti6Al4V from a SBF x 5 solution: influence of magnesium. Biomaterials 2002;23(10):2211-2220.
29. Li PJ. Biomimetic nano-apatite coating capable of promoting bone ingrowth. Journal of Biomedical Materials Research Part A 2003;66A(1):79-85.
30. Chikara Ohtsuki MKTM. Coating bone-like apatite onto organic substrates using solutions mimicking body fluid. Journal of Tissue Engineering and Regenerative Medicine 2007;1(1):33-38.
31. Tate MLK. "Whither flows the fluid in bone?" An osteocyte's perspective. Journal of Biomechanics 2003;36(10):1409-1424.
32. Meinel L, Karageorgiou V, Fajardo R, Snyder B, Shinde-Patil V, Zichner L, Kaplan D, Langer R, Vunjak-Novakovic G. Bone tissue engineering using human mesenchymal stem cells: Effects of scaffold material and medium flow. Annals of Biomedical Engineering 2004;32(1):112-122.
33. Ramila A, Vallet-Regi M. Static and dynamic in vitro study of a sol-gel glass bioactivity. Biomaterials 2001;22(16):2301-2306.
34. Eglin D, Ali SAM, Perry CC. Comparative study of the in vitro apatite-forming ability of poly(epsilon-caprolactone)-silica sol-gels using three osteoconductivity tests (static, dynamic, and alternate soaking process). Journal of Biomedical Materials Research Part A 2004;69A(4):718-727.
35. Vallet-Regi M, Perez-Pariente J, Izquierdo-Barba I, Salinas AJ. Compositional variations in time calcium phosphate layer growth on gel glasses soaked in a simulated body fluid. Chemistry of Materials 2000;12(12):3770-3775.
36. Siriphannon P, Kameshima Y, Yasumori A, Okada K, Hayashi S. Comparative study of the formation of hydroxyapatite in simulated body fluid under static and flowing systems. Journal of Biomedical Materials Research 2002;60(1):175-185.
37. Salinas AJ, Vallet-Regi M, Izquierdo-Barba I. Biomimetic apatite deposition on calcium silicate gel glasses. Journal of Sol-Gel Science and Technology 2001;21(1-2):13-25.
38. Reis R. L. CAM, Allan P. S., Bevis M. J. Mechanical behaviour of injection-moulded starch based polymers. Polymer Advanced Technology 1996;7:784-790.
39. Reis RL, Cunha A. M. Characterization of two biodegradable polymers of potential application within the biomaterials field. Journal of Materials Science: Materials in Medicine 1995;6:786-792.
40. Oliveira AL, Elvira, C., Vásquez, B., San Roman, J., Reis, R. L. Surface Modifications Tailors the Characteristics of Biomimetic Coatings Nucleated on Starch Based Polymers. Journal of Materials Science: Materials in Medicine 1999;10:827.

41. Elvira C, Mano JF, San Roman J, Reis RL. Starch-based biodegradable hydrogels with potential biomedical applications as drug delivery systems. Biomaterials 2002;23(9):1955-66.
42. Gomes ME, Holtorf HL, Reis RL, Mikos AG. Influence of the porosity of starch-based fiber mesh scaffolds on the proliferation and osteogenic differentiation of bone marrow stromal cells cultured in a flow perfusion bioreactor. Tissue Engineering 2006;12(4):801-809.
43. Gomes M. E. SVI, Behravesh E., Reis R.L., Mikos Antonios G. Effect of Flow Perfusion on the Osteogenic Differentiation of Bone Marrow Stromal Cells Cultured on Starch Based Three-Dimensional Scaffolds. Journal of Biomedical Materials Research 2003;67A:87-95.
44. Santos MI, Fuchs S, Gomes ME, Unger RE, Reis RL, Kirkpatrick CJ. Response of micro- and macrovascular endothelial cells to starch-based fiber meshes for bone tissue engineering. Biomaterials 2007;28(2):240-8.
45. Kokubo T, Kushitani H, Sakka S, Kitsugi T, Yamamuro T. Solutions able to reproduce in vivo surface-structure changes in bioactive glass-ceramic A-W. J Biomed Mater Res 1990;24(6):721-34.
46. Oliveira AL, Costa SA, Sousa RA, Reis RL. Studies on the Formation of Biomimetic Apatite Layers on 3D-Printed Biodegradable Polymeric Scaffolds: Effect of Different Dynamic Coating Routes. Society for Biomaterials 2006 Annual Meeting Pittsburgh; 2006.
47. Pawlak A, Mucha A. Thermogravimetric and FTIR studies of chitosan blends. Thermochimica Acta 2003;396(1-2):153-166.
48. Walsh D, Furuzono T, Tanaka J. Preparation of porous composite implant materials by in situ polymerization of porous apatite containing epsilon-caprolactone or methyl methacrylate. Biomaterials 2001;22(11):1205-1212.
49. Takadama H, Kim HM, Kokubo T, Nakamura T. Mechanism of biomineralization of apatite on a sodium silicate glass: TEM-EDX study in vitro. Chemistry of Materials 2001;13(3):1108-1113.
50. Takadama H, Kim HM, Kokubo T, Nakamura T. X-ray photoelectron spectroscopy study on the process of apatite formation on a sodium silicate glass in simulated body fluid. Journal of the American Ceramic Society 2002;85(8):1933-1936.
51. Vallet-Regi M, Romero AM, Ragel CV, LeGeros RZ. XRD, SEM-EDS, and FTIR studies of in vitro growth of an apatite-like layer on sol-gel glasses. Journal of Biomedical Materials Research 1999;44(4):416-421.
52. Rehman I, Bonfield W. Characterization of hydroxyapatite and carbonated apatite by photo acoustic FTIR spectroscopy. Journal of Materials Science-Materials in Medicine 1997;8(1):1-4.
53. Boskey AL, Posner AS. Magnesium Stabilization of Amorphous Calcium-Phosphate - Kinetic Study. Materials Research Bulletin 1974;9(7):907-916.
54. Miyaji F, Kim HM, Handa S, Kokubo T, Nakamura T. Bonelike apatite coating on organic polymers: novel nucleation process using sodium silicate solution. Biomaterials 1999;20(10):913-919.
55. Tanahashi M, Kokubo T, Matsuda T. Quantitative assessment of apatite formation via a biomimetic method using quartz crystal microbalance. J Biomed Mater Res 1996;31(2):243-9.
56. Kokubo T, Takadama H. How useful is SBF in predicting in vivo bone bioactivity? Biomaterials 2006;27(15):2907-2915.
57. Barrere F, van Blitterswijk CA, de Groot K, Layrolle P. Influence of ionic strength and carbonate on the Ca-P coating formation from SBFx5 solution. Biomaterials 2002;23(9):1921-1930.
58. Kim SS, Park MS, Gwak SJ, Choi CY, Kim BS. Accelerated bonelike apatite growth on porous polymer/ceramic composite scaffolds in vitro. Tissue Eng 2006;12(10):2997-3006.
59. Oyane A, Kawashita M, Nakanishi K, Kokubo T, Minoda M, Miyamoto T, Nakamura T. Bonelike apatite formation on ethylene-vinyl alcohol copolymer modified with silane coupling agent and calcium silicate solutions. Biomaterials 2003;24(10):1729-35.
60. Li P, Ohtsuki C, Kokubo T, Nakanishi K, Soga N, Nakamura T, Yamamuro T. Effects of ions in aqueous media on hydroxyapatite induction by silica gel and its relevance to bioactivity of bioactive glasses and glass-ceramics. J Appl Biomater 1993;4(3):221-9.

CHAPTER V

Chapter V

Micro-Computed Tomography (μ-CT) as a Potential Tool to Assess the Effect of Dynamic Coating Routes on the formation of Biomimetic Apatite Layers on 3D-Plotted Biodegradable Polymeric Scaffolds

Abstract

This work studies the influence of dynamic biomimetic coating procedures on the growth of bone-like apatite layers at the surface of starch/polycaprolactone (SPCL) scaffolds produced by a 3D-plotting technology. These systems are newly proposed for bone Tissue Engineering applications. After generating stable apatite layers through a sodium silicate-based biomimetic methodology the scaffolds were immersed in Simulated Body Fluid solutions (SBF) under static, agitation and circulating flow perfusion conditions, for different time periods. Besides the typical characterization techniques, Micro-Computed Tomography analysis (μ-CT) was used to assess scaffold porosity and as a new tool for mapping apatite content. 2D histomorphometric analysis was performed and 3D virtual models were created using specific softwares for CT reconstruction. By the proposed biomimetic routes apatite layers were produced covering the interior of the scaffolds, without compromising their overall morphology and interconnectivity. Dynamic conditions allowed for the production of thicker apatite layers as consequence of higher mineralizing rates, when comparing with static conditions. μ-CT analysis clearly demonstrated that flow perfusion was the most effective condition in order to obtain well-defined apatite layers in the inner parts of the scaffolds. Together with SEM, this technique was a useful complementary tool for assessing the apatite content in a non-destructive way.

*This part of the chapter is based on the following publication:

A.L. Oliveira, P. B. Malafaya, S.A. Costa, R.A. Sousa, R.L. Reis, “Micro-Computed Tomography (μ-CT) as a Potential Tool to Assess the Effect of Dynamic Coating Routes on the formation of Biomimetic Apatite Layers on 3D-Plotted Biodegradable Polymeric Scaffolds”, Journal of Materials Science: Materials in Medicine, Mater Med (2007) 18:211–222.

V.1. Introduction

Tissue Engineering (TE) has been emerging as a striking approach to the current therapies for bone regeneration/substitution. The appropriate surface chemistry for cell attachment and proliferation is a key issue that needs to be addressed while designing a scaffold for Bone TE. To combine Ca-Ps as coatings on the outermost surface of a polymeric scaffold can be a challenging, but yet attractive approach to better promote bone formation. Several methods for producing Ca-P coatings on the surface of different biomaterials have been proposed over the years, as reviewed elsewhere [1]. The biomimetic synthesis of apatite layers under presence of simulated body fluid (SBF) solutions, initially proposed by Kokubo *et al.* [2], has gained attention in recent years as an alternative low-temperature coating methodology. Besides its osteoconductive properties, a biomimetic apatite layer discloses a carrier potential of biologically relevant molecules such as protein growth factors, enzymes or pharmaceutical drugs used in bone related diseases, due to the physiological operating conditions of temperature and pH.

When considering porous biodegradable polymeric scaffolds there are rather few works reporting the coating of these architectures due to the complex features related with coating composition, thickness distribution or the adhesion to the substrate. Moreover, pH changes due to possible degradation of substrates surface during the coating process have also to be taken into consideration. Nevertheless, in our research group these biomimetic coatings have been effectively produced on the surface of starch based biodegradable polymers [3,4]. In fact, in a previous work [3] it was possible to overcome some of these difficulties by developing a biomimetic methodology using a sodium silicate gel as nucleating agent to produce well-defined bone-like apatite coatings covering the surfaces of starch based 3D architectures. In case of bone TE applications, dynamic mineralization environments can better mimic the *in vivo* scenario, where the flow of body fluids is present, besides being suitable to promote a homogeneous formation of the Ca-P layer in the interior of the scaffold. In this work is presented a comparative study of static and dynamic biomimetic routes for producing apatite layers on the surface of biodegradable scaffolds produced by a rapid prototyping technology. These systems are newly proposed for bone Tissue Engineering applications.

To assess the apatite content in the inner parts of a scaffold is another relevant issue that needs to be taken into consideration. Tomography using x-rays is a well established technique that is gaining popularity since the interior of the specimen can be studied in great detail, without resorting to physical sectioning nor using toxic chemicals. On the other hand, it provides precise quantitative and qualitative information on the 3D morphology of the specimen [5]. After scanning, the intact samples can be subjected to other tests, therefore resolving the problem of sample scarcity. One of the main advantages of μ-CT is that it is able to evaluate the material (polymeric or ceramic) volume based on 3D spatial distribution. It can be applied to very large [6] samples such as body parts and whole organs of humans down to the nanometre scale of a single cell [7]. This means tomography can be used in a hierarchical fashion - from the human, to an organ, a tissue and down to the cell. This technique has been used to characterize the 3D trabecular bone microarchitecture and quantify bone repair responses *in vivo* [8]. For Bone TE applications, μ-CT imaging provides an efficient, non-destructive tool to quantitatively measure the amount and distribution of mineralized matrix formation throughout 3D constructs *in vitro* [9] and *in vivo* [10]. In the herein presented study is μ-CT is proposed as a new tool for mapping the distribution of biomimetic Ca-P coatings throughout the surfaces of starch/polycaprolactone (SPCL) 3D architectures.

V.2. Materials and Methods

V.2.1. Preparation of the scaffolds

As a natural polymer, starch exhibits a great potential to be used in bone related applications [11-14]. In this work, the studied material is based on a blend of starch/polycaprolactone (SPCL). The blend contains around 30% of starch and 70% of poly(epsilon-caprolactone) by weight. The selected biomaterial presents a good biological behaviour and has been proposed for Bone Tissue Engineering applications [15-17].

Rapid prototyping (RP) technologies are considered as potential routes for the production of complex scaffolds for Bone TE applications, as they present superior control over design, manufacturing and reproducibility of TE scaffolds [18]. Moreover, when coupled with adequate image acquisition software, RP allows for the production of anatomically adapted 3D scaffolds based on the patient's own defect. SPCL scaffolds were produced using a 3D plotting technology (Bioplotter®, EnvisionTec GmbH, Germany). In this case, consecutive alternated layers were plotted with a 0º/90º/…/0º/90º orientation pattern to

produce cubic samples with a lateral side of L= 5 mm. Each layer was plotted using a distance of 2 mm between layer strands and an in-plane absolute offset distance of 1 mm between consecutive equivalent layers. 3D plotting RP enables high control over scaffold morphology, namely controlled porosity and interconnectivity.

V.2.2. Apatite Coating Formation

To produce an apatite coating on the surfaces of the obtained SPCL scaffolds a biomimetic methodology was used based on a previously developed sodium silicate methodology [3]. Briefly, the samples were "impregnated" for 1 hour with a sodium silicate gel from SIGMA-ALDRICH ($Na_2SiO_3 \bullet H_2O$, containing ~14% NaOH and ~27% SiO_2, pH ≈13), under mild agitation. Sodium silicate gel was herein used with concentration and SiO_2/Na_2O molar ratio as received. After this treatment the solution with the samples was diluted with 50% vol. of distilled water and stirred for 5 minutes. This procedure was aimed at diminishing the viscosity of the gel in order to produce a homogeneous and thin layer of vitrified sodium silicate in the surface of the materials. The scaffolds were then removed from the solution and then dried in vacuum for 3 hours and moved to a controlled atmosphere (23 ± 1 ºC; 55% RH) for 24 hours. A more detailed description on the coating methodology can be found elsewhere [3].

An aqueous solution was prepared comprising all major inorganic ions present in the human's blood plasma and presenting its approximate ion concentration, in order to promote *in vitro* apatite formation. The different salts were dissolved in de-ionized H_2O and the pH adjusted to neutral using tris(hydroxymethyl)aminomethane and hydrochloric acid. This simulated body fluid solution (SBF) was developed by Kokubo and co-workers [19].

The as-treated scaffolds were immersed in the SBF solution for 7 days. During this period the solution was renewed every 2 days and an apatite layer was allowed to nucleate and grow on the surface of the samples. Following this period, the samples were divided into 3 different groups and placed in contact with a renewed SBF solution under different conditions: static, agitation by shaking in a thermostatic bath (Selecta, Unitronic, Spain, 80 strokes/min.) and circulating flow perfusion in a bioreactor (volume flow rate (Q) of 4mL/min; Residence Time (t_R) of 15 s) for periods up to 14 days. In all the conditions the total volume of SBF available per sample was 50 mL and the solution was renewed every

2 days (solid-to-liquid ratio of 1g/400mL/week). Table 1 summarizes the different coating conditions.

Table 1. Static and dynamic conditions for coating apatite layers on the SPCL scaffolds.

Periods (Days)	**SBF**	**Conditions**		
7	1 X	Static	-	-
14	1 X	Static	Agitation	Flow perfusion
21	1.5 X	Static	Agitation	Flow perfusion
Volume of SBF available per sample		50 mL	50 mL	50 mL
Solid-to-liquid ratio		1g/400mL/week	1g/400mL/week	1g/400mL/week
Fluid Flow		None	Turbulent flow (80 strokes/min.)	Laminar flow (Q=4 mL/min; t_R=15s)

SBF- Simulated Body Fluid solution

For circulating flow perfusion a special bioreactor was designed according with the schematic drawing of Figure 1.

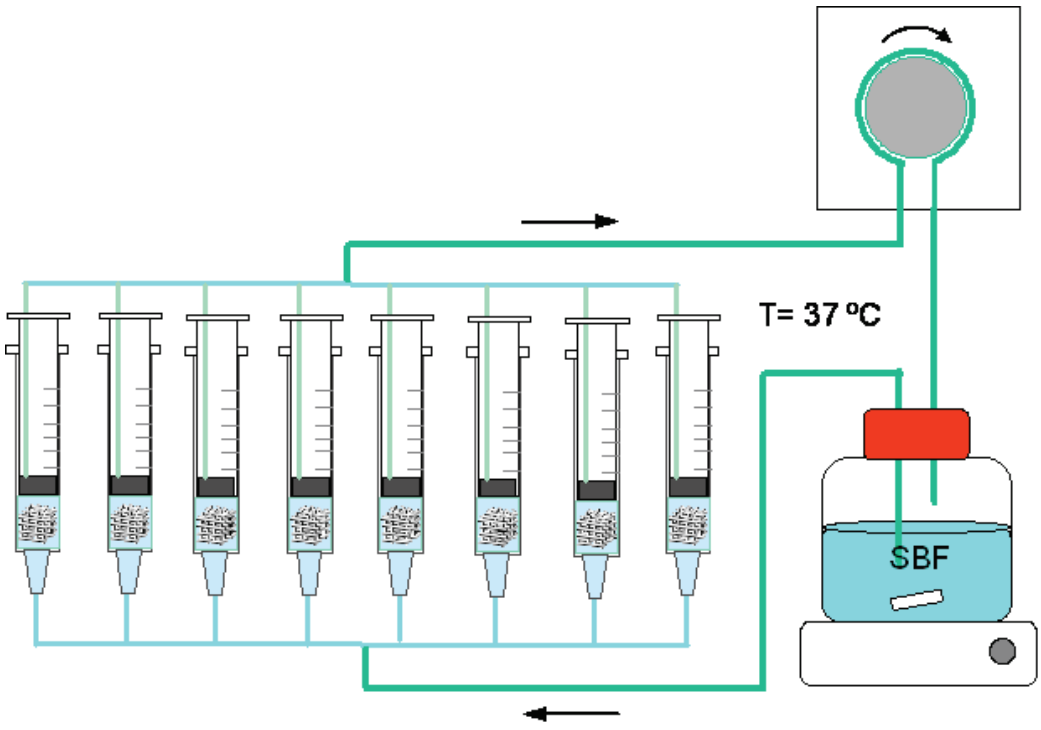


Figure 1. Schematic drawing of the bioreactor designed for coating an apatite layer under flow perfusion.

After 7, 14 and 21 days the samples were removed from solution, washed in distilled water and dried in a controlled atmosphere (23 ± 1 ºC; 55% RH).

V.2.3. Scanning Electron Microscopy (SEM) and Energy Dispersive Spectroscopy (EDS)

The morphological characterisation to the scaffolds was carried out by Scanning Electron Microscopy (SEM) analysis, in a LEICA Cambridge S360, United Kingdom. All the samples were coated with a thin film of carbon, by ion sputtering, prior to any observation. The electron beam energy was 10 KeV and 12 KeV. The scaffolds were observed in 3 different orientations: from the top, lateral side and bottom, for the different tested periods and conditions in SBF. The corresponding cross-sections were also analysed and the thickness of the apatite layers was calculated by performing measurements in six fibres *per* scaffold (3 measurements *per* fibre). Since these coatings are constituted by fused spherical apatite nuclei they present an irregular surface. Therefore, in order to ensure that the measure would be done in the same way for all the conditions the basis of these nuclei was established as the limit for the coating. In this was the measured average values are the minimum thickness values for all the samples.

V.2.4. X-ray Diffraction (TF-XRD)

Thin-Film X-Ray Diffraction (TF-XRD, Philips X'Pert MPD, The Netherlands) was used to identify any crystalline phases present in the apatite layers formed during the immersion in SBF. The data collection was performed by 2θ scan method with 1º as incident beam angle using CuKα X-ray line and a scan speed of 0.05 º/min in 2θ.

V.2.5. Fourier Transformed Infra-Red (FTIR)

The chemical structure of the apatite coatings formed on the surface of the SPCL scaffold fibres after the different time periods and conditions in SBF was analysed by Fourier Transform Infrared Spectroscopy (FTIR). The surface of the fibres was scratched and the resulting particles were milled with KBr powder and shaped by compression into pellets for further analysis. All spectra were recorded using 64 scans and 2 cm^{-1} resolution in an FTIR spectrophotometer (Perkin-Elmer 1600 Series, USA).

V.2.6. Inductively Coupled Plasma Spectroscopy (ICP)

The composition of the resulting Ca-P coatings was accessed by analysing the solution resulting from the dissolution of the coated scaffolds in 0.1 M HCl, under agitation for 24 hours (the scaffolds were examined by SEM afterwards to confirm the total dissolution at the surface). The elemental concentration was measured by Inductively Coupled Plasma Optical Emission Spectroscopy (ICP-OES, JY 70 plus, Jobin Yvon, France). Duplicate samples were analysed for each condition and immersion time. From these results Ca/P ratios were calculated. The following relations were also considered: (Ca+Na+Mg+K)/P; (Ca+Mg+K)/P; Na/Ca; Mg/Ca; K/Ca in order to investigate the possible presence of Mg^{2+}, Na^{+} and K^{+} in the SBF, substituting the Ca^{2+} in the crystalline network of the apatite.

V.2.7. Micro-Computed Tomography (µ-CT)

Micro-Computed Tomography (µ-CT) of the uncoated and coated scaffolds was carried out using µ-CT 20 equipment (SCANCO Medicals, Switzerland). The X-ray scans were performed in high resolution mode of 11 µm x/y/z and an integration time of 250ms x 2 (500 ms). The rotation step used was 500/180º. The energy of the scanner used was 50 keV with 180 µA current. Around 400 slices of the materials were obtained in order to scan the entire scaffolds. Mimics from Materialise (Belgium), CT Analyser and CT Vol Realistic 3D Visualization both from SkyScan (Belgium) were used as image processing softwares, for CT reconstruction, to create and visualize the 3D representation. The 2-D histomorphometric analysis of the scaffolds was performed using a threshold of 51 to determine the porosity and a threshold of 133 to identify the apatite content along the scaffold (from 0-4500 µm) (grey values).

V.3. Results and Discussion

V.3.1. Stabilization of the apatite layer

Figure 2 presents SEM micrographs of the SPCL scaffolds as processed and after the nucleation of a biomimetic apatite layer for 7days.

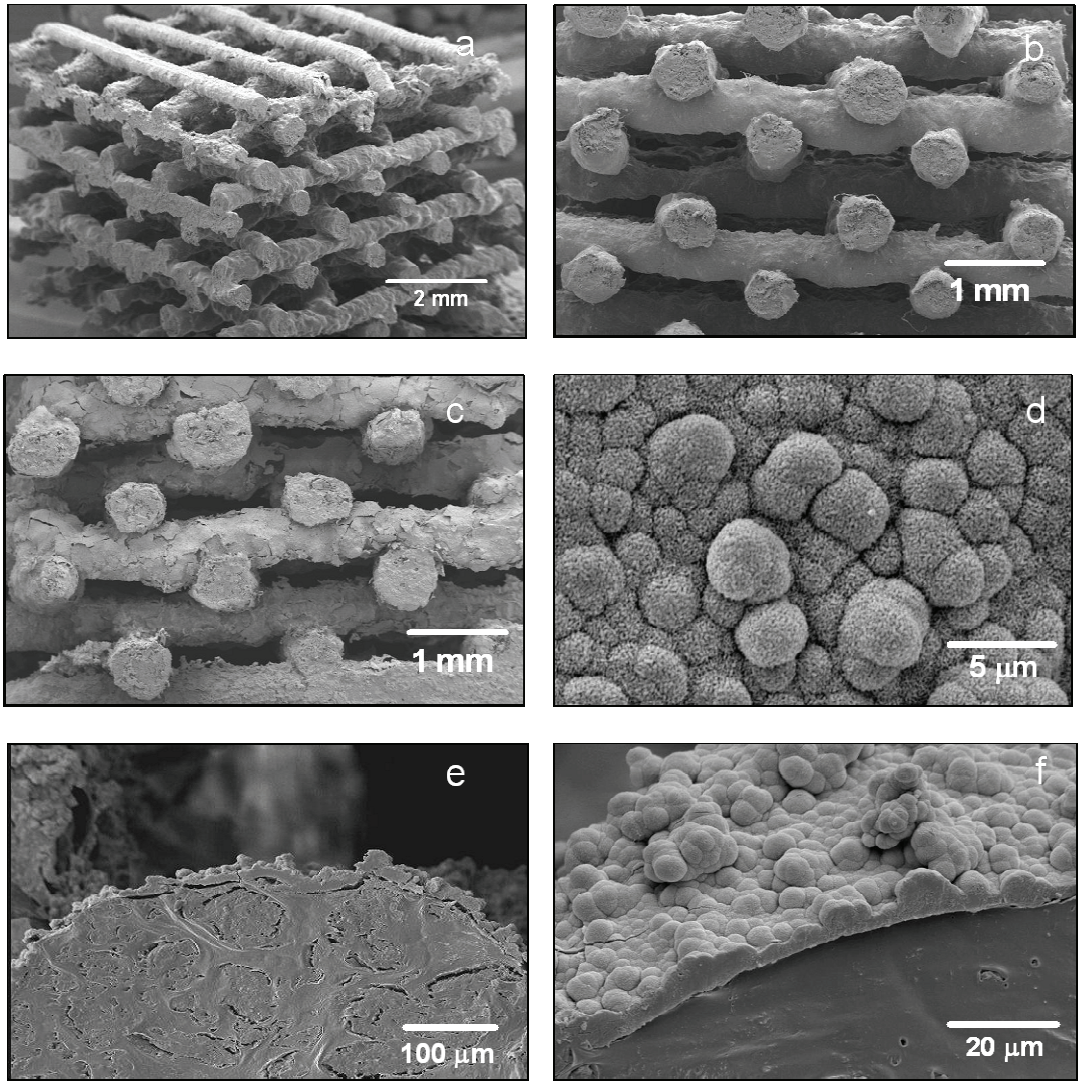


Figure 2. SEM micrographs of SPCL scaffolds a), b) as processed and c), d), e) f) after growing a biomimetic apatite layer for 7 days in SBF.

3D plotting technology allowed for the processing of fibre-based 3D constructs with a controlled morphology and porosity (Figures. 2a and 2b) in a reproducible manner. The Sodium silicate treatment followed by immersion in SBF solution for 7 days has resulted in the nucleation of a well-defined apatite layer at the surface of the fibres which covered the entire surface of these porous materials while maintaining their initial architecture (Figure 2c). The mechanism for the nucleation and growth of an apatite layer on a sodium silicate gel is well known and has been described elsewhere [3,20]. The resulting Ca-P coating presents a needle-like structure (Figures 2d) corresponding to the typical morphology obtained by this biomimetic route [3]. By TF-XRD and FTIR it was possible to confirm that a poorly crystalline carbonated apatite similar to bone was formed after 7 days of

immersion in SBF (data not shown). This coating was present both in the outside and in the interior of the scaffold, as it can be observed in Figs. 2d and 2e that present a cross-section from the interior of the scaffold, from which strong adherence of the coating to the surface of the fibres is evident. Apatite nucleation is clearly controlled by the surface [21,22] , which serves as template for the formation of the apatite layer.

V.3.2. Growing of the apatite layer under static and dynamic conditions

After the formation of a stabilized bone-like apatite layer in the surface of the SPCL constructs for 7 days in static SBF, the scaffolds were divided into 3 groups and immersed in SBF solutions under 3 different hydrodynamic conditions: static, agitation and flow perfusion, for periods up to 21 days.

Figure 3 presents the typical FTIR spectra of the apatite coatings produced in the different SBF conditions, for the periods of 14 and 21 days.

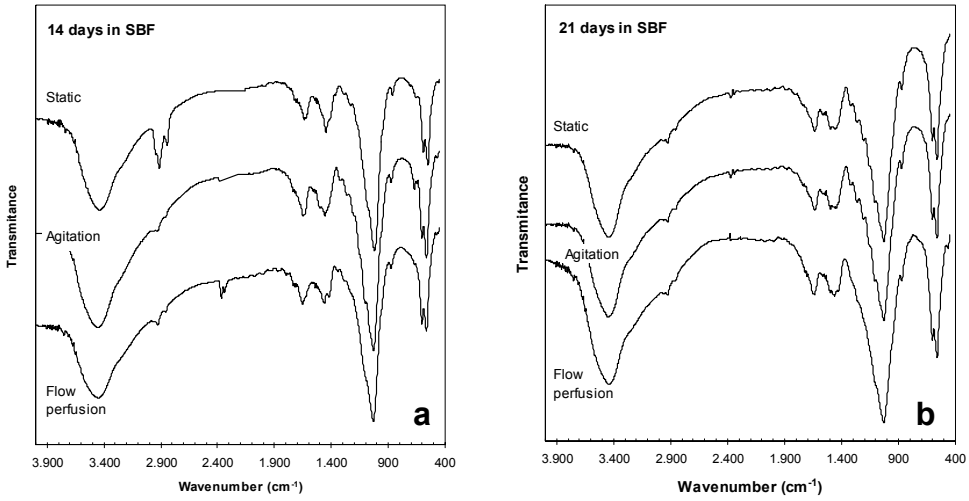


Figure 3. FTIR spectra obtained from the analysis of apatite layers after immersion in SBF for 21 days from which 14 days under static and dynamic conditions. All the spectra were obtained from the same side of the scaffold.

The bands detected at 1630 cm^{-1} are assigned to water molecules in the apatite structure. Another broad band assigned to water was also detected in the region of 3400 cm^{-1}. In fact, apatite contains water incorporated in its structure, either chemically bonded, i.e. structural water or also adsorbed due to its hydroscopic character [23]. The bands at 866, 1412 and 1452 cm^{-1} result from the presence of carbonate (CO_3^{2-}) incorporated in the

apatite lattice [23,24]. The presence of these bands clearly indicates that a carbonated apatite was formed, as it is found in bone apatite. The bands at 558 and 572 are assigned to the ν_4 bending mode of the O-P-O bonds in the apatite, indicating some degree of crystallinity. The bands at 1024 cm^{-1} indicate the ν_3 stretching mode of P-O bonds [23]. The detected FTIR bands correspond to the characteristic ones of a carbonated apatite.

Figure 4 presents the typical TF-XRD spectra of the apatite coatings produced in the various static and dynamic SBF conditions.

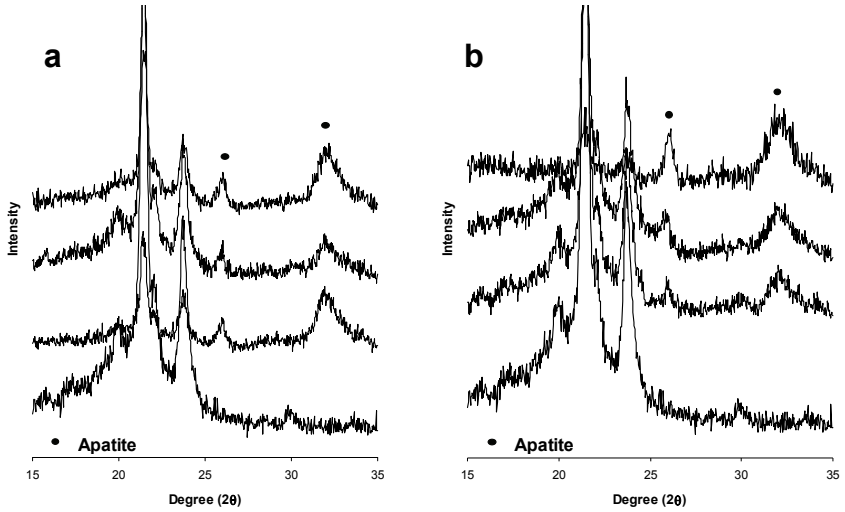


Figure 4. TF-XRD spectra obtained from the analysis of the SPCL scaffolds before and after immersion in SBF for a) 14 and 21 days in static and dynamic conditions.

The peaks detected at 2θ=20, 21 and 24 are assigned to SPCL crystalline phases. After producing the biomimetic coatings in different conditions the main characteristic peaks attributed to HA were detected. The peak at 2θ = 26º is assigned to (002) plane in the apatite crystalline lattice. Another important diffraction peak is detected around 2θ = 32º and is related to the overlapping of planes (211), (112) and (300). This broad peak indicates that the apatite structure is composed by small crystallites. Similar XRD profiles were obtained when comparing the different static and dynamic coating conditions. From 14 to 21 days of immersion in SBF a slight increase in the intensity of the apatite peaks indicates that the apatite coatings tend to be more crystalline in the presence of SBF 1.5 x. The intensity of the SPCL peaks diminishes considerably in case of dynamic conditions after 21 days (Figure 3b), which is related with an increase of thickness of the apatite layers.

When comparing Figure 3a with 3b, and Figure 4a with 4b no marked differences in the obtained spectra were detectable between the apatites coated after 14 days in SBF (Figure 3.a, 4a) and those coated after 21 days (Figure 3.b, 4b) or between each different condition. In the same way, FTIR and TF-XRD analysis performed to different sides in each scaffold did not reveal any clear differences in the spectra (data not shown). The presented results were obtained from the bottom side of the scaffold. By the present technique it was not possible to assess any clear modification of the chemical structure or crystallinity of the apatite layers when dynamic flows were present.

ICP analysis to the solutions resulting from dissolving the apatite coatings allowed for comparing the chemical composition of the coatings prepared under the different biomimetic conditions. In static conditions the calculated Ca/P ratio after 14 days of immersion in SBF was 1.53. Since the established value for bone-apatite is 1.67, the herein prepared biomimetic apatites are Ca-deficient. This ratio increases when considering the presence of other ions in the structure replacing for Ca such as K, Mg and Na to a value of 1.67. The elemental composition obtained for the apatite layers formed under agitation and flow perfusion is very similar (1.57 and 1.51, respectively), indicating that besides the chemical structure and crystallinity, the chemical composition of the apatite layers was also not altered by the presence of the dynamic flow conditions.

In order to evaluate the effect of the studied biomimetic procedures on the morphology and integrity of the resulting apatite layers SEM analysis was performed to the top, bottom and lateral sides of the cubic shaped scaffolds. The interior of the scaffolds was also characterized by examining cross-sections performed in the centre of the scaffolds. Therefore, these observations were intended to investigate the efficiency of the methodologies on coating the overall surfaces of the constructs and were also a useful comparative mean to evaluate the applicability of the μ-CT analysis for the visualization and quantification of the apatite layers throughout the constructs.

Figure 5 presents the lateral sides of the scaffolds after being coated for 14 and 21 days in the different conditions. The correspondent cross-sections are shown in Figure 6.

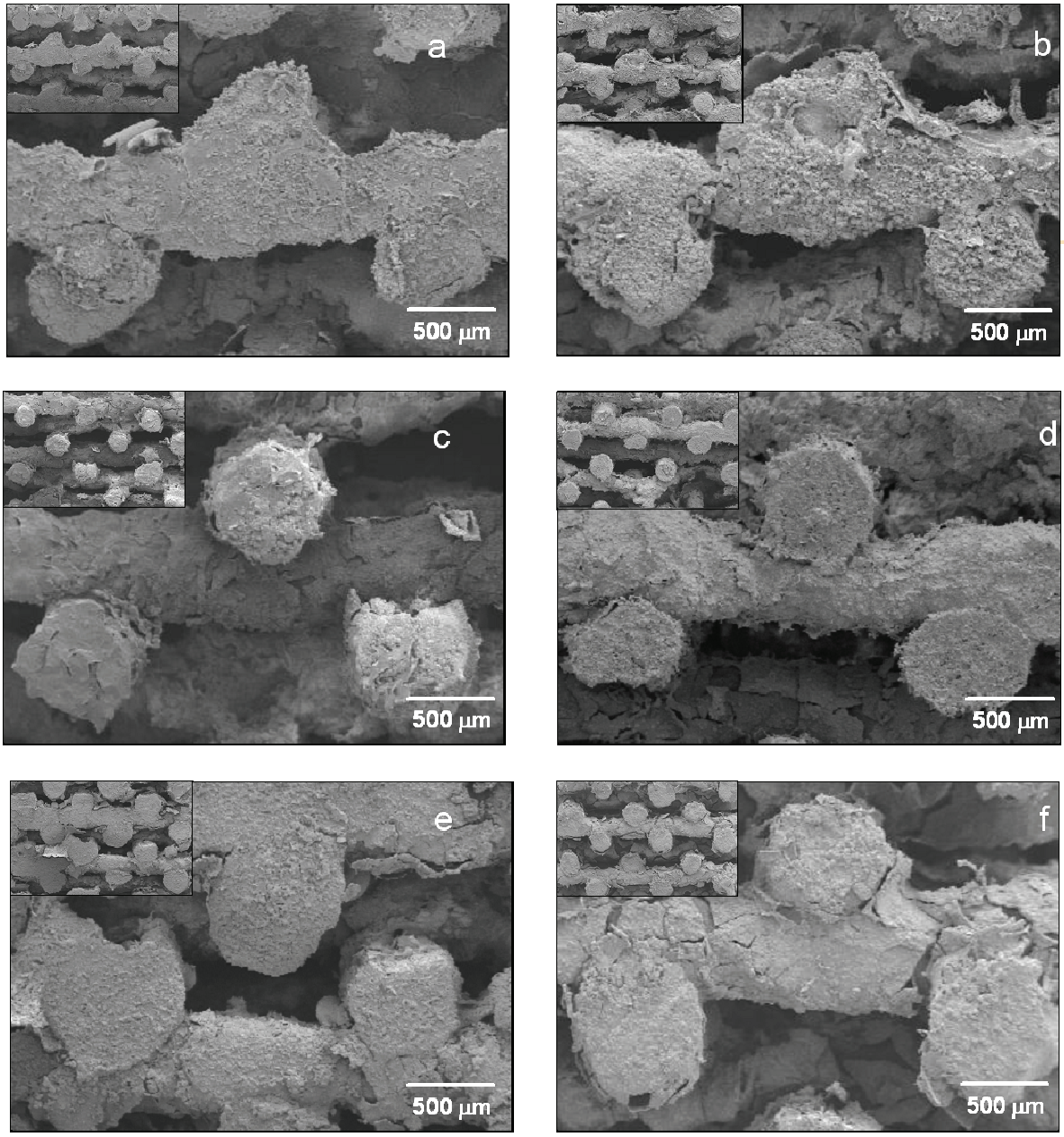


Figure 5. SEM micrographs of the coated lateral sides of the scaffolds after immersion in SBF in static (a,b), agitation (c,d) and flow perfusion (e,f) conditions for 14 (a, c, e) and 21 (b, d, f) days.

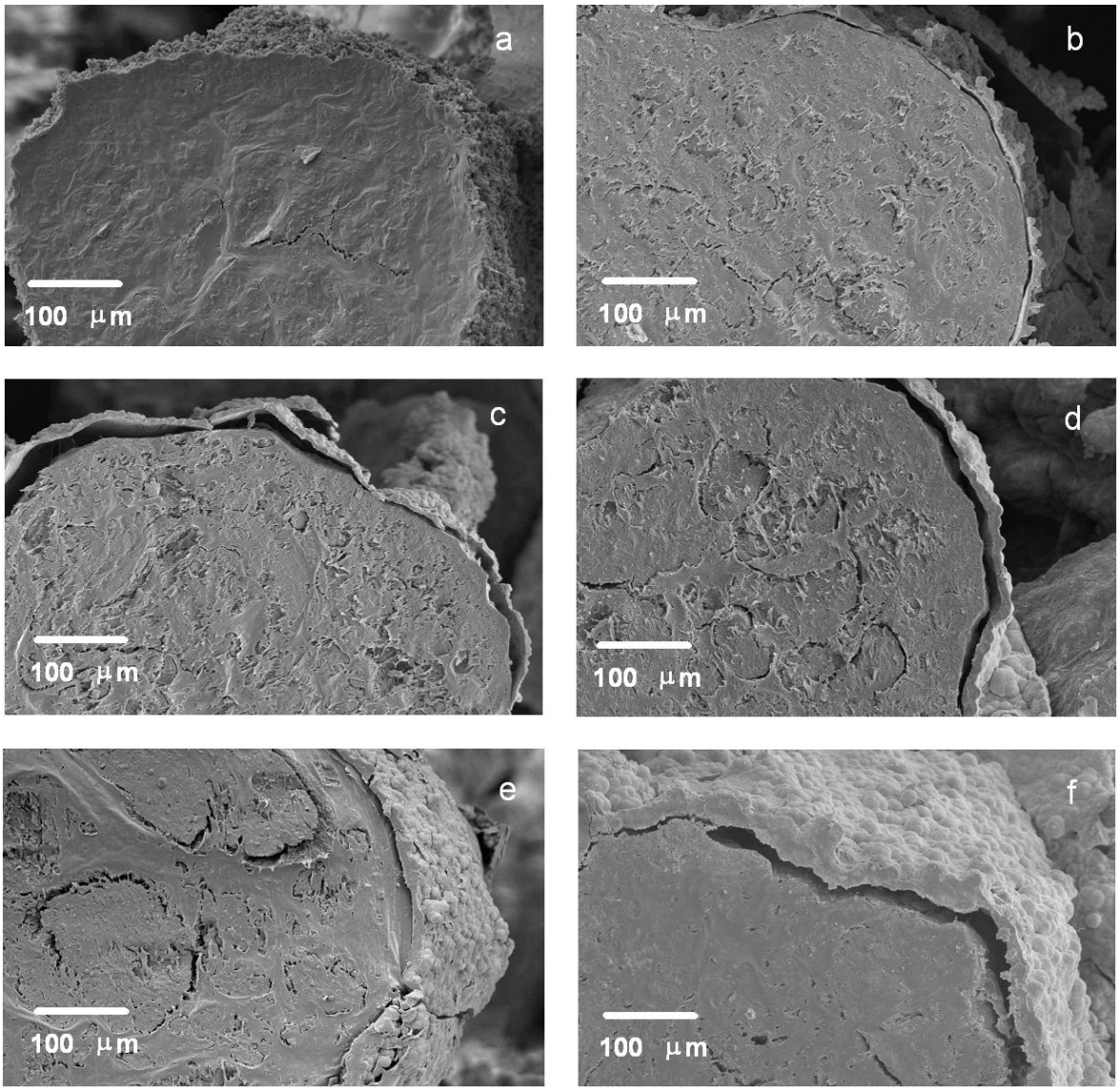


Figure 6. SEM micrographs of the cross-sections of a fibre in the middle of the scaffolds after immersion in SBF in static (a,b), agitation (c,d) and flow perfusion (e,f) conditions for 14 (a, c, e) and 21 (b, d, f) days

For all the studied conditions the integrity of the apatite layer nucleated in static SBF (Figure 2c) was maintained during the growth stage, even when dynamic conditions were present. The apatite layers have grown and clearly covered the fibres of the scaffolds without compromising its overall morphology and porosity. Nevertheless, in case of the static condition (Figure 5a and 5b) apatite tended to accumulate in some of the intersections of the fibres, particularly those at its outer region. A possible explanation for this effect can be a local increase of the concentration of Ca^{2+} and PO_4^{3-} ions in the SBF due to re-dissolution, in some extent, of the pre-established coating, which will induce a higher formation of apatite in those restricted areas. In case of agitation and flow perfusion conditions apatite coating has shown to better follow the fibres contour, as presented in Figs. 5c, 5d, 5e and 5f. However, after 21 days some cracking of the apatite coatings was

observed, particularly in case of agitation (Figure 5d) and flow perfusion (Figure 5f) conditions.

When considering the cross-sections of the centre of the scaffolds it is possible to confirm that for static conditions (Figures 6a and 6b) the formed apatite layers follow the shape of the fibres while for agitation (Figures 6c and 6d) a gap at the interface between the surface and the coating became visible in a considerable number of fibres. In case of flow perfusion a thicker apatite layer was formed after immersion in SBF for 14 days (Figs. 6e and 6f), following better the contour of the substrate. After 21 days the coating presented some extent of detachment which can be attributed mainly to the formation of a thick and cohesive apatite layer (Figs. 6e). In this case the cohesive forces tend to prevail over the adhesive forces at the interface coating/substrate. Nevertheless, one has to take into consideration that the observed coated scaffolds were previously subjected to high vacuum environments during sputtering and SEM observations and also to shear stresses during cross-section preparation which may have affected the coating integrity and adhesion. In spite of these situations, the apatite coating did not completely detach.

The calculated average thickness of the apatite layers measured *per* condition is plotted in Figure 7. The SEM micrograph illustrates the procedure used to perform the measurements, starting from the basis of the apatite nuclei to the interface. In this way, it was assured that the measurements were performed in the same way for all the conditions. The obtained values are the minimum thickness values for all the samples.

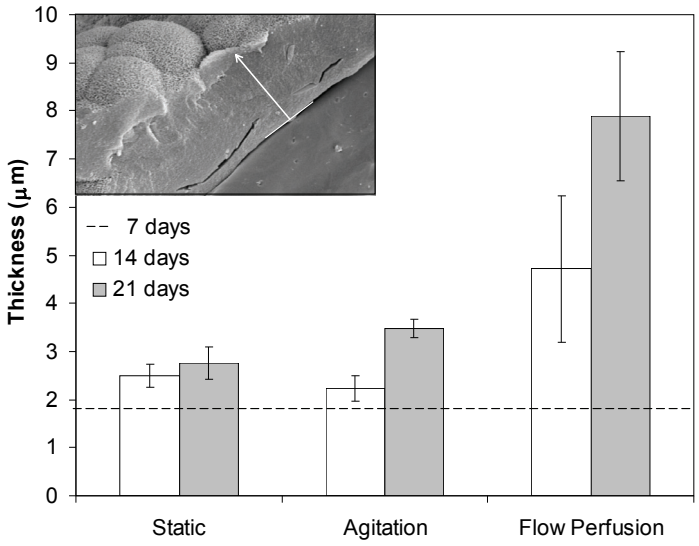


Figure 7. Average thickness of the apatite coatings formed during the biomimetic process in static and dynamic conditions, measured by SEM analysis.

The estimated apatite thickness after 7 days of immersion in SBF was 1.77 ± 0.31 μm (n=6), corresponding to a growth rate of 0.25 μm/day, during nucleation period. Subsequent immersion in SBF allowed for the apatite to grow, particularly in case of dynamic conditions. After 21 days, the calculated average thickness was 2.76 ± 0.33 μm in static conditions, 3.47 ± 0.19 μm in case of agitation and 7.90 ± 1.34 μm for flow perfusion. The rates for apatite growth were respectively: 0.04, 0.17 and 0.45 μm/day. Although a continuous increase in thickness was observed, the apatite has grown at lower rates than in the nucleation stage for all the conditions since the nucleation agent (sodium silicate) was no longer participating in the mineralization process. When dynamic conditions were present the rate for apatite formation increases, which indicates that the growing process is ion transport controlled, possibly by a combination of diffusion and convection phenomena right at the interface surface/fluid [25-27].

Only a few authors have studied the induction and growth of an apatite layer on the surface of bioactive materials on dynamic SBF. In fact, to the authors [28-32] knowledge, this kind of approach has been only proposed for accessing the SBF *in vitro* mineralization of materials in with intrinsic bioactivity like silica-based ceramics [28,30-32] or their composites [29]. However, no straight comparison can be establish with the present study due to the different and conditions used (e.g. solid/liquid ratio, flow rate) and the nature of the substrates.

V.3.3. μ-CT evaluation of the coated scaffolds

In the current study, μ-CT is originally used as an additional tool to complement the SEM morphological characterization, in order to evaluate the *in vitro* apatite coatings for static and dynamic conditions in 3D-plotted polymeric scaffolds as function of time. The average apatite content measured in the scaffolds is presented in Figure 8, as function of time and static/dynamic conditions. The degree of induced *in vitro* mineralization occurring in the polymeric 3D-plotted scaffolds is presented as a percentage of the overall scaffolds' volume.

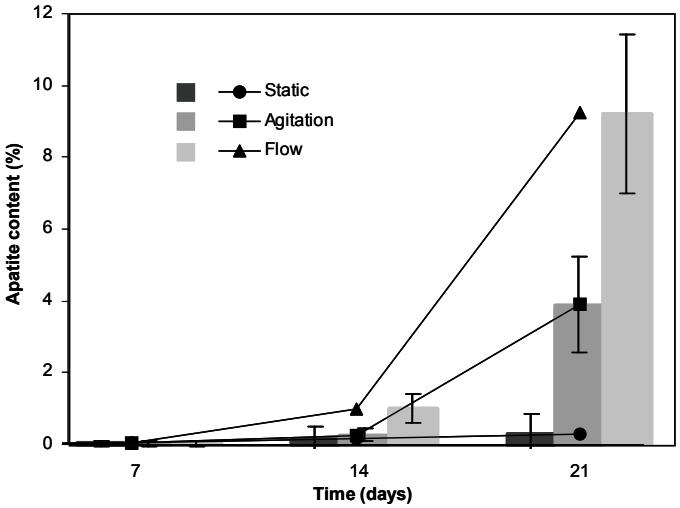


Figure 8. *In vitro* apatite coating progress in the scaffolds measured by μ-CT as function of time and test conditions.

The 2D histomorphometric analysis allowed for comparing the apatite content after coating in static and dynamic conditions. After a period of 14 days, an increase in the apatite content was observed when flow perfusion was applied. The influence of dynamic conditions is even more noticeable after a coating period of 21 days for both agitation and flow perfusion conditions. As one can observe, in static conditions, the evolution of the apatite content with time is negligible. However, there is a general growth in the apatite content observed from 14 to 21 days, related with the conjugated effect of dynamic conditions and an increase in the SBF concentration (from 1 to 1.5 times). These results are consistent with those obtained from the examination of the cross-sections of the coated scaffolds (Figure 6) and the correspondent thickness measurements (Figure 7).

In Figure 9 is plotted the SPCL porosity profile together with the apatite content distribution along the entire scaffolds as function of static and dynamic conditions for 21 days in SBF.

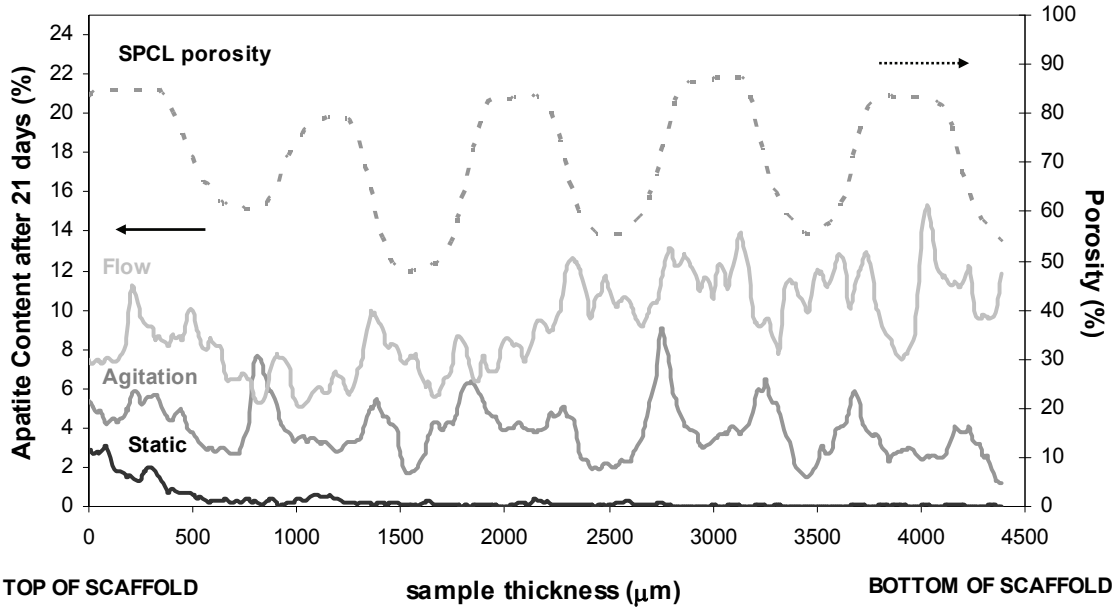


Figure 9. SPCL porosity profile (---) and apatite content distribution (——) along the scaffolds after 21 days period as function of test condition.

As expected, SPCL porosity profile obtained throughout the scaffolds presented a periodic variation, in agreement with the pre-established design of the scaffolds (Figure 2a). The mean porosity of the developed scaffolds is 70.8 ± 12%. As confirmed by SEM (Figure 5) all the scaffolds were coated from the top to the bottom regardless of the coating conditions, following the porosity profile. In static conditions, the average amount of apatite detected throughout the scaffold content was below 1% (Figure 8) of the overall polymer content. The profile of the apatite content followed the scaffolds' periodic trend although this is not clear due to the low values presented for this condition. A higher content was detected in the top of the scaffolds which can be probably related to some deposition of Ca-P precipitates in the scaffold upper side. In dynamic conditions, higher amounts of apatite were detected. In case of agitation, the periodic pattern is clearly indicating that the apatite coating follows the fibre contour. When flow perfusion is used, the coating follows in a more roughly way the periodic porosity profile but, if complemented with the SEM observations (Figs. 5 and 6), one can assure that the coating is well distributed along the fibres while following the geometry of the scaffolds. In case of flow perfusion, a general increase of the apatite coating from the top to the bottom of the 3D-plotted scaffolds is detected. In fact, for flow perfusion conditions, the side of the scaffold facing the flow will have a higher ion supply, since SBF flow rate is higher at the entrance of the chamber than in its centre. This result correlates well with the obtained values for the coating thickness presented in Figure 7 where the calculated apatite thickness presents a high standard deviation due to a thickness gradient observed from

the bottom to the top of the apatite scaffolds. In fact, the fibres from the bottom surface which were facing the flow presented a higher thickness, corresponding to the values in the upper limit of the error bar. To avoid this effect, future studies will include cyclic inversion of the flow.

Although the entire scaffolds were scanned essentially for 2D histomorphometric analysis, a volume of interest (VOI) of the materials was selected from the μ-CT data set for 3D visualization. This VOI corresponds to the central and inner part of the scaffolds as illustrated in Figs. 10a and 10b. The selection of this region included the same area used for performing the cross-sections. In this case, the main advantage of μ-CT over SEM is that sectioning is not required. Furthermore, coating of the inner part of the scaffolds is presented as a key challenge to the *in vitro* Ca-P coating technologies.

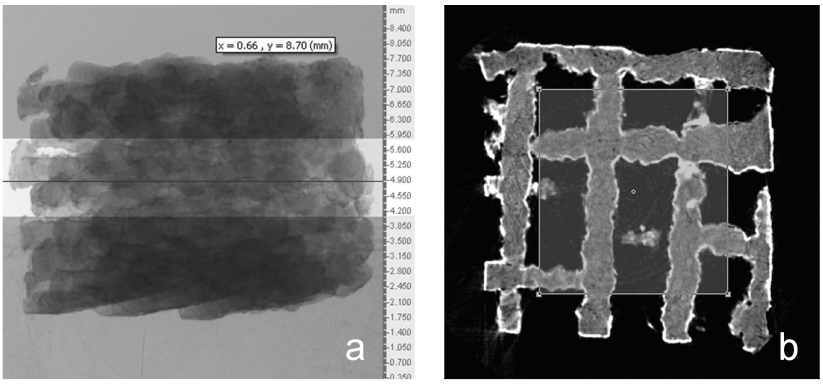


Figure 10. Selected volume of interest (VOI) of the central and inner area of the scaffolds. This selection was applied for all the scanned scaffolds.

In Figure 11 are presented different examples of cross-sections in 2D X-ray images, binary images at the pre-defined threshold used to identify the apatite content and finally, built the 3D models of the selected central VOI. The same threshold for binarization and to build the 3D models was used in all the scaffolds. These results concern a coating period of 21 days for the different tested conditions as the same trend was observed for 14 days and lower amounts of apatite.

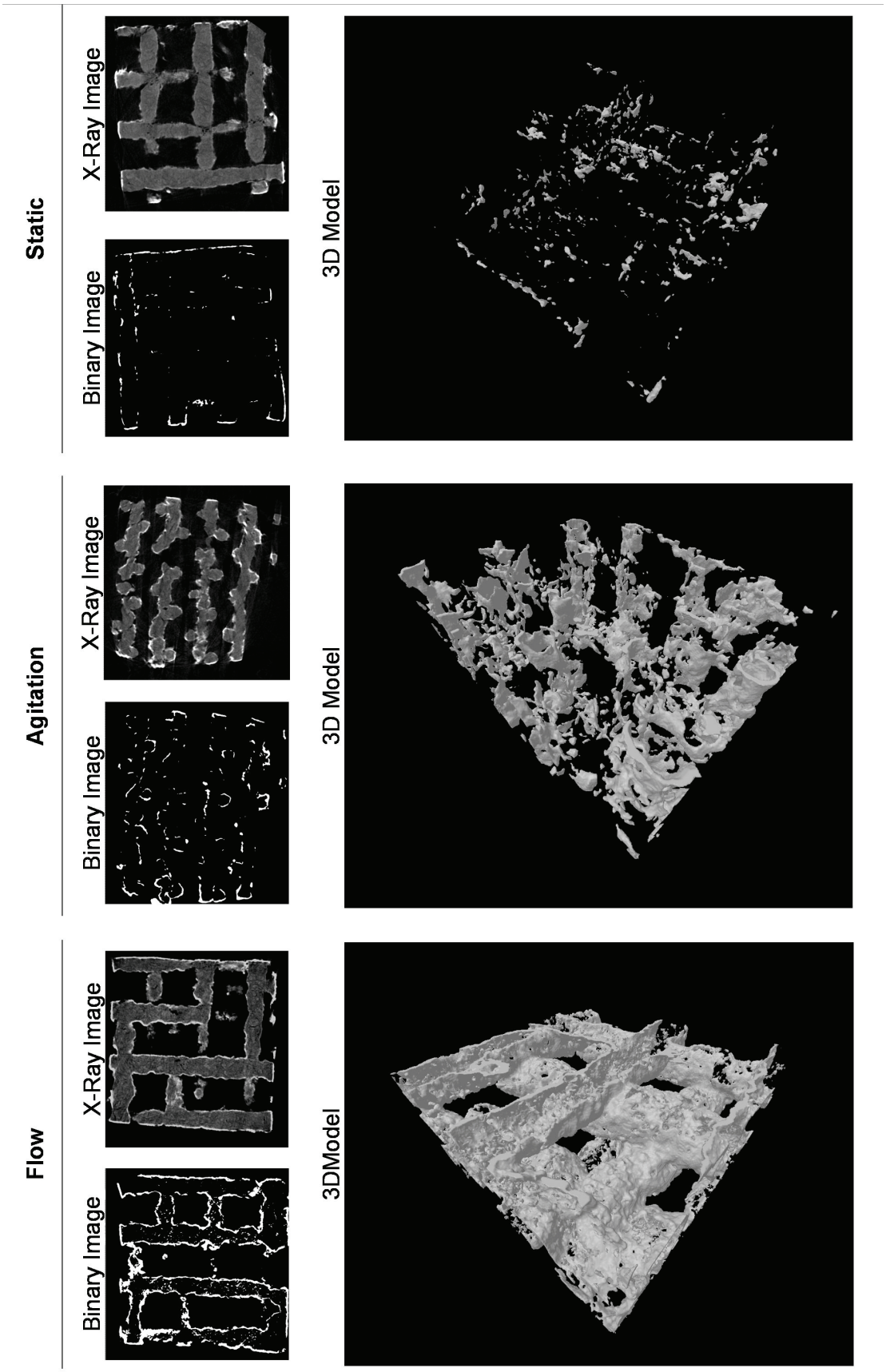


Figure 11. 2D X-Ray, 2D binary images and 3D models for the apatite coatings obtained for 21 days as function of static and dynamic conditions.

The obtained 3D models of the apatite spatial distribution on the inner part of the scaffolds show that for static and agitation conditions the coating only partially covered the SPCL fibres. In the flow perfusion condition, a well-defined apatite layer covers all the inner parts of the scaffold, following the available fibre surface area without compromising the overall morphology and interconnectivity of the 3D-plotted scaffolds. By SEM examination of the different scaffolds' surfaces and cross-sections it was possible to observe the constant presence of a continuous apatite layer covering the entire fibres, which is in disagreement with the apatite 3D models for both static and agitation conditions.

This can be explained by the lower thickness of the produced apatite layers for these conditions. The resolution mode used in these scans was 11 μm, which has shown to be insufficient to detect very thin coatings. In fact, high contrasts between phases are required for better quantification [33]. Theoretically at the pre-established threshold and with the present resolution it would not be possible to visualize the correct 3D representation of apatite layers with a thickness less 11 μm (value obtained from Figure 7). Nevertheless, one can clearly observe the coating on the scaffold in case of flow perfusion condition after 21 days in SBF, being the calculated thickness in this case around 8 μm (please see Figure 7). As explained above, the measured thickness by SEM analysis corresponds to the minimum average values since they refer to the distance starting from the basis of the apatite nuclei to the interface of the coating. This means that considering the nuclei above the most dense layer the coating thickness will be, in average, higher that 8 μm. Furthermore, even though the resolution was 11 μm, (pixel size: 11 μm) the equipment/software is capable of detecting Ca-P coating under this limit due also to the high diffraction of this ceramic when comparing with the polymer. Of course in this case the definition is lower. In future studies high resolution should be applied (decreasing the scaffolds size and increasing, in this way, the scan magnification) in order to obtain 3D models with more reliance. The herein utilized equipment (μ-CT 20) has an optimal resolution of 8 μm/pixel. Nevertheless, by complementing with SEM observations and 2D histomorphometric analysis it is possible to state that the coating is present in all the area of the scaffolds.

Microtomograph histomorphometric analysis revealed to be a useful complementary tool to characterize the induced *in vitro* mineralization and study different static and dynamic influence in the coatings growing. The apatite coating can be also quantified in terms of the overall scaffolds volume and its distribution along the scaffolds can be easily assessed without damaging the constructs. Nevertheless, the correct choice of adequate thresholds

and the use of high resolution modes are extremely important steps in order to obtain the correct visualization of the apatite coatings. The herein presented results provide the first insights on the potential of this non-destructive technique for the overall morphological characterization of biomimetic apatite layers, which would be impossible to achieve with the currently used techniques.

μ-CT analysis has clearly demonstrated that flow perfusion was the most effective apatite coating procedure, as already indicated by SEM technique. The advantages of this system when comparing with simple agitation and static conditions are numerous: i) unlike static conditions, the accumulation of precipitates is avoided; ii) it can closer mimic in vivo apatite mineralization; iii) a higher control of coating process is achieved by the controlling the flow rate; iv). the scaffolds and the coatings can better preserve their integrity because they are static in the chamber, which does not occur for agitation condition; v). a higher rate for apatite formation is obtained which means that the time for the coating process can be greatly reduced. Moreover, flow perfusion conditions can allow for the sequential incorporation of biologically interesting molecules in the context of TE. This subject together with studies on cell differentiation and proliferation will be investigated in the future.

V.4. Conclusions

Static and dynamic biomimetic routes allow for the effective coating of a bone-like apatite layer on newly developed SPCL scaffolds. Dynamic conditions mimic better the biological milieu, allowing for the coating of complex architectures at higher rates for the production the apatite layers, particularly in case of flow perfusion. By this process the time required for apatite formation was highly reduced and more stable and well-defined apatite layers were formed. Morphological analysis by SEM and μ-CT gave valuable information on the architecture of the scaffolds and on the dimension and distribution of the coatings. The herein presented results, obtained using μ-CT, provided the first insights on the potential of this non-destructive technique for the overall morphological characterization of biomimetic apatite layers, which would be impossible to achieve with the typically used characterization techniques.

References

1. Oliveira AL, Mano JF, Reis RL. Nature-inspired calcium phosphate coatings: present status and novel advances in the science of mimicry. Current Opinion in Solid State & Materials Science 2003;7(4-5):309-318.
2. Abe Y, Kokubo T, Yamamuro T. Apatite Coating on Ceramics, Metals and Polymers Utilizing a Biological Process. Journal of Materials Science-Materials in Medicine 1990;1(4):233-238.
3. Oliveira AL, Malafaya PB, Reis RL. Sodium silicate gel as a precursor for the in vitro nucleation and growth of a bone-like apatite coating in compact and porous polymeric structures. Biomaterials 2003;24(15):2575-2584.
4. Oliveira AL, Reis RL. Pre-mineralisation of starch/polycrapolactone bone tissue engineering scaffolds by a calcium-silicate-based process. Journal of Materials Science: Materials in Medicine 2004;15(4):533-540.
5. Mulder L, Koolstra JH, Van Euden TMGJ. Accuracy of MicroCT in the quantitative determination of the degree and distribution of mineralization in developing bone. Acta Radiologica 2004;45(7):769-777.
6. Kubik-Huch RA, Dorffler W, von Schulthess GK, Marincek B, Kochli OR, Seifert B, Haller U, Steinert HC. Value of (18F)-FDG positron emission tomography, computed tomography, and magnetic resonance imaging in diagnosing primary and recurrent ovarian carcinoma. European Radiology 2000;10(5):761-767.
7. Thurner P, Muller B, Sennhauser U, Hubbell J, Muller R. Tomography studies of biological cells on polymer scaffolds. Journal of Physics-Condensed Matter 2004;16(33):S3499-S3510.
8. Ito M. Assessment of bone quality using micro-computed tomography (micro-CT) and synchrotron micro-CT. Journal of Bone and Mineral Metabolism 2005;23:115-121.
9. Cartmell S, Huynh K, Lin A, Nagaraja S, Guldberg R. Quantitative microcomputed tomography analysis of mineralization within three-dimensional scaffolds in vitro. Journal of Biomedical Materials Research Part A 2004;69A(1):97-104.
10. Chen VJ, Smith LA, Ma PX. Bone regeneration on computer-designed nano-fibrous scaffolds. Biomaterials 2006;27(21):3973-3979.
11. Reis RL, Cunha A. M. Characterization of two biodegradable polymers of potential application within the biomaterials field. Journal of Materials Science: Materials in Medicine 1995;6:786-792.
12. Elvira C, Mano JF, San Roman J, Reis RL. Starch-based biodegradable hydrogels with potential biomedical applications as drug delivery systems. Biomaterials 2002;23(9):1955-66.
13. Gomes ME, Reis RL. Biodegradable polymers and composites in biomedical applications: from catgut to tissue engineering - Part 1 - Available systems and their properties. International Materials Reviews 2004;49(5):261-273.
14. Malafaya PB, Elvira C, Gallardo A, San Roman J, Reis RL. Porous starch-based drug delivery systems processed by a microwave route. J Biomater Sci Polym Ed 2001;12(11):1227-41.
15. Gomes M. E. SVI, Behravesh E., Reis R.L., Mikos Antonios G. Effect of Flow Perfusion on the Osteogenic Differentiation of Bone Marrow Stromal Cells Cultured on Starch Based Three-Dimensional Scaffolds. Journal of Biomedical Materials Research 2003;67A:87-95.
16. Tuzlakoglu K, Bolgen N, Salgado AJ, Gomes ME, Piskin E, Reis RL. Nano- and micro-fiber combined scaffolds: a new architecture for bone tissue engineering. J Mater Sci Mater Med 2005;16(12):1099-104.
17. Gomes ME, Reis RL, Cunha AM, Blitterswijk CA, de Bruijn JD. Cytocompatibility and response of osteoblastic-like cells to starch-based polymers: effect of several additives and processing conditions. Biomaterials 2001;22(13):1911-7.
18. Hutmacher DW, Sittinger M, Risbud MV. Scaffold-based tissue engineering: rationale for computer-aided design and solid free-form fabrication systems. Trends in Biotechnology 2004;22(7):354-362.
19. Kokubo T, Kushitani H, Sakka S, Kitsugi T, Yamamuro T. Solutions able to reproduce in vivo surface-structure changes in bioactive glass-ceramic A-W. J Biomed Mater Res 1990;24(6):721-34.

20. Takadama H, Kim HM, Kokubo T, Nakamura T. Mechanism of biomineralization of apatite on a sodium silicate glass: TEM-EDX study in vitro. Chemistry of Materials 2001;13(3):1108-1113.
21. Wu WJ, Gerard DE, Nancollas GH. Nucleation at surfaces: The importance of interfacial energy. Journal of the American Society of Nephrology 1999;10:S355-S358.
22. Wu WJ, Nancollas GH. Kinetics and surface energy approaches to the crystallization of synthetic and biological calcium phosphates. Phosphorus Sulfur and Silicon and the Related Elements 1999;146:125-128.
23. Vallet-Regi M, Romero AM, Ragel CV, LeGeros RZ. XRD, SEM-EDS, and FTIR studies of in vitro growth of an apatite-like layer on sol-gel glasses. Journal of Biomedical Materials Research 1999;44(4):416-421.
24. Rehman I, Bonfield W. Characterization of hydroxyapatite and carbonated apatite by photo acoustic FTIR spectroscopy. Journal of Materials Science-Materials in Medicine 1997;8(1):1-4.
25. Wu WJ, Nancollas GH. Determination of interfacial tension from crystallization and dissolution data: a comparison with other methods. Advances in Colloid and Interface Science 1999;79(2-3):229-279.
26. Hata K, Kokubo T, Nakamura T, Yamamuro T. Growth of a Bonelike Apatite Layer on a Substrate by a Biomimetic Process. Journal of the American Ceramic Society 1995;78(4):1049-1053.
27. Kokubo T, Kim HM, Kawashita M, Takadama H, Miyazaki T, Uchida M, Nakamura T. Nucleation and growth of apatite an amorphous phases in simulated body fluid. Glass Science and Technology-Glastechnische Berichte 2000;73:247-254.
28. Ramila A, Vallet-Regi M. Static and dynamic in vitro study of a sol-gel glass bioactivity. Biomaterials 2001;22(16):2301-2306.
29. Eglin D, Ali SAM, Perry CC. Comparative study of the in vitro apatite-forming ability of poly(epsilon-caprolactone)-silica sol-gels using three osteoconductivity tests (static, dynamic, and alternate soaking process). Journal of Biomedical Materials Research Part A 2004;69A(4):718-727.
30. Vallet-Regi M, Perez-Pariente J, Izquierdo-Barba I, Salinas AJ. Compositional variations in time calcium phosphate layer growth on gel glasses soaked in a simulated body fluid. Chemistry of Materials 2000;12(12):3770-3775.
31. Siriphannon P, Kameshima Y, Yasumori A, Okada K, Hayashi S. Comparative study of the formation of hydroxyapatite in simulated body fluid under static and flowing systems. Journal of Biomedical Materials Research 2002;60(1):175-185.
32. Salinas AJ, Vallet-Regi M, Izquierdo-Barba I. Biomimetic apatite deposition on calcium silicate gel glasses. Journal of Sol-Gel Science and Technology 2001;21(1-2):13-25.
33. Sun W, Lal P. Recent development on computer aided tissue engineering - a review. Computer Methods and Programs in Biomedicine 2002;67(2):85-103.

CHAPTER VI

Chapter VI

Biomimetic Ca-P Coatings Incorporating Bisphosphonates Produced on Starch Based Degradable Biomaterials

Abstract

In the present study sodium clodronate, a well known therapeutic agent from the family of bisphosphonates (BP) is incorporated in a biomimetic apatite coating, previously formed on the surface of a starch based biomaterial by a sodium silicate methodology, as a strategy to develop a site-specific drug delivery system for bone tissue regeneration applications. The effects on the resulting apatite coatings were evaluated in terms of morphology, chemistry and structure. The dissolution of Ca and P form the coating and the release profiles of sodium clodronate were also assessed. As a preliminary approach, this first study also aimed at evaluating the effects of this BP on the viability, growth and function of a human osteoblastic cell line, since there is still little information available on the interaction between BPs and this type of cells. Sodium clodronate could be successfully incorporated, at different doses, in the structure of a biomimetic apatite layer formed by a sodium silicate process. This type of bisphosphonates had a stimulatory effect on osteoblastic activity, particularly at the specific concentration of 0.32 mg/mL. It is foreseen that these coatings can for instances be produced on the surface of degradable polymers and then used for regulating the equilibrium on osteoblastic/osteoclastic activity leading to a controlled regenerative effect at the interface between the biomaterial and bone.

*This part of the chapter is based on the following publication:

AL Oliveira, AJ Pedro, C Saiz Arroyo, JF Mano, G Rodriguez, J San Roman and RL Reis, Biomimetic Ca-P Coatings Incorporating Bisphosphonates Produced on Starch Based Degradable Journal of Biomedical Materials Research Part A, (2007), *submitted.*

VI.1. Introduction

Although remarkable progresses have been made to produce superior bone-like materials, the right balance between surface and bulk properties is still to be achieved. At the present, one of the most interesting solutions to this problem is to use Ca-Ps as coatings on the surface of biomaterials. Using such type of techniques allows to produce Ca-P layers with potential to simultaneously serve as drug-carrier systems in bone Tissue Engineering applications [1,2]. Up to recently, calcium phosphate layers were deposited upon the surfaces of metal implants under highly unphysiological physical conditions, which did not allowed for their use in polymeric substrates. Plasma spraying, for example is a commercially available technique in which the high processing temperatures are clearly above 500 ºC [3-7].

At the present, it is possible to produce calcium phosphate layers under physiological conditions of temperature, pH and pressure, namely by the so-called biomimetic process [8-15]. As a result, there are new opportunities for applying this type of coatings in the field of tissue engineering, as a way to enhance cell adhesion and proliferation and extra-cellular matrix production. On the other hand, new possibilities for incorporating bioactive molecules such as synthetic drugs or proteinaceous osteoinductive molecules are being considered [2]. Due to the slow, but definite degradation of Ca-Ps, as well as their high hydrophilicity [16], they can be very suitable to serve as carriers for these molecules.

Research envisioning Ca-P coatings as carrier systems for the release of therapeutic molecules is still scarce, but its potential have captured the attention of some groups in the recent years. For example, antibiotic loading into calcium phosphate coatings on bone-replacement materials is a clinically relevant concept in the setting of total joint arthroplasty and has been recently addressed. For instances, Radin *et al.* [17] have accomplished the loading of vancomycin by immersion of ceramic-coated discs in vancomycin-containing simulated physiological solution. In a study performed by Campbell *et al.* [18] chlorhexidine was incorporated into an apatite coating by placing the substrate into various chlorhexidine solutions in between mineralization cycles. Calcium phosphate coatings containing tobramycin were produced by Stigter *et al.* [19] on titanium alloy (Ti6Al4V) implants using a biomimetic approach. Although the options for creating a

delivery system in these coatings can be numerous, the affinity of a specific molecule to the Ca-P crystals as well as its size, charge or conformation, are crucial features for an effective incorporation. In fact, some of these agents, due to their chemical structure or conformation, can only be adsorbed superficially, upon preformed layers. Such superficially adsorbed molecules are sometimes released too rapidly within a biological milieu to be effective in their therapeutic/osteoinductive capacity.

Bisphosphonates (BPs) are an important family of drugs in various bone- and calcium-related pathologies like cancer [20], hypercalcemia [21], Paget's disease [22] or osteoporosis [20-26]. The affinity of BPs to bone mineral hydroxylapatite is the basis for their use as inhibitors of bone resorption [25,26]. They are pyrophosphate (P-O-P) analogues in which the oxygen in the P-O-P has been replaced by a carbon to yield a P-C-P backbone. Substitutions on the carbon give rise to a large family of compounds with different properties and potencies which are determined by the nature of the side chains [26]. The physicochemical effects of BPs include binding strongly to the calcium phosphate crystals and inhibiting their growth, aggregation and dissolution [25-27]. Their biological effects in calcium-related disorders are due to the direct interaction with osteoclasts [28] and/or osteoblasts [29] though a variety of biochemical pathways. It is now generally accepted that BPs inhibit osteoclast activity [23-25,29]. However, the major drawback of the clinically utilized BPs is their pharmacokinetics and poor oral absorption from the gastrointestinal tract, which is typically less than 1% [25,26]. In addition, BPs have been associated with adverse gastrointestinal effects in humans [30]. The vast attempts to improve the bioavailability of BPs had only very limited success due to a lack of marked improvement of adsorption and/or side effects [30]. The challenge for novel drug delivery systems is to achieve improved bioavailability and safety. Besides oral administration, different strategies have been proposed over the last years, as nasal delivery [31] and subcutaneous [32-34] or intramuscular injection [35].

In addition of being used in the treatment of the above described pathologies, it has been also discovered [36-38] that BPs can be beneficial when administrated after bone replacement, decreasing the primary failure mode of total hip arthroplasty, which is aseptic loosening following peri-implant osteolysis. Nevertheless, this effect could be improved if the time delay for the bisphosphonate to reach the interface bone-implant could be reduced. In this case a localized delivery of the drug could have a favourable effect in order to produce a more stable and integrated interface between the implant and bone at the early stage of implantation, when a significant bone loss can occur [39]. In fact, this

was already attempted with success in several studies using different BPs [39-42]. For example, Kajiwara *et al.* [40] have treated calcium ion-implanted titanium implants with Pamidronate which significantly accelerated new bone formation in a rat tibia. Yoshinari et al. [41] have studied the effect of the same BP incorporated in a plasma sprayed hydroxyapatite (HA) coated titanium dental implant in beagle mandibular bone, increasing the bone-implant contact area. Recently, Peter *et al.* [42] have grafted Zoledronate to plasma-sprayed HA-coating of titanium implants that were then inserted in rat condyles. A positive concentration-dependent effect was observed on the peri-implant bone density and on different histomorphometric parameters.

Due to its reported effects on bone, one can envision that to incorporate a bisphosphonate in a bone-like apatite coated biodegradable scaffold can be a very promising strategy for designing a site-specific drug delivery system in a Tissue Engineering approach, by locally enhancing tissue integration and regeneration. In the present study sodium clodronate, a well known BP, was incorporated at different doses in an apatite coating, previously formed on the surface of a starch based biomaterial by a sodium silicate methodology. The effects on the resulting apatite coatings were evaluated in terms of morphology, chemistry and structure. The release profile of the drug and the stability of the coatings were assessed at different physiological environments. As a preliminary approach, this study also aimed at screening the ideal sodium clodronate dose to be incorporated in the apatite coatings, that is able to elicit positive effects on the viability, growth and function of a human osteoblastic-like cell line. In fact there is still little information available on the interaction between BPs and this type of cells.

VI.2. Materials & Methods

VI.2.1. Preparation of the samples

As a natural polymer with rather interesting properties [43-45], starch exhibits a great potential to be used in biomedical applications. The studied material is based on a blend of starch/ethylene vinyl alcohol (SEVA-C) supplied by Novamont, Italy. The blend contains around 50% starch by weight, while the copolymer discloses a composition of 60/40 mol/mol. Compact samples were produced by injection moulding on a Klockner Desma FM-20, using a nozzle temperature of 170 ºC. All the samples were shaped into the form of disks with a diameter of 10 mm. Further information on the properties of starch based polymers and its potential for biomedical applications may be found elsewhere [43-46].

VI.2.2. Sodium silicate methodology

To produce the bioactive coatings a commercially available sodium silicate gel from SIGMA-ALDRICH ($Na_2SiO_3 \bullet H_2O$, containing ~14% NaOH and ~27% SiO_2, pH ≈13) was used. The sodium silicate gel was herein used with concentration and SiO_2/Na_2O molar ratio as received [15]. The viscosity of the gel is 6 x 10^{-2} $Pa.s^{-1}$. This high viscosity allowed for the impregnation other than uptaking the gel into the polymer, which would affect the mechanical and degradation behaviour of the material. The materials (SEVA-C disks with ∅ of 10 mm) were "impregnated" for 24 hours with the gel, in a controlled atmosphere (23 ± 1 ºC; 55% RH). After this treatment the gel with the samples was diluted with 50% vol. of distilled water and stirred for 5 minutes. This procedure was aimed at diminishing the viscosity of the gel in order to produce a homogeneous and thin layer of vitrified sodium silicate in the surface of the materials. The samples were then removed from the solution and dried in a controlled atmosphere (23 ± 1 ºC; 55% RH).

VI.2.3. Apatite formation

An aqueous solution was prepared comprising all major inorganic ions present in the human's blood plasma and presenting its approximate ion concentration, in order to promote *in vitro* apatite formation. The different salts were dissolved in de-ionized H_2O

and the pH adjusted to neutral using tris(hydroxymethyl)aminomethane and hydrochloric acid. This simulated body fluid solution (SBF) was developed by Kokubo and co-workers [11].

The treated samples were first soaked in SBF in order to nucleate the apatite layer and after 7 days, soaked in another solution, with ion concentrations 1.5x SBF for allowing this layer to grow. The solutions were renewed every 2 days during the coating process which lasted for 14 days. The average thickness of the apatite layers formed by this methodology is ~ 2.5 μm (measured from the basis of the apatite nuclei to the interface, according to a previously developed method [47])

VI.2.4. Incorporation of sodium clodronate

Bisphosphonates are stable analogues of pyrophosphate in which the P-O-P structure is replaced by a P-C-P structure. Side chains R^1 and R^2 are attached to the geminal carbon atom. The bisphosphonate used in this study was a sodium clodronate in which R^1 and R^2 are replaced by chloride. The structure of this drug is presented in Figure. 1.

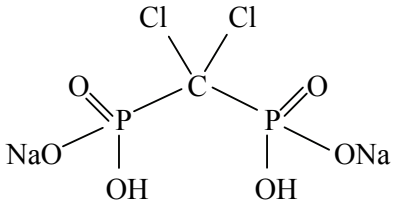


Figure 1. Chemical structure of sodium clodronate

Sodium Clodronate (dichloromethylene-bisphosphonate) is one of the best documented bisphosphonate that is used effectively in medical applications [48]. In the literature the ideal concentration of this BP for inducing a positive effect in bone cells varies from study to study. Therefore, we have chosen two lower concentrations that are considered to be in the therapeutic range [48] and two higher concentrations in order to scale up the effects of this BP in the structure of the apatite coating in order to be detectable by infra-red and x-ray spectroscopies. Solutions of 0.064, 0.32, 8 and 16 mg/mL of sodium clodronate (SIGMA-ALDRICH) were prepared with the pH adjusted to 7.4 with NaOH (1M). Aliquots of 50 μl of each solution were added to the coated disks left for 3 hours followed by drying at 60ºC [49]. The effective concentration of the BP in the coated samples is approximately as follows: 0.004, 0.02, 0.5 and 1 mg/cm^2.

VI.2.5. Structural and morphological characterisation

The morphological characterisation was carried out by Scanning Electron Microscopy (SEM) analysis in a LEICA Cambridge S360, United Kingdom. All the samples were coated with a thin film of carbon, by ion sputtering, prior to any observation. The electron beam energy was 15 KeV. Energy Dispersive Spectroscopy (EDS) was performed qualitatively in a Rontec spectrometer, in order to obtain the compositional profiles of the apatite layers incorporating different amounts of sodium clodronate. Fourier Transform Infrared Spectroscopy with Attenuated total Reflectance (FTIR-ATR) was performed, aiming at detecting any type of chemical modification on the samples chemical structure. The acquisition was performed in transmittance mode from 4000 to 500 cm^{-1}. All spectra were recorded using 64 scans and 2 cm^{-1} resolution in an FTIR spectrophotometer (Perkin-Elmer 1600 Series, USA). Thin-Film X-Ray Diffraction (TF-XRD, Philips X'Pert MPD, The Netherlands) was used to identify the crystalline phases present in the apatite layers formed during the immersion in SBF and after incorporating sodium clodronate. The data collection was performed by 2θ scan method with 1º as incident beam angle using CuKα X-ray line and a scan speed of 0.05 º/min in 2θ.

VI.2.6. Mechanical behaviour

Microhardness tests are usually regarded as a convenient mean of investigating the mechanical properties of materials in a localised and non-destructive manner. Microhardness measurements have been used herein to study the differences and correlation between the composition and the surface or coatings in different kinds of samples. The motivations of such measurements are to probe the mechanical environment that the cells will feel when in contact with the material, and to evaluate the influence of the presence of the drug in the coating in its mechanical properties. A Leica VMHT30 equipment was used to measure the microhardness of the samples at room temperature, (~20ºC), using a Vickers diamond pyramid indented, (included angle α=136ºC). The microhardness, H_v, was calculated from the residual projected diagonal impression using H_v=1.854 F/d^2 equation, where d is the mean diagonal length of the indentation in mm and F the applied force in N. A load of 9.807mN was applied during 10s in all tests. These conditions were chosen, for getting measurements only at level of the coating, avoiding the bulk of the substrate samples. Fifteen measurements at randomly

selected places around coating of each sample were taken in each condition. The same procedure was followed for the samples' substrate.

VI.2.7. Dissolution behaviour

To try to predict the behaviour of the apatite coating when facing the biological milieu is of extreme importance. However, to design a method capable of fully replicate it, is extremely difficult, considering the complexity of the biological fluids, going from minerals to proteins, enzymes and cells. *In vitro* dissolution tests, although far from the ideal method, can give some insights on the stability of the materials prior to implantation. In fact, since these studies are carried out in solution they always simulate the worst case low-end service environment.

Dissolution tests were carried out on the coated samples before and after loading with increasing doses of sodium clodronate. Two different media were used in this study, according to the International Standard ISO/DIS 10993-14 procedure and are presented in Table 1.

Table 1. Solutions used in the dissolution studies.

Solution #	Description	pH (at 37ºC)
1	Simulated Tris/HCl solution	7.4
2	Acidic Buffered solution (simulating osteoclastic activity)	3

Solution 1 simulates, in a very simplistic way, the *in vitro* physiological environment. Solution 2, is aimed at reproducing the worse predictable scenario in which bone is resorbed due to osteoclastic activity. The coated disks, incorporating different amounts of sodium clodronate, were immersed in a volume of 5 mL of each solution. Two replicates of each condition were studied. The experiment was carried out at 37ºC for periods up to 15 days. Aliquots of 2 mL were removed at different periods and replaced by the same volume of fresh solution. The obtained samples were analysed by Induced Coupled Plasma emission (ICP) spectroscopy for the quantification of Ca and P. The final cumulative concentration values were calculated according to the following equation:

$$\Sigma\,[V_n-(V_{n-1}*2/5)]_n \qquad (1)$$

V_n- Volume aliquoted;

V_{n-1}- Subsequent volume aliquoted;

VI.2.8. Sodium clodronate Release studies

The release of sodium clodronate from the Ca-P coatings in the previously described solutions was studied. The analysed solutions and periods of time were the same in which Ca and P were quantified. The release of the drug was monitorized by means of High Permeation Liquid Chromatography (HPLC). The analysis was performed by using a mixture (60:40) of methanol/aqueous solution of PIC A (a solution of Tetrabutylammonium Hydrogen Sulphate in water, supplied by Waters) as the mobile phase and a flow rate of 1 mL/min. The system consisted in a Perkin Elmer LC-250 pump, an UV/VIS detector Perkin Elmer LC-95 and a Waters μBoundapak C-18 column of 3.9 × 300 mm. Measurements were made at 204 nm. Using these conditions, sodium clodronate presented a retention time of 2.31 and 2.35 minutes in pH=7.4 and pH = 3 respectively, as it is shown in Figure 2.The obtained profiles for each solution are presented in Figure 2.

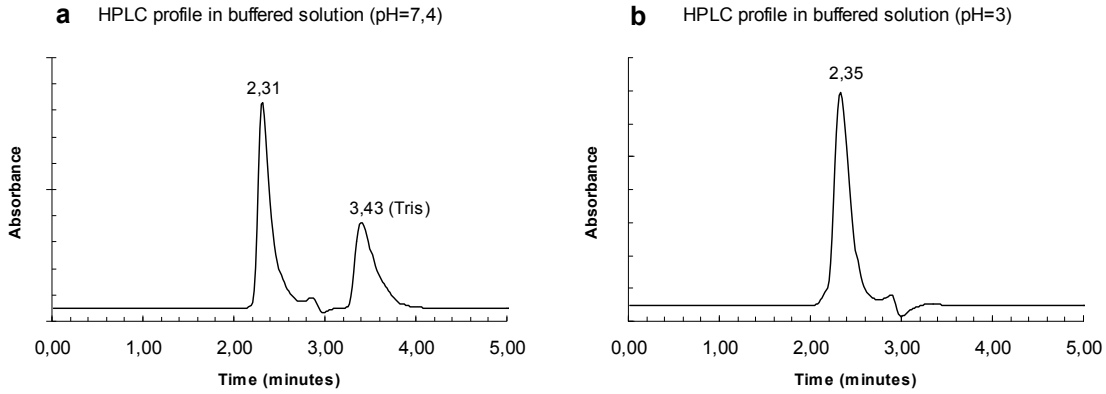


Figure 2. HPLC release profiles of sodium clodronate in a) a solution buffered to pH 7.4, b) a solution buffered to pH 3.

Release studies were carried out from discs loaded with 8 mg/ml solutions of sodium clodronate, which provided an effective concentration of 0.4 mg of drug per coated disk. Discs prepared with lower concentration of drug (0.32 and 0.064 mg/ml) were not evaluated since they are below the detection limit of the HPLC equipment. The effective concentration loaded in the was 0,4 mg per coated disk, which is the result of a 50 μL aliquot of a solution with concentration 8 mg/mL. The results were plotted according with Equation 1.

VI.2.9. Preliminary evaluation of Cell adhesion and proliferation

In order to study the morphology, attachment and proliferation of osteoblast-like cells over pre-calcified loaded SEVA-C surfaces, a human osteoblast-like cell line (SaOs-2) obtained from the European Collection of Cell Cultures was selected. Dulbecco's Modified Eagle's Medium (DMEM, Sigma, USA), supplemented with 10% Foetal Bovine Serum (FBS, Biochrome, Germany) and 1% antibiotic/antimicotic solution (Sigma, USA) was used as cell incubation medium and growth to confluency in controlled atmosphere conditions (37ºC, 5% CO2, 100% humidity). Detachment of confluent low passage cells was performed using 0,25% Trypsin/EDTA solution (Sigma, USA). Subsequently, osteoblast-like cells were cultured over samples in a concentration of 3.3 x 104 cell/mL and incubated for 3, 5 and 7 days in controlled atmosphere conditions. Tissue culture grade polystyrene was used as control and replicates were prepared. After each incubation period, samples were washed with Phosphate Buffer Saline (PBS, Sigma, USA) solution and fixed in Gluteraldehyde 2.5% (V/V) for observation by means of Scanning Electronic Microscopy. After fixation, samples were dehydrated in crescent ethanol concentrations (50%, 70%, 90% and 100%), air-dried and sputter coated with gold.

Cell proliferation of SaOs-2 was assessed using the Micro BCA Protein Assay Kit from PIERCE to quantify the total protein quantity. At each time period each sample was washed with PBS (phosphate-buffered saline), the cells were lysed through cycles of freeze and thawing and the protein present on each lysed suspension was measured. This total protein quantification is directly related with cell proliferation, once it is directly proportional to the cell number.

Cell viability was measured through the MTS test, using the CellTiter 96® AQueous One Solution from PROMEGA, that is based on bioreduction of a substrate (MTS), into a brown product by dehydrogenase enzymes in metabolically active cells and is commonly used for cell viability evaluation. Cells were then incubated for 3 h at 37°C in a humidified atmosphere containing 5% CO2. At this time optical density (OD) was measured with a plate reader at 490 nm. The mean OD value obtained for the positive control (cell seeded on culture plate without any coating) was considered as 100% metabolic activity.
Alkaline phosphatase activity was assessed by the p-nitrophenol phosphate method which consists on the use of the lysed cells (that contains the Enzyme ALP) to cleave the p-nitrophenol phosphate that is added to that solution as a substrate. The resultant products

are phosphate and p-nitrophenol. The last is turns resultant solution into yellow, which can be measured by OD at 405nm. The obtained OD is directly related with the enzyme activity.

VI.3. Results & Discussion

VI.3.1. Morphology, crystallinity and chemical structure of the apatite coatings

The effect of the incorporation of different doses of sodium clodronate on the morphology, crystallinity and chemical structure of the biomimetic coatings was evaluated using SEM/EDS, TF-XRD and FTIR-ATR techniques. In Figure 3 is presented the morphology of the apatite coatings grown on the surface of SEVA-C samples before and after a treatment with sodium clodronate at 8 mg/mL. The corresponding EDS spectra showing the evolution of the elemental composition are presented in Figure 4.

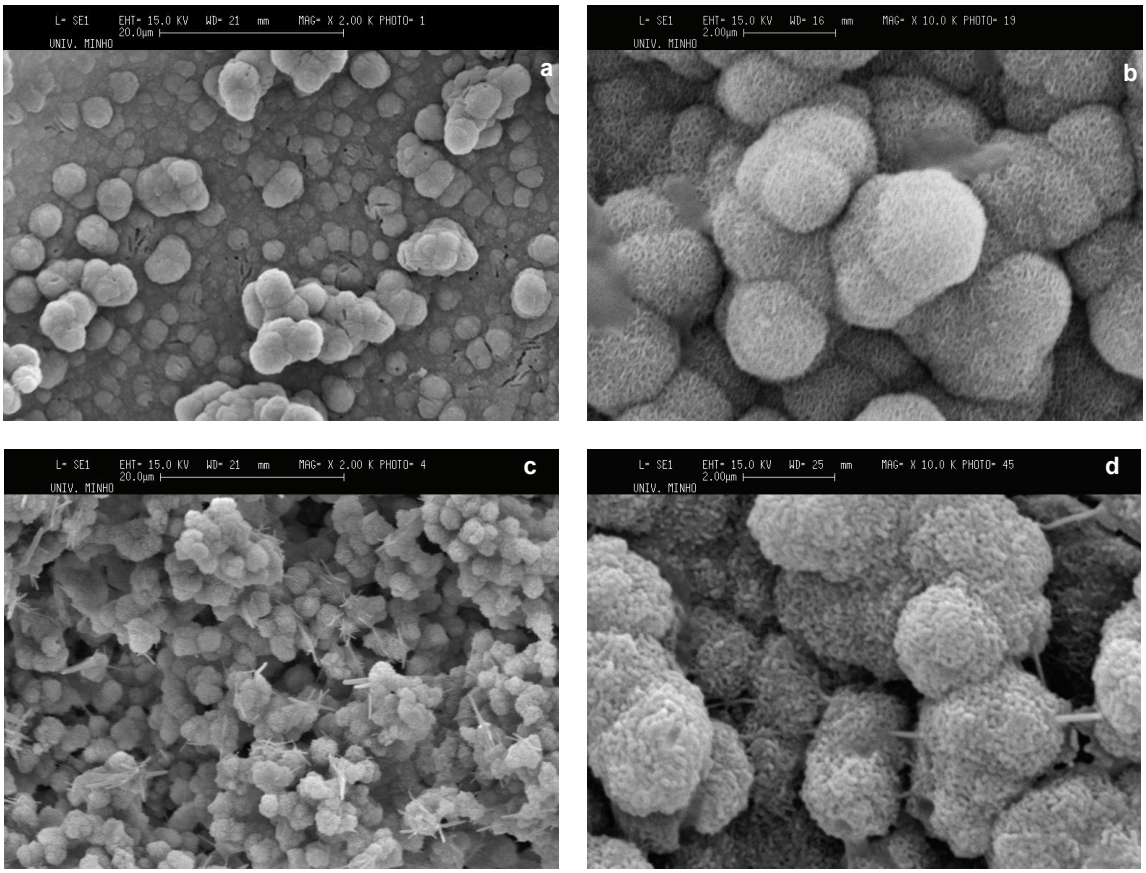


Figure 3. SEM micrographs performed on the apatite coatings grown on the surface of SEVA-C samples a), b) before and c), d) after the treatment with 8 mg/mL of sodium clodronate.

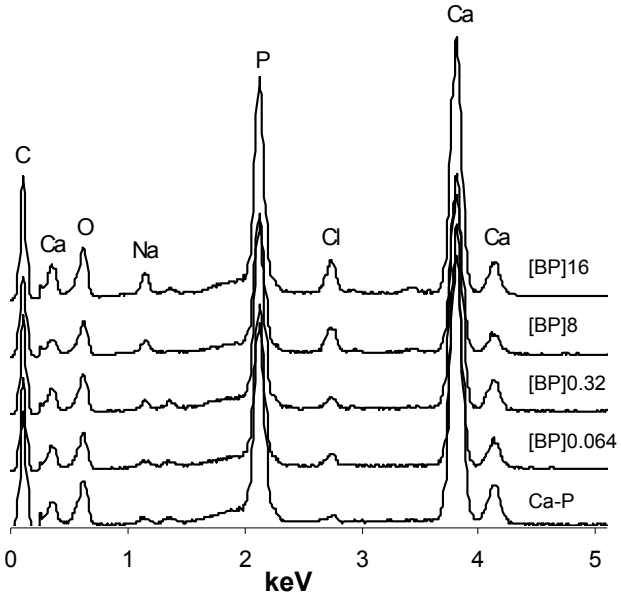


Figure 4. EDS spectra showing the evolution of the elemental composition of the apatite layers with increasing doses of sodium clodronate.

The use of sodium silicate biomimetic coating methodology resulted in the formation of an apatite layer on the surface of SEVA-C after 15 days in SBF, exhibiting a nanocrystalline needle-like structure, as presented in Figures 3.a and 3.b. After incorporating the lowest concentrations studied of sodium clodronate, i.e. 0,064 and 0,32 mg/mL, the apatite crystallites did not present any observable modification in their morphology. Therefore, the micrographs presented in Figure 3a. and 3b. are representative of the obtained morphologies in these cases. When incorporating the highest studied concentrations of the BP (8 and 16 mg/mL), well-defined spicule crystallites started to grow on the surface of the apatite layer, as it can be visible by examining Figures 3c. and 3d, for the case where a solution containing 8 mg/mL was used. By performing localized EDS it was possible to confirm that the elemental composition of these structures exhibited a high content in Cl which is assigned to sodium clodronate (data not shown). On the other hand, by observing the surface of the apatite layer in greater detail (Figure 3.d), it is also possible to find a modification in its morphology. The resulting apatite crystals present a more “worm-like” morphology when comparing with the original “needle-like” shape (Figure 3.b). This modification can be attributed to a partial dissolution at the surface of apatite layer in the presence of the solutions containing high concentrations of sodium clodronate (by calcium depletion) and further re-precipitation under these new conditions, which differ from those present in SBF in terms of composition, ionic strength and buffer capability. On the other hand, due to its high affinity for Ca-compounds (especially to

calcium phosphates [25,26]), it is also predictable to a certain extent the chemical incorporation of the drug onto the apatite structure, causing dimensional re-arrangements.

In Figure 5 is plotted the FTIR spectra performed on the surface of SEVA-C before and after growing an apatite layer and after incorporating the highest doses studied of sodium clodronate. Again, by this technique it was not possible to detect the presence of BP in the samples treated with the lowest concentrations of the drug. The IR spectrum of sodium clodronate powder is also presented as a reference for identifying its characteristic peaks.

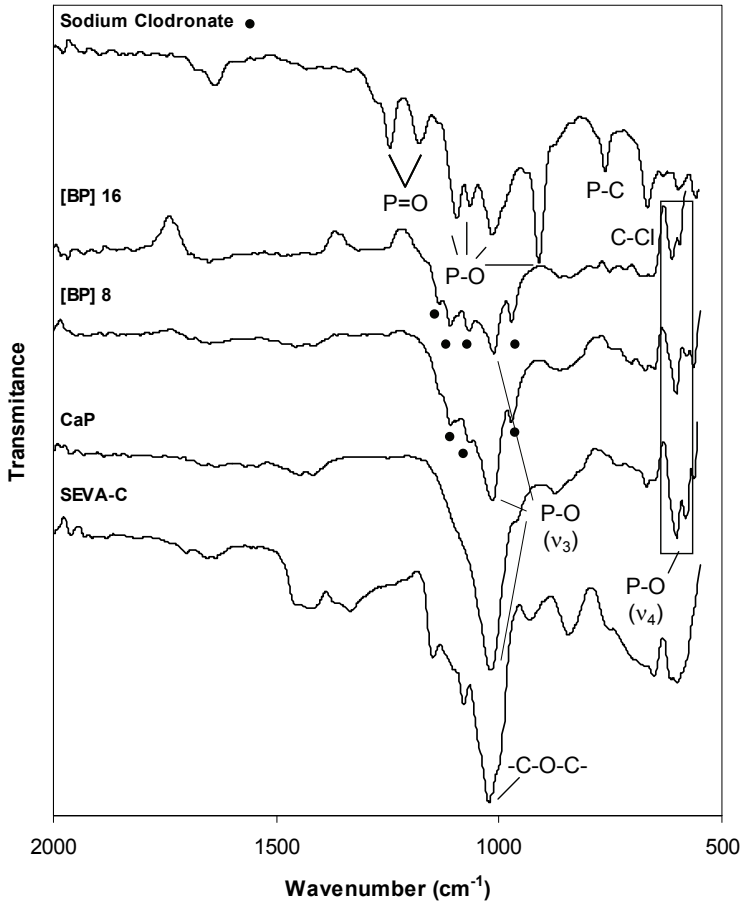


Figure 5. FTIR-ATR spectra of SEVA-C before and after forming an apatite layer and after the incorporation of 8 and 16 mg/mL of sodium clodronate. Sodium clodronate powder was used as reference.

SEVA-C presents -C-O-C- bands at 1015-1140 cm^{-1} which are characteristic of the glycosidic bonds from starch [50,51]. After coating the biomimetic layer it is possible to detect the typical bands of calcium phosphates. The bands at 864, 1406 and 1434 cm^{-1} result from the presence of carbonate (CO_3^{2-}) incorporated in the apatite lattice [52]. These bands clearly indicate that a carbonated apatite was formed, as it is found in bone

apatite and as reported for other biomimetic coating methods [13,53]. The bands at 578 and 598 are assigned to the ν_4 bending mode of the O-P-O bonds in the apatite, indicating some degree of crystallinity. The band at 1012 cm^{-1} indicates the ν_3 stretching mode of P-O bonds [52]. When sodium clodronate is present besides the major P-O bond attributed to the ν_3 vibration of -PO_4, additional bands attributed to the same type of bonds are detected at 968, 1060, 1102, 1122 cm^{-1}. The crystallites newly formed on the apatite layer and detected by SEM can then be assigned to the precipitation of the sodium clodronate..

Figure 6 presents the typical X-Ray Diffraction patterns, for the surface of SEVA-C samples before and after growing the apatite layers and for the same layers after incorporating sodium clodronate at the highest studied doses. The profile of pure sodium clodronate powder was also acquired and is herein presented as a reference pattern.

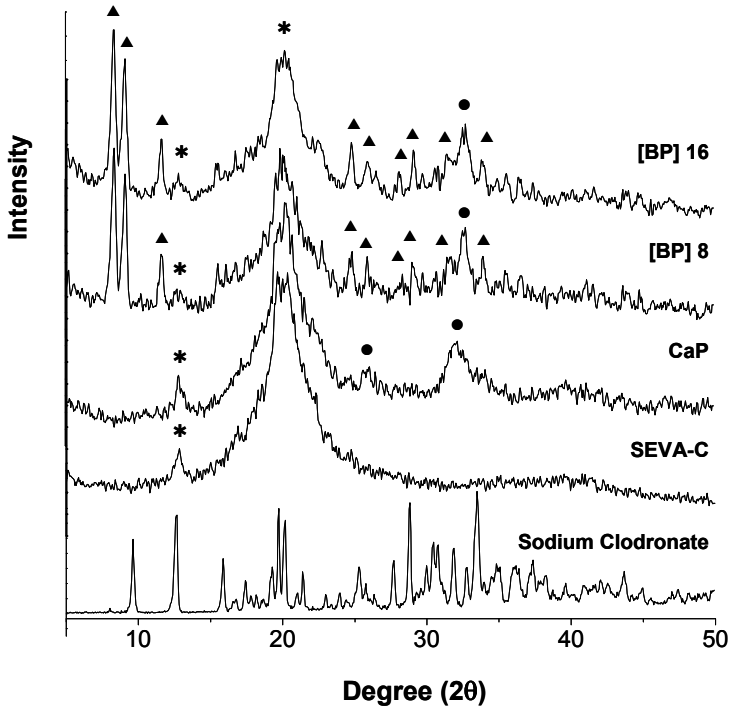


Figure 6. TF-XRD spectra of SEVA-C before and after forming an apatite layer and after the incorporation of 8 and 16 mg/mL of sodium clodronate. Sodium clodronate powder was used as reference. ✱ SEVA-C; ● Apatite; ▲ Sodium clodronate.

SEVA-C diffraction profile presents two characteristic broad peaks, detected at 2θ=12º, and 2θ=20º, assigned to its crystalline phases [51]. After growing the biomimetic layers on its surface it is possible to detect the two main characteristic peaks attributed to HA (JCPDS card 9-432). The peak at 2θ = 26º is assigned to (002) plane in the apatite crystalline lattice. Another important diffraction peak is detected around 2θ = 32º and is

related to the overlapping of planes (211), (112) and (300). This broad peak indicates that the apatite structure is composed by small crystallites. Similar XRD profile was obtained after adding sodium clodronate at 0,064 and 0,32 mg/mL to the coatings. In this way, XRD technique was not suitable for detecting such low amounts drug in the coating. However, when incorporating the drug at concentrations of 8 and 16 mg/mL, several other strong reflections can be detected, as presented in Figure 5. This indicates the presence of a new crystalline phase. These peaks can be well correlated with the diffraction pattern of the drug. Nevertheless, differences between both spectra can be detected, such as the appearance of an intense peak at $2\theta = 8^{o}$ and a shift left of the majority of the diffraction peaks. This result indicates that sodium clodronate crystals have suffered a dimensional rearrangement during crystallization at the surface of the coating.

VI.3.2. Microhardness tests

Figure 7 shows the microhardness of SEVA-C surface and of the coatings as function of the increasing concentrations of sodium clodronate. For the concentrations of 8 mg/mL and 16 mg/mL it was not possible to obtain consistent results due to the high variability of roughness caused by the sodium clodronate crystal spicules at the surface of the apatite coating (as presented in Figure 3c and d).

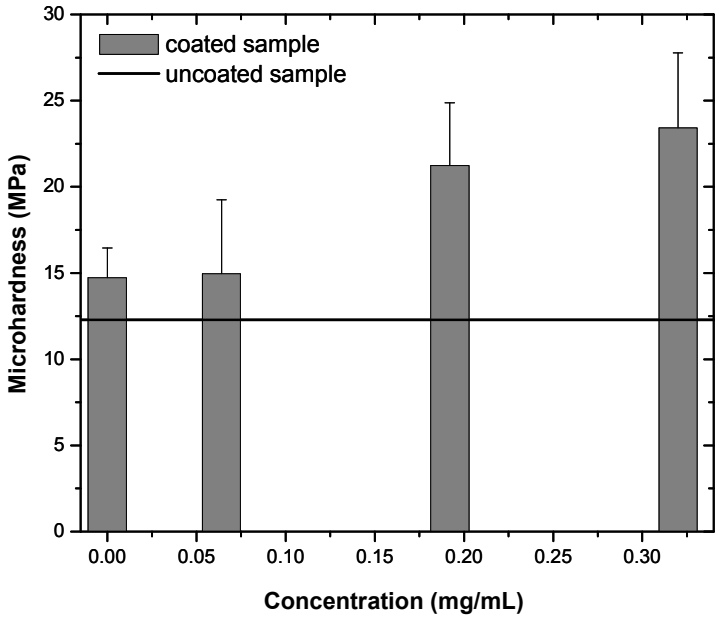


Figure 7. Microhardness of the samples with different concentrations of sodium clodronate in the CaP coatings. The continuous line represents the average corresponding to the microhardness at the level of the bulk substrate (uncoated sample).

After coating SEVA-C samples with the biomimetic apatite layer the microhardness increased from 12 to around 15 MPa. When incorporating sodium clodronate at concentrations from 0.064 to 0.32 mg/mL an increase is observed to values up to 22 MPa. In this way, the microhardness increases significantly with increasing concentration, indicating that the drug will influence the mechanical features of the coating.

VI.3.3. Dissolution of Ca and P

It is important to investigate the solubility of the apatite layers, since they will dictate the release profile of the drug incorporated into it. In Figure 8 are plotted the dissolution profiles of Ca and P from the studied apatite coatings immersed in the different media: a solution buffered to pH 7.4 and another buffered to pH 3. This last solution replicates the worst *in vivo* circumstance resulting from the osteoclasts' activity.

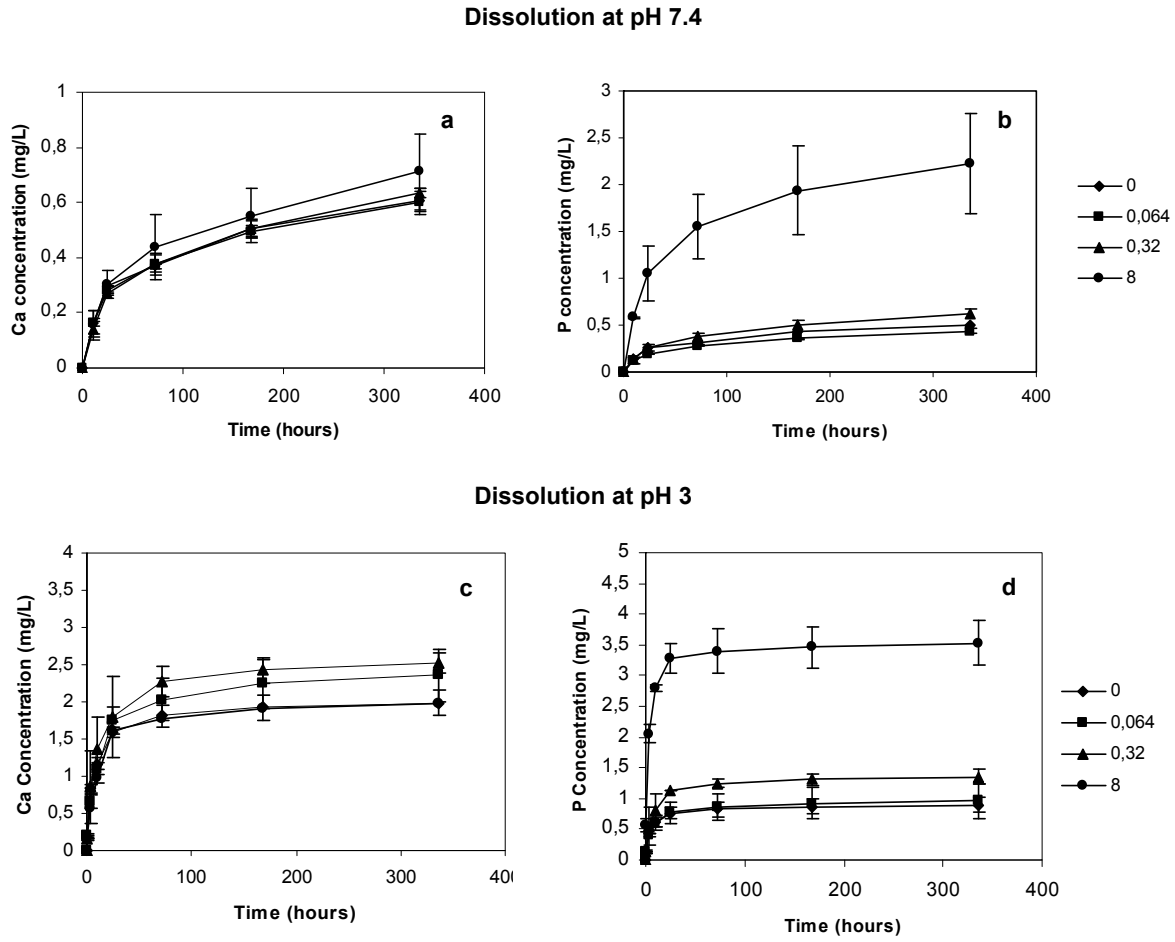


Figure 8. Dissolution profile of Ca and P in a standard solutions buffered at a), b) at pH 7.4 and c),d) at pH 3.

When analysing the dissolution profiles of Ca and P from the apatite coatings, one can observe that for the studied solutions, different dissolution kinetics are observed. The dissolution rates depend heavily on the pH, since Ca-Ps are more soluble in acidic than in neutral conditions [27,54]. As expected, when comparing the two dissolution media, the apatite coatings dissolve at a higher rate when immersed in the acidic solution, at pH 3. Nevertheless the dissolution characteristics of calcium phosphates are governed by a large number of other factors related either with the *in vitro* solution environment or with the properties of the material. Besides the pH, the environmental factors include the type and concentration of the buffered or unbuffered solutions, the degree of saturation, ionic strength, etc.; the material properties include chemical composition, crystallinity, crystal particle size, density, etc [55].

By comparing the dissolution profiles of Ca at pH 7.4 (Figure 8.a), it is possible to observe that the trend of the curves is quite similar, independently of the amount of drug present in the apatite coating. Since the dissolution kinetics was not significantly altered with the presence of the drug, it means that the coating stability was not compromised. When concerning the dissolution profile of P at pH 7.4 (Figure 8.b) this trend is also present, with exception to the case were 8 mg/mL of sodium clodronate was incorporated in the coating. In this case the amount of P detected does not only result from the dissolution of the Ca-P coating, but also from the release of sodium clodronate, that has contributed significantly to the total P measured. The dissolution rate of Ca and P is higher during the first 24 hours. This can be correlated with nature of the apatite coatings. In a dissolution study by Zhang and co-workers [56] using the same Tris-HCl solution it has been clearly demonstrated that at an early stage of the dissolution the process is governed by the morphology, crystallinity and crystal size of the Ca-P layers. Since the apatite coatings are constituted by small crystallites there will be a high surface contact area with the solution (the specific area) that will favour the dissolution process. With time, the dissolution rate decreases and other factors became rather important, as for example, the ionic product of the surrounding medium. The increase of Ca and P in solution will favour some degree of re-precipitation, which can also contribute to the decrease in the dissolution rate.

The dissolution profiles of Ca and P at pH 3 (Figures 8 c. and 8 d.) indicate that after 24 hours the apatite coatings were completely dissolved. Also in this case the dissolution kinetics was not significantly altered with the presence of sodium clodronate, which means that the coating initial stability was preserved. Again, in case of the coatings incorporating 8 mg/mL of sodium clodronate, the released amount of P was higher.

VI.3.4. Sodium clodronate release profiles

The release profiles of sodium clodronate, incorporated at a concentration of 8 mg/mL, in the two studied solutions are plotted in Figure 9. The release profiles at concentrations lower than this value were below the HPLC detection limit.

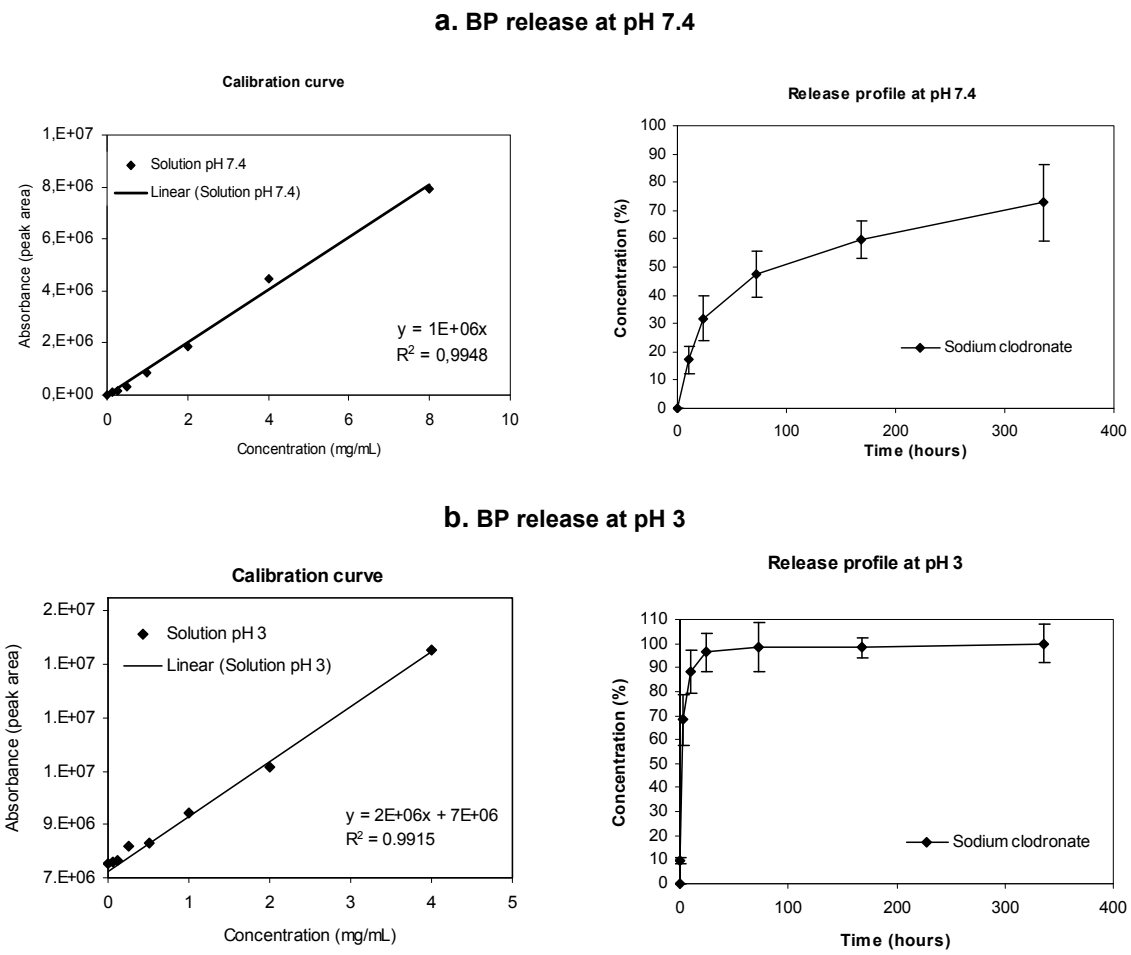


Figure 9. Calibration curves of sodium clodronate and respective release profiles in a) a solution buffered at pH 7.4 and b) a solution buffered at pH 3.

The release profile of sodium clodronate obtained in the solution buffered at pH 7.4 (Figure 9.a and 9.b) follows the same trend of the P release presented in Figure 8.b. Around 30% of the drug is released in the first 24 hours. After 14 days 70 % of the drug was released being the remain incorporated in the structure of the apatite layer, possibly due to a re-precipitation phenomenon [56].

The sodium clodronate release profile at pH 3 (Figure 9.c and 9.d), indicates that the entire drug is released in the first 24 hours of the experiment. Again, this result is consistent with the correspondent dissolution profile of P presented in Figure 8.d. At this

time period all the Ca-P is completely dissolved. The drastic effect of this solution simulates the osteoclastic digestion which, *in vivo* would be characterized by the release of citric acid in the surface of the coating and the formation of the so-called resorption pits [57]. In this extreme situation the stability of the Ca-P is very low, leading to total dissolution. Further *in vitro* osteoclasts studied will help to determine the stability of the apatite coatings in the presence of these cells.

VI.3.5. Preliminary evaluation of the cell adhesion and proliferation

Figure 10 presents SEM micrographs of the morphology of the osteoblasts after 3 days of seeding as function of time and concentration of sodium clodronate. In Figure 11 are plotted the results concerning the ALP activity, protein quantification and cell viability (MTS) for the different times and concentrations of BP studied.

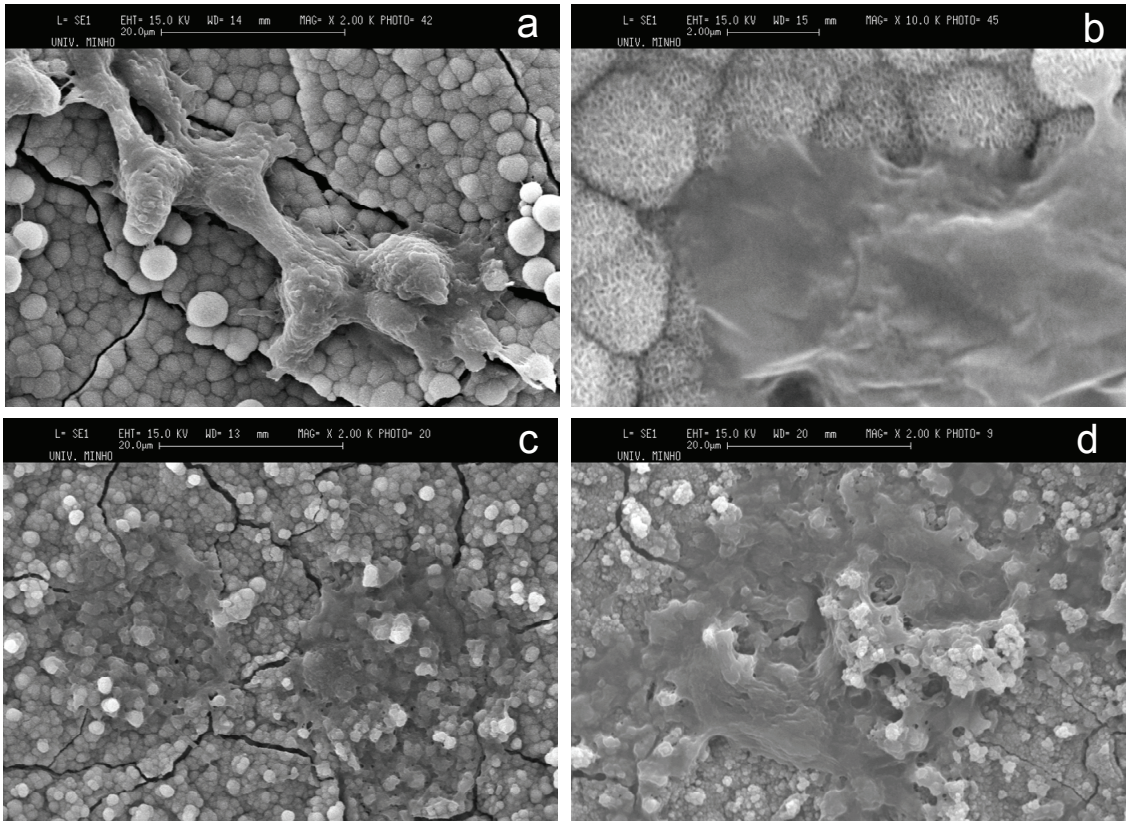


Figure 10. SEM micrographs after 3 days in culture of Osteoblasts Cells (SaOs-2): a), b) SEM micrographs showing the osteoblasts adhesion onto surfaces of apatite coatings material without incorporation of Sodium Clodronate; c), d) SEM micrographs showing the osteoblasts adhesion onto surfaces of apatite coatings material with incorporation of Sodium Clodronate at 0,064 mg/mL and 0,32 mg/mL respectively.

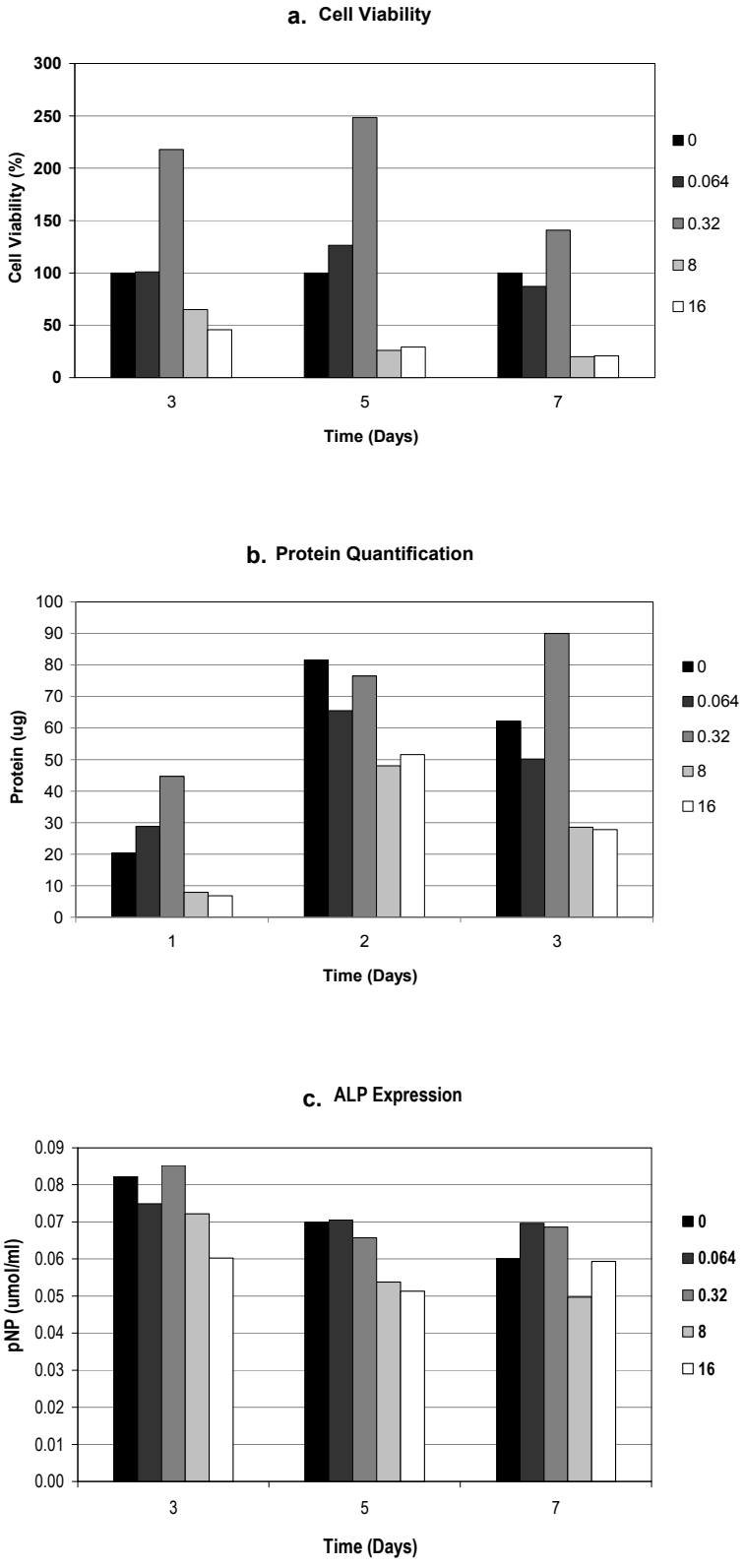


Figure 11. Quantification of the a) cell viability, b) protein quantification and c) ALP expression after different periods of culture on apatite coatings as function of sodium clodronate content.

The incorporation of sodium clodronate on the apatite coating had a significant influence on the adhesion of the cells onto its surface. This can be clearly observed in the example presented in Figure 10 after 3 days of culture, when 0,064 mg/mL and 0,32 mg/mL were present in the apatite coating. With the presence of the BP incorporated in the apatite coating at these doses, the cells presented a more flatten morphology, reflecting higher number of adhesion points to the surface. This behaviour indicates a superior affinity to this type of surface compared with the cells that adhered to the apatite coated surfaces but without the BP. For the higher concentrations of drug used, i.e. 8 and 16 mg/mL a decrease in the cell number was observed and the cells presented a more round morphology (data not shown), indicating that at these levels sodium clodronate induced a toxic behaviour.

Based on the MTS and Protein quantification assays (Figures 11.a and 11.b), bisphosphonate stimulated cellular proliferation and this effect was strongly dependent upon the dose and upon the coating type. The effect of the drug followed a sigmoid curve causing inhibition of cellular activity at the highest dose studied and peaked at 0,32 mg/mL. Along the time, it was also observed a sigmoid curve that peaked at day 5 and decreased at day 7. Although the decrease verified on the two higher concentration was expected, due to its high toxicity, the decrease on the other two could only mean the end of the proliferation period and the start of the osteoblastic activity period. This can be attained because of the diminishing of the protein assessed, also at day 7, and of the increasing of the ALP activity at the same time (Figure 11.c).

VI.4. Discussion

Sodium clodronate could be successfully incorporated, at different doses, in the structure of a biomimetic apatite layer formed by a sodium silicate process. This initial study was aimed at evaluating the effects of this BP i) on the structure and *in vitro* stability of the apatite layers and viability and ii) on the growth and function of a human osteoblast cell line, since there is still little information available on the interaction between BPs and this type of cells. Besides defining the minimum dose to be incorporated in the Ca-P coating, it was also possible to detect a stimulatory effect of the osteoblastic activity when the ideal dose was incorporated.

The properties and composition of the produced biomimetic apatite layers, were tailored in previous studies [15,58] and have dictated the type of interaction with the drug and its loading efficiency. In fact, the choice the adequate Ca-P to be used as carrier for the drug is an important aspect for an effective incorporation. The processing route for obtaining the Ca-P is also a relevant aspect. Although known to be stable under most chemical conditions, bisphosphonates decompose at relatively low temperatures ($<$ 200°C) [59] which makes most coating techniques as for example plasma-spray or sol-gel inapplicable for co-precipitation. In these cases a post-loading methodology has been an adopted solution [60-62], that showed limited success. Due to the more crystalline and dense nature of the apatite coatings the BP could only be incorporated at the outermost surface. Some authors [62,63] have tried to overcome this problem by co-precipitating carbonated apatite layers with the BP over their highly crystalline Ca-P substrates. In a recent study, Peter et al. [63] proposes to co-precipitate Pamidronate with an apatite coating from an SBF solution onto a pre-formed plasma-sprayed coating. The efficiency of this method was however limited. Since plasma sprayed HA presents a highly stable and compact structure the drug was only incorporated in the outer layer of carbonated apatite which was more reactive with the drug. In a study performed by Seshima and co-workers [60] it was demonstrated that the porosity (specific surface area) and crystal size of a Ca-P have a profound influence its solubility and consequently in the ability to incorporate/release the bisphosphonates. Ca-Ps with lower crystal size and higher specific surface area will present a higher solubility as well as a higher ability for incorporating the BP. This effect was also experienced by Josse and co-authors [61] when incorporating the bisphosphonate Zolendronate onto different Ca-P compounds. Using mainly ^{31}P NMR spectroscopy, two different association modes have been observed, according to the nature of the CaP support and/or the initial concentration of the Zoledronate solution. β-tricalcium phosphate (β-TCP) and mixtures of hydroxyapatite and β-TCP appear to promote Zoledronate-containing crystals formation. On the other hand, at low concentrations CDAs (calcium deficient apatites) seem to undergo chemisorption of the drug through a surface adsorption process, due to PO_3 for PO_4 exchange.

In our study we were able to promote the interaction of different amounts of sodium clodronate with a biomimetic apatite layer due to its partially amorphous and nano-crystaline nature. It was possible to detect the presence of this drug by SEM/EDS, TF-XRD and FTIR analysis when incorporated at concentrations of 8 and 16 mg/L. However, for these high concentration levels, the majority of the drug detected resulted from the precipitation of crystal spicules of the drug at the surface of the apatite layer during drying.

Nevertheless, at higher magnifications it is possible to detect a modification of the apatite nanocrystalline structure, indicating that a structural re-arrangement has occurred probably due to a dissolution and re-precipitation phenomena in the presence of the drug [64]. Yet the extent of this modification did not significantly alter the overall structural stability of the apatite coatings, as it can be clearly indicated by the similar dissolution profiles at pHs 7.4 and 3. When 8 mg/mL of BP are incorporated in the apatite coating, after 14 days of release, around 30% of the drug remained in its structure indicating that a chemical interaction is most certainly occurring, since like other bisphosphonates, Sodium Clodronate has a great affinity to Ca ions by forming complexes [25,26,65]. The type of interactions between this drug and apatite layer will be further investigated by NMR studies.

At lower concentrations (0,064 and 0,32 mg/mL) sodium clodronate was not detected by the above mentioned techniques. Nevertheless, it was able to influence the mechanical properties of the coating towards an increase of the microhardness of the surface. It can be extrapolated that the presence of the drug at low amounts will influence the mechanical environment that the cells will feel when in contact with the material together with the new chemical environment. In fact, sodium clodronate incorporated on the apatite have influenced cellular proliferation. This effect was strongly dependent upon the dose incorporated, being 0,32 mg/mL the ideal concentration of BP for enhancing cell viability and osteoblastic profile.

Ganguli and co-workers [66] demonstrated that the synthesis of DNA, protein and collagen was enhanced in osteoblasts when cultured on apatite surfaces coated with Clodronates or Pamidronates, proving to have a potent proliferative effect on osteoblasts. In our study SaOs-2 cells showed a similar response to bisphosphonates in terms of cell proliferation, but a complex response in terms of ALP activity demonstrated by the enhanced alkaline phosphatase activity at 3rd day, and at 7th day of post-treatment with sodium clodronate. SaOs-2 cells are an immortalized cell line, that is, mature cells have a high osteoblastic activity potential even without any treatment. The increased alkaline phosphatase level at the 3rd day is due to the osteoblastic activity (high alkaline phophatase expression) of the existing cells. From the 3rd day until 5th day of culture, proliferative stimuli from bisphosphonates predominated, causing alkaline phosphatase activity to diminish. The increasing of alkaline phosphatase level observed at 7th day may be attributed to maturing osteoblasts from the newly proliferated cells. Since 0,32 mg/mL seems to be the most suitable concentration of biphosphonate for an enhanced cell

viability and osteoblastic profile, it would be expected that this concentration presented a greater alkaline expression. What it could, probably mean, is that this concentration is the one that can more rapidly induce the proliferative profile, which correlates with the fact that the ALP activity at 3rd day was already the lowest, and it's was capable of maintaining this profile for a longer period. By extending the culture period for more days, it would probably be possible to observe a later increase ALP activity. In future studies, this issue will be taken into consideration. This stimulatory effect, together with the potential for inhibiting bone resorption via osteoclasts, without altering the structure of the apatite, can make this approach very effective for improving implant-bone integration and moreover, in applications were regeneration of the tissue is required, as in tissue engineering TE applications. This preliminary results have encouraged further studies, namely to test the osteoclastic activity, that be carried out in the near future. Furthermore, due to the physiological working conditions (T, pH) of this biomimetic methodology new design strategies are presently being considered with the aim of co-precipitate this drug at an early stage of the coating process in order to obtain BP-containing layers for long-term controlled release. It is foreseen that the coatings incorporating there therapeutic agent can for instances be produced on degradable polymeric carriers for the treatment of specific bone diseases regulating the equilibrium on osteoblastic/osteoclastic activity in the direction of a regenerative effect.

VI.5. Conclusions

Sodium clodronate could be successfully incorporated, at different doses, in the structure of a biomimetic apatite layer formed by a sodium silicate process. When incorporated at concentrations of 8 and 16 mg/L its was possible to identify its presence by SEM/EDS, TF-XRD and FTIR analysis. At lower concentrations (0,064 and 0,32 mg/mL) sodium clodronate was not detected by the above mentioned techniques. Nevertheless, it was able to influence the mechanical properties of the coating towards an increase of the microhardness of the surface. It can be extrapolated that the presence of the drug at low amounts will influence the mechanical environment that the cells will feel when in contact with the material together with the new chemical environment. In fact, sodium clodronate incorporated on the apatite have influenced cellular proliferation. This effect was strongly dependent upon the dose incorporated, being 0,32 mg/mL the ideal concentration of BP for enhancing cell viability and osteoblastic profile. This stimulatory effect, together with the potential for inhibiting bone resorption, without altering the structure of the apatite, can

make this approach very effective for improving implant-bone integration and moreover, in applications were regeneration of the tissue is required, as in tissue engineering TE applications.

References

1. Liu Y, De Groot K, Hunziker EB. Osteoinductive implants: The Mise-en-scene for drug-bearing biomimetic coatings. Annals of Biomedical Engineering 2004;32(3):398-406.
2. Oliveira AL, Mano JF, Reis RL. Nature-inspired calcium phosphate coatings: present status and novel advances in the science of mimicry. Current Opinion in Solid State and Materials Science 2003;7(4-5):309-318.
3. Kohn DH. Metals in medical applications. Current Opinion in Solid State & Materials Science 1998;3(3):309-316.
4. Weng J, Liu Q, Wolke JGC, Zhang XD, deGroot K. Formation and characteristics of the apatite layer on plasma-sprayed hydroxyapatite coatings in simulated body fluid. Biomaterials 1997;18(15):1027-1035.
5. Zheng XB, Huang MH, Ding CX. Bond strength of plasma-sprayed hydroxyapatite/Ti composite coatings. Biomaterials 2000;21(8):841-849.
6. Gledhill HC, Turner IG, Doyle C. In vitro dissolution behaviour of two morphologically different thermally sprayed hydroxyapatite coatings. Biomaterials 2001;22(7):695-700.
7. Reis RL, Monteiro FJ. Crystallinity and structural changes in HA plasma-sprayed coatings induced by cyclic loading in physiological media Journal of Materials Science: Materials in Medicine 1996;7:407-411.
8. Leonor IB, Kim HM, Balas F, Kawashita M, Reis RL, Kokubo T, Nakamura T. Functionalization of different polymers with sulfonic groups as a way to coat them with a biomimetic apatite layer. J Mater Sci Mater Med 2007;18(10):1923-30.
9. Tuzlakoglu K, Reis RL. Formation of bone-like apatite layer on chitosan fiber mesh scaffolds by a biomimetic spraying process. J Mater Sci Mater Med 2007;18(7):1279-86.
10. Abe Y, Kokubo T, Yamamuro T. Apatite Coating on Ceramics, Metals and Polymers Utilizing a Biological Process. Journal of Materials Science-Materials in Medicine 1990;1(4):233-238.
11. Kokubo T, Kushitani H, Sakka S, Kitsugi T, Yamamuro T. Solutions able to reproduce in vivo surface-structure changes in bioactive glass-ceramic A-W. J Biomed Mater Res 1990;24(6):721-34.
12. Leonor IB, Azevedo HS, Pashkuleva I, Oliveira AL, Alves CM, Reis RL. Learning From Nature How To Design Biomimetic Calcium-Phosphate Coatings. In: Reis RL, Weiner S, editors. Learning from Nature How to Design New Implantable Biomaterials: From Biomineralization Fundamentals to Biomimetic Materials and Processing Routes. Drodercht: Kluwer Press; 2004. p 123-150.
13. Oliveira AL, Elvira, C., Vásquez, B., San Roman, J., Reis, R. L. Surface Modifications Tailors the Characteristics of Biomimetic Coatings Nucleated on Starch Based Polymers. Journal of Materials Science: Materials in Medicine 1999;10:827.
14. Oliveira AL, Leonor IB, Malafaya PB, Alves CM, Azevedo HS, Reis RL. Tailoring the bioactivity of natural origin inorganic-polymeric based systems. Bioceramics 15 2003;240-2:111-142.
15. Oliveira AL, Malafaya PB, Reis RL. Sodium silicate gel as a precursor for the in vitro nucleation and growth of a bone-like apatite coating in compact and porous polymeric structures. Biomaterials 2003;24(15):2575-2584.
16. Nagano M, Nakamura T, Kokubo T, Tanahashi M, Ogawa M. Differences of bone bonding ability and degradation behaviour in vivo between amorphous calcium phosphate and highly crystalline hydroxyapatite coating. Biomaterials 1996;17(18):1771-1777.
17. Radin S, Campbell JT, Ducheyne P, Cuckler JM. Calcium phosphate ceramic coatings as carriers of vancomycin. Biomaterials 1997;18(11):777-782.
18. Campbell AA, Song L, Li XS, Nelson BJ, Bottoni C, Brooks DE, DeJong ES. Development, characterization, and anti-microbial efficacy of hydroxyapatite-chlorhexidine coatings produced by surface-induced mineralization. J Biomed Mater Res 2000;53(4):400-7.

19. Stigter M, de Groot K, Layrolle P. Incorporation of tobramycin into biomimetic hydroxyapatite coating on titanium. Biomaterials 2002;23(20):4143-4153.
20. Body JJ, Bartl R, Burckhardt P, Delmas PD, Diel IJ, Fleisch H, Kanis JA, Kyle RA, Mundy GR, Paterson AHG and others. Current use of bisphosphonates in oncology. Journal of Clinical Oncology 1998;16(12):3890-3899.
21. Mastrandrea LD, Albini CH. Bisphosphonate treatment of tumor-induced hypercalcemia in a toddler: case report and review of related literature. Endocr Pract 2006;12(6):670-5.
22. Eekhoff ME, Zwinderman AH, Haverkort DM, Cremers SC, Hamdy NA, Papapoulos SE. Determinants of induction and duration of remission of Paget's disease of bone after bisphosphonate (olpadronate) therapy. Bone 2003;33(5):831-8.
23. Rodan GA, Martin TJ. Therapeutic approaches to bone diseases. Science 2000;289(5484):1508-1514.
24. Rodan GA, Fleisch HA. Bisphosphonates: Mechanisms of action. Journal of Clinical Investigation 1996;97(12):2692-2696.
25. Fleisch H. Bisphosphonates: mechanisms of action. Expert Opinion on Therapeutic Patents 2001;11(9):1371-1381.
26. Ezra A, Golomb G. Administration routes and delivery systems of bisphosphonates for the treatment of bone resorption. Adv Drug Deliv Rev 2000;42(3):175-95.
27. Henneman ZJ, Nancollas GH, Ebetino FH, Russell RG, Phipps RJ. Bisphosphonate binding affinity as assessed by inhibition of carbonated apatite dissolution in vitro. J Biomed Mater Res A 2007.
28. Fisher JE, Rodan GA, Reszka AA. In vivo effects of bisphosphonates on the osteoclast mevalonate pathway. Endocrinology 2000;141(12):4793-6.
29. Nishikawa M, Akatsu T, Katayama Y, Yasutomo Y, Kado S, Kugal N, Yamamoto M, Nagata N. Bisphosphonates act on osteoblastic cells and inhibit osteoclast formation in mouse marrow cultures. Bone 1996;18(1):9-14.
30. Adami S, Zamberlan N. Adverse effects of bisphosphonates - A comparative review. Drug Safety 1996;14(3):158-170.
31. Sutton SC, Engle K, Fix JA. Intranasal delivery of the bisphosphonate alendronate in the rat and dog. Pharm Res 1993;10(6):924-6.
32. Duncan AR. The use of subcutaneous pamidronate. J Pain Symptom Manage 2003;26(1):592-3.
33. Osterman T, Lauren L. Level of clodronate in bone after single and repeated subcutaneous injections in rats. Pharmacol Toxicol 1991;69(5):369-71.
34. Walker P, Watanabe S, Lawlor P, Hanson J, Pereira J, Bruera E. Subcutaneous clodronate: a study evaluating efficacy in hypercalcemia of malignancy and local toxicity. Ann Oncol 1997;8(9):915-6.
35. Conte P, Guarneri V. Safety of intravenous and oral bisphosphonates and compliance with dosing regimens. Oncologist 2004;9 Suppl 4:28-37.
36. Venesmaa PK, Kroger HPJ, Miettinen HJA, Jurvelin JS, Suomalainen OT, Alhava EM. Alendronate reduces periprosthetic bone loss after uncemented primary total hip arthroplasty: A prospective randomized study. Journal of Bone and Mineral Research 2001;16(11):2126-2131.
37. Nehme A, Maalouf G, Tricoire JL, Giordano G, Chiron P, Puget J. Effect of alendronate on periprosthetic bone loss after cemented primary total hip arthroplasty: a prospective randomized study. Revue De Chirurgie Orthopedique Et Reparatrice De L Appareil Moteur 2003;89(7):593-598.
38. Yamaguchi K, Masuhara K, Yamasaki S, Nakai T, Fuji T. Cyclic therapy with etidronate has a therapeutic effect against local osteoporosis after cementless total hip arthroplasty. Bone 2003;33(1):144-149.
39. Venesmaa PK, Kroger HPJ, Miettinen HJA, Jurvelin JS, Suomalainen OT, Alhava EM. Monitoring of periprosthetic BMD after uncemented total hip arthroplasty with dual-energy X-ray absorptiometry - a 3-year follow-up study. Journal of Bone and Mineral Research 2001;16(6):1056-1061.
40. Kajiwara H, Yamaza T, Yoshinari M, Goto T, Iyama S, Atsuta I, Kido MA, Tanaka T. The bisphosphonate pamidronate on the surface of titanium stimulates bone formation around tibial implants in rats. Biomaterials 2005;26(6):581-587.
41. Yoshinari M, Oda Y, Inoue T, Matsuzaka K, Shimono M. Bone response to calcium phosphate-coated and bisphosphonate-immobilized titanium implants. Biomaterials 2002;23(14):2879-2885.

42. Peter B, Pioletti DP, Laib S, Bujoli B, Pilet P, Janvier P, Guicheux J, Zambelli PY, Bouler JM, Gauthier O. Calcium phosphate drug delivery system: influence of local zoledronate release on bone implant osteointegration. Bone 2005;36(1):52-60.
43. Reis RL, Cunha AM. Characterization of two biodegradable polymers of potential application within the biomaterials field. Journal of Materials Science-Materials in Medicine 1995;6(12):786-792.
44. Reis RL, Cunha AM, Allan PS, Bevis MJ. Mechanical behavior of injection-molded starch-based polymers. Polymers for Advanced Technologies 1996;7(10):784-790.
45. Sousa RA, Reis RL, Cunha AM, Bevis MJ. Processing and properties of bone-analogue biodegradable and bioinert polymeric composites. Composites Science and Technology 2003;63(3-4):389-402.
46. Reis RL, Mendes SC, Cunha AM, Bevis MJ. Processing and in vitro degradation of starch/EVOH thermoplastic blends. Polymer International 1997;43(4):347-352.
47. Oliveira AL, Malafaya PB, Costa SA, Sousa RA, Reis RL. Micro-computed tomography (mu -CT) as a potential tool to assess the effect of dynamic coating routes on the formation of biomimetic apatite layers on 3D-plotted biodegradable polymeric scaffolds. J Mater Sci Mater Med 2007;18(2):211-223.
48. Plosker GL, Goa KL. Clodronate - a Review of Its Pharmacological Properties and Therapeutic Efficacy in Resorptive Bone-Disease. Drugs 1994;47(6):945-982.
49. Oliveira AL, Santos MI, Pedro AA, Reis RL. Bisphosphonates incorporated on a Ca-P biomimetic coating produced by a sodium silicate based methodology stimulate osteoblastic activity. Bioceramics, Vol 17 2005;17:615-618.
50. Azevedo HS, Gama FM, Reis RL. In vitro assessment of the enzymatic degradation of several starch based biomaterials. Biomacromolecules 2003;4(6):1703-12.
51. Reis RL, Cunha A. M. Characterization of two biodegradable polymers of potential application within the biomaterials field. Journal of Materials Science: Materials in Medicine 1995;6:786-792.
52. Rehman I, Bonfield W. Characterization of hydroxyapatite and carbonated apatite by photo acoustic FTIR spectroscopy. Journal of Materials Science-Materials in Medicine 1997;8(1):1-4.
53. Oliveira AL, Malafaya PB, Reis RL. Sodium silicate gel induced self-mineralization of different compact and porous polymeric structures. Bioceramics 2000;192-1:75-78.
54. Budz JA, Nancollas GH. The Mechanism of Dissolution of Hydroxyapatite and Carbonated Apatite in Acidic Solutions. Journal of Crystal Growth 1988;91(4):490-496.
55. Ducheyne P, Radin S, King L. The Effect Of Calcium-Phosphate Ceramic Composition And Structure On Invitro Behavior .1. Dissolution. Journal Of Biomedical Materials Research 1993;27(1):25-34.
56. Zhang Q, Chen J, Feng J, Cao Y, Deng C, Zhang X. Dissolution and mineralization behaviors of HA coatings. Biomaterials 2003;24(26):4741-4748.
57. Matsuoka H, Nakamura T, Takadama H, Yamada S, Tamura J, Okada Y, Oka M, Kokubo T. Osteoclastic resorption of bone-like apatite formed on a plastic disk as an in vitro assay system. J Biomed Mater Res 1998;42(2):278-85.
58. Oliveira AL, Reis RL. Pre-mineralisation of starch/polycrapolactone bone tissue engineering scaffolds by a calcium-silicate-based process. Journal of Materials Science: Materials in Medicine 2004;15(4):533-540.
59. Ezra A, Golomb G. Administration routes and delivery systems of bisphosphonates for the treatment of bone resorption. Advanced Drug Delivery Reviews 2000;42(3):175-195.
60. Seshima H, Yoshinari M, Takemoto S, Hattori M, Kawada E, Inoue T, Oda Y. Control of bisphosphonate release using hydroxyapatite granules. Journal of Biomedical Materials Research Part B-Applied Biomaterials 2006;78B(2):215-221.
61. Josse S, Faucheux C, Soueidan A, Grimandi G, Massiot D, Alonso B, Janvier P, Laib S, Pilet P, Gauthier O. Novel biomaterials for bisphosphonate delivery. Biomaterials 2005;26(14):2073.
62. Yoshinari M, Oda Y, Ueki H, Yokose S. Immobilization of bisphosphonates on surface modified titanium. Biomaterials 2001;22(7):709-715.
63. Peter B, Gauthier O, Laib S, Bujoli B, Guicheux J, Janvier P, van Lenthe GH, Muller R, Zambelli PY, Bouler JM and others. Local delivery of bisphosphonate from coated orthopedic implants increases implants mechanical stability in osteoporotic rats. Journal of Biomedical Materials Research Part A 2006;76A(1):133-143.

64. Zhang QY, Chen JY, Feng JM, Cao Y, Deng CL, Zhang XD. Dissolution and mineralization behaviors of HA coatings. Biomaterials 2003;24(26):4741-4748.
65. Kontturi M, Peraniemi S, Vepsalainen JJ, Ahlgren M. X-ray diffraction study of bisphosphonate metal complexes: Mg and Ca complexes of (dichloromethylene)bisphosphonic acid P,P'-diisopropyl ester. Polyhedron 2005;24(2):305.
66. Ganguli A, Henderson C, Grant MH, Meikle ST, Lloyd AW, Goldie I. The interactions of bisphosphonates in solution and as coatings on hydroxyapatite with osteoblasts. Journal of Materials Science-Materials in Medicine 2002;13(10):923-931.

SECTION 4

CHAPTER VII

Chapter VII

Strontium-Substituted Apatite Coating on Ti6Al4V Through Biomimetic Synthesis

Abstract

During the last few years Strontium has been shown to have beneficial effects when incorporated at certain doses in bone by stimulating bone formation. It is believed that its presence locally at the interface between an implant and bone will enhance osteointegration and therefore, ensure the longevity of a joint prosthesis. In this study we explore the possibility of incorporating Sr into nano-apatite coatings prepared by a solution-derived process according to an established biomimetic methodology for coating titanium based implants. The way this element is incorporated in the apatite structure and its effects on the stereochemistry and morphology of the resulting apatite layers was investigated, as well as its effect in the mineralization kinetics.

By using the present methodology it was possible to incorporate increasing amounts of Sr in the apatite layers. Sr was found to incorporate in the apatite lattice through a substitution mechanism by replacing Ca in the apatite lattice. The presence of Sr in solution induced an inhibitory effect on mineralization, leading to a decrease in the thickness of the mineral layers. The obtained Sr-substituted biomimetic coatings presented a bone-like structure similar to the one found in the human bone and therefore, are expected to enhance bone formation and osteointegration.

*This part of the chapter is based on the following publication:

A. L. Oliveira, R. L. Reis, P. Li, “Strontium-Substituted Apatite Coating Grown on Ti6Al4V substrate through Biomimetic Synthesis”, Journal of Biomedical Materials Research. Part B: Applied Biomaterials, *in press.*

VII.1. Introduction

Skeletal metabolism of strontium (Sr) has been the subject of extensive study over the past several years. Because of its chemical and physical similarity to calcium, strontium is a natural bone-seeking trace element that accumulates in the skeleton [1]. There is growing evidence that strontium influences bone remodeling by affecting both bone resorption and bone formation [2].

Several studies [3-5] indicate that strontium can affect the activity of cells *in vitro,* acting directly on osteoclasts to inhibit bone resorption. The presence of this trace element on the surface of bone at a level higher than that required for normal cell physiology, can be effective in blocking osteoclastic bone resorption without apparent cytotoxic effect on osteoblasts [4]. Consistent with the *in vitro* data, available *in vivo* studies indicate that Strontium has a metabolic effect on bone [5-9]. Positive effects were observed in different animal models namely those with predominant bone remodeling, like monkeys [10]. The presence of Sr can enhance endosteal and trabecular bone formation without affecting bone mineralization and reducing bone resorption. These effects can directly influence the mechanical properties of bone, increasing the bone strength, while maintaining the bone physiological balance. These *in vivo* studies support the concept that Strontium administration at a correctly defined dose can act on bone resorption, increasing bone formation, and reducing bone loss in animal models of osteopenia, suggesting that controlled doses of strontium may have potential benefits in the treatment of osteopenic disorders, like osteoporosis [8,11]. In dental enamel, strontium was also found to stabilize the apatitic structure and induce higher resistance to degradation by bacterial acids [12,13].

In the recent years human clinical trials have been conducted using a specific molecule, strontium ranelate, composed of an organic moiety which binds two stable strontium atoms for increasing strontium bioavailability. Low doses of strontium ranelate, when orally supplemented, were reported to increase vertebral bone calcification in osteoporotic patients [12,14-16]. Important pharmacological and clinical data have clearly demonstrated that the presence of this Sr-based drug reduces the risk of vertebral [17,18] and non-vertebral fractures [19] in postmenopausal women with good tolerability in patients.

When orally supplemented, Sr can be retained in bone at a certain extent. A study in monkeys by Boivin *et al.* [10] reported that when large doses of Sr were supplemented

over a long period of time the calcium to strontium ratio reached a maximum of 10:1. This means that, low doses of Sr are required to elicit positive effects. In newly formed bone, Sr atoms are incorporated into the crystal by ionic substitution for calcium [9]. Newly formed apatite crystals are more reactive and incorporate more Sr ions than the larger crystals, which grow more slowly. Complex effects of strontium on apatite crystals have been reported [1,11], such as a decrease in the apatite carbonate content and in crystal length. However, crystals containing strontium have demonstrated to be more stable and show more regular shapes [1,11]. In this sense, strontium may also indirectly inhibit the resorption of the calcified matrix by stabilizing hydroxyapatite crystals.

When considering load-bearing cementless metallic implants, biological fixation is crucial for ensuring its long-term viability. Because of this osteoconductivity, hydroxyapatite (HA) ceramic has been used as a coating in joint reconstruction devices such as hip stems and acetabular cups. These coatings, commonly produced using a plasma spraying technique [20,21], have demonstrated direct bone apposition [22]. However, concerns about delamination of the plasma-sprayed HA coating and the potential for generating ceramic particles have discouraged its widespread acceptance. This fact has motivated a continuous search for effective ways of producing calcium phosphates more similar to those formed by the natural processes of bone mineralization, driving the attention over the last years to biomimetic methodologies [23-27]. When coated with a layer similar to the natural mineral of bone, an orthopaedic implant besides exhibiting adequate mechanical properties to be used as bone replacement can also conduct bone formation and thereby, firmly integrate to bone. Following this idea, a solution-derived process was designed to produce a nano-apatite coating with a composition and structure equivalent to bone mineral. This coating is achieved by the immersion of titanium substrates in an aqueous solution comprising all major inorganic components present in the body, mainly, HCO_3^-, Ca^{2+}, HPO_4^{2-} and Mg^{2+} ions [28]. The resulting apatite layers have demonstrated by *in vivo* studies to be capable of inducing bone formation and promoting direct bone apposition [28]. Moreover, due to the physiologically related conditions for the formation of these coatings (in a solution with temperature, pH and inorganic composition close to human blood plasma) they present a high carrier potential at the surface of an implant, since in this environment the biomolecules with therapeutic relevance can preserve their activity. The loading options are therefore numerous, going from protein growth factors [29-31] to different therapeutic agents [32] used in the treatment of bone related diseases.

Considering the beneficial effects of the presence of Sr in bone, reported in literature over the last years and herein shortly summarized, it is believed that its presence locally at the

interface between the implant and bone via a calcium phosphate coating will stimulate bone formation, enhance osteointegration, and therefore ensure the longevity of a cementless implant. In this study we evaluated the possibility of incorporating different amounts of Sr onto the nano-apatite layers during the coating process. The effect on the coating properties like the morphology, chemistry and crystallinity was then evaluated.

VII.2. Materials and Methods

VII.2.1. Materials

Titanium alloys are currently used in the manufacturing of joint implants. Twelve Ti-6A1-4V disks with a 16 mm in diameter and 2 mm in thickness were polished to have a reflective mirror-like finish, and another twelve disks were grit blasted using 20-μm alumina particles, per coating condition. A total of 48 polished and 48 grit blasted samples were used in the study. The distribution of the samples was as following: 3 samples per assay (all 3 used for TF-XRD followed by DR-FTIR and finally 2 for SEM) x 4 [Sr] x 4 time periods in solution: 24 and 50 hours, 4 and 7 days. In this paper we are reporting the results concerning the obtained coating after 7 days of coating. The specimens were ultrasonically cleaned first in a detergent solution, then in acetone, ethanol and finally in de-ionized water and then dried at 60 ºC.

VII.2.2. Apatite coating formation

A biomimetic nano-crystalline apatite coating was grown on the titanium specimens according to a procedure which was adapted from a previously developed process described by Li *et al* [28,33]. An aqueous solution was prepared comprising all major inorganic ions present in the body, based in a simulated body fluid solution (SBF) initially proposed by Kokubo *et al.* [27]. $CaCl_2$, NaCl, KCl, K_2HPO_4, $MgCl_2$, $NaSO_4$, and $NaHCO_3$ were dissolved in de-ionized H_2O and the pH adjusted to neutral using tris(hydroxymethyl)aminomethane-hydrochloric acid. The solution was buffered at time 0. The concentrations of NaCl, KCl, $NaHCO_3$, $MgCl_2$ and $NaSO_4$ were designed to correspond to the nominal levels of human blood plasma, whereas the concentrations of Ca^{2+} and HPO_4^{2-} were 5.0 and 2.4 mM, respectively. Three other solutions were prepared based on the same procedure with the supplement of 0.5, 1.0 and 1.5 mM $SrCl_2$ that results in the atomic ratio of Ca to Sr in solution of 10:1, 5:1 and 10:3, respectively.[34]. The lowest concentration of Sr is in the therapeutic range, when compared to the values

found in human blood plasma in a study carried out in patients receiving a daily strontium supplement [12]. Concerning the ideal concentration of Sr in bone a consensus has not been reached. In the literature several studies report different amounts of strontium found in bone [1,6,12,35-38] which, however, cannot be directly compared, since they are referred to either different animal models or human subjects and different Sr therapies. Nevertheless in a review by Dahl and co-workers [9] 10:1 indicated as the theoretical maximum of the Ca to Sr ratio in bone, based on studies by Boivin *et al*. [10]. The as-prepared solutions were loaded in a 2L double-jacketed glass reactor and the temperature was kept constant at 45 ºC using a water circulating controller. The samples were fixed in tailor-made Teflon holders and placed in the reactors standing vertically in order for the surfaces to be coated. Such arrangement ensures that the coating formed on the surface of Ti disks will not result from sedimentation of precipitates in the solution. Figure 1 illustrates schematically the process. The disks were removed from solution after 7 days and cleaned with de-ionized water.

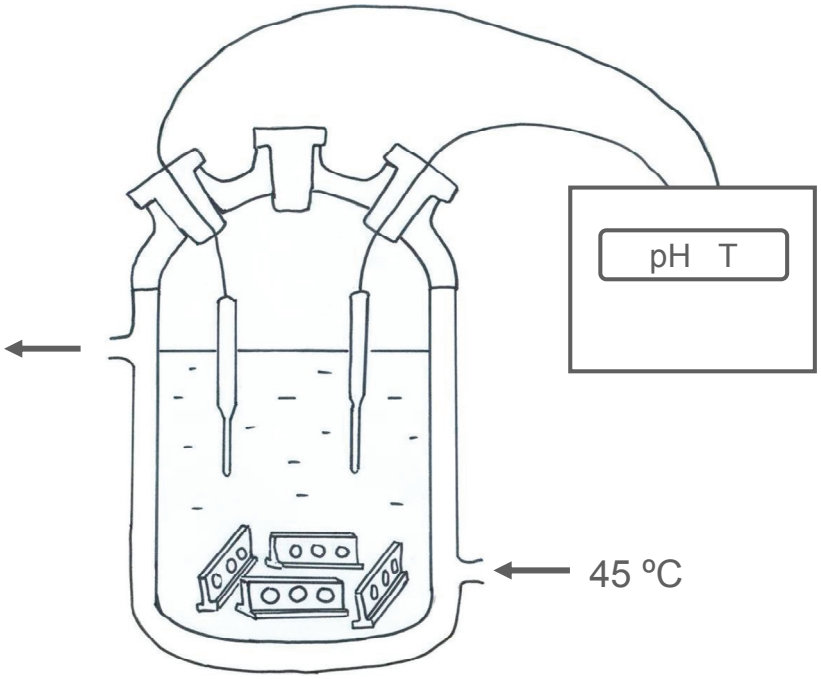


Figure 1. Schematic drawing of the coating experiments in double-jacked glass reactors.

VII.2.3. Solution analysis

During the entire process the pH and temperature of the solutions were monitored (recorded every 10 minutes) by a pH/ion meter (pH/ion Meter 692, Metrohm, Switzerland). The change of Ca, P and Sr concentrations in the coating solutions was followed by means of removing aliquots of 5 mL of solution every 10 to 12 hours. Atomic Absorption Spectroscopy (AA800, Perkin-Elmer, Norwalk, CT) was used to quantify the amount of the Ca and Sr present. To eliminate the interference of phosphate in the measurement of calcium and strontium, 0.1 mL of the sample solution was diluted in 5 mL of 0,625 %wt of $LaCl_3$ that acts as a release agent. The P concentration was analyzed by the "molybdenum blue" method [39] using a UV-light spectrophotometer (Genesys 2, Spectronic Instruments). For both methods, for each time point 3 repetitions *per* 5 replicates were analyzed, and the average values calculated.

VII.2.4. Characterization of the apatite coatings

The formed apatite coatings were analyzed using Diffuse Reflectance Fourier Transform Infra-Red spectroscopy (DR-FTIR, Magna-IR 550, Nicolet, Madison, WI), Thin-Film X-Ray Diffractometry (TF-XRD, X'Pert PW3040, Philips, The Netherlands), and Scanning Electron Microscopy (SEM, S-3500N, Hitashi, Japan) linked with Energy-Dispersive Spectroscopy (EDS). Two samples were used for each assay. To perform the SEM analysis all the samples were coated with a thin film of carbon, by ion sputtering, prior to any observation. The cross-sections of the coatings were also observed by SEM and its thickness calculated from the average of measurements performed in 5 equidistant points (5 μm) along the cross-sections.

VII.3. Results

VII.3.1. Apatite formation: the solution side

The evolution of the Ca, P and Sr composition in solution is presented in Figure 2.

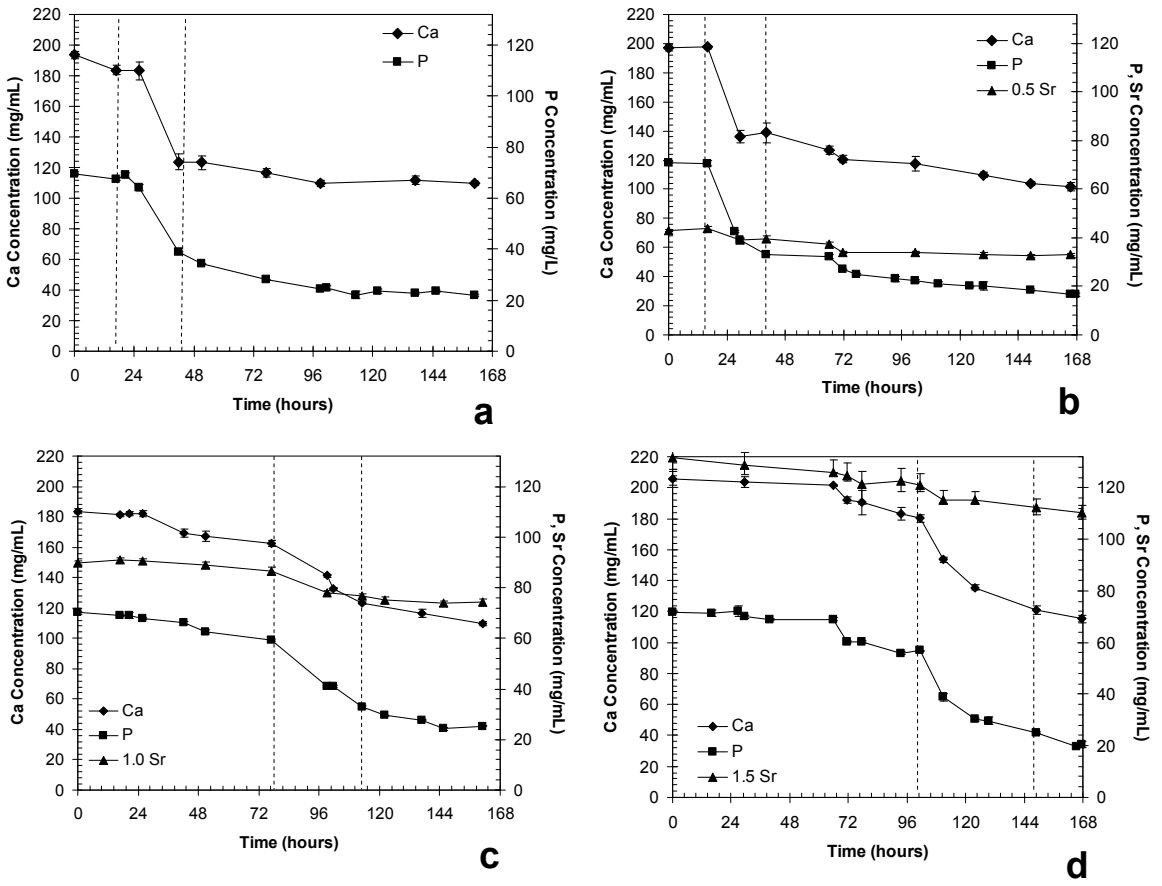


Figure 2. Evolution of Ca, P and Sr composition of the different solutions during the coating process: a) solution in the absence of Sr and with b) 0.5 , c) 1.0 and d) 1.5 mg/mL of Sr.

When comparing the presented curves for each different solution, a concurrent drop in the concentration of Ca, P and Sr is observed, indicating that these ions are being consumed from solution while the apatite coating is being formed. The solution without supplement of $SrCl_2$ (Figure 2.a), shows a drop in the concentration of Ca from approximately 200 to 123 mg/L and the P concentration from approximately 70 to 40 mg/mL between the first 24 and 48 hours. When 0.5 mM of Sr is added to the solution (Figure 2.b) the change of Ca and P concentrations is not considerably altered, suggesting that this amount of Sr does not affect significantly the driving forces for apatite formation. However, when Sr is raised to 1.0 (Figure 2.c) and 1.5 mM (Figure 2.d) the Ca and P drop is delayed to approximately 77 and 90 hours respectively. A retarding effect of Sr is, therefore, observed at these concentrations. This indicates an inhibitory effect of Sr. At the same time the concentration of this element in solution follows the same trend as of Ca and P concentration (Figures 2a, b and c). This result indicates that the Sr ions can be incorporated in the structure of the apatite, possibly by competing with Ca ions for its substitution.

VII.3.2. Apatite formation: the coating side

Figure 3 presents the morphologies of the apatite coatings formed after 7 days in the solution without Sr and with increasing concentrations of this element. The coating shows similar morphologies when formed on polished surfaces as compared with the coating on grit-blasted samples. Therefore, these micrographs concern the polished samples, being representative of the obtained morphologies for both cases.

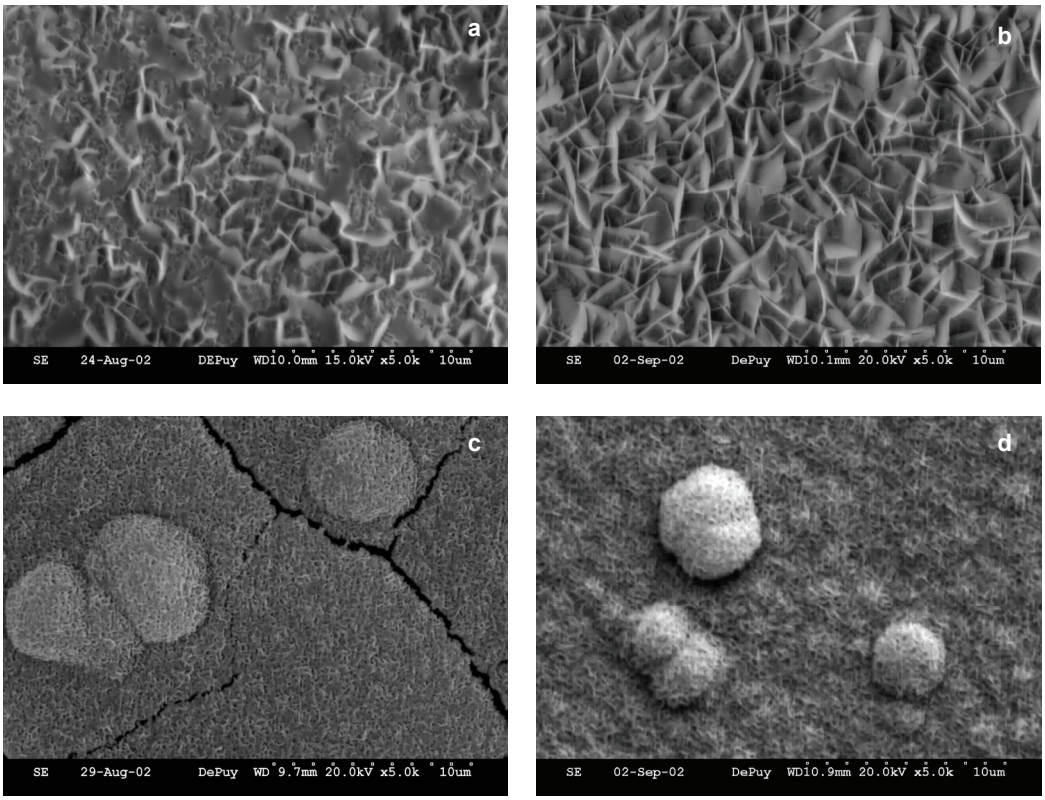


Figure 3. Morphologies of the apatite coatings formed after 7 days in the solutions containing: a) 0, b) 0.5, c) 1.0 and d) 1.5 mM of Sr, concerning a polished sample.

After immersion in solution without the presence of Sr (Figure 3.a), it was possible to observe a uniform coating on the surface of the samples, exhibiting a needle-like structure. When adding 0.5 mM of Sr to the solution the structure of crystals presented a more regular shape (Figure 3.b). These morphologies are typically found when octacalcium phosphate is present [40]. When the amount of Sr in solution rises to 1.0 and 1.5 mM (Figures 3.c and 3.d respectively) a remarkable change in the morphology is observed. The apatite crystals decrease from an approximate size of $\cong$ 2.5 μm to the sub-micron level. This result indicates that the presence of Sr inhibits the apatite crystals from growing, leading to the formation of a nano-apatite structure. Figure 4 presents SEM micrographs of the apatite layers' cross-sections after 7 days, for polished and grit-blasted

samples as function of the amount of Sr in solution. The correspondent thickness evolution is plotted in Figure 5.

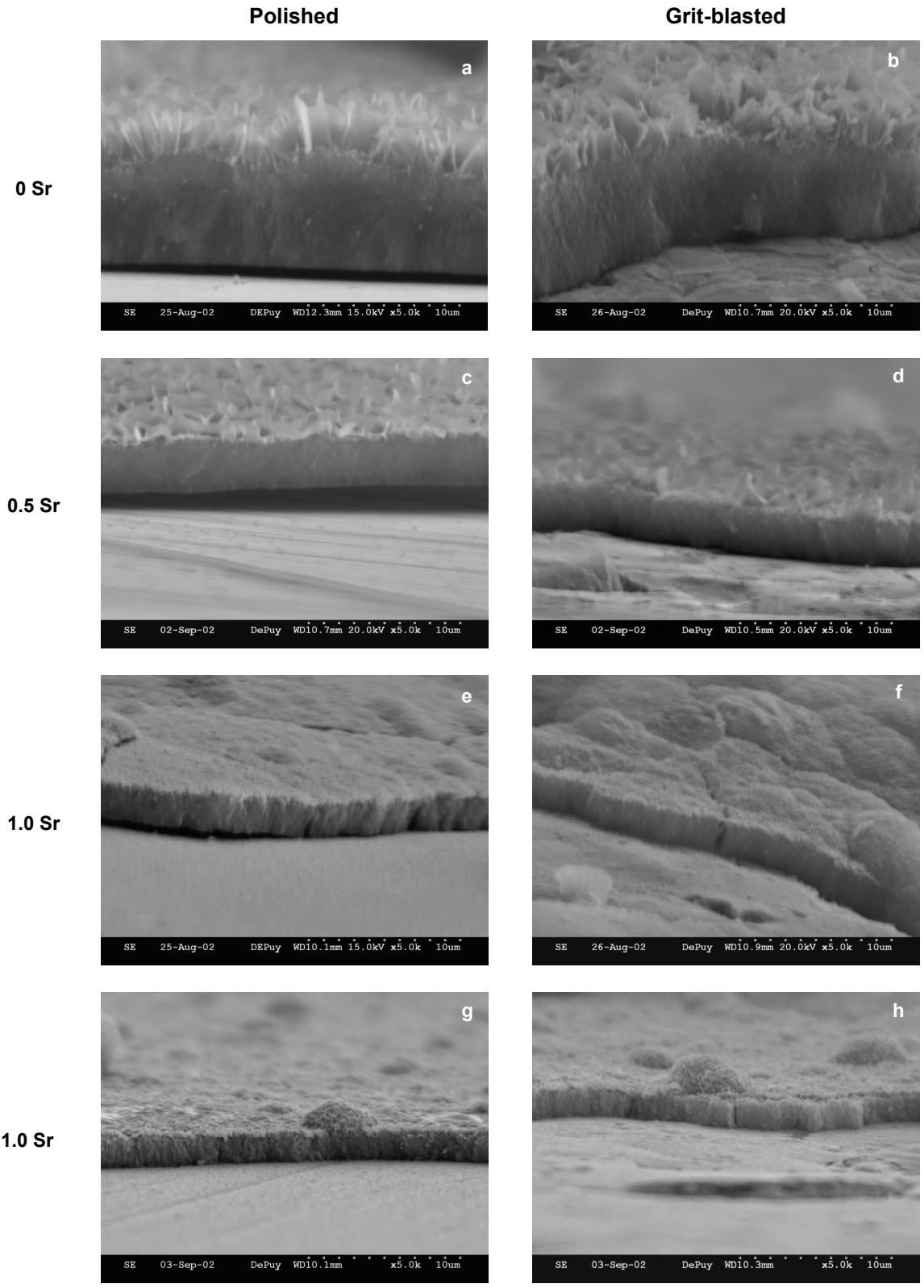


Figure 4. Morphology and thickness of the apatite layers formed on polished (a,c,e,g) and grit-blasted (b,d,f,h) surfaces after 7 days in SBF containing increasing amounts of Sr in solution: 0 mM (a, b), 0.5 mM (c, d), 1.0 mM (e, f), 1.5 mM (g, h).

When comparing the apatite layers formed on the two types of surfaces studied, it is possible to observe that neither the morphology nor the thickness were influenced by the roughness of the Ti substrates (Figures 4. a,c,e,g and 4 b,d,f,h). However, an increase in substrate roughness have improved adhesion of apatite coating to substrate due to a better mechanical interlocking with the apatite layer [25]. When adding only 0.5 M Sr to the solution, a marked decrease in the thickness of the coating is observed.

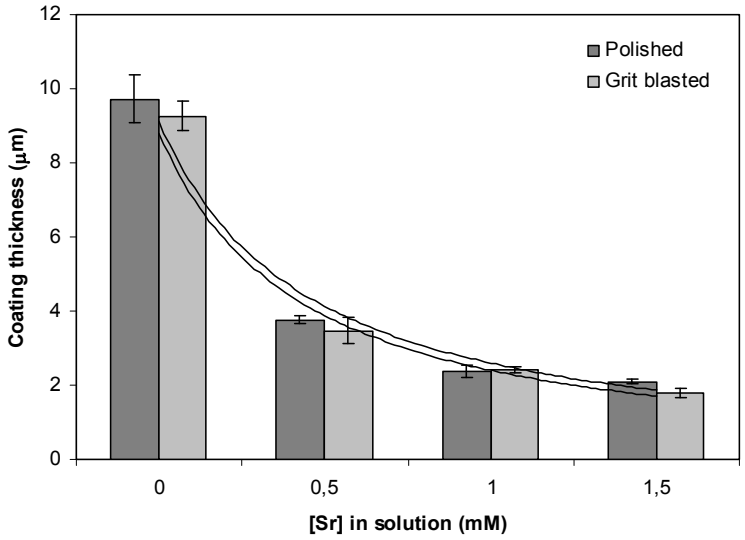


Figure 5. Average thickness of the apatite layers formed in solutions containing increasing amounts of Sr.

Figure 6 shows a typical EDS spectrum obtained after 7 days for the coating produced in a solution containing 1mM of Sr, where it is possible to identify the presence of this element. This spectrum is representative of the profiles obtained after Sr was incorporated at the different doses. After the coating process, the samples were washed in de-ionized water to remove a residue of coating source solution. The absence of Na or Cl indicates that the surface is clean. The Sr detected on the surface is the element that is chemically incorporated in the apatite structure. Sr was identified even when a lower amount of Sr (0.5 mM) was added to solution. Trace amounts of Mg were also detected together with Sr. In fact the affinity of this ion for the apatite structure increased with the presence of Sr. Titanium and Aluminum are also detected from the substrate, which is composed of a commercially available Ti alloy (Ti6Al4V).

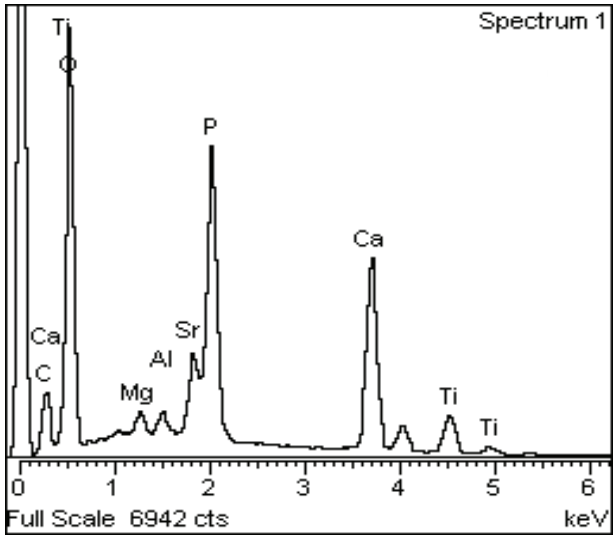


Figure 6. Typical EDS spectra obtained for the formed Sr-apatite layers after 7 days of the coating process.

Figure 7 presents the most important region of the DR-FTIR spectra of the apatite coatings produced in the various solutions.

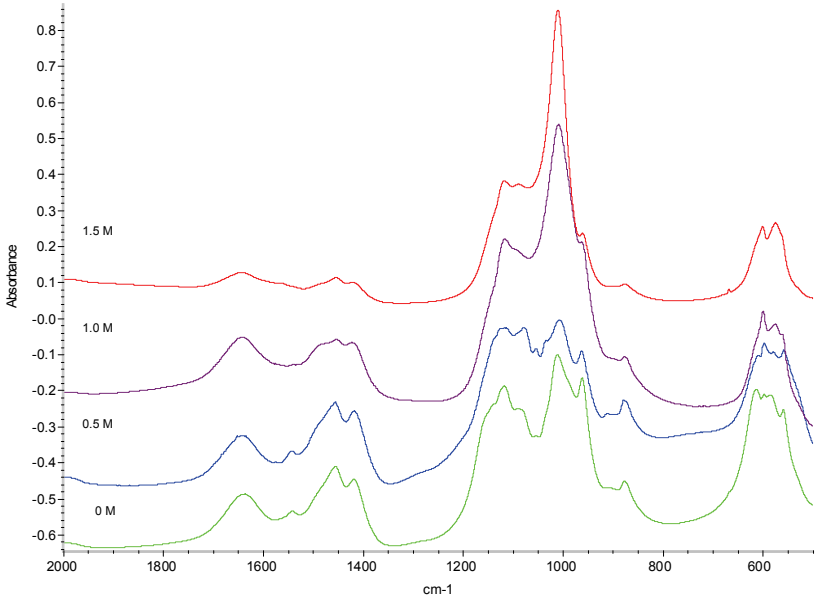


Figure 7. DR-FTIR of the apatite coatings formed in the solutions containing increasing concentrations of Sr.

The bands detected at 1636 cm^{-1} are assigned to water molecules in the apatite structure. Another broad band assigned to water was also detected in the region of 3200 cm^{-1} (data not shown). In fact, apatite contains water incorporated in its structure, either chemically bonded, i.e. structural water or also adsorbed due to its hydroscopic character [41]. The bands at 870, 1410 and 1446 cm^{-1} result from the presence of carbonate (CO_3^{2-}) incorporated in the apatite lattice [41,42]. The presence of these bands clearly indicates

that a carbonated apatite was formed, as it is found in bone apatite. The bands at 602 and 578 are assigned to the ν_4 bending mode of the O-P-O bonds in the apatite. The bands at 1072 and 1112 cm^{-1} indicate the ν_3 stretching mode of P-O bonds [41].

Figure 8 presents the TF-XRD spectra of the apatite coatings with increasing Sr content. Figure 9 presents in detail the region of the (002) plane.

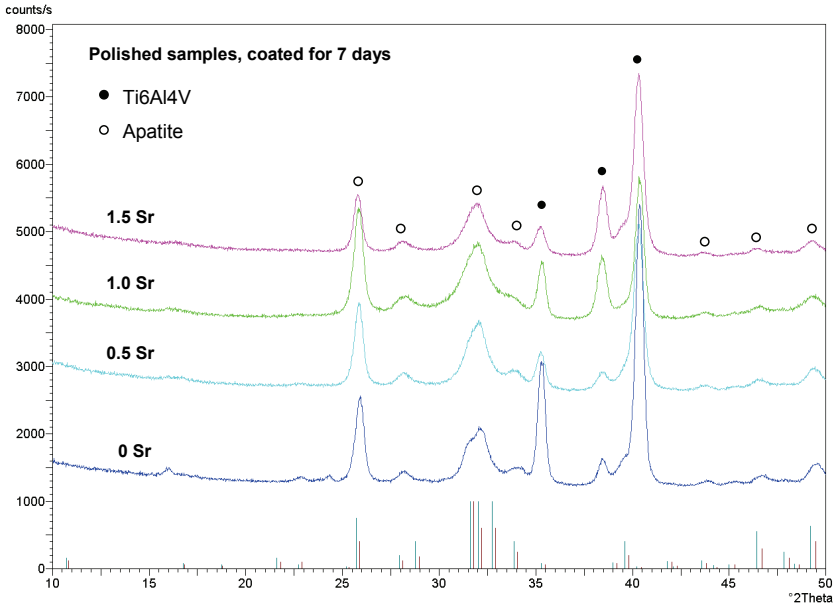


Figure 8. TF-XRD of the apatite coatings formed in the solutions containing increasing concentrations of Sr.

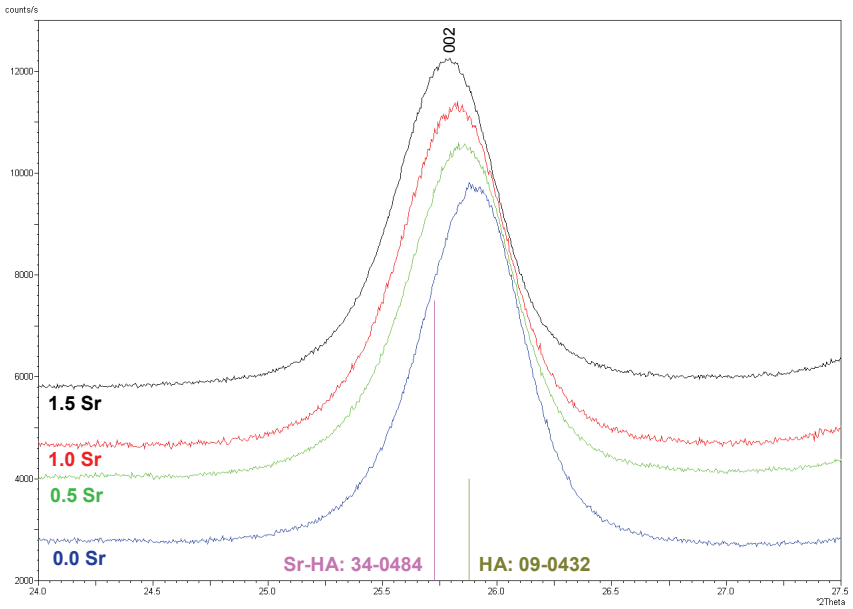


Figure 9. Detail of the XRD peaks assigned to the (002) lattice plane indicating a shift to the left on coatings formed in solutions with increasing Sr.

By TF-XRD (Figure 8) it was possible to identify the main characteristic peaks attributed to HA. The peak at $2\theta = 26^{\circ}$ is assigned to (002) plane in the lattice of apatite crystal. The strong diffraction intensity of this peak suggests a preferential orientation of the crystals. Another important diffraction peak is detected around $2\theta = 32^{\circ}$ and is related to the overlapping of planes (211), (112) and (300). This broad peak indicates that the apatite is poorly crystalline. When comparing in detail the apatite peaks it is possible to note a shift to the left that is progressive as function of the amount of Sr in the coating solution. An example of this shift is found in Figure 9, in a detailed analysis of the region correspondent to the (002) plane. This shift is a close match to the reference pattern for composition $(Ca)_9Sr(PO4)_6(HO)_2$, indicating that Ca is being replaced by Sr during the coating process.

VII.4. Discussion

The process of apatite formation in the herein studied solution is a complex phenomenon [28]. It involves a number of reactions concerning the association/dissociation of the various ions and ion groups in solution, which will be affected by interactions with the titanium substrate and with the environment to which the solution is exposed. During apatite coating formation, a concurrent drop in the concentrations of Ca, P and Sr (when present) in solution is detected, together with a drop of the solutions' pH (data not shown). This phenomenon has been studied and reported in a previous work [28]. In brief, at the initial stage of the coating processes the pH of the solution increases due to the release of CO_2 from the dissociation of HCO_3^- ions, resulting in the generation of hydroxyl ions. This is a rather well known phenomena studied by several authors [28,43,44] when using comparable supersaturated solutions. However, at a certain time point a pH drop is observed which is coincident with a drop in the Ca and P composition. The pH drop results from the dissociation of HPO_4^{2-} and $H_2PO_4^-$ ionic groups into PO_4^{3-} which will then bond to Ca^{2+} to the form the apatite coating.

When Sr is present in higher amounts in solution the Ca and P drop is delayed (as well as the correspondent pH drop), indicating delay in the coating formation due to an inhibitory effect of this ion. This effect was reflected in the resulting apatite layers' morphology. A decrease in the crystal size was observed when adding increasing amounts of Sr to the solution, indicating that its presence inhibits the growing of the apatite crystals, increasing the nano-character of the apatite structure. This result suggests that Sr can have an inhibitory effect similar to the well-known effect of Mg, as reported by several authors [40,45,46]. A pronounced inhibitory effect is observed when only 0.5 mM Sr is added to

the solution, resulting in a marked decrease in the thickness of the apatite layer. When increasing the Sr content the thickness continues to decrease, however not in such a prominent way. Therefore, it can be said that increasing [Sr] in solution has a negligible effect on the coating thickness.

When comparing the FTIR spectra, the intensity of the band at 1072 cm^{-1} (ν_3 stretching mode of P-O bonds) increases in case of the coatings formed in solutions containing 1.0 and 1.5 mM of Sr. This type of profile was also observed in the case of apatite coatings formed in the absence of Sr in the first days of the coating process (data not shown). The higher intensity of this band might be related to the thickness of the coating or to its overall composition. In fact, absorbance is related to the quantity of function group determined by the coating thickness. On the other hand, since the solution is not replenished during the 7 days of the experiment, the degree of solution supersaturation decreases over time, which might be affecting the composition of the apatite over time of immersion. Nevertheless, FTIR analysis neither reveals a significant shift of PO_4 bands nor demonstrates addition of any other bands, indicating that these possible compositional changes are not significant.

Although FTIR analysis did not reveal any significant difference between the spectra of the Sr-free and Sr-containing apatite coatings, by TF-XRD analysis a progressive shift of the main apatite peaks was observed towards the typical composition of Sr substituted apatite. Sr atoms, although having a higher ionic radii than Ca are able to replace them, which will lead to a distortion in the crystal lattice and consequently to a deviation of the diffraction planes. These results qualitatively associate with the observations made of the solutions evolution during the process. The mechanism by which Sr is being incorporated in the apatite structure is, therefore, by the substitution of Sr for Ca. Further studies, however, are required in order to determine the exact composition of these new biomimetic strontium-substituted apatite coatings.

VII.5. Conclusions

In this study it was possible to incorporate different amounts of Sr into the structure of the apatite layer by adding $SrCl_2$ in biomimetic apatite coating source solution. Sr ions are extracted from the solution to substitute for Ca in apatite coating during its formation, leading to the formation of a Sr-substituted apatite coating. The presence of Sr ions in solution could inhibit the coating formation and results in the decrease of coating thickness. The formed Sr-containing biomimetic coatings presented a bone-like structure

similar to the one found in the human bone. This new Sr-apatite coatings are expected to have a positive effect in enhancing bone formation and therefore to contributing to better osteointegration.

References

1. Grynpas MD, Marie PJ. Effects of Low-Doses of Strontium on Bone Quality and Quantity in Rats. Bone 1990;11(5):313-319.
2. Marie PJ, Ammann P, Boivin G, Rey C. Mechanisms of action and therapeutic potential of strontium in bone. Calcified Tissue International 2001;69(3):121-129.
3. Canalis E, Hott M, Deloffre P, Tsouderos Y, Marie PJ. The divalent strontium salt S12911 enhances bone cell replication and bone formation in vitro. Bone 1996;18(6):517-523.
4. Su Y, Bonnet J, Deloffre P, Tsouderos Y, Baron R. The Strontium Salt-S12911 Inhibits the Expression of Carbonic-Anhydrase and the Vitronectin Receptor in Chicken Bone-Marrow Cultures and Bone-Resorption in Mouse Calvaria and Isolated Rat Osteoclasts. Journal of Bone and Mineral Research 1992;7:S306-S306.
5. Marie PJ. Strontium as therapy for osteoporosis. Curr Opin Pharmacol 2005;5(6):633-6.
6. Marie PJ, Garba MT, Hott M, Miravet L. Effect of Low-Doses of Stable Strontium on Bone Metabolism in Rats. Mineral and Electrolyte Metabolism 1985;11(1):5-13.
7. Marie PJ, Hott M. Short-Term Effects of Fluoride and Strontium on Bone-Formation and Resorption in the Mouse. Metabolism-Clinical and Experimental 1986;35(6):547-551.
8. Buehler J, Chappuis P, Saffar JL, Tsouderos Y, Vignery A. Strontium ranelate inhibits bone resorption while maintaining bone formation in alveolar bone in monkeys (Macaca fascicularis). Bone 2001;29(2):176-179.
9. Dahl SG, Allain P, Marie PJ, Mauras Y, Boivin G, Ammann P, Tsouderos Y, Delmas PD, Christiansen C. Incorporation and distribution of strontium in bone. Bone 2001;28(4):446-453.
10. Boivin G, Deloffre P, Perrat B, Panczer G, Boudeulle M, Mauras Y, Allain P, Tsouderos Y, Meunier PJ. Strontium distribution and interactions with bone mineral in monkey iliac bone after strontium salt (S 12911) administration. Journal of Bone and Mineral Research 1996;11(9):1302-1311.
11. Christoffersen J, Christoffersen MR, Kolthoff N, Barenholdt O. Effects of strontium ions on growth and dissolution of hydroxyapatite and on bone mineral detection. Bone 1997;20(1):47-54.
12. Skoryna SC. Effects of Oral Supplementation with Stable Strontium. Canadian Medical Association Journal 1981;125(7):703-712.
13. Curzon MEJ, Spector PC. Strontium Uptake and Enamel Dissolution in Bovine and Human-Enamel. Caries Research 1983;17(3):249-252.
14. Mccaslin FE, Janes JM. The Effect of Strontium Lactate in the Treatment of Osteoporosis. Proceedings of the Staff Meetings of the Mayo Clinic 1959;34(13):329-334.
15. Reginster JY, Lecart MP, Deroisy R, Lousberg C. Strontium ranelate: a new paradigm in the treatment of osteoporosis. Expert Opinion on Investigational Drugs 2004;13(7):857-864.
16. Reginster JY, Deroisy R, Jupsin I. Strontium ranelate: A new paradigm in the treatment of osteoporosis. Drugs of Today 2003;39(2):89-101.
17. Meunier PJ, Roux C, Seeman E, Ortolani S, Badurski JE, Spector TD, Cannata J, Balogh A, Lemmel EM, Pors-Nielsen S and others. The effects of strontium ranelate on the risk of vertebral fracture in women with postmenopausal osteoporosis. N Engl J Med 2004;350(5):459-68.
18. Roux C, Reginster JY, Fechtenbaum J, Kolta S, Sawicki A, Tulassay Z, Luisetto G, Padrino JM, Doyle D, Prince R and others. Vertebral fracture risk reduction with strontium ranelate in women with postmenopausal osteoporosis is independent of baseline risk factors. J Bone Miner Res 2006;21(4):536-42.
19. Reginster JY, Seeman E, De Vernejoul MC, Adami S, Compston J, Phenekos C, Devogelaer JP, Curiel MD, Sawicki A, Goemaere S and others. Strontium ranelate reduces

the risk of nonvertebral fractures in postmenopausal women with osteoporosis: Treatment of Peripheral Osteoporosis (TROPOS) study. J Clin Endocrinol Metab 2005;90(5):2816-22.
20. Degroot K, Geesink R, Klein CPAT, Serekian P. Plasma Sprayed Coatings of Hydroxylapatite. Journal of Biomedical Materials Research 1987;21(12):1375-1381.
21. Jaffe WL, Scott DF. Total hip arthroplasty with hydroxyapatite-coated prostheses. Journal of Bone and Joint Surgery-American Volume 1996;78A(12):1918-1934.
22. Geesink RGT, Degroot K, Klein CPAT. Chemical Implant Fixation Using Hydroxyl-Apatite Coatings - the Development of a Human Total Hip-Prosthesis for Chemical Fixation to Bone Using Hydroxyl-Apatite Coatings on Titanium Substrates. Clinical Orthopaedics and Related Research 1987(225):147-170.
23. Li PJ, Ducheyne P. Quasi-biological apatite film induced by titanium in a simulated body fluid. Journal of Biomedical Materials Research 1998;41(3):341-348.
24. Oliveira AL, Gomes ME, Malafaya PB, Reis RL. Biomimetic coating of starch based polymeric foams produced by a calcium silicate based methodology. Bioceramics 15 2003;240-2:101-104.
25. Oliveira AL, Elvira C, Reis RL, Vazquez B, San Roman J. Surface modification tailors the characteristics of biomimetic coatings nucleated on starch-based polymers. Journal of Materials Science-Materials in Medicine 1999;10(12):827-835.
26. Li P, Nakanishi K, Kokubo T, de Groot K. Induction and morphology of hydroxyapatite, precipitated from metastable simulated body fluids on sol-gel prepared silica. Biomaterials 1993;14(13):963-8.
27. Kokubo T, Kushitani H, Sakka S, Kitsugi T, Yamamuro T. Solutions able to reproduce in vivo surface-structure changes in bioactive glass-ceramic A-W. J Biomed Mater Res 1990;24(6):721-34.
28. Li PJ. Biomimetic nano-apatite coating capable of promoting bone ingrowth. Journal of Biomedical Materials Research Part A 2003;66A(1):79-85.
29. Rose FRAJ, Hou QP, Oreffo ROC. Delivery systems for bone growth factors - the new players in skeletal regeneration. Journal of Pharmacy and Pharmacology 2004;56(4):415-427.
30. Luginbuehl V, Meinel L, Merkle HP, Gander B. Localized delivery of growth factors for bone repair. European Journal of Pharmaceutics and Biopharmaceutics 2004;58(2):197-208.
31. Krout A, Wen HB, Hippensteel E, Li PJ. A hybrid coating of biomimetic apatite and osteocalcin. Journal of Biomedical Materials Research Part A 2005;73A(4):377-387.
32. Rodan GA, Martin TJ. Therapeutic approaches to bone diseases. Science 2000;289(5484):1508-1514.
33. Li P; DePuy Orthopaedics, Inc., assignee. Bioactive ceramic coating and method. USA patent 6, 569,489. 2000.
34. Li P; DePuy Products, Inc., assignee. Strontium-substituted apatite coating. USA patent 6905723. 2005.
35. Morohashi T, Sano T, Yamada S. Effects of Strontium on Calcium-Metabolism in Rats.1. A Distinction between the Pharmacological and Toxic Doses. Japanese Journal of Pharmacology 1994;64(3):155-162.
36. Marie PJ, Hott M, Modrowski D, Depollak C, Guillemain J, Deloffre P, Tsouderos Y. An Uncoupling Agent Containing Strontium Prevents Bone Loss by Depressing Bone-Resorption and Maintaining Bone-Formation in Estrogen-Deficient Rats. Journal of Bone and Mineral Research 1993;8(5):607-615.
37. Marie PJ, Hott M. Short-Term Effects of Fluoride and Strontium on Bone Forming and Bone Resorbing Cells in the Mouse. Calcified Tissue International 1986;38(Ns):S17-S17.
38. Grynpas MD, Hamilton E, Cheung R, Tsouderos Y, Deloffre P, Hott M, Marie PJ. Strontium increases vertebral bone volume in rats at a low dose that does not induce detectable mineralization defect. Bone 1996;18(3):253-259.
39. Dick WA, Tabatabai MA. Determination of Orthophosphate in Aqueous-Solutions Containing Labile Organic and Inorganic Phosphorus-Compounds. Journal of Environmental Quality 1977;6(1):82-85.
40. Barrere F, Layrolle P, Van Blitterswijk CA, De Groot K. Biomimetic calcium phosphate coatings on Ti6Al4V: A crystal growth study of octacalcium phosphate and inhibition by Mg2+ and HCO3-. Bone 1999;25(2):107s-111s.
41. Vallet-Regi M, Romero AM, Ragel CV, LeGeros RZ. XRD, SEM-EDS, and FTIR studies of in vitro growth of an apatite-like layer on sol-gel glasses. Journal of Biomedical Materials Research 1999;44(4):416-421.

42. Rehman I, Bonfield W. Characterization of hydroxyapatite and carbonated apatite by photo acoustic FTIR spectroscopy. Journal of Materials Science-Materials in Medicine 1997;8(1):1-4.
43. Barralet J, Best S, Bonfield W. Carbonate substitution in precipitated hydroxyapatite: An investigation into the effects of reaction temperature and bicarbonate ion concentration. Journal of Biomedical Materials Research 1998;41(1):79-86.
44. Barrere F, van Blitterswijk CA, de Groot K, Layrolle P. Influence of ionic strength and carbonate on the Ca-P coating formation from SBFx5 solution. Biomaterials 2002;23(9):1921-1930.
45. Barrere F, van Blitterswijk CA, de Groot K, Layrolle P. Nucleation of biomimetic Ca-P coatings on Ti6Al4V from a SBF x 5 solution: influence of magnesium. Biomaterials 2002;23(10):2211-2220.
46. Li P, Ohtsuki C, Kokubo T, Nakanishi K, Soga N, Nakamura T, Yamamuro T. Effects of ions in aqueous media on hydroxyapatite induction by silica gel and its relevance to bioactivity of bioactive glasses and glass-ceramics. J Appl Biomater 1993;4(3):221-9.

SECTION 5.

CHAPTER VIII

Chapter VIII

General Conclusions & Final Remarks

General Conclusions

The main goal of the present thesis was to design innovative biomimetic coating routes able to produce bone-like tailored apatite layers at the surface of compact and porous biomaterials, as a strategy for promoting bone-bonding and enhance tissue regeneration when in contact with the natural bone tissue.

Different biomimetic routes were herein originally proposed in order to meet the requirements imposed by the type of substrate and the application context of the coatings. The process of apatite formation in solution is a complex phenomenon, involving a number of reactions concerning the association/dissociation of various ions and ion groups in solution, which will be affected by interactions with the substrate and with the environment to which the solutions are exposed [1-5].

For being able to coat natural origin biodegradable starch-based polymers, a novel biomimetic sodium silicate methodology has been previously developed [6]. Based on this method, different studies were conducted for coating both compact and porous starch-based polymers taking into account several important aspects, namely:

- The ionic strength of the Simulated Body Fluid (SBF): the influence of the ionic strength of the SBF solution on apatite layer formation was investigated and consequently its influence osteoblast-like cell behaviour.
- The use of dynamic coating conditions: the possibility of using dynamic conditions to enhance the coating efficiency in 3D complex architectures substrates was also investigated;

- The assessment of coatings using non-destructive techniques: the possibility to evaluate the overall apatite coating distribution on 3D complex architectures using a non-destructive technique was also studied;
- The incorporation of a therapeutic molecule: the incorporation of a therapeutic molecule with affinity for Ca-P was also demonstrated. Sodium clodronate, aimed at stimulating bone formation, was used as a biomolecule model;
- The biomimetic coating of a metallic substrate: the development of a biomimetic coating methodology aimed at stimulating bone formation through the incorporation of Strontium into its structure.

VII.1. Biomimetic Calcium-Phosphate Coatings Produced by a Sodium Silicate Gel Methodology

An innovative biomimetic methodology for producing bioactive coatings at the surface of compact and porous starch based biodegradable materials has been developed [6], using a sodium silicate gel as an alternative nucleating agent to the traditional approach based on bioactive glass proposed by Kokubo *et al.* [7,8] and adapted by Reis *et al.* [9]. This methodology relies on the swelling ability of the substrate and proved to be suitable to hygroscopic substrates such as the starch-based blends herein investigated. By this way, the surface of the materials can be impregnated with the nucleating agent. The water uptake ability of the substrates is regarded as an important requirement as demonstrated in an earlier study conducted for HMWPE and PU foam for which it was not possible to induce any Ca-P layer formation [6].

Besides acting as a nucleating agent, sodium silicate can increase the hydration degree and surface hydrophilicity (determined for compact structures by contact angle measurements) of the starch based blends. These effects will contribute to the increase of the polar groups at the surface which will improve the adhesion between the coating and the substrate. These changes were justified by an alkali attack produced by the sodium silicate gel, comparable to the effect induced by a surface pre-treatment with KOH, performed for SEVA-C substrates as presented in a previous study [10,11]. As a consequence, upon SBF immersion, the number of favourable sites for apatite formation on the surface of the substrates has increased, allowing for the formation of a well-adhered and uniform apatite layer.

For both compact and porous structures, it was possible to observe the formation of a very cohesive apatite-like layer after only 6 hours of immersion in SBF. The main advantages of this metod as compared to the traditional biomimetic approach include:

- Improved coating of porous substrates: the produced layer could be observed within the pores, clearly covering the surface of the fibres. When comparing with the traditional biomimetic treatment, the later is not so effective at the bulk of porous structures.
- Shorter induction period: sodium silicate gel methodology proved to be a very effective and simple methodology to reduce the induction period for the formation of a well-defined apatite-like layer on the surface of starch based biodegradable polymers.

VII.1.2 Influence of the ionic strength of the SBF solution

One of the most interesting aspects of biomimetic preparation of Ca-P coatings is that, although initially designed to be conducted at physiological conditions, slight variations in the processing conditions can lead to diferences on the resulting apatite layer and on further cell behaviour. This was reflected in Chapter III, were an increase in the ionic strength of the SBF solution resulted in slight changes in the crystallinity of the formed apatite layers, which in turn have positively influenced the way osteoblast-like cells adhere to the surface. A very good osteoblast adhesion and an undisrupted morphology were obtained, which is an indicator of the biocompatibility of the apatite coatings. This study served as a starting point for developing the subsequent studies in this thesis.

VII.1.3. Effect of Dynamic Conditions on coating the Surface and Bulk of Complex Architectures

Sodium silicate treatment is a methodology particularly suitable for coating 3D complex architectures, as the gel can penetrate along the pores of the scaffolds allowing the coating of their entire surface. Albeit the coating formation within the scaffold is possible, there are still challenges remaining on what concerns the control of coating distribution. In fact, the rate for apatite formation within the bulk of the scaffold is significantly lower as compared to the outer part, leading to marked differences in thickness distribution. This effect results from the difficult access of the ions to the scaffold inner pores and consequent ion concentration gradient across the scaffold thickness. To avoid this concentration gradient, a new dynamic coating route was proposed in Chapters IV and V

aimed to be applied to SPCL scaffolds produced by a 3D plotting technology. This strategy, intended to improve the coating efficiency of the scaffold materials, by attempting to mimick Nature in the sense that bone mineralization occurs in the presence of fluids that continuously circulate in the body. Therefore, an *in vitro* biomimetic approach capable of replicating dynamic conditions is of great significance as it better mimics the *in vivo* milieu. In this context, bone-like apatite layers were produced both at the surface and at the bulk of SPCL scaffolds under different conditions: static, agitation and flow perfusion (inside a bioreactor). For the studied periods of immersion in SBF, the composition, chemical structure and crystallinity of the obtained apatite layers grown under static, agitation and flow perfusion conditions was not significantly altered. However, in case of the flow perfusion, the coating thickness was greatly enhanced. By means of this process, the time required for apatite formation can be greatly reduced and more stable and well-defined apatite layers could be produced. The advantages of this system when comparing with both static and agitation conditions are various, namely:

- True biomimetic approach: it better mimics *in vivo* apatite mineralization processes;
- No precipitate formation: unlike static methods, the accumulation of precipitates is avoided;
- Greater process control: control over the coating kinetics is achieved through flow rate adjustment;
- More efficient coating: higher rate for apatite formation that strongly reduces duration of coating time.
- High integrity of the coating: scaffolds are immobilized within the chamber which preserves the integrity of the coating as compared to agitation conditions;

Morphological analysis by SEM and μ-CT gave valuable information on both the architecture of the scaffolds and the thickness distribution of the coatings. The results presented in Chapter V using μ-CT provided the first insights on the potential of this non-destructive technique for the overall morphological characterization of biomimetic apatite layers, which would be impossible to achieve using traditional characterisation techniques. It was possible to clearly observe the differences between the coating conditions. Nevertheless it is important to have in mind that the adequate resolution of the CT scans is very important as it dictates the accuracy of the obtained information, particularly in the case of thin coatings.

VII.1.4. Incorporation of a therapeutic molecule: Sodium Clodronate

Due to the physiological working conditions in terms of pH and temperature, the proposed biomimetic methodology offers the possibility of incorporating molecules of biological relevance. The selection of Bisphosphonate as a model drug to be incorporated in the produced coatings was based on its affinity to Ca-P, its positive effect when administrated for the treatment of bone-related diseases and its availability at a relative low cost. The first criterion is very important as it is very difficult to design a controlled release system using calcium phosphates as carriers due to their low loading efficiency. Amorphous calcium phosphates tend to be more reactive and thus more suitable to be used as drug delivery vehicles [12-16]. In this way, biomimetic coatings are good candidates to be used as carriers, due to its poorly crystalline nature and their nanocrystalline porous (cauliflower) structure (higher surface contact area).

Sodium clodronate is a well known bisphosphonate that was successfully incorporated, at different doses in the structure of biomimetic apatite layers formed using a sodium silicate based process. In this preliminary approach, a screening of the optimal bisphosphonate concentration in terms of osteoblastic response was performed, having in mind the necessity of conducting complementary studies with osteoclasts in order to fully investigate its inhibitory effect. It was interesting to note that for certain doses, sodium clodronate exhibited a non toxic effect and even stimulated cell function. It is foreseen that the coatings incorporating this therapeutic agent could be potentially used for the localized treatment of specific bone diseases by regulating the equilibrium on osteoblastic/osteoclastic activity.

VII.2. Development of a Biomimetic Technology to produce a Strontium-Substituted Apatite Coating

In this study, a different biomimetic route was applied to coat the surface of a titanium alloy. This methodology, initially proposed by Li *et al.* [2], uses a solution derived from the well-known SBF. This specially designed mineralization solution differs from SBF on its composition, on the temperature and pH used during the coating process. The ionic concentration of the solution is approximately 2X SBF, the temperature used is 45 ºC and the pH around 6.7. Under these conditions the precipitation of the Ca-P occurs

spontaneously without the intervention of a nucleating agent which can allow for the coating of any type of surface inside the reactor chamber. While the nucleation and growth of the apatite layer in SBF is governed by a heterogeneous process [4], in which the nuclei start to form in the presence of a nucleation agent or bioactive surface, in this solution the precipitation is homogeneous, occurring through the overall solution and in the surfaces that are in contact with it. In this way, during the coating process the solution becomes turbid, which does not happens when SBF is used. At the presented conditions the coating can be achieved in a short time period such as 24 hours.

Although it operates under less pysiological conditions, this methodology has allowed for the formation of a uniform bone-like apatite coating at the surface of Ti, exhibiting typical needle-like shape morphology. When adding increasingly amounts of strontium chloride ($SrCl_2$) to the solution, a remarkable change in the apatite morphology was observed indicating that the presence of Sr has inhibited the growth of the apatite crystals, and increased the nano-character of the apatite structure. At the same time a delay in the coating process was observed that resulted in a decrease of the coating thickness. Sr ions are depleted from solution to substitute for Ca in apatite lattice during its formation, leading to the formation of a Sr-substituted apatite coating. Because of its chemical and physical similarity to calcium [17], strontium is a natural bone-seeking trace element that accumulates in the skeleton, influencing bone remodelling by affecting both bone resorption and formation [18,19] This new Sr-apatite coatings are expected to have a positive effect in enhancing bone formation.

V.II.3. Final Remarks and Future work

The herein proposed biomimetic concepts intend to give a contribute for the development of nature-inspired calcium phosphate coatings aimed to mimic, in the best possible way, the composition and structure of natural bone. The concept of coating scaffolds featuring 3D architectures has motivated the development of alternative coating procedures for the production of apatite layers with improved quality, homogeneous distribution and high reproducibility. One of the important achievements in this thesis was the development of a bioreactor based flow perfusion system capable of continuously coating complex substrate architectures at higher apatite formation rates. Using this methodology, the distribution of the coating thickness was remarkably improved. Even so, the external surface of the scaffold opposite to the main direction of flow (the bottom side) presented a higher coating thickness. In fact, this side had a higher ion supply, as the flow velocity is higher at the entrance of the

hamber, decreasing along distance. To avoid this gradient effect, a new bioreactor concept is presently being designed which includes the cyclic inversion of the flow (Figure 1).

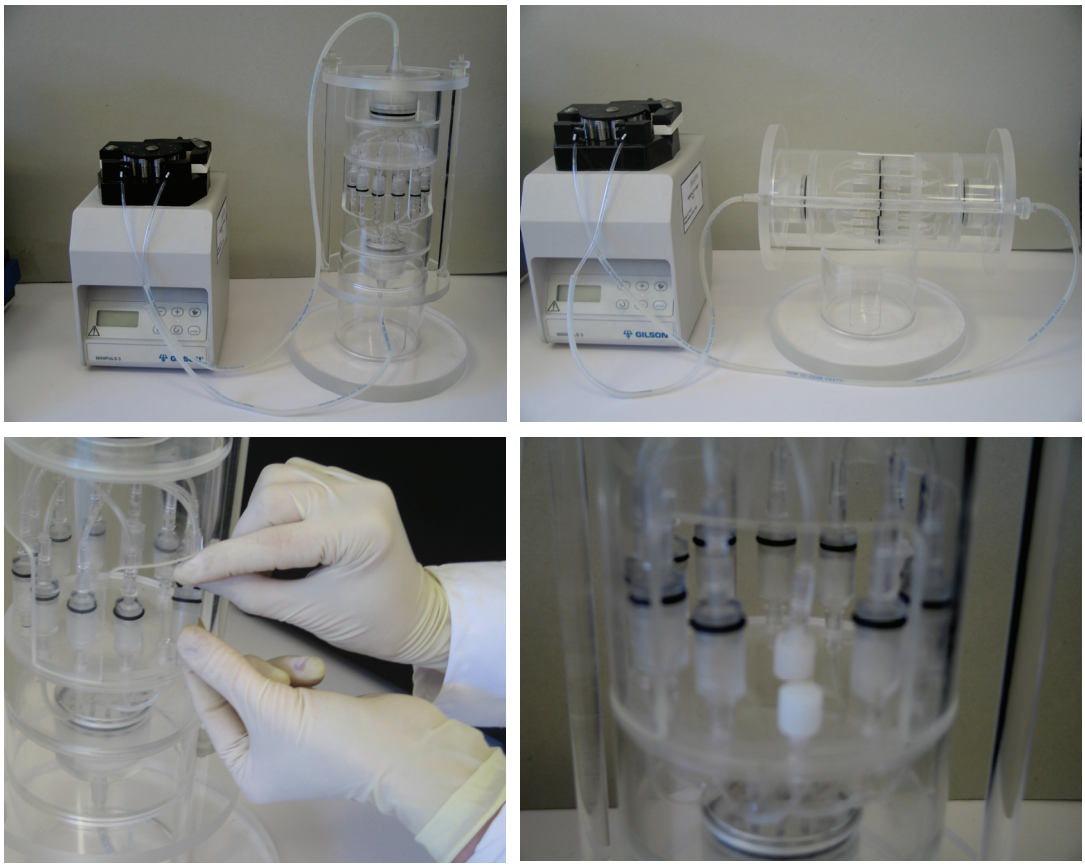


Figure 1. New bioreactor including the cyclic inversion of the flow.

This novel bioreactor system will incorporate several functioning innovations which will ensure a higher operating efficiency of this technology in two main aspects:

- Improved coating thickness distribution: This new system will periodically alternate the flow direction inside the chamber, allowing for a homogeneous distribution of the coating thickness.
- Sterile operation of the bioreactor: The system will allow for the removal of the samples from the bioreactor without stopping the coating process or opening the system, making it suitable to be operated under sterile conditions.

Another issue addressed in this thesis was the possibility of adding a therapeutic function to the apatite layers, either by post-loading sodium clodronate or by incorporating Sr in the apatite structure. The incorporation of both substances in the biomimetic coatings was demonstrated. The choice of either a bisphosphonate or a metallic element such as Sr to be incorporated in the apatite lattice has relied on their known effect in stabilizing the

structure of the apatite [17,20-23] and inhibiting bone resorption [19,24-27]. In the authors Opinion, these options constitute attractive strategies for improving apatite layer performance by specifically promoting bone remodelling at the bone-material interface.

In the case of sodium clodronate, the optimum therapeutic dose to be incorporated in the apatite layer was identified**.** In this way, and due to the mild working conditions (T, pH) of the presented biomimetic methodologies, the next step will be to co-precipitate this drug at an early stage of the coating process in order to obtain BP-containing layers for long-term controlled release. The ability of the developed loaded coatings in inhibiting *in vitro* osteoclastic behaviour, i.e. evaluating their capability in preventing bone resorption, is another important subject that will be studied in the future. It is foreseen that these coatings could be used in clinical situations for which a regenerative effect could be produced by regulating the osteoblastic/osteoclastic activity.

Using the complementary knowledge acquired in the herein presented studies, an innovative technology is ultimately proposed as an outcome of this thesis through the integration of the several concepts developed. The recently developed bioreactor (Figure 1) will comprise new functionalities integrating the following stages: i. coating of an apatite layer; ii. incorporation of a therapeutic agent and iii. replacement of SBF by osteogenic medium followed by cell seeding and iv. implantation.

By using this multi-function bioreactor, it will be possible to assure minimal manual manipulation of the constructs prior to implantation. This aspect is very important in order to guarantee the integrity of the produced apatite coatings, as the coated scaffolds are not subjected to any drying step that is the main cause for coating detachment.

References

1. Lu X, Leng Y. Theoretical analysis of calcium phosphate precipitation in simulated body fluid. Biomaterials 2005;26(10):1097-108.
2. Li PJ. Biomimetic nano-apatite coating capable of promoting bone ingrowth. Journal of Biomedical Materials Research Part A 2003;66A(1):79-85.
3. Li P, Ohtsuki C, Kokubo T, Nakanishi K, Soga N, Nakamura T, Yamamuro T. Effects of ions in aqueous media on hydroxyapatite induction by silica gel and its relevance to bioactivity of bioactive glasses and glass-ceramics. J Appl Biomater 1993;4(3):221-9.
4. Kokubo T, Takadama H. How useful is SBF in predicting in vivo bone bioactivity? Biomaterials 2006;27(15):2907-2915.
5. Leonor IB, Kim HM, Balas F, Kawashita M, Reis RL, Kokubo T, Nakamura T. Surface potential change in bioactive polymer during the process of biomimetic apatite formation in a simulated body fluid. Journal of Materials Chemistry 2007;17(38):4057-4063.
6. Oliveira AL, Malafaya PB, Reis RL. Sodium silicate gel as a precursor for the in vitro nucleation and growth of a bone-like apatite coating in compact and porous polymeric structures. Biomaterials 2003;24(15):2575-2584.
7. Abe Y, Kokubo T, Yamamuro T. Apatite Coating on Ceramics, Metals and Polymers Utilizing a Biological Process. Journal of Materials Science-Materials in Medicine 1990;1(4):233-238.
8. Kokubo T, Kushitani H, Sakka S, Kitsugi T, Yamamuro T. Solutions able to reproduce in vivo surface-structure changes in bioactive glass-ceramic A-W. J Biomed Mater Res 1990;24(6):721-34.
9. Reis RL, Cunha, A. M., Fernandes, M. H., Correia, R. N. Treatments to Induce the Nucleation and Growth of Apatite Like Layers onto Polymeric Surfaces and Foams. Journal of Materials Science: Materials in Medicine 1997;8:897.
10. Oliveira AL, Elvira C, Reis RL, Vazquez B, San Roman J. Surface modification tailors the characteristics of biomimetic coatings nucleated on starch-based polymers. Journal of Materials Science-Materials in Medicine 1999;10(12):827-835.
11. Oliveira AL, Leonor IB, Elvira C, Azevedo MC, Pashkuleva I, Reis RL. Surface Treatments and Pre-calcification Routes to Enhance Cell Adhesion and Proliferation. In: Reis RL, Cohn D, editors. Polymer Based Systems on Tissue Engineering, Replacement and Regeneration. Drodercht: Kluwer Press; 2002. p 183-217.
12. Paschalis EP, Wikiel K, Nancollas GH. Dual Constant Composition Kinetics Characterization of Apatitic Surfaces. Journal of Biomedical Materials Research 1994;28(12):1411-1418.
13. Budz JA, Nancollas GH. The Mechanism of Dissolution of Hydroxyapatite and Carbonated Apatite in Acidic Solutions. Journal of Crystal Growth 1988;91(4):490-496.
14. Nancollas GH, Wu W, Tang R. The mechanisms of crystallization and dissolution of caclium phosphates at surfaces. Glass Science and Technology-Glastechnische Berichte 2000;73:318-325.
15. Nancollas GH, Wu WJ. Biomineralization mechanisms: a kinetics and interfacial energy approach. Journal of Crystal Growth 2000;211(1-4):137-142.
16. Tang RK, Henneman ZJ, Nancollas GH. Constant composition kinetics study of carbonated apatite dissolution. Journal of Crystal Growth 2003;249(3-4):614-624.
17. Bigi A, Boanini E, Capuccini C, Gazzano M. Strontium-substituted hydroxyapatite nanocrystals. Inorganica Chimica Acta 2007;360(3):1009-1016.
18. Marie PJ, Ammann P, Boivin G, Rey C. Mechanisms of action and therapeutic potential of strontium in bone. Calcified Tissue International 2001;69(3):121-129.
19. Ni GX, Chiu KY, Lu WW, Wang Y, Zhang YG, Hao LB, Li ZY, Lam WM, Lu SB, Luk KDK. Strontium-containing hydroxyapatite bioactive bone cement in revision hip arthroplasty. Biomaterials 2006;27(24):4348-4355.
20. Curzon MEJ, Spector PC. Strontium Uptake and Enamel Dissolution in Bovine and Human-Enamel. Caries Research 1983;17(3):249-252.
21. Fleisch H. Bisphosphonates: mechanisms of action. Expert Opinion on Therapeutic Patents 2001;11(9):1371-1381.
22. Henneman ZJ, Nancollas GH, Ebetino FH, Russell RG, Phipps RJ. Bisphosphonate binding affinity as assessed by inhibition of carbonated apatite dissolution in vitro. J Biomed Mater Res A 2007.

23. Peter B, Gauthier O, Laib S, Bujoli B, Guicheux J, Janvier P, van Lenthe GH, Muller R, Zambelli PY, Bouler JM and others. Local delivery of bisphosphonate from coated orthopedic implants increases implants mechanical stability in osteoporotic rats. Journal of Biomedical Materials Research Part A 2006;76A(1):133-143.
24. Rodan GA, Martin TJ. Therapeutic approaches to bone diseases. Science 2000;289(5484):1508-1514.
25. Rodan GA, Reszka AA. Osteoporosis and bisphosphonates. Journal of Bone and Joint Surgery-American Volume 2003;85A:8-12.
26. Shanbhag AS. Use of bisphosphonates to improve the durability of total joint replacements. Journal of the American Academy of Orthopaedic Surgeons 2006;14(4):215-225.
27. McLeod K, Anderson GI, Dutta NK, Smart RS, Voelcker NH, Sekel R, Kumar S. Adsorption of bisphosphonate onto hydroxyapatite using a novel co-precipitation technique for bone growth enhancement. Journal of Biomedical Materials Research Part A 2006;79A(2):271-281.